COUPLED SURFACE AND GROUNDWATER FLOWS: QUASISTATIC LIMIT AND A SECOND-ORDER, UNCONDITIONALLY STABLE, PARTITIONED METHOD

by

Marina Moraiti

B.S. in Applied Mathematics, University of Crete, 2006

M.S. in Mathematics, University of Crete, 2009

M.A. in Mathematics, University of Pittsburgh, 2010

Submitted to the Graduate Faculty of

the Kenneth P. Dietrich School of Arts and Sciences in partial

fulfillment

of the requirements for the degree of

Doctor of Philosophy

University of Pittsburgh

2015

UNIVERSITY OF PITTSBURGH

KENNETH P. DIETRICH SCHOOL OF ARTS AND SCIENCES

This dissertation was presented

by

Marina Moraiti

It was defended on

December 2, 2014

and approved by

Prof. William Layton, Dept. of Mathematics, University of Pittsburgh

Prof. Catalin Trenchea, Dept. of Mathematics, University of Pittsburgh

Prof. Yibiao Pan, Dept. of Mathematics, University of Pittsburgh

Prof. Jorge Abad, Dept. of Civil & Environmental Engineering, University of Pittsburgh

Dissertation Director: Prof. William Layton, Dept. of Mathematics, University of

Pittsburgh

COUPLED SURFACE AND GROUNDWATER FLOWS: QUASISTATIC LIMIT AND A SECOND-ORDER, UNCONDITIONALLY STABLE, PARTITIONED METHOD

Marina Moraiti, PhD

University of Pittsburgh, 2015

In this thesis we study the fully evolutionary Stokes-Darcy and Navier-Stokes/Darcy models for the coupling of surface and groundwater flows versus the quasistatic models, in which the groundwater flow is assumed to instantaneously adjust to equilibrium. Further, we develop and analyze an efficient numerical method for the Stokes-Darcy problem that decouples the sub-physics flows, and is second-order convergent, uniformly in the model parameters.

We first investigate the linear, fully evolutionary Stokes-Darcy problem and its quasistatic approximation, and prove that the solution of the former converges to the solution of the latter as the specific storage parameter converges to zero. The proof reveals that the quasistatic problem predicts the solution accurately only under certain parameter regimes.

Next, we develop and analyze a partitioned numerical method for the evolutionary Stokes-Darcy problem. We prove that the new method is asymptotically stable, and second-order, uniformly convergent with respect to the model parameters. As a result, it can be used to solve the quasistatic Stokes-Darcy problem. Several numerical tests are performed to support the theoretical efficiency, stability, and convergence properties of the proposed method.

Finally, we consider the nonlinear Navier-Stokes/Darcy problem and its quasistatic approximation under a modified balance of forces interface condition. We show that the solution of the fully evolutionary problem converges to the quasistatic solution as the specific storage converges to zero. To prove convergence in three spatial dimensions, we assume more regularity on the solution, or small data.

TABLE OF CONTENTS

LIST OF TABLES

LIST OF FIGURES

PREFACE

I would like to express my deepest gratitude to my dissertation advisor, Professor William Layton, for his guidance, support, and encouragement throughout my graduate school years at the University of Pittsburgh. I thank him for his contagious enthusiasm about research and mathematics, for always being available, for equipping me with the tools to grow into an independent researcher, for his helpful advice in both academic and life matters, and for being, above all, a great human being and friend. I could not have imagined a better advisor.

I thank Professor Catalin Trenchea for serving on my committee, for his support and his great comments on my research. I thank Professors Yibiao Pan and Jorge Abad for serving on my committee and for being available to discuss about my research and provide feedback. A special thanks goes to Mike Sussman and Professor Michael Neilan for their willingness to discuss and give helpful comments on my research. I also thank my former Master's thesis advisor, Professor Michail Loulakis, for encouraging me to pursue a Ph.D. in Mathematics.

A big thanks goes to all my classmates, officemates, and collaborators in the Department of Mathematics at the University of Pittsburgh, and especially to Michaela Kubacki, Hoang Tran, Martina Bukač, Nan Jiang, Yong Li, Nick Hurl, and Xin Xiong.

I want to thank my friends, both back in Greece as well as in the United States, for making my graduate school years more fun. I thank my Pittsburgh friends especially for making the many hours we spent together studying or working on research more enjoyable.

Finally, I thank my family, and especially my parents, Christina and Stavros, my sister, Danai, and my parents in-law for their love, support, and encouragement. Most of all, I thank my husband, Michael, for his love and for his encouragement every step of the way.

1.0 INTRODUCTION

Groundwater constitutes the world's most vast and valuable source of freshwater [18]. It is essential in a wide range of everyday human activities, such as irrigation in agriculture, industrial processes, urban development, household activities, and in many areas it serves as the only source of drinking water. However, these same activities inevitably lead to groundwater contamination and the deterioration of freshwater aquifers. For example, pesticides or heavy chemical and radioactive industrial waste (Figure 1) can be transported by free surface streams and permeate the ground, polluting groundwater. On the other hand, rising sea levels due to the effects of climate change can potentially lead to salt-water intrusion into freshwater aquifers. Oil extraction occasionally results in spills which also threaten to severely pollute groundwater. Moreover, the recently adapted method of hydraulic fracturing for the extraction of gas poses new challenges for the effective protection of the environment, and in particular freshwater supplies. Considering the rise in population, and consequently, the increasing demand for fresh and clean water, and on the other hand the growing demand for oil and natural gas, precise modeling and accurate prediction of the fluid flow in coupled surface and subsurface settings are critical. This thesis addresses both modeling and numerical solution of coupled groundwater and surface-water flows.

Modeling the interaction between groundwater and surface-water flows involves two different physical processes taking place in two adjacent domains: the groundwater flow region and the surface-water flow region (Figure 1). The groundwater flow region may consist of different porous materials, such as clay, rock or sand. In this thesis, we focus on the coupling between incompressible Navier-Stokes or Stokes flow in the fluid region, and the groundwater flow equation (Darcy's law plus conservation of mass in the pores) in the porous media region. We denote the fluid and porous media domains by Ω_f and Ω_p respectively, $\Omega_{f/p} \subset \mathbb{R}^d$,

1
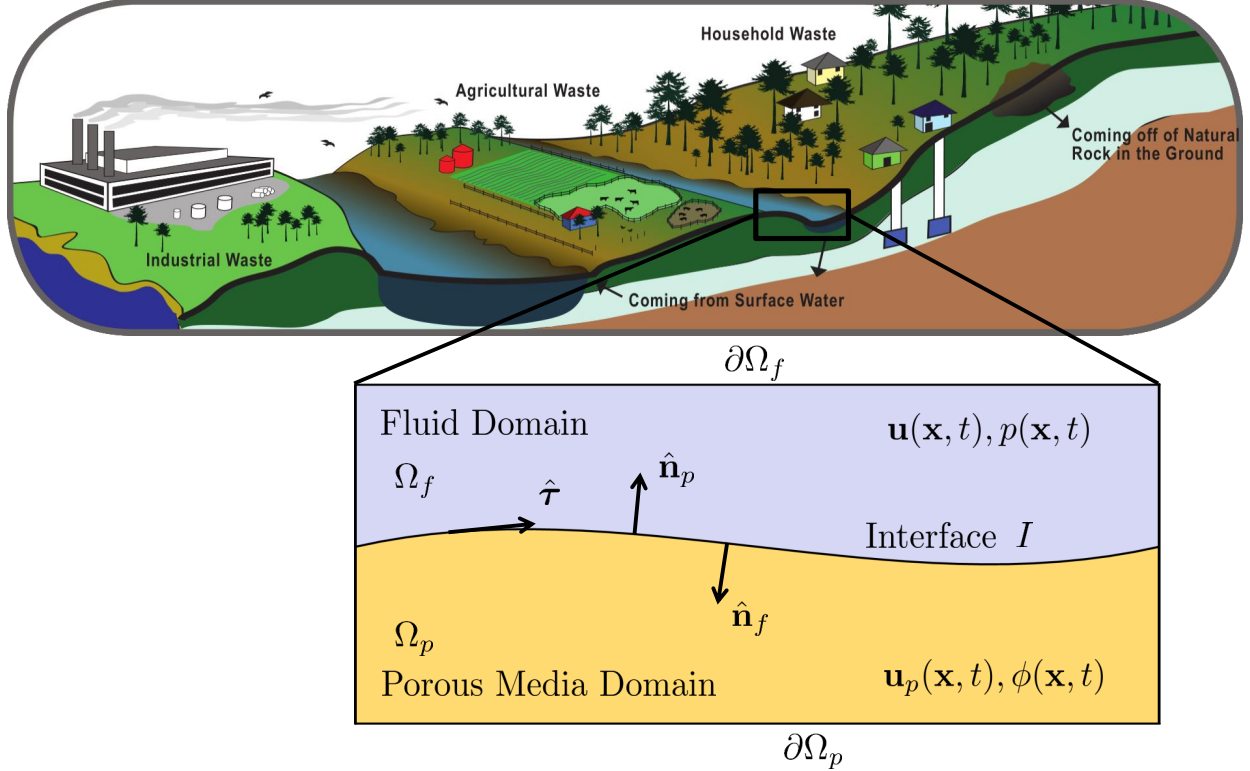
Figure 1: Groundwater pollution sources and modeling of coupled surface and groundwater flows. (Image adapted from [93] and used with permission from the NC Department of Health and Human Services.)

$d = 2$ or 3, and assume they lie across an interface, I, as shown in Figure 1. Both domains are assumed to be bounded and regular, with smooth enough boundaries, $\partial \Omega_{f/p}$. We further denote by $\hat{\mathbf{n}}_f, \hat{\mathbf{n}}_p$ the unit normal vectors on Ω_f, Ω_p, respectively, which satisfy $\hat{\mathbf{n}}_f = -\hat{\mathbf{n}}_p$. Appropriate coupling and boundary conditions are assumed at the interface and exterior boundaries of the domains respectively. We are interested in determining the velocity field, $\mathbf{u}$ and $\mathbf{u}_p$, in each domain, the pressure, p, in the fluid domain, and the hydraulic head, ϕ, in the porous media domain (Figure 1). The evolutionary problem occurs when we are interested in remediation or estimation of contaminated subsurface, or oil spills, for instance.

The challenges in modeling and solving the coupled (time-dependent) problem are many. First, it is a multi-physics, multi-domain problem, and the coupling of the sub-physics pro-

cesses across the interface is exactly conservative (skew symmetric). Second, the model parameters depend on the porous materials' properties, and also on the degree of saturation in the aquifer, and are therefore typically inhomogeneous, anisotropic, and in certain settings, very small in value. Third, the flow in the porous media region is commonly much slower than the surface flow, and thus multi-rate formulations, where different time steps are assumed in each domain, are necessary. Further, because of the low permeability and thus low hydraulic conductivity and/or low specific storage of certain confined or semi-permeable, large aquifers, we often need to solve the evolutionary problem over long time intervals. Finally, in the case of the Navier-Stokes/Darcy model, tackling the nonlinearity adds to the problem's complexity. These observations further emphasize the need for numerical methods that are efficient, stable, and uniformly convergent with respect to the model parameters. This thesis addresses the modeling of time-dependent, coupled surface and groundwater flows governed by the Navier-Stokes/Darcy or Stokes-Darcy systems and further involves the development, analysis, and testing of a partitioned numerical method for the evolutionary Stokes-Darcy equations that allows for parallel solving of the sub-physics processes at each times step, and that is second-order, asymptotically stable and uniformly convergent with respect to the model parameters. In the analysis, we assume that the porous media region is fully saturated, and that all model parameters are homogeneous.

The literature on coupled fluid and porous media flows has expanded considerably in recent years. Since Beavers and Joseph [12] first investigated the coupling conditions between a fluid and a porous medium experimentally, further studies have been conducted in [101, 86, 95, 67, 89, 24, 112]. The Stokes-Darcy model and its associated numerical analysis and solution, has been studied since [33] and [82] in [33, 35, 88, 32, 36, 98, 99, 57, 37, 60, 19, 5, 91, 20, 68, 61, 30, 22, 24, 23, 42, 50, 109] for the steady case and in [115, 92, 24, 83, 21] for the time-dependent case. The Navier-Stokes/Darcy coupling has been analyzed in, e.g., [32, 52, 8] for the steady case and in [1] for the time-dependent case. See [34] for an overview of analysis and numerical methods for the Stokes-Darcy and Navier-Stokes/Darcy couplings for surface and groundwater flows.

One common model used in, e.g., [1, 52, 25, 8], drops a term involving the time derivative of the hydraulic head in the equation modeling the groundwater flow. The simplified model

will be referred to as the quasistatic model, because one of the two sub-physics processes in the coupling is assumed to instantaneously adjust to equilibrium. However, due to the effect of poroelasticity, the flow in the pores is slightly compressible, and the model adjusts slower to equilibrium. In this thesis we investigate under which circumstances it is justified to use the quasistatic model and drop the time-derivative term from the groundwater flow equation. We prove that the solution of the fully evolutionary Stokes-Darcy problem converges to the quasistatic solution as the specific storage parameter converges to zero, see also [90]. Further, we analyze the Navier-Stokes/Darcy coupling and prove that the solution of the fully evolutionary model converges to the quasistatic solution. For the convergence in the nonlinear case we modify the balance of normal forces coupling condition to include an "inertia" term. To show convergence in three spatial dimensions in the nonlinear case, we assume more regularity on the solution or small data. Several numerical tests are performed to confirm the theoretical rate of convergence to the quasistatic solution.

One approach in the numerical solution of the coupled problem is monolithic discretization by an implicit method and iterative solution of the resulting system by domain decomposition. Partitioned methods, on the other hand, uncouple the two sub-physics flows and allow for parallel solution of each sub problem, and thus require only two symmetric positive-definite solves per time step. The decoupling is achieved by using implicit methods for the discretization of the sub-physics flows, and explicit methods for the coupling terms. In this thesis, we analyze a partitioned method that uses a combination of the Crank-Nicolson and Leapfrog time-marching schemes with added stabilization terms for the temporal discretization of the fully evolutionary Stokes-Darcy problem.

One typical limitation of partitioned methods is their conditional stability under time step conditions that often depend on the model parameters. Since several of the physical parameters in modeling surface and groundwater flows are small in value, this often results in a computationally impractical time step size for stability. The first partitioned methods for the fully evolutionary Stokes-Darcy problem were studied in [92], and were first-order accurate. Additional partitioned methods were analyzed in [83, 102], and higher-order partitioned methods were studied in [85, 21]. Methods with different time steps in each domain were studied in [103]. In [75], it was shown that the combination of Crank-Nicolson and

Leapfrog for the time discretization results in a second-order partitioned method for the Stokes-Darcy system that is conditionally stable under a time step condition that is highly sensitive to small values of the specific storage parameter.

The implicit-explicit combination of Crank-Nicolson and Leapfrog (CNLF), which results in a second-order method, is widely used in the coupling of atmospheric and oceanic flows and in climate modeling and prediction, see, e.g., [100, 7, 105, 114, 28, 27]. The method was first analyzed in [70], and stability for systems was recently proven in [85]. The two limitations of the method are a strong time step condition required for stability and also a weak instability exhibited through the unstable mode of Leapfrog, $(\mathbf{u}^{n+1}+\mathbf{u}^{n-1})$, (for which $\mathbf{u}^{n+1}+\mathbf{u}^{n-1} \equiv \mathbf{0}$), see, e.g., [55, 74]. In [64], we prove asymptotic stability of the unstable mode under the usual time step condition of the method. Due to the strong time step condition, modular time filters, such as the Robert-Asselin-Williams (RAW) filter, [100, 7, 105, 114, 63, 43, 65], have been developed. However, even with the use of time filters like RAW, CNLF can be too restrictive computationally. For a general theory of implicit-explicit methods, see, e.g., [29, 108, 6, 44, 62, 4, 107, 26, 110].

In this thesis, we analyze the CNLF method first applied to a general evolution equation, and develop a non-modular stabilization that increases accuracy while it also eliminates all time step conditions for stability and is long-time stable, in the sense of, e.g., [73, 106, 84, 54, 83]. The stabilization is similar to tools developed in [4, 77, 40, 31]. Further, we prove that the method is asymptotically stable in the unstable mode of Leapfrog, see also [69]. We perform numerical tests to support asymptotic, unconditional stability and second-order, increased accuracy of the method. We next, extend the stabilized CNLF method to the fully evolutionary Stokes-Darcy coupling, see [76]. The resulting partitioned method eliminates all time step conditions for stability and is asymptotically stable in the unstable mode of Leapfrog. In addition, the method retains second-order accuracy of CNLF. We analyze the method's stability and convergence properties and prove unconditional, asymptotic stability and uniform convergence with respect to the model parameters. We further perform a series of numerical tests to demonstrate the method's unconditional stability under small parameter values, verify its second-order accuracy, and show its effectiveness versus fully coupled methods by comparing computational costs.

1.1 THESIS OUTLINE

In Chapter 2 we introduce the necessary notation and analytical tools used in the analysis. Chapter 3 introduces the fully evolutionary Stokes-Darcy (SD) model for coupled surface and groundwater flows. We start with the conservation laws that describe each sub-physics process and the coupling across the interface, and derive the equivalent weak formulation. We also prove a two-domain embedding inequality that is important in the analysis.

Chapter 4 deals with the quasistatic approximation in the SD model. We prove that the solution of the fully evolutionary SD problem converges to the solution of the quasistatic problem as the specific storage parameter converges to zero. The proof reveals that the quasistatic model predicts the solution accurately only under specific parameter regimes.

In Chapter 5 we develop a stabilization for the well known Crank-Nicolson Leapfrog time stepping scheme for a general evolution equation. We prove that the resulting method is unconditionally, asymptotically stable, while increasing accuracy.

In Chapter 6 we extend the stabilization from Chapter 5 to the fully evolutionary SD problem. We prove that the resulting partitioned algorithm is unconditionally, asymptotically stable, and second-order convergent, uniformly in the model parameters.

In Chapter 7 we introduce the nonlinear, fully evolutionary Navier-Stokes/Darcy (NSD) model for coupled surface and groundwater flows, and consider its quasistatic limit. We prove that the solution of the fully evolutionary NSD model converges to the quasistatic solution as the specific storage converges to zero under a modified coupling condition. In three spatial dimensions we assume higher regularity or small data.

In Chapter 8 we conduct numerical tests to support the results of Chapters 4, 5, and 6.

Finally, we present concluding remarks and discuss future research objectives in Chapter 9. Some complementary proofs to the analysis are given in Appendix A, and the code used in the numerical tests in Appendix B.

Remark 1. *The work in Chapter 4 is based on [90], Chapter 5 on [69, 64], and Chapter 6 on [76].*

2.0   PRELIMINARIES

2.1   NOTATION

We begin by introducing the necessary notation. In the definitions below, u and v are scalar functions, $\mathbf{u} = (u_1, \ldots, u_d)^\tau$ and $\mathbf{v} = (v_1, \ldots, v_d)^\tau$ are vector-valued functions, $d \in \{2, 3\}$, and $\mathbf{M}$ and $\mathbf{N}$ are second-order tensors with elements $\{M_{ij}\}_{i,j=1}^d$ and $\{N_{ij}\}_{i,j=1}^d$ respectively. We allow these functions to depend on both space and time. We denote the Euclidean norm of $\mathbf{v}$ by

$$|\mathbf{v}| := \left(\sum_{i=1}^d |v_i|^2 \right)^{\frac{1}{2}},$$

the inner product of $\mathbf{u}$ and $\mathbf{v}$ by

$$\mathbf{u} \cdot \mathbf{v} := \sum_{i=1}^d u_i v_i,$$

and the inner product of $\mathbf{M}$ and $\mathbf{N}$ by

$$\mathbf{M} : \mathbf{N} := \sum_{i,j=1}^d M_{ij} N_{ij}.$$

Further, we write $\mathbf{u} \cdot \mathbf{M} \cdot \mathbf{v}$ for the scalar quantity $\mathbf{u}^\tau \mathbf{M} \mathbf{v}$:

$$\mathbf{u} \cdot \mathbf{M} \cdot \mathbf{v} := \mathbf{u}^\tau \mathbf{M} \mathbf{v} = \sum_{i,j=1}^d \mathbf{u}_i \mathbf{M}_{ij} \mathbf{v}_j.$$

Let $\Omega \subset \mathbb{R}^d$ be an open set, $d \in \{2, 3\}$. We indicate by $L^p(\Omega)$, $1 \leq p < \infty$, the space

$$L^p(\Omega) := \left\{ v : \Omega \to \mathbb{R}, \ v \text{ Lebesgue-measurable function} \ \middle| \ \int_\Omega |v(\mathbf{x})|^p \, d\mathbf{x} < \infty \right\}.$$

$L^p(\Omega)$ is a Banach space endowed with the norm

$$\|v\|_{L^p(\Omega)} := \left(\int_\Omega |v(\mathbf{x})|^p \, d\mathbf{x} \right)^{1/p}, \quad 1 \le p < \infty.$$

In the special case when $p = 2$, $L^2(\Omega)$ is a Hilbert space equipped with the inner product

$$(u, v)_{L^2(\Omega)} := \int_\Omega u(\mathbf{x}) v(\mathbf{x}) \, d\mathbf{x}.$$

We let $L_0^2(\Omega)$ be the space

$$L_0^2(\Omega) := \left\{ v \in L^2(\Omega) \; \middle| \; \int_\Omega v(\mathbf{x}) \, d\mathbf{x} = 0 \right\}.$$

Furthermore, we denote by $L^\infty(\Omega)$ (case $p = \infty$) the space

$$L^\infty(\Omega) := \left\{ v : \Omega \to \mathbb{R} \; \middle| \; \inf \{ C \ge 0 \; : \max |v(\mathbf{x})| \le C \} < \infty \text{ almost everywhere in } \Omega \right\},$$

which is equipped with the norm

$$\|v\|_{L^\infty(\Omega)} := \inf \{ C \ge 0 \; : \max |v(\mathbf{x})| \le C \text{ almost everywhere in } \Omega \}.$$

Here, "almost everywhere in Ω" means

$$\text{meas} \left(\mathbf{x} \in \Omega \; : \; \inf \{ C \ge 0 \; : \max |v(\mathbf{x})| \le C \} = \infty \right) = 0,$$

where "meas" represents the Lebesgue measure in $\mathbb{R}$.

For a vector function $\mathbf{v} \in (L^p(\Omega))^d$, we define the corresponding norms as

$$\|\mathbf{v}\|_{L^p(\Omega)} := \left(\int_\Omega \sum_{i=1}^d |v_i(\mathbf{x})|^p \, d\mathbf{x} \right)^{1/p}, \quad \text{for } 1 \le p < \infty, \quad \text{and}$$

$$\|\mathbf{v}\|_{L^\infty(\Omega)} := \inf \left\{ C \ge 0 \; : \max_{i \in \{1,\dots,d\}} |v_i(\mathbf{x})| \le C \text{ almost everywhere in } \Omega \right\}, \quad \text{for } p = \infty.$$

In the special case $p = 2$, we define the inner product of $\mathbf{u}, \mathbf{v} \in L^2(\Omega)$ through

$$(\mathbf{u}, \mathbf{v})_{L^2(\Omega)} := \int_\Omega \mathbf{u}(\mathbf{x}) \cdot \mathbf{v}(\mathbf{x}) \, d\mathbf{x}.$$

8

We use the short notation $v_t(\mathbf{x}, t) := \frac{\partial v(\mathbf{x},t)}{\partial t}$ for the derivative of v with respect to time t. We indicate by "∇" the gradient operator defined for a vector function as

$$(\nabla \mathbf{v})_{ij} := \frac{\partial v_j}{\partial x_i}, \quad i, j = 1, \ldots, d,$$

and by "$\mathbf{D}(\cdot)$" the deformation tensor, defined as

$$(\mathbf{D}(\mathbf{v}))_{ij} := \frac{1}{2} \left\{ (\nabla \mathbf{v})_{ij} + (\nabla \mathbf{v})_{ji} \right\}, \quad i, j = 1, \ldots, d.$$

Further, the divergence operator for vector functions is given by

$$\nabla \cdot \mathbf{v} := \sum_{i=1}^{d} \frac{\partial v_i}{\partial x_i},$$

and for second-order tensor functions by

$$(\nabla \cdot \mathbf{M})_i := \sum_{j=1}^{d} \frac{\partial M_{ji}}{\partial x_j}, \quad i = 1, \ldots, d.$$

In addition, "Δ" represents the Laplace operator

$$(\Delta \mathbf{v})_i := \sum_{j=1}^{d} \frac{\partial^2 v_i}{\partial x_i^2}, \quad i = 1, \ldots, d.$$

Next, we introduce the usual notation for Sobolev spaces. Let $k \in \mathbb{N}$ and $1 \leq p \leq \infty$. The space $W^{k,p}$ is defined as follows:

$$W^{k,p}(\Omega) := \{ v \in L^p(\Omega) \ : \ D^{\boldsymbol{\alpha}} v \in L^p(\Omega), \forall \text{ multi-indeces } \boldsymbol{\alpha} \text{ with } |\boldsymbol{\alpha}| \leq k \},$$

where $\boldsymbol{\alpha} = (\alpha_1, \ldots, \alpha_d)$, $\alpha_i \in \mathbb{N}$, and $|\boldsymbol{\alpha}| = \alpha_1 + \ldots + \alpha_d$. $D^{\boldsymbol{\alpha}} v$ indicates the distributional derivative of v:

$$D^{\boldsymbol{\alpha}} v := \frac{\partial^{|\boldsymbol{\alpha}|} v}{\partial x_1^{\alpha_1} \ldots \partial x_d^{\alpha_d}}.$$

In the special case when $p = 2$, the Sobolev space $W^{k,2}(\Omega)$ is denoted by $H^k(\Omega)$ and stands for the space of functions v that belong to $L^2(\Omega)$ and whose distributional derivatives up to and including order k also belong to $L^2(\Omega)$:

$$H^k(\Omega) := \left\{ v \in L^2(\Omega) \ : \ D^{\boldsymbol{\alpha}} v \in L^2(\Omega), \forall \text{ multi-indeces } \boldsymbol{\alpha} \text{ with } |\boldsymbol{\alpha}| \leq k \right\}.$$

$H^k(\Omega)$ is a Hilbert space equipped with the norm

$$\|v\|_{H^k(\Omega)} := \left(\sum_{|\boldsymbol{\alpha}| \le k} \|D^{\boldsymbol{\alpha}} v\|_{L^2(\Omega)}^2 \right)^{\frac{1}{2}}$$

and the inner product defined through the L^2 inner product as

$$(u, v)_{H^k(\Omega)} := \sum_{|\boldsymbol{\alpha}| \le k} (D^{\boldsymbol{\alpha}} u, D^{\boldsymbol{\alpha}} v)_{L^2(\Omega)}.$$

Finally, we define the space $H_0^1(\Omega)$ to be the closure with respect to the H^1-norm of the space of smooth functions with compact support, that is,

$$H_0^1(\Omega) := \overline{C_c^\infty(\Omega)}^{\|\cdot\|_{H^1(\Omega)}}.$$

For simplicity, we will use the following short notation to distinguish between the various inner products and norms over the domains Ω_f, Ω_p, the boundaries of the domains $\partial\Omega_f$, $\partial\Omega_p$, and the interface I:

$$(u, v)_{f/p} := (u, v)_{L^2(\Omega_{f/p})} = \int_{\Omega_{f/p}} u(\mathbf{x}) \, v(\mathbf{x}) \, d\mathbf{x},$$

$$(\mathbf{u}, \mathbf{v})_{f/p} := (\mathbf{u}, \mathbf{v})_{L^2(\Omega_{f/p})} = \int_{\Omega_{f/p}} \mathbf{u}(\mathbf{x}) \cdot \mathbf{v}(\mathbf{x}) \, d\mathbf{x},$$

$$(\mathbf{M}, \mathbf{N})_{f/p} := \int_{\Omega_{f/p}} \mathbf{M}(\mathbf{x}) : \mathbf{N}(\mathbf{x}) \, d\mathbf{x},$$

$$\langle u, v \rangle_{f/p/I} := \int_{\partial\Omega_f/\partial\Omega_p/I} u \, v \, d\boldsymbol{\sigma},$$

$$\langle \mathbf{u}, \mathbf{v} \rangle_{f/p/I} := \int_{\partial\Omega_f/\partial\Omega_p/I} \mathbf{u} \cdot \mathbf{v} \, d\boldsymbol{\sigma},$$

$$\|v\|_{f/p} := \|v\|_{L^2(\Omega_{f/p})} = \left(\int_{\Omega_{f/p}} |v(\mathbf{x})|^2 \, d\mathbf{x} \right)^{\frac{1}{2}},$$

$$\|\mathbf{v}\|_{f/p} := \|\mathbf{v}\|_{L^2(\Omega_{f/p})} = \left(\int_{\Omega_{f/p}} \sum_{i=1}^d |v_i(\mathbf{x})|^2 \, d\mathbf{x} \right)^{\frac{1}{2}},$$

$$\|\mathbf{M}\|_{f/p} := \left(\int_{\Omega_{f/p}} \sum_{i,j=1}^d |M_{ij}(\mathbf{x})|^2 \, d\mathbf{x} \right)^{\frac{1}{2}},$$

$$\|v\|_{1,f/p} := \|v\|_{H^1(\Omega_{f/p})} = \left(\|v\|_{f/p}^2 + \|\nabla v\|_{f/p}^2 \right)^{\frac{1}{2}},$$

$$\|\mathbf{v}\|_{1,f/p} := \|\mathbf{v}\|_{H^1(\Omega_{f/p})} = \left(\|\mathbf{v}\|_{f/p}^2 + \|\nabla \mathbf{v}\|_{f/p}^2 \right)^{\frac{1}{2}}.$$

Further, we denote by

$$H^1_{\mathrm{div}}(\Omega) := \{\mathbf{v} \in (L^2(\Omega))^d : \ \nabla \cdot \mathbf{v} \in L^2(\Omega)\}$$

the Hilbert space H^1-div, which is endowed with the norm

$$\|\mathbf{v}\|_{\mathrm{div},f} := \left(\|\mathbf{v}\|_f^2 + \|\nabla \cdot \mathbf{v}\|_f^2\right)^{\frac{1}{2}}.$$

Last, we let

$$L^2(0,T;X) = \{\mathbf{v} : [0,T] \to X : \int_0^T \|\mathbf{v}(t)\|_X^2 \ dt < \infty\},$$

$$L^\infty(0,T;X) = \{\mathbf{v} : [0,T] \to X : \sup_{t\in[0,T]} \{\|\mathbf{v}(t)\|_X\} < \infty\},$$

for any Hilbert space X, where $T > 0$, with the corresponding norms respectively

$$\|\mathbf{v}\|_{L^2(0,T;X)} := \left(\int_0^T \|\mathbf{v}(t)\|_X^2 \ dt\right)^{1/2},$$

$$\|\mathbf{v}\|_{L^\infty(0,T;X)} := \sup_{t\in[0,T]} \|\mathbf{v}(t)\|_X.$$

2.2   USEFUL INEQUALITIES

Throughout this thesis we will use the results listed below.

1. Hölder's inequality, which states that for all p, q with $1 \leq p, q \leq \infty$ such that $\frac{1}{p} + \frac{1}{q} = 1$, there holds

$$| (u, v)_{L^2(\Omega)} | \leq \|u\|_{L^p(\Omega)} \|v\|_{L^q(\Omega)}. \tag{2.1}$$

In the special case when $p = 2$ we have the Cauchy-Schwarz inequality:

$$| (u, v)_{L^2(\Omega)} | \leq \|u\|_{L^2(\Omega)} \|v\|_{L^2(\Omega)}. \tag{2.2}$$

Furthermore, by applying Hölder's inequality twice, we also have: for all p, q, r with $1 \leq p, q, r \leq \infty$ such that $\frac{1}{p} + \frac{1}{q} + \frac{1}{r} = 1$,

$$\int_\Omega |u||v||w| \; dx \leq \|u\|_{L^p(\Omega)} \|v\|_{L^q(\Omega)} \|w\|_{L^r(\Omega)}. \tag{2.3}$$

2. Young's inequality, which states that for any two non-negative numbers a, b, any $\epsilon > 0$, and any p, q with $1 \leq p, q \leq \infty$ such that $\frac{1}{p} + \frac{1}{q} = 1$, there holds

$$ab \leq \frac{\epsilon}{p} a^p + \frac{1}{q \epsilon^{q/p}} b^q. \tag{2.4}$$

For $p = 2$ we have the elementary case of Young's inequality:

$$ab \leq \frac{\epsilon}{2} a^2 + \frac{1}{2\epsilon} b^2. \tag{2.5}$$

3. The Poincaré-Friedrichs inequality [46], which holds for all $\mathbf{v} \in \left(H_0^1(\Omega_{f/p}) \right)^d$, given by

$$\|\mathbf{v}\|_{f/p} \leq C_{PF,f/p} \|\nabla \mathbf{v}\|_{f/p}, \tag{2.6}$$

where $C_{PF,f/p}$ is a positive constant that depends on the domain $\Omega_{f/p}$.

4. One form of Korn's inequality [48, 53], which states that the H^1 semi-norm of $\mathbf{v} \in (H^1(\Omega))^d$ is bounded by the L^2-norm of the deformation tensor of $\mathbf{v}$:

$$\|\nabla \mathbf{v}\|_{L^2(\Omega)}^2 \leq C_K \|\mathbf{D}(\mathbf{v})\|_{L^2(\Omega)}^2, \tag{2.7}$$

where C_K is a positive constant.

5. The standard inequality

$$\|\nabla \cdot \mathbf{v}\|_{L^2(\Omega)} \leq \sqrt{d}\|\nabla \mathbf{v}\|_{L^2(\Omega)}. \tag{2.8}$$

6. The standard trace estimate

$$\|\mathbf{v}\|_{L^2(\partial\Omega_{f/p})} \leq C_{T,f/p}\|\mathbf{v}\|_{f/p}^{1/2}\|\nabla\mathbf{v}\|_{f/p}^{1/2}, \tag{2.9}$$

where $C_{T,f/p}$ is a positive constant that depends on the domain $\Omega_{f/p}$, see, for example, [14, Chapter 1.6, p. 36-38].

7. The integral form of Grönwall's lemma: assume that $t \in \mathcal{I} = [a, b], [a, b), or [a, \infty), a < b$, β is a non-negative, continuous function, α is a non-negative, non-decreasing function, and u is continuous and satisfies the integral inequality

$$u(t) \leq \alpha(t) + \int_a^t \beta(s)u(s)ds, \quad \forall t \in \mathcal{I}.$$

Then

$$u(t) \leq \alpha(t) \exp\left(\int_a^t \beta(s)ds\right), \quad \forall t \in \mathcal{I}. \tag{2.10}$$

13

3.0 THE STOKES-DARCY MODEL

In this chapter we present the fully evolutionary Stokes-Darcy problem and derive its equivalent weak formulation. The Stokes and the groundwater flow equations are introduced along with appropriate coupling conditions across the interface between the two domains.

3.1 THE EVOLUTIONARY STOKES-DARCY PROBLEM
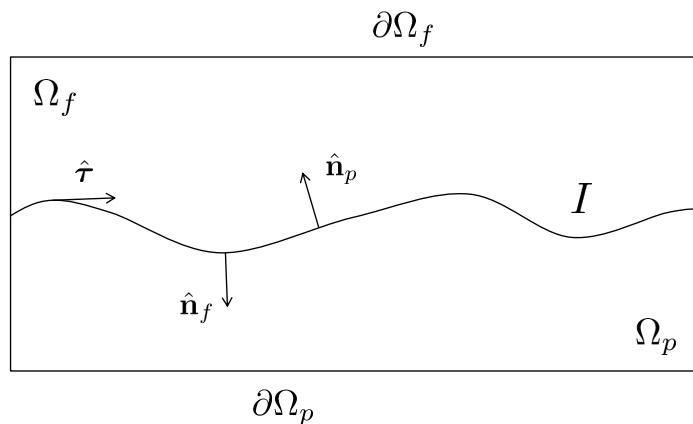
Figure 2: Fluid and porous media domains (example of a 2d cross-section).

To model the interaction between surface and groundwater flows we assume Stokes flow in the fluid domain, Ω_f, and the groundwater flow equation in the porous media domain, Ω_p (Figure 2). The system of equations along with the boundary conditions and the appropriate coupling conditions at the interface I are presented next. We denote by $\hat{\mathbf{n}}_{f/p}$ the outward pointing unit normal vector on $\Omega_{f/p}$ respectively, where $\hat{\mathbf{n}}_p = -\hat{\mathbf{n}}_f$. The velocity, $\mathbf{u} = \mathbf{u}(\mathbf{x}, t)$,

and the pressure, $p = p(\mathbf{x}, t)$, defined in $\Omega_f \times [0, T]$, $T > 0$, satisfy

$$\rho \mathbf{u}_t - \nabla \cdot \mathbf{\Pi}(\mathbf{u}, p) = \mathbf{f}_f \qquad \text{in } \Omega_f \times (0, T], \tag{3.1}$$

$$\nabla \cdot \mathbf{u} = 0 \qquad \text{in } \Omega_f \times (0, T], \tag{3.2}$$

$$\mathbf{u} = \mathbf{0} \qquad \text{in } (\partial \Omega_f \backslash I) \times (0, T], \tag{3.3}$$

$$\mathbf{u}(\mathbf{x}, 0) = \mathbf{u}_0(\mathbf{x}) \qquad \text{in } \Omega_f, \tag{3.4}$$

and the velocity, $\mathbf{u}_p = \mathbf{u}(\mathbf{x}, t)$, and the hydraulic head, $\phi = \phi(\mathbf{x}, t)$, defined in $\Omega_p \times [0, T]$, satisfy

$$S_0 \phi_t + \nabla \cdot \mathbf{q} = f_p \qquad \text{in } \Omega_p \times (0, T], \tag{3.5}$$

$$\mathbf{q} = -\mathbf{K} \nabla \phi \qquad \text{in } \Omega_p \times (0, T], \tag{3.6}$$

$$\mathbf{u}_p = \frac{\mathbf{q}}{n} \qquad \text{in } \Omega_p \times (0, T], \tag{3.7}$$

$$\phi = 0 \qquad \text{in } (\partial \Omega_p \backslash I) \times (0, T], \tag{3.8}$$

$$\phi(\mathbf{x}, 0) = \phi_0(\mathbf{x}) \qquad \text{in } \Omega_p, \tag{3.9}$$

where

$\mathbf{\Pi}(\mathbf{u}, p) = -p\mathbf{I} + 2\mu \mathbf{D}(\mathbf{u})$ is the stress tensor,

$\mathbf{q}$ is the specific discharge, defined as the volume of the fluid flowing per unit time through

a unit cross-sectional area normal to the direction of the flow,

$S_0 > 0$ is the specific storage,

$\mathbf{K} = \mathbf{K}(\mathbf{x})$ is the hydraulic conductivity tensor,

$\mathbf{f}_f$ & f_p are the body forces in Ω_f and the sources or sinks in Ω_p,

$\mu > 0$ & $\rho > 0$ are the dynamic viscosity and density of the fluid respectively, and

$n \in (0, 1]$ is the volumetric porosity.

The hydraulic (or piezometric) head ϕ can be expressed as

$$\phi = \frac{p_p}{\rho g} + z,$$

where

p_p is the pressure in Ω_p,

$g > 0$ is the gravitational acceleration constant, and

z is the elevation head (the elevation at the bottom of a piezometer).

For simplicity, we will assume that $z = 0$, so that $p_p = \rho g \phi$. The equations describing the incompressible Stokes flow in the fluid region are conservation of momentum (3.1) and conservation of mass or the incompressibility condition (3.2). For a rigorous derivation of the equations describing the surface flow (3.1)-(3.2) see, e.g., [46]. We further assume no slip (condition (3.3)) at the exterior boundary of Ω_f (not including the interface I). The equations representing the groundwater flow in the porous media region are conservation of mass (3.5) and Darcy's law (3.6). See [11] for a derivation of (3.5) from conservation laws and also Remark 2 below. We assume homogeneous Dirichlet boundary conditions at the exterior boundary of Ω_p. The analysis in the upcoming chapters extends to other exterior boundary conditions as well. In the next section, we present the coupling conditions assumed at the interface I.

3.2 COUPLING CONDITIONS

The two systems of equations, (3.1)-(3.3) and (3.5)-(3.8), describing the flow in each subdomain, are coupled by the following conditions across the interface I:

1. *Conservation of mass*:

$$\mathbf{u} \cdot \hat{\mathbf{n}}_f + \mathbf{u}_p \cdot \hat{\mathbf{n}}_p = 0, \quad \text{on } I. \tag{3.10}$$

2. *Balance of normal forces*:
   Let $\overrightarrow{t} = \overrightarrow{t}(\mathbf{u}, p)$ denote the Cauchy stress vector, $\overrightarrow{t} = \hat{\mathbf{n}}_f \cdot \mathbf{\Pi}$. Then, continuity of

forces gives

$$p_p = -\overrightarrow{t}(\mathbf{u}, p) \cdot \hat{\mathbf{n}}_f$$
$$\Rightarrow \rho g \phi = -\hat{\mathbf{n}}_f \cdot \mathbf{\Pi}(\mathbf{u}, p) \cdot \hat{\mathbf{n}}_f$$
$$= p - 2\mu \; \hat{\mathbf{n}}_f \cdot \mathbf{D}(\mathbf{u}) \cdot \hat{\mathbf{n}}_f, \quad \text{on } I. \tag{3.11}$$

3. *The Beavers-Joseph-Saffman (BJS) slip condition:*

Let $\{\hat{\boldsymbol{\tau}}_i\}_{i=1}^{d-1}$ denote an orthonormal basis of tangent vectors on I. The Beavers-Joseph-Saffman condition on the tangential velocity is

$$-2 \; \hat{\boldsymbol{n}}_f \cdot \mathbf{D}(\mathbf{u}) \cdot \hat{\boldsymbol{\tau}}_i = \frac{\alpha}{\sqrt{\hat{\boldsymbol{\tau}}_i \cdot \mathbf{K} \cdot \hat{\boldsymbol{\tau}}_i}} \; \mathbf{u} \cdot \hat{\boldsymbol{\tau}}_i, \quad \text{for } i = 1, \ldots, d-1, \quad \text{on } I, \tag{3.12}$$

which is a simplification of the original and more physically realistic Beavers-Joseph condition, see [12]:

$$\frac{1}{\mu} \left(-\overrightarrow{t}(\mathbf{u}, p) \right) \cdot \hat{\boldsymbol{\tau}}_i = \frac{\alpha}{\sqrt{\hat{\boldsymbol{\tau}}_i \cdot \mathbf{K} \cdot \hat{\boldsymbol{\tau}}_i}} \; (\mathbf{u} - \mathbf{u}_p) \cdot \hat{\boldsymbol{\tau}}_i, \quad \text{for } i = 1, \ldots, d-1, \quad \text{on } I. \tag{3.13}$$

The latter states that the tangential component of the normal stress of the flow in the conduit at the interface is proportional to the tangential velocity in the conduit at the interface. In (3.12) and (3.13), $\alpha > 0$ is a dimensionless, experimentally determined constant. The former condition is due to Saffman who further studied condition (3.13) and found that the term "$\mathbf{u}_p$" was much smaller than the rest of the terms in the condition, and proposed that the term be dropped [101]. For more information about the Beavers-Joseph-Saffman condition see also [72, 95, 67]. In light of the simplified condition (3.12), it is clear that the coupling between the two flows happens through the first two interface conditions, (3.10) and (3.11).

17

3.3 IMPORTANT PHYSICAL PARAMETERS

Before we present the variational formulation of the Stokes-Darcy problem we take a closer look at two physical parameters of the problem that are of particular importance in this thesis: the specific storage and the hydraulic conductivity.

The hydraulic conductivity tensor, $\mathbf{K}$, appearing in Darcy's law, (3.6), is symmetric, uniformly positive definite, satisfying

$$k_{\min}|\boldsymbol{\xi}|^2 \leq \boldsymbol{\xi} \cdot \mathbf{K}(\mathbf{x}) \cdot \boldsymbol{\xi} \leq k_{\max}|\boldsymbol{\xi}|^2, \tag{3.14}$$

for some $0 < k_{\min} \leq k_{\max}$ and for all $\boldsymbol{\xi} \in \mathbb{R}^d$. The hydraulic conductivity is a property of porous materials such as rocks and soils that measures the ease with which a fluid (usually water) moves through the pore spaces or fractures of the porous medium. It depends on the intrinsic permeability of the material, the degree of saturation, as well as the density and viscosity of the fluid. In particular, its components take the form

$$\mathbf{K}_{ij} = \frac{nl^2 \rho g}{\mu},$$

where l is the characteristic length of the pores. The hydraulic conductivity has units of length/time. Its values are either determined experimentally through Darcy's law (3.6) or empirically from soil properties, like pore or particle size. Table 1, taken from [10], presents typical values of the hydraulic conductivity for different materials.

The specific storage, S_0, represents the volume of water that a portion of a fully saturated porous medium will release (or absorb) from storage per unit volume, per unit change in hydraulic head, see [58, 45]. It can be defined as $S_0 = S/b$, where S is the storativity coefficient (dimensionless) and b is the height (or thickness) of the aquifer [113]. Therefore, it has units 1/length. In confined aquifers[1], the values of S_0 range from 10^{-6} or smaller for rock to 10^{-2} for plastic clay, see [39], while in unconfined aquifers S_0 is larger. In Table 2 we give a few representative values of S_0 in confined aquifers, see [38, 71, 2, 9].

---

[1]A confined aquifer is one bounded above and below by impervious formations. In a well penetrating such an aquifer, the water level will rise above the base of the confining formation. An unconfined aquifer is one with a water table serving as its upper boundary, see [11].

Table 1: Hydraulic conductivity values for different materials

Material	Hydraulic conductivity (m/s)
Well sorted gravel	$10^{-1} - 10^{0}$
Highly fractured rocks	$10^{-3} - 10^{0}$
Well sorted sand or sand & gravel	$10^{-4} - 10^{-2}$
Oil reservoir rocks	$10^{-6} - 10^{-4}$
Very fine sand, silt, loess, loam	$10^{-8} - 10^{-5}$
Layered clay	$10^{-8} - 10^{-6}$
Fresh sandstone, limestone, dolomite, granite	$10^{-12} - 10^{-7}$
Fat/unweathered clay	$10^{-12} - 10^{-9}$

Remark 2 (Poroelasticity and the origin of the critical term $S_0\phi_t$.). *The term "$S_0\phi_t$" in (3.5) arises because aquifers consist of elastic media and the porous matrix responds slowly, but not instantaneously, to changes in the pressure of the fluid, [13, 111]. Moreover, soil particles consolidate as pressure drops, and liquids are slightly compressible, [96]. Thus, $n = n(p_p)$, and $\rho = \rho(p_p)$, where n is the volumetric porosity, ρ the density of the fluid, and p_p the pressure in the porous region. Conservation of mass in the pores gives:*

$$\frac{\partial}{\partial t}(n\rho) + \nabla \cdot (\rho \mathbf{q}) = 0. \tag{3.15}$$

We have

$$
\begin{aligned}
\frac{\partial}{\partial t}(n\rho) &= n_t \rho + n\rho_t \\
&= \left(\frac{\partial n}{\partial p_p} \frac{\partial p_p}{\partial t} \right) \rho + n \left(\frac{\partial \rho}{\partial p_p} \frac{\partial p_p}{\partial t} \right) \\
&= \rho(n\beta_c + c_v) \frac{\partial p_p}{\partial t},
\end{aligned}
$$

Table 2: Specific storage values for different materials

Material	Specific Storage S_0 (m^{-1})
Plastic clay	$2.0 \times 10^{-2} - 2.6 \times 10^{-3}$
Stiff clay	$2.6 \times 10^{-3} - 1.3 \times 10^{-3}$
Medium hard clay	$1.3 \times 10^{-3} - 9.2 \times 10^{-4}$
Loose sand	$1.0 \times 10^{-3} - 4.9 \times 10^{-4}$
Dense sand	$2.0 \times 10^{-4} - 1.3 \times 10^{-4}$
Dense sandy gravel	$1.0 \times 10^{-4} - 4.9 \times 10^{-5}$
Rock, fissured jointed	$6.9 \times 10^{-5} - 3.3 \times 10^{-6}$
Rock, sound	less than 3.3×10^{-6}

where

$$\beta_c := \frac{1}{\rho}\frac{d\rho}{dp_p} \quad \textit{is the compressibility of the fluid, and}$$

$$c_v := \frac{dn}{dp_p} \quad \textit{is the coefficient of consolidation in soil mechanics.}$$

The hydraulic head ϕ and pressure p_p satisfy

$$\frac{\partial \phi}{\partial t} = \frac{1}{g\rho(p_p)}\frac{\partial p_p}{\partial t}.$$

Consequently, (3.15) *becomes*

$$g\rho^2(n\beta_c + c_v)\frac{\partial \phi}{\partial t} - \nabla \cdot (\rho \mathbf{q}) = 0.$$

It is common to assume, based on experimental data, that $|\partial \rho/\partial x_i| \ll \mathcal{O}(1)$ and thus one factor of ρ can be canceled. Hence, defining the specific storage to be

$$S_0 := g\rho(n\beta_c + c_v),$$

we obtain the conservation law of flow through porous media, (3.5).

3.4 VARIATIONAL FORMULATION OF THE STOKES-DARCY PROBLEM

In this section we derive the variational formulation of the evolutionary Stokes-Darcy problem described by the system of equations (3.1)-(3.12). Let

$$\mathbf{X}_f = \{\mathbf{v} \in (H^1(\Omega_f))^d \; : \; \mathbf{v} = \mathbf{0} \text{ on } \partial\Omega_f \backslash I\}, \quad Q_f = L_0^2(\Omega_f)$$

denote the velocity and pressure spaces in Ω_f respectively, and let

$$X_p = \{\psi \in H^1(\Omega_p) \; : \; \psi = 0 \text{ on } \Omega_p \backslash I\}$$

denote the hydraulic head space in Ω_p. To arrive at the equivalent variational formulation we first multiply the groundwater flow equation (3.5) by $\psi \in X_p$ and integrate over Ω_p. Using integration by parts, Darcy's law (3.6), equation (3.7), the fact that $\psi \in X_p$, and the coupling condition (3.10), we obtain

$$
\begin{aligned}
(f_p, \psi)_p &= (S_0\phi_t, \psi)_p + (\nabla \cdot \mathbf{q}, \psi)_p \\
&= (S_0\phi_t, \psi)_p - (\mathbf{q}, \nabla\psi)_p + \langle \mathbf{q} \cdot \hat{\mathbf{n}}_p, \psi \rangle_p \\
&= (S_0\phi_t, \psi)_p + (\mathbf{K}\nabla\phi, \nabla\psi)_p + \langle n\mathbf{u}_p \cdot \hat{\mathbf{n}}_p, \psi \rangle_I \\
&= (S_0\phi_t, \psi)_p + (\mathbf{K}\nabla\phi, \nabla\psi)_p - n\langle \mathbf{u} \cdot \hat{\mathbf{n}}_f, \psi \rangle_I.
\end{aligned}
\tag{3.16}
$$

Next, we multiply the Stokes equation (3.1) by $\mathbf{v} \in \mathbf{X}_f$ and equation (3.2) by $q \in Q_f$, and integrate over Ω_f:

$$
\begin{aligned}
(\mathbf{f}_f, \mathbf{v})_f &= \rho(\mathbf{u}_t, \mathbf{v})_f - (\nabla \cdot \mathbf{\Pi}, \mathbf{v})_f \\
&= \rho(\mathbf{u}_t, \mathbf{v})_f + (\nabla p, \mathbf{v})_f - 2\mu(\nabla \cdot \mathbf{D}(\mathbf{u}), \mathbf{v})_f,
\end{aligned}
\tag{3.17}
$$

$$(\nabla \cdot \mathbf{u}, q)_f = 0. \tag{3.18}$$

Using integration by parts and the fact that $(\mathbf{D}(\mathbf{u}), \nabla\mathbf{v}) = (\mathbf{D}(\mathbf{u}), \mathbf{D}(\mathbf{v}))$ for $\mathbf{v} \in \mathbf{X}_f$, (3.17) becomes

$$
\begin{aligned}
(\mathbf{f}_f, \mathbf{v})_f &= \rho(\mathbf{u}_t, \mathbf{v})_f - (p, \nabla \cdot \mathbf{v})_f + \langle p, \mathbf{v} \cdot \hat{\mathbf{n}}_f \rangle_f + 2\mu(\mathbf{D}(\mathbf{u}), \nabla\mathbf{v})_f - 2\mu\langle \mathbf{D}(\mathbf{u}) \cdot \hat{\mathbf{n}}_f, \mathbf{v} \rangle_f \\
&= \rho(\mathbf{u}_t, \mathbf{v})_f - (p, \nabla \cdot \mathbf{v})_f + \langle p, \mathbf{v} \cdot \hat{\mathbf{n}}_f \rangle_I + 2\mu(\mathbf{D}(\mathbf{u}), \mathbf{D}(\mathbf{v}))_f - 2\mu\langle \mathbf{D}(\mathbf{u}) \cdot \hat{\mathbf{n}}_f, \mathbf{v} \rangle_I.
\end{aligned}
\tag{3.19}
$$

We express the test function $\mathbf{v}$ in terms of the orthonormal basis of $\mathbb{R}^d$ consisting of the normal vector $\hat{\mathbf{n}}_f$ and the tangent vectors $\hat{\boldsymbol{\tau}}_i, i = 1, \ldots, d-1$:

$$
\mathbf{v} = \sum_{i=1}^{d-1} (\mathbf{v} \cdot \hat{\boldsymbol{\tau}}_i)\hat{\boldsymbol{\tau}}_i + (\mathbf{v} \cdot \hat{\mathbf{n}}_f)\hat{\mathbf{n}}_f.
$$

Then,

$$
\begin{aligned}
\langle \mathbf{D}(\mathbf{u}) \cdot \hat{\mathbf{n}}_f, \mathbf{v} \rangle_I &= \left\langle \mathbf{D}(\mathbf{u}) \cdot \hat{\mathbf{n}}_f, \sum_{i=1}^{d-1} (\mathbf{v} \cdot \hat{\boldsymbol{\tau}}_i)\hat{\boldsymbol{\tau}}_i \right\rangle_I + \langle \mathbf{D}(\mathbf{u}) \cdot \hat{\mathbf{n}}_f, (\mathbf{v} \cdot \hat{\mathbf{n}}_f)\hat{\mathbf{n}}_f \rangle_I \\
&= \sum_{i=1}^{d-1} \langle \hat{\boldsymbol{\tau}}_i \cdot \mathbf{D}(\mathbf{u}) \cdot \hat{\mathbf{n}}_f, \mathbf{v} \cdot \hat{\boldsymbol{\tau}}_i \rangle_I + \langle \hat{\mathbf{n}}_f \cdot \mathbf{D}(\mathbf{u}) \cdot \hat{\mathbf{n}}_f, \mathbf{v} \cdot \hat{\mathbf{n}}_f \rangle_I.
\end{aligned}
$$

By substituting this last term into (3.19) we have

$$
\begin{aligned}
(\mathbf{f}_f, \mathbf{v})_f &= \rho(\mathbf{u}_t, \mathbf{v})_f - (p, \nabla \cdot \mathbf{v})_f + 2\mu(\mathbf{D}(\mathbf{u}), \mathbf{D}(\mathbf{v}))_f + \langle p - 2\mu \, \hat{\mathbf{n}}_f \cdot \mathbf{D}(\mathbf{u}) \cdot \hat{\mathbf{n}}_f, \mathbf{v} \cdot \hat{\mathbf{n}}_f \rangle_I \\
&\quad - 2\mu \sum_{i=1}^{d-1} \langle \hat{\boldsymbol{\tau}}_i \cdot \mathbf{D}(\mathbf{u}) \cdot \hat{\mathbf{n}}_f, \mathbf{v} \cdot \hat{\boldsymbol{\tau}}_i \rangle_I.
\end{aligned}
$$

Applying the interface conditions (3.11) and (3.12) we obtain

$$
\begin{aligned}
(\mathbf{f}_f, \mathbf{v})_f &= \rho(\mathbf{u}_t, \mathbf{v})_f - (p, \nabla \cdot \mathbf{v})_f + 2\mu(\mathbf{D}(\mathbf{u}), \mathbf{D}(\mathbf{v}))_f + \rho g\langle \phi, \mathbf{v} \cdot \hat{\mathbf{n}}_f \rangle_I \\
&\quad + \mu\alpha \sum_{i=1}^{d-1} \left\langle \frac{\mathbf{u} \cdot \hat{\boldsymbol{\tau}}_i}{\sqrt{\hat{\boldsymbol{\tau}}_i \cdot \mathbf{K} \cdot \hat{\boldsymbol{\tau}}_i}}, \mathbf{v} \cdot \hat{\boldsymbol{\tau}}_i \right\rangle_I.
\end{aligned}
$$

Dividing both sides by ρ, and letting $\nu = \mu/\rho$ denote the kinematic viscosity, we finally have

$$
\begin{aligned}
(\tilde{\mathbf{f}}_f, \mathbf{v})_f &= (\mathbf{u}_t, \mathbf{v})_f - (\tilde{p}, \nabla \cdot \mathbf{v})_f + 2\nu(\mathbf{D}(\mathbf{u}), \mathbf{D}(\mathbf{v}))_f + g\langle \phi, \mathbf{v} \cdot \hat{\mathbf{n}}_f \rangle_I \\
&\quad + \nu\alpha \sum_{i=1}^{d-1} \left\langle \frac{\mathbf{u} \cdot \hat{\boldsymbol{\tau}}_i}{\sqrt{\hat{\boldsymbol{\tau}}_i \cdot \mathbf{K} \cdot \hat{\boldsymbol{\tau}}_i}}, \mathbf{v} \cdot \hat{\boldsymbol{\tau}}_i \right\rangle_I,
\end{aligned}
\tag{3.20}
$$

where $\tilde{\mathbf{f}}_f = \mathbf{f}_f/\rho$ and $\tilde{p} = p/\rho$. We now multiply (3.20) by n and (3.16) by g to obtain

$$n(\tilde{\mathbf{f}}_f, \mathbf{v})_f = n(\mathbf{u}_t, \mathbf{v})_f - n(\tilde{p}, \nabla \cdot \mathbf{v})_f + 2n\nu(\mathbf{D}(\mathbf{u}), \mathbf{D}(\mathbf{v}))_f + ng\langle \phi, \mathbf{v} \cdot \hat{\mathbf{n}}_f \rangle_I$$

$$+ n\nu\alpha \sum_{i=1}^{d-1} \left\langle \frac{\mathbf{u} \cdot \hat{\boldsymbol{\tau}}_i}{\sqrt{\hat{\boldsymbol{\tau}}_i \cdot \mathbf{K} \cdot \hat{\boldsymbol{\tau}}_i}}, \mathbf{v} \cdot \hat{\boldsymbol{\tau}}_i \right\rangle_I, \tag{3.21}$$

$$g(f_p, \psi)_p = g(S_0\phi_t, \psi)_p + g(\mathbf{K}\nabla\phi, \nabla\psi)_p - ng\langle \mathbf{u} \cdot \hat{\mathbf{n}}_f, \psi \rangle_I. \tag{3.22}$$

Finally, letting $a_f : \mathbf{X}_f \times \mathbf{X}_f \to \mathbb{R}$, $a_p : X_p \times X_p \to \mathbb{R}$, $b : \mathbf{X}_f \times Q_f \to \mathbb{R}$, and $c_I : \mathbf{X}_f \times X_p \to \mathbb{R}$ denote the bilinear forms defined respectively by

$$a_f(\mathbf{v}, \mathbf{w}) := 2n\nu(\mathbf{D}(\mathbf{v}), \mathbf{D}(\mathbf{w}))_f + n\nu\alpha \sum_{i=1}^{d-1} \left\langle \frac{\mathbf{v} \cdot \hat{\boldsymbol{\tau}}_i}{\sqrt{\hat{\boldsymbol{\tau}}_i \cdot \mathbf{K} \cdot \hat{\boldsymbol{\tau}}_i}}, \mathbf{w} \cdot \hat{\boldsymbol{\tau}}_i \right\rangle_I, \tag{3.23}$$

$$a_p(\psi, \xi) := g(\mathbf{K}\nabla\psi, \nabla\xi)_p, \tag{3.24}$$

$$b_f(\mathbf{v}, q) := -(q, \nabla \cdot \mathbf{v})_f, \tag{3.25}$$

$$c_I(\mathbf{v}, \psi) := ng\langle \psi, \mathbf{v} \cdot \hat{\mathbf{n}}_f \rangle_I, \tag{3.26}$$

the variational formulation of the evolutionary Stokes-Darcy problem is:

Find $(\mathbf{u}, \tilde{p}, \phi) : (0, T] \to \mathbf{X}_f \times Q_f \times X_p$ *such that for all* $(\mathbf{v}, q, \psi) \in \mathbf{X}_f \times Q_f \times X_p,$

$$n(\mathbf{u}_t, \mathbf{v})_f + nb_f(\mathbf{v}, \tilde{p}) + a_f(\mathbf{u}, \mathbf{v}) + c_I(\mathbf{v}, \phi) = n(\tilde{\mathbf{f}}_f, \mathbf{v})_f, \tag{3.27}$$

$$b_f(\mathbf{u}, q) = 0, \tag{3.28}$$

$$g(S_0\phi_t, \psi)_p + a_p(\phi, \psi) - c_I(\mathbf{u}, \psi) = g(f_p, \psi)_p, \tag{3.29}$$

given the initial data $\mathbf{u}(\mathbf{x}, 0) = \mathbf{u}_0(\mathbf{x})$ *and* $\phi(\mathbf{x}, 0) = \phi_0(\mathbf{x})$.

It is important to notice the exactly skew-symmetric (conservative) coupling between (3.27) and (3.29) through the interface term $c_I(\cdot, \cdot)$.

3.5 ANALYSIS OF THE VARIATIONAL FORMULATION

We now analyze the variational formulation of the Stokes-Darcy problem, (3.27)-(3.29), and briefly discuss its well-posedness.

Lemma 1. *The bilinear form $b_f(\cdot, \cdot)$ defined in (3.25) is continuous and satisfies*

$$|b_f(\mathbf{v}, q)| \leq \sqrt{d}\|q\|_f\|\nabla\mathbf{v}\|_f, \tag{3.30}$$

for all $q \in Q_f$ and $\mathbf{v} \in \mathbf{X}_f$. It follows that the divergence-free subspace $\mathbf{V}_f$ of $\mathbf{X}_f$,

$$\mathbf{V}_f := \{\mathbf{v} \in \mathbf{X}_f : (q, \nabla \cdot \mathbf{v})_f = 0, \ \forall q \in Q_f\}, \tag{3.31}$$

is a closed subspace of $\mathbf{X}_f$.

Proof. The continuity bound follows by applying the Cauchy-Schwarz inequality and inequality (2.8). □

Proposition 1 (The continuous inf-sup condition)**.** *There exists a constant $\beta^* > 0$ such that*

$$\inf_{\substack{q \in Q_f \\ q \neq 0}} \sup_{\substack{\mathbf{v} \in \mathbf{X}_f \\ \mathbf{v} \neq \mathbf{0}}} \frac{b_f(\mathbf{v}, q)}{\|\nabla\mathbf{v}\|_f\|q\|_f} \geq \beta^* > 0. \tag{3.32}$$

The continuous inf-sup condition (3.32), also known as the Ladyzhenskaya-Babúska-Brezzi (LBB) condition [78], is a compatibility condition that guarantees the existence and uniqueness of p in the Stokes problem, given the velocity $\mathbf{u}$, and further, it guarantees that p is stable.

Lemma 2. *The bilinear forms $a_f(\cdot, \cdot)$ and $a_p(\cdot, \cdot)$ given in (3.23) and (3.24) respectively are symmetric, continuous and coercive, and satisfy*

$$|a_f(\mathbf{v}, \mathbf{w})| \leq n\nu \left(2 + \frac{\alpha C_{T,f}^2 C_{PF,f}}{2\sqrt{k_{min}}}\right) \|\nabla\mathbf{v}\|_f\|\nabla\mathbf{w}\|_f, \tag{3.33}$$

$$a_f(\mathbf{v}, \mathbf{v}) \geq \frac{2n\nu}{C_K}\|\nabla\mathbf{v}\|_f^2 + \frac{n\nu\alpha}{\sqrt{k_{max}}} \sum_{i=1}^{d-1} \int_I (\mathbf{v} \cdot \hat{\boldsymbol{\tau}}_i)^2 \, d\boldsymbol{\sigma} =: \frac{2n\nu}{C_K}\|\nabla\mathbf{v}\|_f^2 + \frac{n\nu\alpha}{\sqrt{k_{max}}}\|\mathbf{v} \cdot \hat{\boldsymbol{\tau}}\|_I^2, \tag{3.34}$$

$$|a_p(\psi, \xi)| \leq gk_{max}\|\nabla\psi\|_p\|\nabla\xi\|_p, \tag{3.35}$$

$$a_p(\psi, \psi) \geq gk_{min}\|\nabla\psi\|_p^2, \tag{3.36}$$

for all $\mathbf{v}, \mathbf{w} \in \mathbf{X}_f$ *and all* $\psi, \xi \in X_p$.

Proof. Let $\psi, \xi \in X_p$. Since $\mathbf{K}$ is positive definite, and $0 < k_{min} \leq \lambda(\mathbf{K}) \leq k_{max}$, where $\lambda(\mathbf{K})$ is the spectrum of $\mathbf{K}$, (3.35) and (3.36) are straightforward. For $\mathbf{v}, \mathbf{w} \in \mathbf{X}_f$, and using $\hat{\boldsymbol{\tau}}_i \cdot \mathbf{K} \cdot \hat{\boldsymbol{\tau}}_i \geq k_{min}$, $\forall i$, the Cauchy-Schwarz inequality, and the trace inequality (2.9), we have

$$|a_f(\mathbf{v}, \mathbf{w})| \leq 2n\nu \|\nabla \mathbf{v}\|_f \|\nabla \mathbf{w}\|_f + \frac{n\nu\alpha C_{T,f}^2}{\sqrt{k_{min}}} \sqrt{\|\mathbf{v}\|_f \|\nabla \mathbf{v}\|_f} \sqrt{\|\mathbf{w}\|_f \|\nabla \mathbf{w}\|_f}.$$

Applying the Poincaré-Friedrichs inequality (2.6) twice we obtain

$$|a_f(\mathbf{v}, \mathbf{w})| \leq 2n\nu \|\nabla \mathbf{v}\|_f \|\nabla \mathbf{w}\|_f + \frac{n\nu\alpha C_{T,f}^2 C_{PF,f}}{\sqrt{k_{min}}} \|\nabla \mathbf{v}\|_f \|\nabla \mathbf{w}\|_f.$$

Finally, using Korn's inequality, (2.7), and $\hat{\boldsymbol{\tau}}_i \cdot \mathbf{K} \cdot \hat{\boldsymbol{\tau}}_i \leq k_{max}$, $\forall i$, we get

$$a_f(\mathbf{v}, \mathbf{v}) \geq \frac{2n\nu}{C_K} \|\nabla \mathbf{v}\|_f^2 + \frac{n\nu\alpha}{\sqrt{k_{max}}} \sum_{i=1}^{d-1} \int_I (\mathbf{v} \cdot \hat{\tau}_i)^2 \, d\boldsymbol{\sigma}.$$

$\square$

We next turn our attention to the interface coupling term, $c_I(\cdot, \cdot)$, which is a key quantity in the analysis of the Stokes-Darcy problem.

Lemma 3. *The bilinear form* $c_I(\cdot, \cdot)$ *is continuous and satisfies*

$$c_I(\mathbf{v}, \psi)| \leq ng C_{T,f} C_{T,p} C_{PF,f}^{1/2} C_{PF,p}^{1/2} \|\nabla \mathbf{v}\|_f \|\nabla \psi\|_p, \tag{3.37}$$

for all $\mathbf{v} \in \mathbf{X}_f, \psi \in X_p$.

Proof. (3.37) follows by applying the Cauchy-Schwarz inequality and then the trace (2.9) and the Poincaré-Friedrichs (2.6) inequalities for $\mathbf{v}$ and ψ. $\square$

25

In view of Proposition 1 and Lemmas 1-3, existence and uniqueness of a solution $(\mathbf{u}, p, \phi)$ to the problem (3.27)-(3.29) follow by the theory of saddle point problems found in, e.g., [16, 15], see also [82].

We will often use the equivalent variational formulation of the Stokes-Darcy system over the divergence-free space $\mathbf{V}_f$:

Find $(\mathbf{u}, \phi) : (0, T] \to \mathbf{V}_f \times X_p$ such that for all $(\mathbf{v}, \psi) \in \mathbf{V}_f \times X_p$,

$$n(\mathbf{u}_t, \mathbf{v})_f + a_f(\mathbf{u}, \mathbf{v}) + c_I(\mathbf{v}, \phi) = n(\tilde{\mathbf{f}}_f, \mathbf{v})_f, \tag{3.38}$$

$$g(S_0\phi_t, \psi)_p + a_p(\phi, \psi) - c_I(\mathbf{u}, \psi) = g(f_p, \psi)_p, \tag{3.39}$$

given the initial data $\mathbf{u}(\mathbf{x}, 0) = \mathbf{u}_0(\mathbf{x})$ and $\phi(\mathbf{x}, 0) = \phi_0(\mathbf{x})$.

3.6   A TWO-DOMAIN EMBEDDING INEQUALITY

In the upcoming chapters we will use a two-domain embedding inequality, which we prove next in Theorems 1 and 2. It is a continuity bound on the coupling term $\int_I \phi \mathbf{u} \cdot \hat{\mathbf{n}}_f \, d\boldsymbol{\sigma}$. In Theorem 1 we obtain a bound for the integral under the assumption that there exists a $\mathcal{C}^1-$diffeomorphism between the domains Ω_f and Ω_p. In Theorem 2 we show that a similar inequality holds without any extra restrictions on Ω_f and Ω_p, but assuming instead that the interface I between the two domains is of the form $x_d = f(x_1, \ldots, x_{d-1})$ for some $\mathcal{C}^1-$function f (Figure 3). The resulting inequality is a standard result in the case when $\Omega_p = \Omega_f$ and $I = \partial\Omega_f$, see, e.g., [51], or in the special case when Ω_p is contained in Ω_f and $I = \partial\Omega_p$. However, it is not known what the most general domains and shared boundaries are for the inequality to hold. In Theorems 1 and 2 we show that the inequality holds for many special cases without any extra assumptions or constraints on ϕ or $\mathbf{u}$.

Theorem 1. *Assume that there exists a $\mathcal{C}^1-$diffeomorphism $\mathbf{F} : \Omega_f \to \Omega_p$, so that there exist constants $C_1, C_2 > 0$ such that*

$$\frac{1}{\sqrt{|det(\mathbf{F}')|}} \leq C_1, \ in \ \Omega_f, \tag{3.40}$$

$$|\mathbf{F}'|_{Hilb} \leq C_2, \ in \ \Omega_f, \tag{3.41}$$
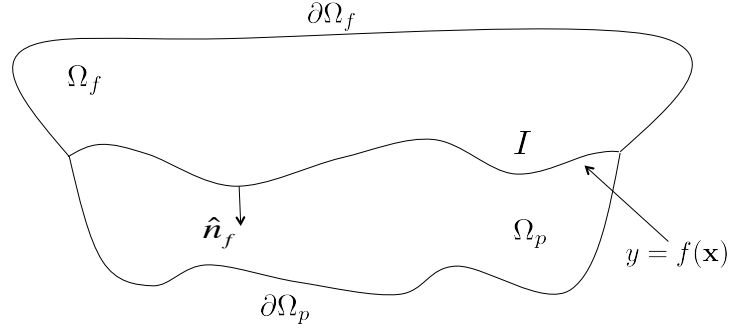
Figure 3: Domains Ω_f and Ω_p (example of a $2d$ cross-section).

where $\mathbf{F}'$ is the Jacobian matrix of $\mathbf{F}$, and $|\cdot|_{Hilb}$ denotes the Hilbert norm. Then

$$\left| \int_I \phi \mathbf{u} \cdot \hat{\mathbf{n}}_f \, d\boldsymbol{\sigma} \right| \leq C \|\mathbf{u}\|_{div,f} \|\phi\|_{1,p}, \tag{3.42}$$

where the constant C is given by $C := C_1 \max\{1, C_2\}$.

Proof. We define $\tilde{\phi} : \Omega_f \to \Omega_p$ by

$$\tilde{\phi}(\mathbf{x}) = \begin{cases} (\phi \circ \mathbf{F})(\mathbf{x}) & , \mathbf{x} \in \Omega_f \\ \phi(\mathbf{x}) & , \mathbf{x} \in I. \end{cases}$$

By the divergence theorem we have

$$\int_I \phi \mathbf{u} \cdot \hat{\mathbf{n}}_f \, d\boldsymbol{\sigma} = \int_I \tilde{\phi} \mathbf{u} \cdot \hat{\mathbf{n}}_f \, d\boldsymbol{\sigma} = \int_{\partial\Omega_f} \tilde{\phi} \mathbf{u} \cdot \hat{\mathbf{n}}_f \, d\boldsymbol{\sigma} = \int_{\Omega_f} \nabla \cdot \left(\tilde{\phi} \mathbf{u} \right) \, d\boldsymbol{\sigma}$$

$$= \int_{\Omega_f} \tilde{\phi} \nabla \cdot \mathbf{u} \, d\mathbf{x} + \int_{\Omega_f} \nabla \tilde{\phi} \cdot \mathbf{u} \, d\mathbf{x}.$$

Thus, by the Cauchy-Schwarz inequality we obtain

$$\left| \int_I \phi \mathbf{u} \cdot \hat{\mathbf{n}}_f \, d\boldsymbol{\sigma} \right| \leq \|\mathbf{u}\|_{\mathrm{div},f} \|\tilde{\phi}\|_{1,f}. \tag{3.43}$$

27

Next, the change of variables theorem yields

$$\|\tilde{\phi}\|_{1,f} = \left(\int_{\Omega_f} \left(|\phi \circ \mathbf{F}|^2 + |\nabla(\phi \circ \mathbf{F})|^2 \right) \frac{|det(\mathbf{F}')|}{|det(\mathbf{F}')|} \ d\mathbf{x} \right)^{\frac{1}{2}}$$

$$\leq \left(\int_{\Omega_f} \left(|\phi \circ \mathbf{F}|^2 + |\nabla(\phi \circ \mathbf{F})|^2 \right) |det(\mathbf{F}')| C_1^2 \ d\mathbf{x} \right)^{\frac{1}{2}}$$

$$= C_1 \left(\int_{\Omega_p} \left(|\phi|^2 + |\nabla_x \phi|^2 \right) \ d\boldsymbol{\eta} \right)^{\frac{1}{2}}$$

$$\leq C_1 \left(\int_{\Omega_p} \left(|\phi|^2 + |\mathbf{F}'|^2_{Hilb} |\nabla_{\boldsymbol{\eta}} \phi|^2 \right) \ d\boldsymbol{\eta} \right)^{\frac{1}{2}}$$

$$\leq C_1 \max\{1, C_2\} \left(\int_{\Omega_p} \left(|\phi|^2 + |\nabla_{\boldsymbol{\eta}} \phi|^2 \right) \ d\boldsymbol{\eta} \right)^{\frac{1}{2}} = C\|\phi\|_{1,p}, \qquad (3.44)$$

where $\nabla_{\mathbf{x}} = \nabla_{(x_1,\ldots,x_d)}, \mathbf{x} \in \Omega_f$, denotes the gradient operator in Ω_f and $\nabla_{\boldsymbol{\eta}} = \nabla_{(\eta_1,\ldots,\eta_d)}, \boldsymbol{\eta} \in \Omega_p$, denotes the gradient operator in Ω_p. The inequality now follows by combining (3.43) and (3.44). $\qquad \square$

Remark 3. *In the special case when the field $\mathbf{u}$ is divergence-free $(\nabla \cdot \mathbf{u} = 0)$ a similar inequality holds. Assuming $\nabla \cdot \mathbf{u} = 0$ in Ω_f and following the same steps as in the proof of Theorem 1 we obtain*

$$\left| \int_I \phi \mathbf{u} \cdot \hat{\mathbf{n}}_f \ d\boldsymbol{\sigma} \right| \leq C\|\mathbf{u}\|_f \|\nabla \phi\|_p, \qquad (3.45)$$

where $C = C_1 C_2$ instead.

Theorem 2. *If $\Omega_f, \Omega_p \subset \mathbb{R}^d, \ d = 2, 3, \ldots,$ are two domains that lie across an interface I from each other given by $I = \{(x_1, \ldots, x_d) \in \mathbb{R}^d : x_d = f(x_1, \ldots, x_{d-1})\}$, where $f : \mathbb{R}^{d-1} \to \mathbb{R}$ is a $\mathcal{C}^1-$function, then*

$$\left| \int_I \phi \mathbf{u} \cdot \hat{\mathbf{n}}_f \ d\boldsymbol{\sigma} \right| \leq C\|\mathbf{u}\|_{div,f} \|\phi\|_{1,p}, \qquad (3.46)$$

where the constant C is given by $C = 1 + 2\sup\left\{ |\nabla_{\mathbf{x}} f|, \ \mathbf{x} \in \times_{i=1}^{d-1}[a_i, b_i] \right\}$, and

$$a_i := \min\{x_i : (x_1, \ldots, x_d) \in \Omega_f \cup \Omega_p\} \in \mathbb{R},$$

$$b_i := \max\{x_i : (x_1, \ldots, x_d) \in \Omega_f \cup \Omega_p\} \in \mathbb{R},$$

$i = 1, \ldots, d-1.$

Proof. We restrict the interface I as follows, and denote the restricted interface by I:

$$I = \{(x_1, \ldots, x_d) \in \mathbb{R}^d : x_i \in [a_i, b_i], i = 1, \ldots, d-1, \ x_d = f(x_1, \ldots, x_{d-1})\}.$$

Next, we embed the two domains Ω_f, Ω_p in domains $D^+, D^- \subset \mathbb{R}^d$ respectively, defined as

$$D^+ := \{(x_1, \ldots, x_{d-1}) \in [a_1, b_1] \times \ldots \times [a_{d-1}, b_{d-1}], f \leq x_d \leq f + M\},$$

$$D^- := \{(x_1, \ldots, x_{d-1}) \in [a_1, b_1] \times \ldots \times [a_{d-1}, b_{d-1}], f - M \leq x_d \leq f\},$$

where $M := \max\{|x_d - f(x_1, \ldots, x_{d-1})| : (x_1, \ldots, x_d) \in \Omega_f \cup \Omega_p\}$, as shown in Figure 4. We
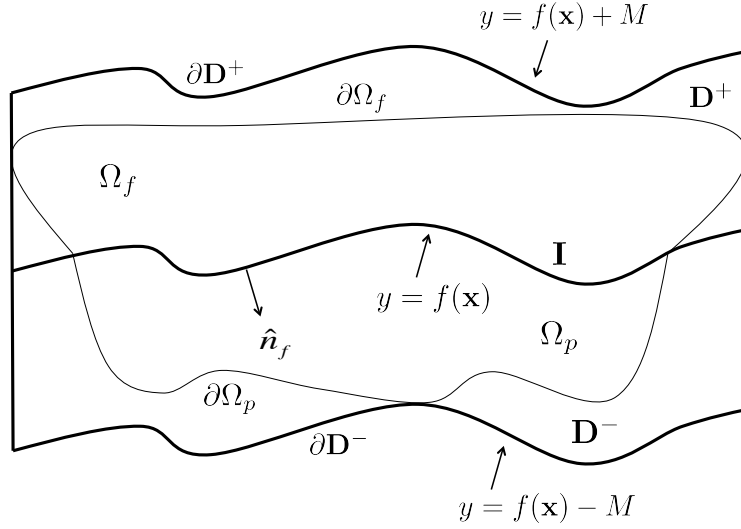
Figure 4: Domains D^+ and D^- (example of a 2d cross-section).

extend the functions $\mathbf{u}/\phi$ by zero on $D^{+/-}$, and denote the extended functions by $\mathbf{u}/\phi$. Let

$$\mathbf{F}(x_1, \ldots, x_d) = \begin{cases} (x_1, \ldots, x_{d-1}, 2f(x_1, \ldots, x_{d-1}) - x_d) & \text{in} \quad D^+ \\ \\ (x_1, \ldots, x_d) & \text{on} \quad \partial D^+. \end{cases}$$

The Jacobian matrix of $\mathbf{F}$ is given by

$$\mathbf{F}' = \left[\begin{array}{c|c} \mathbb{I}_{(d-1)} & \mathbf{0}_{(d-1) \times 1} \\ \hline 2\nabla_{\mathbf{x}}f & -1 \end{array} \right]$$

29

and thus the Jacobian determinant is $\det(\mathbf{F}') = -1$. Defining $\tilde{\phi} : D^+ \to \mathbb{R}$ as $\tilde{\phi} = \phi \circ \mathbf{F}$, we have by the divergence theorem

$$
\begin{aligned}
\int_I \phi \mathbf{u} \cdot \hat{\mathbf{n}}_f \, d\boldsymbol{\sigma} &= \int_I \tilde{\phi} \mathbf{u} \cdot \hat{\mathbf{n}}_f \, d\boldsymbol{\sigma} \\
&= \int_{\partial D^+} \tilde{\phi} \mathbf{u} \cdot \hat{\mathbf{n}}_f \, d\boldsymbol{\sigma} \\
&= \int_{D^+} \nabla \cdot (\tilde{\phi} \mathbf{u}) \, d\mathbf{x} \\
&= \int_{D^+} \left(\nabla \tilde{\phi} \cdot \mathbf{u} + \tilde{\phi} \nabla \cdot \mathbf{u} \right) \, d\mathbf{x}.
\end{aligned}
$$

Using the Cauchy-Schwarz inequality we get

$$
\begin{aligned}
\left| \int_I \phi \mathbf{u} \cdot \hat{\mathbf{n}}_f \, d\boldsymbol{\sigma} \right| &\leq \int_{D^+} \left(|\nabla \tilde{\phi}||\mathbf{u}| + |\tilde{\phi}||\nabla \cdot \mathbf{u}| \right) \, d\mathbf{x} \\
&\leq \int_{D^+} \left(|\nabla \tilde{\phi}|^2 + |\tilde{\phi}|^2 \right)^{1/2} \left(|\mathbf{u}|^2 + |\nabla \cdot \mathbf{u}| \right)^{1/2} \, d\mathbf{x} \\
&\leq \left(\int_{D^+} \left(|\nabla \tilde{\phi}|^2 + |\tilde{\phi}|^2 \right) \, d\mathbf{x} \right)^{1/2} \left(\int_{D^+} \left(|\mathbf{u}|^2 + |\nabla \cdot \mathbf{u}|^2 \right) \, d\mathbf{x} \right)^{1/2} \\
&= \left(\int_{D^+} \left(|\nabla \tilde{\phi}|^2 + |\tilde{\phi}|^2 \right) \, d\mathbf{x} \right)^{1/2} \left(\int_{\Omega_f} \left(|\mathbf{u}|^2 + |\nabla \cdot \mathbf{u}|^2 \right) \, d\mathbf{x} \right)^{1/2} \\
&= \|\mathbf{u}\|_{\mathrm{div},f} \left(\int_{D^+} \left(|\nabla \tilde{\phi}|^2 + |\tilde{\phi}|^2 \right) \, d\mathbf{x} \right)^{1/2}.
\end{aligned}
$$

By the change of variables theorem we have

$$
\int_{D^+} \left(|\nabla \tilde{\phi}|^2 + |\tilde{\phi}|^2 \right) \, d\mathbf{x} = \int_{D^+} \left(|\nabla(\phi \circ \mathbf{F})|^2 + |\phi \circ \mathbf{F}|^2 \right) |\det(\mathbf{F}')| \, d\mathbf{x} = \int_{D^-} \left(|\nabla_{\mathbf{x}} \phi|^2 + |\phi|^2 \right) \, d\boldsymbol{\eta},
$$

where $\nabla_{\mathbf{x}}$ denotes differentiation with respect to $\mathbf{x} \in D^+$, and where $\boldsymbol{\eta} = (\eta_1, \ldots, \eta_d) \in D^-$. We have

$$
\begin{aligned}
\nabla_{\mathbf{x}} \phi &= \left(\sum_{i=1}^d \frac{\partial \phi}{\partial \eta_i} \frac{\partial \eta_i}{\partial x_1}, \sum_{i=1}^d \frac{\partial \phi}{\partial \eta_i} \frac{\partial \eta_i}{\partial x_2}, \ldots, \sum_{i=1}^d \frac{\partial \phi}{\partial \eta_i} \frac{\partial \eta_i}{\partial x_d} \right) \\
&= \left(\frac{\partial \phi}{\partial \eta_1} + 2 \frac{\partial \phi}{\eta_d} \frac{\partial f}{\partial x_1}, \frac{\partial \phi}{\partial \eta_2} + 2 \frac{\partial \phi}{\eta_d} \frac{\partial f}{\partial x_2}, \ldots, \frac{\partial \phi}{\partial \eta_{d-1}} + 2 \frac{\partial \phi}{\eta_d} \frac{\partial f}{\partial x_{d-1}}, -\frac{\partial \phi}{\partial \eta_d} \right) \\
&= \left(\frac{\partial \phi}{\partial \eta_1}, \frac{\partial \phi}{\partial \eta_2}, \ldots, \frac{\partial \phi}{\partial \eta_{d-1}}, -\frac{\partial \phi}{\partial \eta_d} \right) + 2 \frac{\partial \phi}{\eta_d} \left(\frac{\partial f}{\partial x_1}, \frac{\partial f}{\partial x_2}, \ldots, \frac{\partial f}{\partial x_{d-1}}, 0 \right).
\end{aligned}
$$

If $\nabla_{\boldsymbol{\eta}}$ denotes differentiation with respect to $\boldsymbol{\eta} \in D^-$, then

$$|\nabla_{\mathbf{x}}\phi| \leq \left|\left(\frac{\partial\phi}{\partial\eta_1}, \frac{\partial\phi}{\partial\eta_2}, \ldots, \frac{\partial\phi}{\partial\eta_{d-1}}, -\frac{\partial\phi}{\partial\eta_d}\right)\right| + 2\left|\frac{\partial\phi}{\eta_d}\right|\left|\left(\frac{\partial f}{\partial x_1}, \frac{\partial f}{\partial x_2}, \ldots, \frac{\partial f}{\partial x_{d-1}}, 0\right)\right|$$

$$\leq |\nabla_{\boldsymbol{\eta}}\phi| + 2\left|\frac{\partial\phi}{\eta_d}\right||\nabla_{\mathbf{x}}f|$$

$$\leq |\nabla_{\boldsymbol{\eta}}\phi|(1 + 2|\nabla_{\mathbf{x}}f|).$$

Therefore,

$$\left|\int_I \phi\mathbf{u}\cdot\hat{\mathbf{n}}_f \, d\boldsymbol{\sigma}\right| \leq (1 + 2|\nabla_{\mathbf{x}}f|)\|\mathbf{u}\|_{\mathrm{div},f}\|\phi\|_{1,D^-}$$

$$= (1 + 2|\nabla_{\mathbf{x}}f|)\|\mathbf{u}\|_{\mathrm{div},f}\|\phi\|_{1,p}$$

$$\leq \left(1 + 2\sup\left\{|\nabla_{\mathbf{x}}f|, \ \mathbf{x} \in \times_{i=1}^{d-1}[a_i, b_i]\right\}\right)\|\mathbf{u}\|_{\mathrm{div},f}\|\phi\|_{1,p}.$$

$\square$

Remark 4. *In the special case when the field $\mathbf{u}$ is divergence-free $(\nabla\cdot\mathbf{u} = 0)$ a similar inequality holds. Assuming $\nabla\cdot\mathbf{u} = 0$ in Ω_f and following the same steps as in the proof of Theorem 2 we obtain*

$$\left|\int_I \phi\mathbf{u}\cdot\hat{\mathbf{n}}_f \, d\boldsymbol{\sigma}\right| \leq C\|\mathbf{u}\|_f\|\nabla\phi\|_p, \tag{3.47}$$

where C is the same constant as in Theorem 2.

Remark 5. *The result in Theorem 2 can be extended to piecewise linear interfaces. If the interface I is given by $I = \{(x_1, \ldots, x_d) \in \mathbb{R}^d : x_d = f(x_1, \ldots, x_{d-1})\}$, where $f : \mathbb{R}^{d-1} \to \mathbb{R}$ is a piecewise linear function that consists of k linear pieces, $\{I_i\}_{i=1}^k$, given by*

$$I_i = \left\{(x_1, \ldots, x_d) \in \mathbb{R}^d : \ x_d = \beta_i + \sum_{j=1}^{d-1}\alpha_{ij}x_j; \ \beta_i, \alpha_{ij} \in \mathbb{R}\right\}, \quad i = 1, \ldots, k,$$

then, following the same steps as in the proof of Theorem 2 on each piece I_i, we get

$$\left|\int_I \phi\mathbf{u}\cdot\hat{\mathbf{n}}_f \, d\boldsymbol{\sigma}\right| \leq \left(1 + 2\max_{i=1,\ldots,k}|\mathbf{A}_i|\right)\|\mathbf{u}\|_{div,f}\|\phi\|_{1,p},$$

where $\mathbf{A}_i = (\alpha_{i1}, \ldots, \alpha_{i,d-1})$, $i = 1, \ldots, k$.

Remark 6. *It is worth noting that in the special case when the interface I is flat (i.e., when f is constant and $\nabla_{\mathbf{x}} f = \mathbf{0}$), inequalities (3.46) and (3.47) hold with $C = 1$:*

$$\left| \int_I \phi \mathbf{u} \cdot \hat{\mathbf{n}}_f \, d\boldsymbol{\sigma} \right| \leq \|\mathbf{u}\|_{div,f} \|\phi\|_{1,p}, \qquad and \tag{3.48}$$

$$\left| \int_I \phi \mathbf{u} \cdot \hat{\mathbf{n}}_f \, d\boldsymbol{\sigma} \right| \leq \|\mathbf{u}\|_f \|\nabla \phi\|_p. \tag{3.49}$$

4.0 THE QUASISTATIC STOKES-DARCY APPROXIMATION

In this chapter we study the validity of the quasistatic approximation in the fully evolutionary Stokes-Darcy problem (3.1)-(3.12), which is obtained by setting $S_0 = 0$ in (3.5). In particular, we prove that the weak solution of the fully evolutionary Stokes-Darcy problem converges to the weak solution of the quasistatic problem as $S_0 \to 0$. We also estimate the rate of convergence. Numerical tests confirming the rate of convergence are presented in Chapter 8, in Section 8.3.

4.1 INTRODUCTION

In the fully evolutionary Stokes-Darcy model (3.1)-(3.12), the term "$S_0\phi_t$" arises because aquifers are poroelastic media and the space between the pores responds to changes in the pressure of the water, as we presented in Remark 2 of Chapter 3. The effects of poroelasticity have been extensively studied, see, e.g., [13, 111, 96]. One common model used in, e.g., [1, 8], is based on the assumption that the porous media pressure adjusts instantaneously, and the term "$S_0\phi_t$" is dropped from the Stokes-Darcy equations. This is equivalent to an inelastic assumption on the aquifer and leads to replacing (3.1)-(3.12) by the quasistatic

approximation:

$$\rho \mathbf{u}_t^{QS} - \nabla \cdot \mathbf{\Pi}(\mathbf{u}^{QS}, p^{QS}) = \mathbf{f}_f \qquad \text{in } \Omega_f \times (0, T], \tag{4.1}$$

$$\nabla \cdot \mathbf{u}^{QS} = 0 \qquad \text{in } \Omega_f \times (0, T], \tag{4.2}$$

$$\mathbf{u}^{QS} = \mathbf{0} \qquad \text{in } (\partial \Omega_f \backslash I) \times (0, T], \tag{4.3}$$

$$\mathbf{u}^{QS}(\mathbf{x}, 0) = \mathbf{u}_0(\mathbf{x}) \qquad \text{in } \Omega_f, \tag{4.4}$$

$$\nabla \cdot \mathbf{q}^{QS} = f_p \qquad \text{in } \Omega_p \times (0, T], \tag{4.5}$$

$$\mathbf{q}^{QS} = -\mathbf{K} \nabla \phi^{QS} \qquad \text{in } \Omega_p \times (0, T], \tag{4.6}$$

$$\mathbf{u}_p^{QS} = \frac{\mathbf{q}^{QS}}{n} \qquad \text{in } \Omega_p \times (0, T], \tag{4.7}$$

$$\phi^{QS} = 0 \qquad \text{in } (\partial \Omega_p \backslash I) \times (0, T], \tag{4.8}$$

$$\mathbf{u}^{QS} \cdot \hat{\mathbf{n}}_f + \mathbf{u}_p^{QS} \cdot \hat{\mathbf{n}}_p = 0 \qquad \text{on } I, \tag{4.9}$$

$$\rho g \phi^{QS} = p^{QS} - 2\mu \, \hat{\mathbf{n}}_f \cdot \mathbf{D}(\mathbf{u}^{QS}) \cdot \hat{\mathbf{n}}_f, \qquad \text{on } I, \tag{4.10}$$

$$-2 \, \hat{\boldsymbol{n}}_f \cdot \mathbf{D}(\mathbf{u}^{\mathbf{QS}}) \cdot \hat{\boldsymbol{\tau}}_i = \frac{\alpha}{\sqrt{\hat{\boldsymbol{\tau}}_i \cdot \mathbf{K} \cdot \hat{\boldsymbol{\tau}}_i}} \, \mathbf{u}^{QS} \cdot \hat{\boldsymbol{\tau}}_i, \qquad \text{for } i = 1, \ldots, d-1 \quad \text{on } I, \tag{4.11}$$

where $(\mathbf{u}^{QS}, p^{QS}, \phi^{QS})$ denotes the quasistatic solution. We consider the mathematical foundation for this simplification. Problems of the type "$\epsilon u_t + Au = 0$", where ϵ small, are treated in [87]. However, the coupled flow problem (3.1)-(3.12), with S_0 small, does not fit within the general theory in [87].

In Section 4.2 we obtain à priori bounds for the velocity and hydraulic head for both the fully evolutionary Stokes-Darcy problem and its quasistatic approximation. In Section 4.4, Theorems 5 and 6, we prove that the solution $(\mathbf{u}, \phi)$ of the fully evolutionary Stokes-Darcy model converges to the quasistatic solution $(\mathbf{u}^{QS}, \phi^{QS})$, as $S_0 \to 0$, with order one half or one, under mild assumptions on the initial data and body forces. This analysis justifies the inelastic or quasistatic approximation provided that

$$0 < S_0 << k_{min} << 1.$$

4.2 À PRIORI ESTIMATES

We recall from Chapter 2 the definitions of the spaces

$$\mathbf{X}_f := \left\{ \mathbf{v} \in (H^1(\Omega_f))^d : \mathbf{v} = \mathbf{0} \text{ on } \partial\Omega_f \backslash I \right\},$$

$$X_p := \left\{ \psi \in H^1(\Omega_p) : \psi = 0 \text{ on } \partial\Omega_p \backslash I \right\},$$

$$Q_f := L_0^2(\Omega_f),$$

$$\mathbf{V}_f := \left\{ \mathbf{v} \in \mathbf{X}_f : (q, \nabla \cdot \mathbf{v})_f = 0 \ \forall q \in Q_f \right\},$$

and define the norms on the dual spaces of $\mathbf{X}_f$, X_p respectively, by

$$\|\mathbf{f}\|_{-1,f} := \sup_{\mathbf{0} \neq \mathbf{v} \in \mathbf{X}_f} \frac{(\mathbf{f}, \mathbf{v})_f}{\|\nabla\mathbf{v}\|_f},$$

$$\|f\|_{-1,p} := \sup_{0 \neq \psi \in X_p} \frac{(f, \psi)_p}{\|\nabla\psi\|_p},$$

where $\| \cdot \|_{f/p}$ denotes the L^2 norm on $\Omega_{f/p}$, and $(\cdot, \cdot)_{f/p}$ denotes the corresponding inner product on $\Omega_{f/p}$. We further recall

$$L^2(0, T; \mathbf{X}) = \{\mathbf{v} : [0, T] \to \mathbf{X} : \int_0^T \|\mathbf{v}(t)\|_{\mathbf{X}}^2 \ dt < \infty\},$$

$$L^\infty(0, T; \mathbf{X}) = \{\mathbf{v} : [0, T] \to \mathbf{X} : \sup_{t \in [0,T]} \{\|\mathbf{v}(t)\|_{\mathbf{X}}\} < \infty\},$$

for any Hilbert space $\mathbf{X}$, and the Poincaré-Friedrichs inequality (2.6) for each domain $\Omega_{f/p}$,

$$\|\mathbf{v}\|_f \leq C_{PF,f} \|\nabla\mathbf{v}\|_f, \tag{4.12}$$

$$\|\phi\|_p \leq C_{PF,p} \|\nabla\phi\|_p, \tag{4.13}$$

where $C_{PF,f/p} > 0$. Finally, we denote by $C^* = C^*(\mathbf{u}_0, \phi_0, \mathbf{f}_f, f_p)$ a positive, finite constant.

As we presented in Chapter 3, the variational formulation of the Stokes-Darcy problem over the divergence-free space $\mathbf{V}_f$ is to find $\mathbf{u} : [0, T] \to \mathbf{V}_f$, $\phi : [0, T] \to X_p$ such that

$$n(\mathbf{u}_t, \mathbf{v})_f + a_f(\mathbf{u}, \mathbf{v}) + c_I(\mathbf{v}, \phi) = n(\tilde{\mathbf{f}}_f, \mathbf{v})_f, \tag{4.14}$$

$$gS_0(\phi_t, \psi)_p + a_p(\phi, \psi) - c_I(\mathbf{u}, \psi) = g(f_p, \psi)_p, \tag{4.15}$$

35

$\forall \mathbf{v} \in \mathbf{V}_f$, $\forall \psi \in X_p$, where $\mathbf{u}(\mathbf{x}, 0) = \mathbf{u}_0(\mathbf{x})$, $\phi(\mathbf{x}, 0) = \phi_0(\mathbf{x})$ are given. The variational formulation of the quasistatic approximation is obtained by setting $S_0 = 0$ in (4.14)-(4.15):

Find $\mathbf{u}^{QS} : [0, T] \to \mathbf{V}_f$, $\phi^{QS} : [0, T] \to X_p$ satisfying

$$n(\mathbf{u}_t^{QS}, \mathbf{v})_f + a_f(\mathbf{u}^{QS}, \mathbf{v}) + c_I(\mathbf{v}, \phi^{QS}) = n(\tilde{\mathbf{f}}_f, \mathbf{v})_f, \tag{4.16}$$

$$a_p(\phi^{QS}, \psi) - c_I(\mathbf{u}^{QS}, \psi) = g(f_p, \psi)_p, \tag{4.17}$$

$\forall \mathbf{v} \in \mathbf{V}_f$, $\forall \psi \in X_p$, where $\mathbf{u}^{QS}(\mathbf{x}, 0) = \mathbf{u}_0(\mathbf{x})$ is given. $\phi^{QS}(\mathbf{x}, 0)$ is defined through (4.17), by solving

$$a_p(\phi^{QS}(\mathbf{x}, 0), \psi(\mathbf{x})) = c_I(\mathbf{u}_0(\mathbf{x}), \psi(\mathbf{x})) + g(f_p(\mathbf{x}, 0), \psi(\mathbf{x})), \ \forall \psi \in X_p,$$

for the unknown $\phi^{QS}(\mathbf{x}, 0)$.

The difference between variational formulations (4.14)-(4.15) and (4.16)-(4.17) is the term "$gS_0(\phi_t, \psi)_p$". Thus, convergence to the quasistatic solution will hinge on à priori bounds on the time derivative of the hydraulic head ϕ. We define

$$\mathbf{u}_t(0) := \mathbf{u}_t(\mathbf{x}, 0) := \lim_{t \to 0^+} \mathbf{u}_t(\mathbf{x}, t) = \tfrac{1}{\rho} \lim_{t \to 0^+} (\nabla \cdot \mathbf{\Pi}(\mathbf{u}, p) + \mathbf{f}_f),$$

$$\mathbf{u}_t^{QS}(0) := \mathbf{u}_t^{QS}(\mathbf{x}, 0) := \lim_{t \to 0^+} \mathbf{u}_t^{QS}(\mathbf{x}, t) = \tfrac{1}{\rho} \lim_{t \to 0^+} (\nabla \cdot \mathbf{\Pi}(\mathbf{u}^{QS}, p^{QS}) + \mathbf{f}_f),$$

$$\phi_t(0) := \phi_t(\mathbf{x}, 0) := \lim_{t \to 0^+} \phi_t(\mathbf{x}, t) = \tfrac{1}{S_0} \lim_{t \to 0^+} (-\nabla \cdot \mathbf{q} + f_p).$$

In Theorem 3 Part 1 we obtain à priori bounds for the velocity and hydraulic head for both the fully evolutionary Stokes-Darcy problem and its quasistatic approximation. The second part of the theorem provides bounds on the time derivatives of the same quantities for each problem.

Theorem 3. *1. In the variational formulations (4.14)-(4.15) and (4.16)-(4.17) assume that the initial data and body forces satisfy*

$$\mathbf{u}_0 \in (L^2(\Omega_f))^d, \ \mathbf{f}_f \in (L^2(0,T;H^{-1}(\Omega_f)))^d, \ f_p \in L^2(0,T;H^{-1}(\Omega_p)).$$

a. Then for $\mathbf{u}^{QS}, \phi^{QS}$ given by (4.16)-(4.17) we have

$$\mathbf{u}^{QS} \in (L^\infty(0,T;L^2(\Omega_f)))^d, \ \nabla\mathbf{u}^{QS} \in (L^2(0,T;L^2(\Omega_f)))^{d\times d},$$

$$\mathbf{u}^{QS} \cdot \hat{\boldsymbol{\tau}}_i \in L^2(0,T;L^2(I)), \ i=1,\ldots,d-1, \ \nabla\phi^{QS} \in (L^2(0,T;L^2(\Omega_p)))^d. \tag{4.18}$$

b. If in addition $\phi_0 \in L^2(\Omega_p)$, then for $\mathbf{u}, \phi$ given by (4.14)-(4.15) it holds

$$\mathbf{u} \in (L^\infty(0,T;L^2(\Omega_f)))^d, \ \sqrt{S_0}\phi \in L^\infty(0,T;L^2(\Omega_p)),$$

$$\nabla\mathbf{u} \in (L^2(0,T;L^2(\Omega_f)))^{d\times d}, \ \mathbf{u} \cdot \hat{\boldsymbol{\tau}}_i \in L^2(0,T;L^2(I)), \ i=1,\ldots,d-1, \tag{4.19}$$

$$\nabla\phi \in (L^2(0,T;L^2(\Omega_p)))^d.$$

2. Assume that the body forces satisfy

$$\mathbf{f}_{f,t} \in (L^2(0,T;H^{-1}(\Omega_f)))^d, \ f_{p,t} \in L^2(0,T;H^{-1}(\Omega_p)),$$

where $\mathbf{f}_{f,t}, f_{p,t}$ denote the derivative of $\mathbf{f}_f, f_p$ with respect to time respectively.

a. If the initial data for (4.14)-(4.15) satisfy $\mathbf{u}_t(0) \in (L^2(\Omega_f))^d$, $\phi_t(0) \in L^2(\Omega_p)$, then

$$\mathbf{u}_t \in (L^\infty(0,T;L^2(\Omega_f)))^d, \ \sqrt{S_0}\phi_t \in L^\infty(0,T;L^2(\Omega_p)),$$

$$\nabla\mathbf{u}_t \in (L^2(0,T;L^2(\Omega_f)))^{d\times d}, \ \mathbf{u}_t \cdot \hat{\boldsymbol{\tau}}_i \in L^2(0,T;L^2(I)), \ i=1,\ldots,d-1, \tag{4.20}$$

$$\nabla\phi_t \in (L^2(0,T;L^2(\Omega_p)))^d.$$

b. If the initial data for (4.16)-(4.17) satisfy $\mathbf{u}_t^{QS}(0) \in (L^2(\Omega_f))^d$, then

$$\mathbf{u}_t^{QS} \in (L^\infty(0,T;L^2(\Omega_f)))^d, \ \nabla\mathbf{u}_t^{QS} \in (L^2(0,T;L^2(\Omega_f)))^{d\times d},$$

$$\mathbf{u}_t^{QS} \cdot \hat{\boldsymbol{\tau}}_i \in L^2(0,T;L^2(I)), \ i=1,\ldots,d-1, \ \nabla\phi_t^{QS} \in (L^2(0,T;L^2(\Omega_p)))^d. \tag{4.21}$$

Proof. The claims 1b, 1a, 2a, and 2b of the theorem are straightforward corollaries of Propositions 2-5, respectively, stated and proven below. □

Proposition 2 is the first energy estimate for the Stokes-Darcy weak formulation (4.14)-(4.15):

Proposition 2. *Consider the weak formulation of the fully evolutionary Stokes-Darcy problem (4.14)-(4.15) over the divergence-free space $\mathbf{V}_f$. Assume that the initial data and body forces satisfy*

$$\mathbf{u}_0 \in (L^2(\Omega_f))^d, \phi_0 \in L^2(\Omega_p), \mathbf{f}_f \in (L^2(0,T;H^{-1}(\Omega_f)))^d, f_p \in L^2(0,T;H^{-1}(\Omega_p)). \quad (4.22)$$

Then we have

$$\sup_{t\in[0,T]} \left\{ n\|\mathbf{u}(t)\|_f^2 + gS_0\|\phi(t)\|_p^2 \right\} + \int_0^T \left\{ \frac{2n\nu}{C_K}\|\nabla\mathbf{u}(t)\|_f^2 + \frac{2n\nu\alpha}{\sqrt{k_{max}}} \sum_{i=1}^{d-1} \|\mathbf{u}(t)\cdot\hat{\boldsymbol{\tau}}_i\|_I^2 \right.$$
$$\left. + gk_{min}\|\nabla\phi(t)\|_p^2 \right\} dt$$
$$\leq n\|\mathbf{u}_0\|_f^2 + gS_0\|\phi_0\|_p^2 + \int_0^T \left\{ \frac{nC_K}{2\rho^2\nu}\|\mathbf{f}_f(t)\|_{-1,f}^2 + \frac{g}{k_{min}}\|f_p(t)\|_{-1,p}^2 \right\} dt \leq C^*. \quad (4.23)$$

Proof. We fix $t > 0$ and set $\mathbf{v} = \mathbf{u}(t)$ and $\psi = \phi(t)$ in (4.14)-(4.15). By adding the two equations together, the two coupling terms exactly cancel. Applying the coercivity estimates (3.34) and (3.36) on the left-hand side and also Young's inequality (2.5) on the right-hand side we then obtain

$$\frac{1}{2}\frac{d}{dt}\left\{ n\|\mathbf{u}(t)\|_f^2 + gS_0\|\phi(t)\|_p^2 \right\} + \frac{2n\nu}{C_K}\|\nabla\mathbf{u}(t)\|_f^2 + \frac{n\nu\alpha}{\sqrt{k_{max}}} \sum_{i=1}^{d-1} \|\mathbf{u}(t)\cdot\hat{\boldsymbol{\tau}}_i\|_I^2$$
$$+ gk_{min}\|\nabla\phi(t)\|_p^2$$
$$\leq \frac{n}{\rho}\|\mathbf{f}_f(t)\|_{-1,f}\|\nabla\mathbf{u}(t)\|_f + g\|f_p(t)\|_{-1,p}(t)\|\nabla\phi(t)\|_p$$
$$\leq \frac{n\nu}{C_K}\|\nabla\mathbf{u}(t)\|_f^2 + \frac{nC_K}{4\rho^2\nu}\|\mathbf{f}_f(t)\|_{-1,f}^2 + \frac{gk_{min}}{2}\|\nabla\phi(t)\|_p^2 + \frac{g}{2k_{min}}\|f_p(t)\|_{-1,p}^2.$$

Rearranging and integrating over $[0,t]$ for any t in $(0,T]$ and $T < \infty$, yields

$$n\|\mathbf{u}(t)\|_f^2 + gS_0\|\phi(t)\|_p^2 + \int_0^t \left\{ \frac{2n\nu}{C_K}\|\nabla\mathbf{u}(s)\|_f^2 + \frac{2n\nu\alpha}{\sqrt{k_{max}}} \sum_{i=1}^{d-1} \|\mathbf{u}(s)\cdot\hat{\boldsymbol{\tau}}_i\|_I^2 \right.$$
$$\left. + gk_{min}\|\nabla\phi(s)\|_p^2 \right\} ds$$
$$\leq n\|\mathbf{u}_0\|_f^2 + gS_0\|\phi_0\|_p^2 + \int_0^t \left\{ \frac{nC_K}{2\rho^2\nu}\|\mathbf{f}_f(s)\|_{-1,f}^2 + \frac{g}{k_{min}}\|f_p(s)\|_{-1,p}^2 \right\} ds.$$

Finally, the result in (4.23) follows by taking the supremum over $[0, T]$ and applying the assumptions (4.22) on the right-hand side above. □

The next proposition gives the corresponding energy estimate for the quasistatic weak formulation (4.16)-(4.17).

Proposition 3. *Consider the quasistatic weak formulation (4.16)-(4.17) and assume that the initial data and body forces satisfy*

$$\mathbf{u}_0 \in (L^2(\Omega_f))^d, \mathbf{f}_f \in (L^2(0, T; H^{-1}(\Omega_f)))^d, f_p \in L^2(0, T; H^{-1}(\Omega_p)). \qquad (4.24)$$

Then we have

$$n \sup_{t \in [0,T]} \|\mathbf{u}^{QS}(t)\|_f^2 + \int_0^T \left\{ \frac{2n\nu}{C_K} \|\nabla \mathbf{u}^{QS}(t)\|_f^2 + \frac{2n\nu\alpha}{\sqrt{k_{max}}} \sum_{i=1}^{d-1} \|\mathbf{u}^{QS}(t) \cdot \hat{\boldsymbol{\tau}}_i\|_I^2 \right.$$
$$\left. + gk_{min} \|\nabla \phi^{QS}(t)\|_p^2 \right\} dt$$
$$\leq n\|\mathbf{u}_0\|_f^2 + \int_0^T \left\{ \frac{nC_K}{2\rho^2\nu} \|\mathbf{f}_f(t)\|_{-1,f}^2 + \frac{g}{k_{min}} \|f_p(s)\|_{-1,p}^2 \right\} dt \leq C^*.$$

Proof. We fix $t > 0$ and pick $\mathbf{v} = \mathbf{u}^{QS}(t), \psi = \phi^{QS}(t)$ in (4.16)-(4.17). After adding the equations together and canceling the coupling terms, the result follows by the assumptions (4.24) and manipulations similar to the ones in the proof of Proposition 2. □

Propositions 4 and 5 below provide à priori bounds for the time derivatives of $\mathbf{u}$ and ϕ in the evolutionary Stokes-Darcy problem and the quasistatic approximation, respectively.

Proposition 4. *Consider the fully evolutionary Stokes-Darcy problem (4.14)-(4.15). If the initial data and body forces satisfy*

$$\mathbf{u}_t(0) \in (L^2(\Omega_f))^d, \ \phi_t(0) \in L^2(\Omega_p),$$

$$\mathbf{f}_{f,t} \in (L^2(0, T; H^{-1}(\Omega_f)))^d, \ f_{p,t} \in L^2(0, T; H^{-1}(\Omega_p)),$$

39

then

$$\sup_{t \in [0,T]} \left\{ n \|\mathbf{u}_t(t)\|_f^2 + g S_0 \|\phi_t(t)\|_p^2 \right\} + \int_0^T \left\{ \frac{2n\nu}{C_K} \|\nabla \mathbf{u}_t(t)\|_f^2 + \frac{2n\nu\alpha}{\sqrt{k_{max}}} \sum_{i=1}^{d-1} \|\mathbf{u}_t(t) \cdot \hat{\boldsymbol{\tau}}_i\|_I^2 \right.$$

$$\left. + g k_{min} \|\nabla \phi_t(t)\|_p^2 \right\} dt$$

$$\leq n \|\mathbf{u}_t(0)\|_f^2 + g S_0 \|\phi_t(0)\|_p^2 + \int_0^T \left\{ \frac{n C_K}{2\rho^2 \nu} \|\mathbf{f}_{f,t}(t)\|_{-1,f}^2 + \frac{g}{k_{min}} \|f_{p,t}(t)\|_{-1,p}^2 \right\} dt \leq C^*.$$

Proof. Starting with the weak formulation (4.14)-(4.15), we take the derivative with respect to time to get

$$n(\mathbf{u}_{tt}, \mathbf{v})_f + a_f(\mathbf{u}_t, \mathbf{v}) + c_I(\mathbf{v}, \phi_t) = n(\tilde{\mathbf{f}}_{f,t}, \mathbf{v})_f, \tag{4.25}$$

$$g S_0(\phi_{tt}, \psi)_p + a_p(\phi_t, \psi) - c_I(\mathbf{u}_t, \psi) = g(f_{p,t}, \psi)_p. \tag{4.26}$$

We now fix $t > 0$, choose $\mathbf{v} = \mathbf{u}_t(t), \psi = \phi_t(t)$ in (4.25)-(4.26), and add the equations together. The coupling terms will cancel and the rest of the proof is similar to the proof of Proposition 2. $\square$

Proposition 5. *Consider the quasistatic weak formulation (4.16)-(4.17) and assume that*

$$\mathbf{u}_t^{QS}(0) \in (L^2(\Omega_f))^d, \mathbf{f}_{f,t} \in (L^2(0, T; H^{-1}(\Omega_f)))^d, f_{p,t} \in L^2(0, T; H^{-1}(\Omega_p)).$$

Then,

$$n \sup_{t \in [0,T]} \|\mathbf{u}_t^{QS}(t)\|_f^2 + \int_0^T \left\{ \frac{2n\nu}{C_K} \|\nabla \mathbf{u}_t^{QS}(t)\|_f^2 + \frac{2n\nu\alpha}{\sqrt{k_{max}}} \sum_{i=1}^{d-1} \|\mathbf{u}_t^{QS}(t) \cdot \hat{\boldsymbol{\tau}}_i\|_I^2 \right.$$

$$\left. + g k_{min} \|\nabla \phi_t^{QS}(t)\|_p^2 \right\} dt$$

$$\leq n \|\mathbf{u}_t^{QS}(0)\|_f^2 + \int_0^T \left\{ \frac{n C_K}{2\rho^2 \nu} \|\mathbf{f}_{f,t}(t)\|_{-1,f}^2 + \frac{g}{k_{min}} \|f_{p,t}(s)\|_{-1,p}^2 \right\} dt \leq C^*.$$

Proof. We start with the weak formulation (4.16)-(4.17) and take the derivative with respect to time:

$$(\mathbf{u}_{tt}^{QS}, \mathbf{v})_f + a_f(\mathbf{u}_t^{QS}, \mathbf{v}) + c_I(\mathbf{v}, \phi_t^{QS}) = n(\tilde{\mathbf{f}}_{f,t}, \mathbf{v})_f, \tag{4.27}$$

$$a_p(\phi_t^{QS}, \psi) - c_I(\mathbf{u}_t^{QS}, \psi) = g(f_{p,t}, \psi)_p. \tag{4.28}$$

By fixing $t > 0$, choosing $\mathbf{v} = \mathbf{u}_t^{QS}(t), \psi = \phi_t^{QS}(t)$ in (4.27)-(4.28), and adding so that the coupling terms cancel, we obtain the result similarly as in the proof of Proposition 2. $\square$

In the next section we obtain á priori bounds for $\mathbf{u}$ and ϕ by assuming less regularity on the body forces.

4.3 À PRIORI ESTIMATES ASSUMING LESS REGULAR BODY FORCES

In this section, we obtain á priori bounds on the velocity $\mathbf{u}$ and hydraulic head ϕ by assuming less regularity on the body forces. In this case, however, we restrict the domains Ω_f and Ω_p by assuming that either the hypotheses of Theorem 1 or those of Theorem 2 hold. That is, we assume either that there exists a C^1-diffeomorphism from Ω_f to Ω_p, so that the bound given in (3.45) holds, or that the interface I is of the form $x_d = f(x_1, \ldots, x_{d-1})$, $f \in C^1(\mathbb{R}^{d-1})$, and Ω_f, Ω_p are any bounded, regular domains, and inequality (3.47) holds instead. In either case, we assume that the domains Ω_f and Ω_p are such that the following bound on the coupling integral term $\langle \phi, \mathbf{u} \cdot \hat{\mathbf{n}}_f \rangle_I$ holds true

$$|\langle \phi, \mathbf{u} \cdot \hat{\mathbf{n}}_f \rangle_I| = \left| \int_I \phi \mathbf{u} \cdot \hat{\mathbf{n}}_f \ d\boldsymbol{\sigma} \right| \leq C^\dagger \|\mathbf{u}\|_f \|\nabla \phi\|_p, \tag{4.29}$$

where $C^\dagger > 0$ is either the constant from Theorem 1 or the one from Theorem 2.

Theorem 4. *Assume that the initial data and body forces satisfy*

$$\mathbf{u}_0 \in (L^2(\Omega_f))^d, \mathbf{D}(\mathbf{u}_0) \in (L^2(\Omega_f))^{d \times d}, \mathbf{u}_0 \cdot \hat{\boldsymbol{\tau}}_i \in L^2(I), i = 1, \ldots, d-1,$$
$$\phi_0 \in L^2(\Omega_p), \nabla \phi(0) \in (L^2(\Omega_p))^d,$$
$$\mathbf{f}_f \in (L^2(0, T; L^2(\Omega_f)))^d, f_p \in L^2(0, T; L^2(\Omega_p)),$$

and that the domains Ω_f, Ω_p are such that (4.29) holds. Then we have

$$\frac{n}{2}\int_0^T \|\mathbf{u}_t(t)\|_f^2 \, dt + gS_0\int_0^T \|\phi_t(t)\|_p^2 \, dt + \sup_{t\in[0,T]}\left\{\frac{2n\nu}{C_K}\|\nabla\mathbf{u}\|_f^2 + \frac{n\nu\alpha}{\sqrt{k_{max}}}\|\mathbf{u}\cdot\hat{\boldsymbol{\tau}}\|_I^2\right.$$

$$\left.+\frac{gk_{min}}{2}\|\nabla\phi\|_p^2\right\}(t)$$

$$\le \frac{n}{\rho^2}\int_0^T \|\mathbf{f}_f(t)\|_f^2 \, dt + \frac{g}{S_0}\int_0^T \|f_p(t)\|_p^2 \, dt + 8n(gC^\dagger)^2\int_0^T \|\nabla\phi(t)\|_p^2 \, dt$$

$$+\frac{2n^2g(C^\dagger)^2}{k_{min}}\sup_{t\in[0,T]}\|\mathbf{u}(t)\|_f^2 + 2n\nu\|\mathbf{D}(\mathbf{u}_0)\|_f^2 + \sum_{i=1}^{d-1}\int_I \frac{n\nu\alpha}{\sqrt{\hat{\boldsymbol{\tau}}_i\cdot\mathbf{K}\cdot\hat{\boldsymbol{\tau}}_i}}(\mathbf{u}_0\cdot\hat{\boldsymbol{\tau}}_i)^2 \, d\boldsymbol{\sigma}$$

$$+g(\mathbf{K}\nabla\phi(0), \nabla\phi(0))_p - 2c_I(\mathbf{u},\phi)(0) \le C^*.$$

Then, specifically

$$\mathbf{u}_t \in (L^2(0,T;L^2(\Omega_f)))^d, \sqrt{S_0}\phi_t \in L^2(0,T;L^2(\Omega_p)),$$

$$\nabla\mathbf{u} \in (L^\infty(0,T;L^2(\Omega_f)))^d, \mathbf{u}\cdot\hat{\boldsymbol{\tau}} \in L^\infty(0,T;L^2(I)), \nabla\phi \in (L^\infty(0,T;L^2(\Omega_p)))^d.$$

Proof. We fix $t > 0$, set $\mathbf{v} = \mathbf{u}_t(t), \psi = \phi_t(t)$ in (4.14)-(4.15), and add together to obtain:

$$n(\mathbf{u}_t,\mathbf{u}_t)_f + gS_0(\phi_t,\phi_t)_p + a_f(\mathbf{u},\mathbf{u}_t) + a_p(\phi,\phi_t) + c_I(\mathbf{u}_t,\phi) - c_I(\mathbf{u},\phi_t)$$

$$= n(\tilde{\mathbf{f}}_f,\mathbf{u}_t)_f + g(f_p,\phi_t)_p.$$

Thus,

$$n\|\mathbf{u}_t\|_f^2 + gS_0\|\phi_t\|_p^2 + \frac{1}{2}\frac{d}{dt}\{a_f(\mathbf{u},\mathbf{u}) + a_p(\phi,\phi)\} + c_I(\mathbf{u}_t,\phi) - c_I(\mathbf{u},\phi_t)$$

$$= n(\tilde{\mathbf{f}}_f,\mathbf{u}_t)_f + g(f_p,\phi_t)_p.$$

Using the Cauchy-Schwarz and Young's inequalities we obtain

$$n\|\mathbf{u}_t\|_f^2 + gS_0\|\phi_t\|_p^2 + \frac{1}{2}\frac{d}{dt}\{a_f(\mathbf{u},\mathbf{u}) + a_p(\phi,\phi)\} + c_I(\mathbf{u}_t,\phi) - c_I(\mathbf{u},\phi_t)$$

$$\le n\|\tilde{\mathbf{f}}_f\|_f\|\mathbf{u}_t\|_f + g\|f_p\|_p\|\phi_t\|_p \le \frac{n}{2}\|\mathbf{u}_t\|_f^2 + \frac{n}{2}\|\tilde{\mathbf{f}}_f\|_f^2 + \frac{gS_0}{2}\|\phi_t\|_p^2 + \frac{g}{2S_0}\|f_p\|_p^2.$$

Rearranging then gives

$$n\|\mathbf{u}_t\|_f^2 + gS_0\|\phi_t\|_p^2 + \frac{d}{dt}\left\{a_f(\mathbf{u},\mathbf{u}) + a_p(\phi,\phi)\right\} + 2\left\{c_I(\mathbf{u}_t,\phi) - c_I(\mathbf{u},\phi_t)\right\}$$
$$\leq n\|\tilde{\mathbf{f}}_f\|_f^2 + \frac{g}{S_0}\|f_p\|_p^2.$$

Using

$$c_I(\mathbf{u}_t,\phi) - c_I(\mathbf{u},\phi_t) = -\frac{d}{dt}c_I(\mathbf{u},\phi) + 2c_I(\mathbf{u}_t,\phi),$$

the inequality becomes

$$n\|\mathbf{u}_t\|_f^2 + gS_0\|\phi_t\|_p^2 + \frac{d}{dt}\left\{a_f(\mathbf{u},\mathbf{u}) + a_p(\phi,\phi) - 2c_I(\mathbf{u},\phi)\right\}$$
$$\leq n\|\tilde{\mathbf{f}}_f\|_f^2 + \frac{g}{S_0}\|f_p\|_p^2 - 4c_I(\mathbf{u}_t,\phi). \tag{4.30}$$

Now, since $\nabla \cdot \mathbf{u} = 0$ in Ω_f implies that $\nabla \cdot \mathbf{u}_t = 0$ in Ω_f, we may use (4.29) to bound the term $-4c_I(\mathbf{u}_t,\phi)$ on the right-hand side of (4.30) as follows:

$$-4c_I(\mathbf{u}_t,\phi) = -4ng\langle\phi, \mathbf{u}\cdot\hat{\mathbf{n}}_f\rangle_I \leq 4ngC^\dagger\|\mathbf{u}_t\|_f\|\nabla\phi\|_p \leq \frac{n}{2}\|\mathbf{u}_t\|_f^2 + 8n(gC^\dagger)^2\|\nabla\phi\|_p^2. \tag{4.31}$$

Using (4.31) in (4.30) and rearranging terms gives

$$\frac{n}{2}\|\mathbf{u}_t\|_f^2 + gS_0\|\phi_t\|_p^2 + \frac{d}{dt}\left\{a_f(\mathbf{u},\mathbf{u}) + a_p(\phi,\phi) - 2c_I(\mathbf{u},\phi)\right\}$$
$$\leq n\|\tilde{\mathbf{f}}_f\|_f^2 + \frac{g}{S_0}\|f_p\|_p^2 + 8n(gC^\dagger)^2\|\nabla\phi\|_p^2.$$

Integrating this over $(0,t]$, for $t \leq T$, gives

$$\frac{n}{2}\int_0^t \|\mathbf{u}_t(s)\|_f^2\,ds + gS_0\int_0^t \|\phi_t(s)\|_p^2\,ds + \left\{a_f(\mathbf{u},\mathbf{u}) + a_p(\phi,\phi) - 2c_I(\mathbf{u},\phi)\right\}(t)$$
$$\leq n\int_0^t \|\tilde{\mathbf{f}}_f(s)\|_f^2\,ds + \frac{g}{S_0}\int_0^t \|f_p(s)\|_p^2\,ds + 8n(gC^\dagger)^2\int_0^t \|\nabla\phi(s)\|_p^2\,ds$$
$$+ \left\{a_f(\mathbf{u},\mathbf{u}) + a_p(\phi,\phi) - 2c_I(\mathbf{u},\phi)\right\}(0). \tag{4.32}$$

Next, we use (4.29) and Young's inequality once more for the term $-2c_I(\mathbf{u},\phi)$ on the left-hand side of (4.32), and estimate

$$-2c_I(\mathbf{u},\phi) = -2ng\langle\phi, \mathbf{u}\cdot\hat{\mathbf{n}}_f\rangle_I \geq -2ngC^\dagger\|\mathbf{u}\|_f\|\nabla\phi\|_p \geq -\frac{2n^2g(C^\dagger)^2}{k_{min}}\|\mathbf{u}\|_f^2 - \frac{gk_{min}}{2}\|\nabla\phi\|_p^2. \tag{4.33}$$

Using (4.33) along with the coercivity estimates (3.34) and (3.36), yields

$$
\{a_f(\mathbf{u}, \mathbf{u}) + a_p(\phi, \phi) - 2c_I(\mathbf{u}, \phi)\}(t)
$$
$$
\geq \left\{ \frac{2n\nu}{C_K}\|\nabla\mathbf{u}\|_f^2 + \frac{n\nu\alpha}{\sqrt{k_{max}}}\|\mathbf{u}\cdot\hat{\boldsymbol{\tau}}\|_I^2 + \frac{gk_{min}}{2}\|\nabla\phi\|_p^2 - \frac{2n^2 g(C^\dagger)^2}{k_{min}}\|\mathbf{u}\|_f^2 \right\}(t). \qquad (4.34)
$$

With (4.34) and after rearranging, (4.32) becomes

$$
\frac{n}{2}\int_0^t \|\mathbf{u}_t(s)\|_f^2\, ds + gS_0 \int_0^t \|\phi_t(s)\|_p^2\, ds + \left\{ \frac{2n\nu}{C_K}\|\nabla\mathbf{u}\|_f^2 + \frac{n\nu\alpha}{\sqrt{k_{max}}}\|\mathbf{u}\cdot\hat{\boldsymbol{\tau}}\|_I^2 + \frac{gk_{min}}{2}\|\nabla\phi\|_p^2 \right\}(t)
$$
$$
\leq n\int_0^t \|\tilde{\mathbf{f}}_f(s)\|_f^2\, ds + \frac{g}{S_0}\int_0^t \|f_p(s)\|_p^2\, ds + 8n(gC^\dagger)^2 \int_0^t \|\nabla\phi(s)\|_p^2\, ds + \frac{2n^2 g(C^\dagger)^2}{k_{min}}\|\mathbf{u}(t)\|_f^2
$$
$$
+ \{a_f(\mathbf{u}, \mathbf{u}) + a_p(\phi, \phi) - 2c_I(\mathbf{u}, \phi)\}(0),
$$

for all $t \leq T$. Taking the *supremum* over $[0, T]$ finally results in

$$
\frac{n}{2}\int_0^T \|\mathbf{u}_t(t)\|_f^2\, dt + gS_0 \int_0^T \|\phi_t(t)\|_p^2\, dt + \sup_{t\in[0,T]} \left\{ \frac{2n\nu}{C_K}\|\nabla\mathbf{u}\|_f^2 + \frac{n\nu\alpha}{\sqrt{k_{max}}}\|\mathbf{u}\cdot\hat{\boldsymbol{\tau}}\|_I^2 \right.
$$
$$
\left. + \frac{gk_{min}}{2}\|\nabla\phi\|_p^2 \right\}(t)
$$
$$
\leq \frac{n}{\rho^2}\int_0^T \|\mathbf{f}_f(t)\|_f^2\, dt + \frac{g}{S_0}\int_0^T \|f_p(t)\|_p^2\, dt + 8n(gC^\dagger)^2 \int_0^T \|\nabla\phi(t)\|_p^2\, dt
$$
$$
+ \frac{2n^2 g(C^\dagger)^2}{k_{min}} \sup_{t\in[0,T]} \|\mathbf{u}(t)\|_f^2 + \left\{ 2n\nu\|\mathbf{D}(\mathbf{u})\|_f^2 + \sum_{i=1}^{d-1} \int_I \frac{n\nu\alpha}{\sqrt{\hat{\boldsymbol{\tau}}_i \cdot \mathbf{K}\cdot\hat{\boldsymbol{\tau}}_i}}(u\cdot\hat{\boldsymbol{\tau}}_i)^2\, d\boldsymbol{\sigma} \right.
$$
$$
\left. + g(\mathbf{K}\nabla\phi, \nabla\phi)_p - 2c_I(\mathbf{u}, \phi) \right\}(0). \qquad (4.35)
$$

Since $\|\cdot\|_{-1, f/p} \leq C\|\cdot\|_{f/p}$, for some $C > 0$, it follows by (4.19) of Theorem 3 that $\mathbf{u} \in (L^\infty(0, T; L^2(\Omega_f)))^d$ and $\nabla\phi \in (L^2(0, T; L^2(\Omega_p)))^d$. Thus, all the terms on the right-hand side of (4.35) are bounded, and the claim of the theorem follows. $\qquad\square$

4.4 CONVERGENCE TO THE QUASISTATIC SOLUTION

In this section we prove that the solution of the fully evolutionary Stokes-Darcy problem, $(\mathbf{u}, \phi)$, determined through (4.14)-(4.15), converges to the quasistatic solution, $(\mathbf{u}^{QS}, \phi^{QS})$, given by (4.16)-(4.17), as S_0 approaches zero. We will use the à priori estimates from the previous sections to obtain error estimates for the velocity and hydraulic head. For the case of less regular body forces we prove one half order convergence in S_0. For the more regular case, we obtain first order convergence.

We denote the errors in $\mathbf{u}$ and ϕ, respectively, by

$$\mathbf{e_u}(\mathbf{x}, t) := \mathbf{u}(\mathbf{x}, t) - \mathbf{u}^{QS}(\mathbf{x}, t),$$

$$e_\phi(\mathbf{x}, t) := \phi(\mathbf{x}, t) - \phi^{QS}(\mathbf{x}, t).$$

By definition, $\mathbf{e_u}(\mathbf{x}, 0) = \mathbf{0}$ and $e_\phi = \phi_0(\mathbf{x}) - \phi^{QS}(\mathbf{x}, 0)$. Subtracting (4.16) from (4.14) and (4.17) from (4.15) we find that the errors satisfy the quasistatic weak formulation (4.16)-(4.17):

$$n(\mathbf{e_{u,t}}, \mathbf{v})_f + a_f(\mathbf{e_u}, \mathbf{v}) + c_I(\mathbf{v}, e_\phi) = 0, \tag{4.36}$$

$$a_p(e_\phi, \psi) - c_I(\mathbf{e_u}, \psi) = -gS_0(\phi_t, \psi)_p. \tag{4.37}$$

This can also be written in the form of the Stokes-Darcy weak formulation (4.14)-(4.15):

$$(\mathbf{e_{u,t}}, \mathbf{v})_f + a_f(\mathbf{e_u}, \mathbf{v}) + c_I(\mathbf{v}, e_\phi) = 0, \tag{4.38}$$

$$gS_0(e_{\phi,t}, \psi)_p + ga_p(e_\phi, \psi) - c_I(\mathbf{e_u}, \psi) = -gS_0(\phi_t^{QS}, \psi)_p. \tag{4.39}$$

In Theorem 5 below we give a result of first order convergence of the solution $(\mathbf{u}, \phi)$ to the quasistatic solution $(\mathbf{u}^{QS}, \phi^{QS})$, as S_0 converges to zero.

Theorem 5. *Consider the weak formulation (4.38)-(4.39) and assume that the initial data and body forces satisfy*

$$\mathbf{u}_t^{QS}(0) \in (L^2(\Omega_f))^d, \|\phi_t(0)\|_{-1,p} < \infty,$$

$$\mathbf{f}_{f,t} \in (L^2(0,T;H^{-1}(\Omega_f)))^d, f_{p,t} \in L^2(0,T;H^{-1}(\Omega_p)).$$

Then

$$\sup_{t\in[0,T]} \left\{ n\|\mathbf{e_u}(t)\|_f^2 + gS_0\|e_\phi(t)\|_p^2 \right\} + \int_0^T \left\{ \frac{2n\nu}{C_K}\|\nabla\mathbf{e_u}(t)\|_f^2 + \frac{2n\nu\alpha}{\sqrt{k_{max}}}\|\mathbf{e_u}(t)\cdot\hat{\boldsymbol{\tau}}\|_I^2 \right.$$

$$\left. + gk_{min}\|\nabla e_\phi(t)\|_p^2 \right\} dt$$

$$\leq gS_0\|\phi_0 - \phi^{QS}(0)\|_p^2 + \frac{S_0^2}{k_{min}}C^* \leq \frac{C^*}{k_{min}}\left(\frac{S_0}{k_{min}}+1\right)S_0^2.$$

Proof. We apply the energy estimate obtained in Proposition 2 to the weak formulation for the error (4.38)-(4.39), with $\mathbf{f}_f \equiv \mathbf{0}$, $f_p = -S_0\phi_t^{QS}$, $\mathbf{e_u}$ replacing $\mathbf{u}$ and e_ϕ replacing ϕ, and have the first error estimate:

$$\sup_{t\in[0,T]} \left\{ n\|\mathbf{e_u}(t)\|_f^2 + gS_0\|e_\phi(t)\|_p^2 \right\} + \int_0^T \left\{ \frac{2n\nu}{C_K}\|\nabla\mathbf{e_u}(t)\|_f^2 + \frac{2n\nu\alpha}{\sqrt{k_{max}}}\|\mathbf{e_u}(t)\cdot\hat{\boldsymbol{\tau}}\|_I^2 \right.$$

$$\left. + gk_{min}\|\nabla e_\phi(t)\|_p^2 \right\} dt$$

$$\leq gS_0\|\phi_0 - \phi^{QS}(0)\|_p^2 + \frac{gS_0^2}{k_{min}}\int_0^T \|\phi_t^{QS}(t)\|_{-1,p}^2 \, dt. \tag{4.40}$$

Using the Poincaré-Friedrichs inequality (4.13) we have

$$\|\phi_t^{QS}\|_{-1,p} \leq C\|\phi_t^{QS}\|_p \leq C_{PF,p}\|\nabla\phi_t^{QS}\|_p. \tag{4.41}$$

By (4.21) of Theorem 3 we have $\nabla\phi_t^{QS} \in (L^2(0,T;L^2(\Omega_p)))^d$. Inequality (4.41) then implies that $\phi_t^{QS} \in L^2(0,T;H^{-1}(\Omega_p))$. Therefore, (4.40) gives

$$\sup_{t\in[0,T]} \left\{ n\|\mathbf{e_u}(t)\|_f^2 + gS_0\|e_\phi(t)\|_p^2 \right\} + \int_0^T \left\{ \frac{2n\nu}{C_K}\|\nabla\mathbf{e_u}(t)\|_f^2 + \frac{2n\nu\alpha}{\sqrt{k_{max}}}\|\mathbf{e_u}(t)\cdot\hat{\boldsymbol{\tau}}\|_I^2 \right.$$

$$\left. + gk_{min}\|\nabla e_\phi(t)\|_p^2 \right\} dt$$

$$\leq gS_0\|\phi_0 - \phi^{QS}(0)\|_p^2 + \frac{C^*}{k_{min}}S_0^2, \tag{4.42}$$

46

which proves the first part of the theorem. For the last inequality, we set $t = 0$ in (4.15) and (4.17) and subtract the second from the first equation to obtain

$$gS_0(\phi_t(0), \psi)_p + a_p(\phi_0 - \phi^{QS}(0), \psi) = 0, \quad \forall \psi \in X_p, \tag{4.43}$$

where we used that $u^{QS}(x, 0) = u_0(x)$. We then set $\psi = \phi_0 - \phi^{QS}(0)$ in (4.43):

$$a_p(\phi_0 - \phi^{QS}(0), \phi_0 - \phi^{QS}(0)) = gS_0(\phi_t(0), \phi^{QS}(0) - \phi_0)_p.$$

Using the coercivity estimate (3.36) and the definition of the $\| \cdot \|_{-1}$ norm we have

$$k_{min}\|\nabla(\phi_0 - \phi^{QS}(0))\|_p^2 \le S_0\|\phi_t(0)\|_{-1,p}\|\nabla(\phi_0 - \phi^{QS}(0))\|_p,$$

so that

$$\|\nabla(\phi_0 - \phi^{QS}(0))\|_p \le \frac{S_0}{k_{min}}\|\phi_t(0)\|_{-1,p}. \tag{4.44}$$

Finally, using the Poincaré-Friedrichs inequality (4.13) on the left-hand side of (4.44) yields

$$\|\phi_0 - \phi^{QS}(0)\|_p \le \frac{C_{PF,p}S_0}{k_{min}}\|\phi_t(0)\|_{-1,p}. \tag{4.45}$$

The last inequality of the theorem now follows by combining (4.42) and (4.45). $\qquad\square$

In Theorem 6 we assume less regularity on the body forces and prove one-half order convergence of the Stokes-Darcy solution to the quasistatic solution as $S_0 \to 0$.

Theorem 6. *Consider the weak formulation (4.36)-(4.37) and assume that the initial data and body forces satisfy*

$$\mathbf{u}_0 \in (L^2(\Omega_f))^d, \mathbf{D}(\mathbf{u}_0) \in (L^2(\Omega_f))^{d\times d}, \mathbf{u}_0 \cdot \hat{\boldsymbol{\tau}}_i \in L^2(I), i = 1, \dots, d-1,$$

$$\phi_0 \in L^2(\Omega_p), \nabla\phi(0) \in (L^2(\Omega_p))^d,$$

$$\mathbf{f}_f \in (L^2(0, T; L^2(\Omega_f)))^d, f_p \in L^2(0, T; L^2(\Omega_p)).$$

Further, assume that the domains Ω_f and Ω_p are such that inequality (4.29) holds. Then

$$n \sup_{t\in[0,T]} \|\mathbf{e_u}(t)\|_f^2 + \int_0^T \left\{ \frac{2n\nu}{C_K}\|\nabla\mathbf{e_u}(t)\|_f^2 + \frac{2n\nu\alpha}{\sqrt{k_{max}}}\|\mathbf{e_u}(t) \cdot \hat{\boldsymbol{\tau}}\|_I^2 + gk_{min}\|\nabla e_\phi(t)\|_p^2 \right\} dt$$

$$\le \frac{gS_0}{k_{min}} \int_0^T \left(\sqrt{S_0}\|\phi_t(t)\|_p \right)^2 dt \le \frac{C^*}{k_{min}}S_0.$$

47

Proof. We first apply the energy estimate obtained in Proposition 3 to the weak formulation for the error (4.36)-(4.37), with $\mathbf{f}_f \equiv \mathbf{0}$, $f_p = -S_0\phi_t$, and with $\mathbf{e_u}$ in place of $\mathbf{u}^{QS}$ and e_ϕ in place of ϕ^{QS}:

$$n \sup_{t\in[0,T]} \|\mathbf{e_u}(t)\|_f^2 + \int_0^T \left\{ \frac{2n\nu}{C_K}\|\nabla\mathbf{e_u}(t)\|_f^2 + \frac{2n\nu\alpha}{\sqrt{k_{max}}}\|\mathbf{e_u}(t)\cdot\hat{\boldsymbol{\tau}}\|_I^2 + gk_{min}\|\nabla e_\phi(t)\|_p^2 \right\} dt$$
$$\leq \frac{gS_0}{k_{min}} \int_0^T \left(\sqrt{S_0}\|\phi_t(t)\|_p \right)^2 dt.$$

By Theorem 4 we have in addition that $\sqrt{S_0}\phi_t \in L^2(0,T;L^2(\Omega_p))$. Thus, we conclude that

$$n \sup_{t\in[0,T]} \|\mathbf{e_u}(t)\|_f^2 + \int_0^T \left\{ \frac{2n\nu}{C_K}\|\nabla\mathbf{e_u}(t)\|_f^2 + \frac{2n\nu\alpha}{\sqrt{k_{max}}}\|\mathbf{e_u}(t)\cdot\hat{\boldsymbol{\tau}}\|_I^2 + gk_{min}\|\nabla e_\phi(t)\|_p^2 \right\} dt \leq \frac{C^*}{k_{min}}S_0.$$

$\square$

Remark 7. *Theorem 6 is important because it proves convergence of the Stokes-Darcy solution to the quasistatic solution as S_0 converges to zero assuming less regular body forces. We note that the assumption on the body forces in Theorem 5 is that the time derivatives of the body forces in $\Omega_{f/p}$ belong to $L^2(0,T;H^{-1}(\Omega_{f/p}))$ respectively, while the requirement in Theorem 6 is that the body forces lie in $L^2(0,T;L^2(\Omega_{f/p}))$. Less regular body forces occur, for instance, in settings involving wells.*

We now summarize the conclusions of Theorems 5 and 6. In each case, C denotes the constant of proportionality in the error estimate, and "$\sim$" means "proportional to":

- Under the assumptions of Theorem 5:

$$\|\mathbf{u}-\mathbf{u}^{QS}\|_{L^\infty(0,T;L^2(\Omega_f))} = \mathcal{O}(S_0), \quad C \sim \frac{1}{\sqrt{nk_{min}}},$$
$$\|\nabla(\mathbf{u}-\mathbf{u}^{QS})\|_{L^2(0,T;L^2(\Omega_f))} = \mathcal{O}(S_0), \quad C \sim \frac{1}{\sqrt{n\nu k_{min}}},$$
$$\|\phi-\phi^{QS}\|_{L^\infty(0,T;L^2(\Omega_p))} = \mathcal{O}(\sqrt{S_0}), \quad C \sim \frac{1}{\sqrt{k_{min}}},$$
$$\|\nabla(\phi-\phi^{QS})\|_{L^2(0,T;L^2(\Omega_p))} = \mathcal{O}(S_0), \quad C \sim \frac{1}{k_{min}}.$$

- Under the assumptions of Theorem 6:

$$\|\mathbf{u}-\mathbf{u}^{QS}\|_{L^\infty(0,T;L^2(\Omega_f))} = \mathcal{O}(\sqrt{S_0}), \quad C \sim \frac{1}{\sqrt{nk_{min}}},$$
$$\|\nabla(\mathbf{u}-\mathbf{u}^{QS})\|_{L^2(0,T;L^2(\Omega_f))} = \mathcal{O}(\sqrt{S_0}), \quad C \sim \frac{1}{\sqrt{n\nu k_{min}}},$$
$$\|\nabla(\phi-\phi^{QS})\|_{L^2(0,T;L^2(\Omega_p))} = \mathcal{O}(\sqrt{S_0}), \quad C \sim \frac{1}{k_{min}}.$$

Remark 8. *From the results in Theorems 5 and 6, summarized above, it is clear that dropping the term "$S_0 \phi_t$" from the fully evolutionary Stokes-Darcy equations, if S_0 is small, is justified provided that $S_0 << \{k_{min}, n\}$, that is, provided that the specific storage is smaller in orders of magnitude than both the minimum eigenvalue of the hydraulic conductivity tensor and the porosity. In real aquifers, it is known that $S_0 < n \leq 1$ and often $S_0 << n$. However, it is often the case that $0 < k_{min} << S_0 << 1$, and therefore, dropping the term in those cases should be questioned.*

Remark 9. *Numerical tests that verify first-order convergence to the quasistatic solution and confirm sensitivity of the convergence to the parameter k_{min} are presented in Chapter 8, in Section 8.3.*

5.0   A LINEAR STABILIZATION OF THE CNLF METHOD

In this chapter we present a linear stabilization of the Crank-Nicolson Leapfrog time stepping scheme for a general evolution equation. We analyze the method for stability and consistency, and show that it is unconditionally stable (requiring no time step condition) while it increases accuracy, and we further prove that it is unconditionally, asymptotically stable in both the stable and unstable modes of Leapfrog. An extension of this method for the Stokes-Darcy problem is the topic of Chapter 6.

5.1   INTRODUCTION AND THE CNLF-STAB METHOD

We let X, L, X' be Hilbert spaces satisfying $X \hookrightarrow L \hookrightarrow X'$. We denote by $(\cdot, \cdot), \| \cdot \|$ the inner product and norm on L respectively, and by $\langle \cdot, \cdot \rangle$ the duality pairing between X and X' which is an extension of the L-inner product. We denote the operator norm of Λ by

$$\|\Lambda\| = \sup_{\mathbf{0} \neq \mathbf{v} \in L} \frac{\|\Lambda \mathbf{v}\|}{\|\mathbf{v}\|}.$$

For $\mathbf{u} : [0, T] \to X$, $0 < T < \infty$, we consider an evolution equation of the form

$$\mathbf{u}_t + A\mathbf{u} + \Lambda \mathbf{u} = \mathbf{0}, \quad \text{for } t \in (0, T],$$
$$\mathbf{u}(0) = \mathbf{u}_0, \tag{5.1}$$

where $A : X \to X'$ is a linear operator that satisfies

$$\langle A\mathbf{u}, \mathbf{u} \rangle \geq 0 \quad \forall \mathbf{u} \in X, \tag{5.2}$$

and $\Lambda : L \to L$ is a linear operator such that

$$1. \ \|\Lambda\| < \infty, \quad \text{and} \tag{5.3}$$

$$2. \ \langle \Lambda \mathbf{u}, \mathbf{v} \rangle = -\langle \mathbf{u}, \Lambda \mathbf{v} \rangle, \quad \forall \mathbf{u}, \mathbf{v} \in L. \tag{5.4}$$

Under these assumptions the following fundamental stability properties hold, which must be preserved under any discretization:

1. $\|\mathbf{u}(t)\|^2 \leq \|\mathbf{u}_0\|^2 \quad \forall t,$

2. $\|\mathbf{u}(t)\|^2 = \|\mathbf{u}_0\|^2 \quad \forall t,$ if $A \equiv \mathbf{0},$ and

3. $\|\mathbf{u}(t)\| \to 0$ as $t \to \infty,$ if $\langle A\mathbf{u}, \mathbf{u} \rangle \geq a_0 \|\mathbf{u}\|^2$ for some $a_0 > 0$ and all $\mathbf{u} \in X.$

We now let $\Delta t > 0$ denote the time step size in our discretization, and denote $\mathbf{v}^k := \mathbf{v}(t^k),$ $k = 0, 1, \ldots, N,$ $T = N\Delta t,$ for any function $\mathbf{v} \in X.$ The Crank-Nicolson Leapfrog (CNLF) method for (5.1) is as follows:

Given $\mathbf{u}^0, \mathbf{u}^1 \in X,$ find $\mathbf{u}^{n+1} \in X$ for $n \geq 1$ such that

$$\frac{\mathbf{u}^{n+1} - \mathbf{u}^{n-1}}{2\Delta t} + A \, \frac{\mathbf{u}^{n+1} + \mathbf{u}^{n-1}}{2} + \Lambda \mathbf{u}^n = \mathbf{0}. \tag{CNLF}$$

The CNLF method involves three levels in time, and therefore requires approximations of sufficient accuracy for the first two approximations, $\mathbf{u}_0$ and $\mathbf{u}_1,$ see, e.g., [110]. These first approximations will affect the overall order of convergence of the scheme. As was shown in [85], (CNLF) is stable under the time step condition

$$\Delta t \|\Lambda\| < 1. \tag{5.5}$$

Proof. See Appendix A.1. □

Further, under condition (5.5), (CNLF) is asymptotically stable in both the stable and unstable modes (see Appendix A.2 for the proof and also [64]). However, energy stability of (CNLF) under condition (5.5) is not completely descriptive of computational practice. It has long been noted that (CNLF) is marginally stable (described in [55] as "slightly unstable"). If the linear term includes a viscous mechanism of the form

$$\langle A\mathbf{u}, \mathbf{u} \rangle \geq a_0 \|\mathbf{u}\|^2, \text{ for some } a_0 > 0 \text{ and all } \mathbf{u} \in X, \tag{5.6}$$

then $\|\mathbf{u}(t)\| \to 0$ as $t \to \infty$. In this common case, the CNLF method damps the energy in the stable mode, $(\mathbf{u}^{n+1} + \mathbf{u}^{n-1})$, however, it often exhibits growth in the unstable mode, $(\mathbf{u}^{n+1} - \mathbf{u}^{n-1})$. One possible explanation is that when Λ is an implicitly defined operator, $\|\Lambda\|$ is estimated in terms of physical wave speeds or calculated under, e.g., periodic, or uniform spatial mesh assumptions that only approximate Λ, leading to a possible slight violation of the time step condition. This drawback has led to the addition of filters such as the Robert-Asselin-Williams (RAW) time filter, see, [100, 7, 114]. However, even when time filters such as the RAW filter are included, condition (5.5) can still be too restrictive,.

In contrast, we present next the CNLF method with an added stabilization term (CNLF-stab), that achieves unconditional asymptotic stability for both the stable and unstable modes and removes all time step conditions for stability, while it also increases accuracy. In the next section we show that it contributes an additional $\mathcal{O}(\Delta t^2)$ consistency error which has the opposite sign of the consistency error of Leapfrog. The CNLF-stab method is:

Given $\mathbf{u}^0, \mathbf{u}^1 \in X$, find $\mathbf{u}^{n+1} \in X$ for $n \geq 1$ such that

$$\frac{\mathbf{u}^{n+1} - \mathbf{u}^{n-1}}{2\Delta t} + \beta \Delta t \Lambda^* \Lambda \left(\mathbf{u}^{n+1} - \mathbf{u}^{n-1} \right) + A \frac{\mathbf{u}^{n+1} + \mathbf{u}^{n-1}}{2} + \Lambda \mathbf{u}^n = \mathbf{0}, \qquad \text{(CNLF-stab)}$$

where $\beta > 1/8$. The added stabilization term, $\beta \Delta t \Lambda^* \Lambda \left(\mathbf{u}^{n+1} - \mathbf{u}^{n-1} \right)$, is linear and symmetric positive definite in the unknown $\mathbf{u}^{n+1}$. We analyze the method's consistency and stability in the next two sections respectively.

5.2   CONSISTENCY ERROR ANALYSIS

In this section we analyze the (CNLF-stab) method for consistency by comparing the consistency errors of the Crank-Nicolson (CN), Leapfrog (LF), and Leapfrog with stabilization (LF-stab) methods applied to (5.1) with $A \equiv 0$:

$$\mathbf{u}_t + \Lambda \mathbf{u} = \mathbf{0}, \ \Lambda^* = -\Lambda. \tag{5.7}$$

The CN method for (5.7) (with time step $2\Delta t$) is

$$\frac{\mathbf{u}^{n+1} - \mathbf{u}^{n-1}}{2\Delta t} + \Lambda \frac{\mathbf{u}^{n+1} + \mathbf{u}^{n-1}}{2} = \mathbf{0}, \tag{CN}$$

while the LF-stab method is ((CNLF-stab) with $A \equiv 0$)

$$\frac{\mathbf{u}^{n+1} - \mathbf{u}^{n-1}}{2\Delta t} + 2\beta\Delta t^2 \Lambda^* \Lambda \frac{\mathbf{u}^{n+1} - \mathbf{u}^{n-1}}{2\Delta t} + \Lambda \mathbf{u}^n = \mathbf{0}, \tag{LF-stab}$$

and the LF method is (LF-stab) with $\beta = 0$:

$$\frac{\mathbf{u}^{n+1} - \mathbf{u}^{n-1}}{2\Delta t} + \Lambda \mathbf{u}^n = \mathbf{0}. \tag{LF}$$

We denote by τ_{method} the consistency error of each method = LF-stab, LF, or CN. Substituting the true solution into (CN) and (LF-stab), we find, respectively

$$\frac{\mathbf{u}(t^{n+1}) - \mathbf{u}(t^{n-1})}{2\Delta t} + \Lambda \frac{\mathbf{u}(t^{n+1}) + \mathbf{u}(t^{n-1})}{2}$$
$$= \mathbf{u}_t(t^n) + \tfrac{1}{6}\Delta t^2 \mathbf{u}_{ttt}(t^n) + \Lambda \mathbf{u}(t^n) + \tfrac{1}{2}\Delta t^2 \Lambda \mathbf{u}_{tt}(t^n) + \mathcal{O}(\Delta t^4),$$
$$\frac{\mathbf{u}(t^{n+1}) - \mathbf{u}(t^{n-1})}{2\Delta t} + 2\beta\Delta t^2 \Lambda^* \Lambda \frac{\mathbf{u}(t^{n+1}) - \mathbf{u}(t^{n-1})}{2\Delta t} + \Lambda \mathbf{u}(t^n)$$
$$= \mathbf{u}_t(t^n) + \tfrac{1}{6}\Delta t^2 \mathbf{u}_{ttt}(t^n) + 2\beta\Delta t^2 \Lambda^* \Lambda \mathbf{u}_t(t^n) + \Lambda \mathbf{u}(t^n) + \mathcal{O}(\Delta t^4).$$

Since $\mathbf{u}_t = -\Lambda \mathbf{u}$, the consistency errors are

$$\tau_{\text{CN}} = \tfrac{1}{6}\Delta t^2 \mathbf{u}_{ttt} + \tfrac{1}{2}\Delta t^2 \Lambda \mathbf{u}_{tt} + \mathcal{O}(\Delta t^4),$$

$$\tau_{\text{LFSTAB}}(\beta) = 2\beta\Delta t^2 \Lambda^* \Lambda \mathbf{u}_t + \tfrac{1}{6}\Delta t^2 \mathbf{u}_{ttt} + \mathcal{O}(\Delta t^4),$$

$$\tau_{\text{LF}} = \tau_{\text{LFSTAB}}(0) = \tfrac{1}{6}\mathbf{u}_{ttt}\Delta t^2 + \mathcal{O}(\Delta t^4).$$

Table 3: Consistency errors of (CN), (LF), and (LF-stab).

Method	Leading consistency error term	Evaluated at solution u(t)
(CN)	$\frac{\Delta t^2}{6}\mathbf{u}_{ttt} + \Lambda\frac{\Delta t^2}{2}\mathbf{u}_{tt}$	$\frac{1}{3}\Delta t^2\Lambda^*\Lambda\mathbf{u}_t$
(LF)	$\frac{\Delta t^2}{6}\mathbf{u}_{ttt}$	$-\frac{1}{6}\Delta t^2\Lambda^*\Lambda\mathbf{u}_t$
(LFstab)	$\frac{\Delta t^2}{6}\mathbf{u}_{ttt} + 2\beta\Delta t^2\Lambda^*\Lambda\mathbf{u}_t$	$(2\beta - \frac{1}{6})\Delta t^2\Lambda^*\Lambda\mathbf{u}_t$

Further, by the skew symmetry of Λ, we may write $\mathbf{u}_{tt} = -\Lambda\mathbf{u}_t$ and $\mathbf{u}_{ttt} = \Lambda^2\mathbf{u}_t = -\Lambda^*\Lambda\mathbf{u}_t$. Hence, the consistency errors for (CN), (LF), and (LF-stab) become

$$\tau_{\mathrm{CN}} = \tfrac{1}{3}\Delta t^2\Lambda^*\Lambda\mathbf{u}_t + \mathcal{O}(\Delta t^4),$$

$$\tau_{\mathrm{LF}} = -\tfrac{1}{6}\Delta t^2\Lambda^*\Lambda\mathbf{u}_t + \mathcal{O}(\Delta t^4),$$

$$\tau_{\mathrm{LFSTAB}}(\beta) = \left(2\beta - \tfrac{1}{6}\right)\Delta t^2\Lambda^*\Lambda\mathbf{u}_t + \mathcal{O}(\Delta t^4).$$

Thus, the leading terms of $\tau_{\mathrm{LFSTAB}}(\beta)$ and τ_{LF} have the same form and opposite signs. This is consistent with the observation that the stabilization term errs by slowing waves, while (LF) errs by accelerating waves. See, for example, [41, p. 61, Section 2.4]. This also implies that it is possible to cancel out the leading-order term of the error by selecting $\beta = 1/12$. The leading order terms of the consistency errors for all three methods are summarized in Table 3. Up to $\mathcal{O}(\Delta t^4)$ terms, we draw the following conclusions:

1. (LF) requires fewer floating point operations than (CN), while being twice as accurate as (CN) with time step $2\Delta t$, and is comparably accurate to (CN) with time step Δt.

2. (LF-stab) is unconditionally stable and has smaller consistency errors than (LF) for $1/8 < \beta < 1/6$ (see Section 5.3 for stability results).

3. For $\beta = 1/12$, the leading-order consistency error term cancels and (LF-stab) is $\mathcal{O}(\Delta t^4)$ accurate. (LF-stab) with $\beta = 1/12$ is conditionally stable, and requires a time step condition of approximately $\Delta t\|\Lambda\| < 1.27$, which is 27% larger than (LF) (see Theorem 19 in Appendix A.3).

5.3   STABILITY ANALYSIS

In this section we prove unconditional stability of (CNLF-stab) by tracking the discrete energy in the method. The kinetic energy of (CNLF-stab) is:

$$\text{Energy}^{n+1/2} = \|\mathbf{u}^{n+1}\|^2 + \|\mathbf{u}^n\|^2 + 2\beta\Delta t^2(\|\Lambda\mathbf{u}^{n+1}\|^2 + \|\Lambda\mathbf{u}^n\|^2)$$
$$+ 2\Delta t\langle\Lambda\mathbf{u}^{n+1}, \mathbf{u}^{n+1}\rangle.$$

The first step is to establish

$$\text{Energy}^{n+1/2} - \text{Energy}^{n-1/2} + \Delta t\langle A(\mathbf{u}^{n+1} + \mathbf{u}^{n-1}), \mathbf{u}^{n+1} + \mathbf{u}^{n-1}\rangle = 0. \tag{5.8}$$

The term $\Delta t\langle A(\mathbf{u}^{n+1} + \mathbf{u}^{n-1}), \mathbf{u}^{n+1} + \mathbf{u}^{n-1}\rangle$ is nonnegative, so it dissipates energy, thereby increasing stability. When $A \equiv 0$, the method exactly conserves energy. This energy estimate implies stability if $\text{Energy}^{n+1/2} > 0$ whenever $\mathbf{u} \neq 0$. We verify this by applying the Cauchy-Schwarz and Young inequalities to show that the term with indefinite sign, $2\Delta t\langle\Lambda\mathbf{u}^n, \mathbf{u}^{n+1}\rangle$, can be absorbed into the positive terms as a part of the total system energy.

Theorem 7 (Unconditional stability of (CNLF-stab) for $\beta > 1/8$). *Consider* (5.1) *under conditions* (5.2) *and* (5.4). *Then,* (CNLF-stab) *with* $\beta > 1/8$ *is unconditionally stable:*

$$\text{Energy}^{N-1/2} + \Delta t \sum_{n=1}^{N-1}\langle A(\mathbf{u}^{n+1} + \mathbf{u}^{n-1}), \mathbf{u}^{n+1} + \mathbf{u}^{n-1}\rangle = \text{Energy}^{1/2}, \quad \forall N > 1, \tag{5.9}$$

$$\text{and} \quad \text{Energy}^{n+1/2} \geq \kappa^* \left(\|\mathbf{u}^{n+1}\|^2 + \|\mathbf{u}^n\|^2\right) > 0, \quad \forall n, \quad \text{for} \quad \mathbf{u}^{n+1}, \mathbf{u}^n \neq \mathbf{0},$$

where $\kappa^* := \left(1 - \frac{1}{8\beta}\right) > 0.$

Proof. Taking the inner product of (CNLF-stab) with $(\mathbf{u}^{n+1} + \mathbf{u}^{n-1})$ and multiplying by $2\Delta t$ gives

$$\|\mathbf{u}^{n+1}\|^2 - \|\mathbf{u}^{n-1}\|^2 + 2\beta\Delta t^2 \left\langle \Lambda^*\Lambda\left(\mathbf{u}^{n+1} - \mathbf{u}^{n-1}\right), \mathbf{u}^{n+1} + \mathbf{u}^{n-1}\right\rangle$$
$$+ \Delta t\left\langle A(\mathbf{u}^{n+1} + \mathbf{u}^{n-1}), \mathbf{u}^{n+1} + \mathbf{u}^{n-1}\right\rangle + 2\Delta t\left\langle \Lambda\mathbf{u}^n, \mathbf{u}^{n+1} + \mathbf{u}^{n-1}\right\rangle = 0. \tag{5.10}$$

The added stabilization term can be written as

$$2\beta\Delta t^2 \left\langle \Lambda^*\Lambda \left(\mathbf{u}^{n+1} - \mathbf{u}^{n-1}\right), \mathbf{u}^{n+1} + \mathbf{u}^{n-1}\right\rangle$$

$$= 2\beta\Delta t^2 \langle \Lambda\left(\mathbf{u}^{n+1} - \mathbf{u}^{n-1}\right), \Lambda(\mathbf{u}^{n+1} + \mathbf{u}^{n-1})\rangle$$

$$= 2\beta\Delta t^2 \left(\|\Lambda\mathbf{u}^{n+1}\|^2 - \|\Lambda\mathbf{u}^{n-1}\|^2\right)$$

$$= 2\beta\Delta t^2 \left\{\left(\|\Lambda\mathbf{u}^{n+1}\|^2 + \|\Lambda\mathbf{u}^n\|^2\right) - \left(\|\Lambda\mathbf{u}^n\|^2 + \|\Lambda\mathbf{u}^{n-1}\|^2\right)\right\}.$$

We define the stabilized system energy as

$$E^{n+1/2} := \|\mathbf{u}^{n+1}\|^2 + \|\mathbf{u}^n\|^2 + 2\beta\Delta t^2 \left(\|\Lambda\mathbf{u}^{n+1}\|^2 + \|\Lambda\mathbf{u}^n\|^2\right),$$

and let

$$C^{n+1/2} := \left\langle \Lambda\mathbf{u}^n, \mathbf{u}^{n+1}\right\rangle.$$

Since Λ is skew-symmetric, we have

$$\left\langle \Lambda\mathbf{u}^n, \mathbf{u}^{n+1} + \mathbf{u}^{n-1}\right\rangle = \left\langle \Lambda\mathbf{u}^n, \mathbf{u}^{n+1}\right\rangle - \left\langle \Lambda\mathbf{u}^{n-1}, \mathbf{u}^n\right\rangle = C^{n+1/2} - C^{n-1/2}.$$

Thus, (5.10) becomes

$$(E^{n+1/2} + 2\Delta t C^{n+1/2}) - (E^{n-1/2} + 2\Delta t C^{n-1/2}) + \Delta t \left\langle A(\mathbf{u}^{n+1} + \mathbf{u}^{n-1}), \mathbf{u}^{n+1} + \mathbf{u}^{n-1}\right\rangle = 0.$$

This has the form of (5.8), where the total system energy is given by

$$\text{Energy}^{n+1/2} := E^{n+1/2} + 2\Delta t C^{n+1/2}.$$

Summing the above from $n = 1$ to $N - 1$ we obtain

$$\text{Energy}^{N-1/2} + \Delta t \sum_{n=1}^{N-1} \left\langle A(\mathbf{u}^{n+1} + \mathbf{u}^{n-1}), \mathbf{u}^{n+1} + \mathbf{u}^{n-1}\right\rangle = \text{Energy}^{1/2}, \ \forall N > 1, \qquad (5.11)$$

which is (5.9). Thus, stability follows provided $\text{Energy}^{N-1/2} > 0$ for $\mathbf{u}^N, \mathbf{u}^{N-1} \neq \mathbf{0}$. We have

$$\begin{aligned}
\text{Energy}^{N-1/2} = E^{N-1/2} + 2\Delta t C^{N-1/2} &= \|\mathbf{u}^N\|^2 + \|\mathbf{u}^{N-1}\|^2 \\
&+ 2\beta\Delta t^2(\|\Lambda\mathbf{u}^N\|^2 + \|\Lambda\mathbf{u}^{N-1}\|^2) + 2\Delta t\langle\Lambda\mathbf{u}^{N-1}, \mathbf{u}^N\rangle.
\end{aligned} \qquad (5.12)$$

56

We bound the indefinite term, $2\Delta t \langle \Lambda \mathbf{u}^{N-1}, \mathbf{u}^N \rangle$, by Cauchy-Schwarz and Young as follows:

$$\begin{aligned}
|2\Delta t \langle \Lambda \mathbf{u}^{N-1}, \mathbf{u}^N \rangle| &= \Delta t |\langle \Lambda \mathbf{u}^{N-1}, \mathbf{u}^N \rangle - \langle \Lambda \mathbf{u}^N, \mathbf{u}^{N-1} \rangle| \\
&\leq \Delta t \left(\|\Lambda \mathbf{u}^{N-1}\| \|\mathbf{u}^N\| + \|\Lambda \mathbf{u}^N\| \|\mathbf{u}^{N-1}\| \right) \\
&\leq \tfrac{1}{8\beta} \left(\|\mathbf{u}^N\|^2 + \|\mathbf{u}^{N-1}\|^2 \right) + 2\beta \Delta t^2 \left(\|\Lambda \mathbf{u}^N\|^2 + \|\Lambda \mathbf{u}^{N-1}\|^2 \right).
\end{aligned} \quad (5.13)$$

Combining (5.12) and (5.13) yields

$$\text{Energy}^{N-1/2} \geq (1 - \tfrac{1}{8\beta})(\|\mathbf{u}^N\|^2 + \|\mathbf{u}^{N-1}\|^2),$$

which is positive definite for $\beta > \frac{1}{8}$, and thus stability follows. $\qquad \square$

Next we prove unconditional asymptotic stability of (CNLF-stab) for $\beta > 1/8$ when A is a symmetric positive-definite, bounded, linear operator. We denote by $\|\mathbf{u}\|_A := \sqrt{\langle A\mathbf{u}, \mathbf{u} \rangle}$ the norm induced by A.

Theorem 8 (Asymptotic stability of (CNLF-stab) for $\beta > 1/8$). *Consider* (CNLF-stab) *with $\beta > 1/8$. If A is a symmetric, positive-definite, bounded, linear operator satisfying* (5.6), *then*

$$(\mathbf{u}^{n+1} + \mathbf{u}^{n-1}) \xrightarrow{n \to \infty} \mathbf{0} \quad and \quad (\mathbf{u}^{n+1} - \mathbf{u}^{n-1}) \xrightarrow{n \to \infty} \mathbf{0}, \qquad (5.14)$$

and thus $\mathbf{u}^n \xrightarrow{n \to \infty} \mathbf{0}$.

Proof. By (5.9) and (5.6), we have that the stable mode, $(\mathbf{u}^{n+1} + \mathbf{u}^{n-1})$, satisfies

$$\Delta t a_0 \sum_{n=1}^{N-1} \|\mathbf{u}^{n+1} + \mathbf{u}^{n-1}\|^2 \leq \text{Energy}^{1/2}, \quad \forall N > 1. \qquad (5.15)$$

Thus, the series $\sum_{n=1}^{\infty} \|\mathbf{u}^{n+1} + \mathbf{u}^{n-1}\|^2$ converges, implying $(\mathbf{u}^{n+1} + \mathbf{u}^{n-1}) \xrightarrow{n \to \infty} \mathbf{0}$. To complete the proof, it remains to derive a similar estimate for the unstable mode, $(\mathbf{u}^{n+1} - \mathbf{u}^{n-1})$, since $\mathbf{u}^n = \frac{1}{2}(\mathbf{u}^n + \mathbf{u}^{n-2}) + \frac{1}{2}(\mathbf{u}^n - \mathbf{u}^{n-2})$ for all $n \geq 2$. Taking the inner product of (CNLF-stab) with the unstable mode, $(\mathbf{u}^{n+1} - \mathbf{u}^{n-1})$, and multiplying by $2\delta \Delta t$ with $\delta > 0$ (to be determined later, see (5.21)), we have:

$$\begin{aligned}
\delta \|\mathbf{u}^{n+1} - \mathbf{u}^{n-1}\|^2 + 2\beta\delta\Delta t^2 \left\langle \Lambda^* \Lambda (\mathbf{u}^{n+1} - \mathbf{u}^{n-1}), \mathbf{u}^{n+1} - \mathbf{u}^{n-1} \right\rangle \\
+ \delta\Delta t \left\langle A(\mathbf{u}^{n+1} + \mathbf{u}^{n-1}), \mathbf{u}^{n+1} - \mathbf{u}^{n-1} \right\rangle + 2\delta\Delta t \left\langle \Lambda \mathbf{u}^n, \mathbf{u}^{n+1} - \mathbf{u}^{n-1} \right\rangle = 0.
\end{aligned} \qquad (5.16)$$

Using symmetry of the operator A, and letting $\mathcal{A}^{n+1/2} := \|\mathbf{u}^{n+1}\|_A^2 + \|\mathbf{u}^n\|_A^2$, (5.16) becomes

$$
\begin{aligned}
& \delta\|\mathbf{u}^{n+1} - \mathbf{u}^{n-1}\|^2 + 2\beta\delta\Delta t^2 \left\langle \Lambda^*\Lambda(\mathbf{u}^{n+1} - \mathbf{u}^{n-1}), \mathbf{u}^{n+1} - \mathbf{u}^{n-1} \right\rangle \\
& + \delta\Delta t \left\{ \mathcal{A}^{n+1/2} - \mathcal{A}^{n-1/2} \right\} + 2\delta\Delta t \left\langle \Lambda\mathbf{u}^n, \mathbf{u}^{n+1} - \mathbf{u}^{n-1} \right\rangle = 0.
\end{aligned}
\tag{5.17}
$$

Summing (5.17) from $n = 1, \ldots, N-1$ results in

$$
\begin{aligned}
& \delta \sum_{n=1}^{N-1} \left\{ \|\mathbf{u}^{n+1} - \mathbf{u}^{n-1}\|^2 + 2\beta\Delta t^2 \|\Lambda(\mathbf{u}^{n+1} - \mathbf{u}^{n-1})\|^2 \right\} \\
& + 2\delta\Delta t \sum_{n=1}^{N-1} \left\langle \Lambda\mathbf{u}^n, \mathbf{u}^{n+1} - \mathbf{u}^{n-1} \right\rangle + \delta\Delta t \mathcal{A}^{N-1/2} = \delta\Delta t \mathcal{A}^{1/2}.
\end{aligned}
\tag{5.18}
$$

Adding together (5.15) and (5.18) yields

$$
\begin{aligned}
& \sum_{n=1}^{N-1} \left\{ a_0\Delta t \|\mathbf{u}^{n+1} + \mathbf{u}^{n-1}\|^2 + \delta\|\mathbf{u}^{n+1} - \mathbf{u}^{n-1}\|^2 + 2\beta\delta\Delta t^2 \|\Lambda(\mathbf{u}^{n+1} - \mathbf{u}^{n-1})\|^2 \right\} \\
& + 2\delta\Delta t \sum_{n=1}^{N-1} \left\langle \Lambda\mathbf{u}^n, \mathbf{u}^{n+1} - \mathbf{u}^{n-1} \right\rangle + \delta\Delta t \mathcal{A}^{N-1/2} \leq \text{Energy}^{1/2} + \delta\Delta t \mathcal{A}^{1/2}.
\end{aligned}
\tag{5.19}
$$

The next step involves bounding and subsuming the critical term:

$$
2\delta\Delta t \sum_{n=1}^{N-1} \left\langle \Lambda\mathbf{u}^n, \mathbf{u}^{n+1} - \mathbf{u}^{n-1} \right\rangle.
$$

Let $0 < \epsilon < 1$. By Cauchy-Schwarz and Young's inequality, we have

$$
\left| 2\delta\Delta t \sum_{n=1}^{N-1} \left\langle \Lambda\mathbf{u}^n, \mathbf{u}^{n+1} - \mathbf{u}^{n-1} \right\rangle \right| \leq \sum_{n=1}^{N-1} \left\{ \delta\epsilon\|\mathbf{u}^{n+1} - \mathbf{u}^{n-1}\|^2 + \tfrac{\delta}{\epsilon}\Delta t^2 \|\Lambda\mathbf{u}^n\|^2 \right\}.
$$

We now use the identity

$$
\|a\|^2 = \frac{1}{4}\|a + b\|^2 + \frac{1}{4}\|a - b\|^2 + \frac{1}{2}\left(\|a\|^2 - \|b\|^2 \right),
$$

to express the term $\|\Lambda\mathbf{u}^n\|^2$ in terms of the stable and unstable modes for all $n \geq 2$:

$$
\|\Lambda\mathbf{u}^n\|^2 = \left\| \Lambda\left(\frac{\mathbf{u}^n + \mathbf{u}^{n-2}}{2} \right) \right\|^2 + \left\| \Lambda\left(\frac{\mathbf{u}^n - \mathbf{u}^{n-2}}{2} \right) \right\|^2 + \tfrac{1}{2}\left(\|\Lambda\mathbf{u}^n\|^2 - \|\Lambda\mathbf{u}^{n-2}\|^2 \right).
$$

58

Using this, we bound $\sum_{n=1}^{N-1} \|\Lambda \mathbf{u}^n\|^2$ as follows.

$$
\sum_{n=1}^{N-1} \|\Lambda \mathbf{u}^n\|^2 = \|\Lambda \mathbf{u}^1\|^2 + \tfrac{1}{4} \sum_{n=2}^{N-1} \left\{ \|\Lambda(\mathbf{u}^n + \mathbf{u}^{n-2})\|^2 + \|\Lambda(\mathbf{u}^n - \mathbf{u}^{n-2})\|^2 \right\}
$$
$$
+ \tfrac{1}{2}(\|\Lambda \mathbf{u}^N\|^2 + \|\Lambda \mathbf{u}^{N-1}\|^2) - \tfrac{1}{2}(\|\Lambda \mathbf{u}^1\|^2 + \|\Lambda \mathbf{u}^0\|^2)
$$
$$
= \tfrac{1}{4} \sum_{n=1}^{N-2} \left\{ \|\Lambda(\mathbf{u}^{n+1} + \mathbf{u}^{n-1})\|^2 + \|\Lambda(\mathbf{u}^{n+1} - \mathbf{u}^{n-1})\|^2 \right\}
$$
$$
+ \tfrac{1}{2}(\|\Lambda \mathbf{u}^N\|^2 + \|\Lambda \mathbf{u}^{N-1}\|^2) + \tfrac{1}{2}(\|\Lambda \mathbf{u}^1\|^2 - \|\Lambda \mathbf{u}^0\|^2)
$$
$$
\le \tfrac{1}{4}\|\Lambda\|^2 \sum_{n=1}^{N-1} \|\mathbf{u}^{n+1} + \mathbf{u}^{n-1}\|^2 + \tfrac{1}{4} \sum_{n=1}^{N-1} \|\Lambda(\mathbf{u}^{n+1} - \mathbf{u}^{n-1})\|^2
$$
$$
+ \tfrac{1}{2}(\|\Lambda \mathbf{u}^N\|^2 + \|\Lambda \mathbf{u}^{N-1}\|^2) + \tfrac{1}{2}(\|\Lambda \mathbf{u}^1\|^2 + \|\Lambda \mathbf{u}^0\|^2).
$$

Hence, the bound on the critical term becomes

$$
\left| 2\delta\Delta t \sum_{n=1}^{N-1} \langle \Lambda \mathbf{u}^n, \mathbf{u}^{n+1} - \mathbf{u}^{n-1} \rangle \right| \le \delta\epsilon \sum_{n=1}^{N-1} \|\mathbf{u}^{n+1} - \mathbf{u}^{n-1}\|^2
$$
$$
+ \tfrac{\delta}{4\epsilon}\Delta t^2 \|\Lambda\|^2 \sum_{n=1}^{N-1} \|\mathbf{u}^{n+1} + \mathbf{u}^{n-1}\|^2 + \tfrac{\delta}{4\epsilon}\Delta t^2 \sum_{n=1}^{N-1} \|\Lambda(\mathbf{u}^{n+1} - \mathbf{u}^{n-1})\|^2
$$
$$
+ \tfrac{\delta}{2\epsilon}\Delta t^2 (\|\Lambda \mathbf{u}^N\|^2 + \|\Lambda \mathbf{u}^{N-1}\|^2) + \tfrac{\delta}{2\epsilon}\Delta t^2 (\|\Lambda \mathbf{u}^1\|^2 + \|\Lambda \mathbf{u}^0\|^2).
$$

Using the above, we subsume the critical term into the positive terms in (5.19):

$$
\Delta t \left(a_0 - \tfrac{\delta}{4\epsilon}\|\Lambda\|^2\Delta t \right) \sum_{n=1}^{N-1} \|\mathbf{u}^{n+1} + \mathbf{u}^{n-1}\|^2 + \delta(1-\epsilon) \sum_{n=1}^{N-1} \|\mathbf{u}^{n+1} - \mathbf{u}^{n-1}\|^2
$$
$$
+ \delta\Delta t^2 \left(2\beta - \tfrac{1}{4\epsilon} \right) \sum_{n=1}^{N-1} \|\Lambda(\mathbf{u}^{n+1} - \mathbf{u}^{n-1})\|^2 + \delta\Delta t \mathcal{A}^{N-1/2}
$$
$$
\le \text{Energy}^{1/2} + \delta\Delta t \mathcal{A}^{1/2} + \tfrac{\delta}{2\epsilon}\Delta t^2 (\|\Lambda \mathbf{u}^N\|^2 + \|\Lambda \mathbf{u}^{N-1}\|^2)
$$
$$
+ \tfrac{\delta}{2\epsilon}\Delta t^2 (\|\Lambda \mathbf{u}^1\|^2 + \|\Lambda \mathbf{u}^0\|^2)
$$
$$
\le \text{Energy}^{1/2} + \delta\Delta t \mathcal{A}^{1/2} + \tfrac{\delta}{2\epsilon}\|\Lambda\|^2\Delta t^2 (\|\mathbf{u}^N\|^2 + \|\mathbf{u}^{N-1}\|^2)
$$
$$
+ \tfrac{\delta}{2\epsilon}\Delta t^2 (\|\Lambda \mathbf{u}^1\|^2 + \|\Lambda \mathbf{u}^0\|^2).
$$

By Theorem 7, the term $\|\mathbf{u}^N\|^2 + \|\mathbf{u}^{N-1}\|^2$ is bounded above by $(1/\kappa^*)\text{Energy}^{1/2}$. Thus,

$$\Delta t \left(a_0 - \tfrac{\delta}{4\epsilon}\|\Lambda\|^2 \Delta t\right) \sum_{n=1}^{N-1} \|\mathbf{u}^{n+1} + \mathbf{u}^{n-1}\|^2 + \delta(1-\epsilon) \sum_{n=1}^{N-1} \|\mathbf{u}^{n+1} - \mathbf{u}^{n-1}\|^2$$

$$+ \delta \Delta t^2 \left(2\beta - \tfrac{1}{4\epsilon}\right) \sum_{n=1}^{N-1} \|\Lambda(\mathbf{u}^{n+1} - \mathbf{u}^{n-1})\|^2 + \delta \Delta t \mathcal{A}^{N-1/2} \qquad (5.20)$$

$$\leq (1 + \tfrac{8\beta\delta}{2\epsilon(8\beta-1)}\|\Lambda\|^2 \Delta t^2)\text{Energy}^{1/2} + \delta \Delta t \mathcal{A}^{1/2} + + \tfrac{\delta}{2\epsilon}\Delta t^2(\|\Lambda \mathbf{u}^1\|^2 + \|\Lambda \mathbf{u}^0\|^2).$$

The above implies asymptotic stability of the unstable mode provided

$$\left(a_0 - \tfrac{\delta}{4\epsilon}\|\Lambda\|^2 \Delta t\right) \geq 0,$$

$$\delta(1-\epsilon) > 0,$$

$$2\beta - \tfrac{1}{4\epsilon} \geq 0.$$

Since $0 < \epsilon < 1$ and $\beta > \tfrac{1}{8}$ the second and third inequalities are true. Therefore, (CNLF-stab) is unconditionally, asymptotically stable if the first inequality holds. Thus, if we choose

$$\delta = \frac{4a_0\epsilon}{2\Delta t\|\Lambda\|^2}, \qquad (5.21)$$

(5.20) implies that

$$\sum_{n=1}^{N-1} \|\mathbf{u}^{n+1} - \mathbf{u}^{n-1}\|^2 \leq C(\mathbf{u}^0, \mathbf{u}^1),$$

where $C(\mathbf{u}^0, \mathbf{u}^1)$ is a constant depending on $\mathbf{u}^0, \mathbf{u}^1$, but independent of N. Consequently,

$$\sum_{n=1}^{\infty} \|\mathbf{u}^{n+1} - \mathbf{u}^{n-1}\|^2 < \infty,$$

and hence $(\mathbf{u}^{n+1} - \mathbf{u}^{n-1}) \xrightarrow{n\to\infty} \mathbf{0}$, concluding the proof. □

Remark 10. *The previous conclusions imply asymptotic stability about zero. By linearity, these results extend to nonzero forcing terms, $\mathbf{F}^n = \mathbf{F}(t^n)$, on the right-hand side of (5.1), provided $\mathbf{F}_n \xrightarrow{n\to\infty} \mathbf{F}_\infty$, where $\mathbf{F}_\infty$ is the forcing term in the related equilibrium problem, in the sense that the series $\sum_{n=1}^{\infty} \|\mathbf{F}^n - \mathbf{F}_\infty\|_*^2$ converges. If this holds, then following the steps of Theorems 7 and 8, we conclude that, $(\mathbf{u}^{n+1} + \mathbf{u}^{n-1}) \xrightarrow{n\to\infty} 2\mathbf{u}_\infty$, $(\mathbf{u}^{n-1} - \mathbf{u}^{n+1}) \xrightarrow{n\to\infty} \mathbf{0}$, and $\mathbf{u}^n \xrightarrow{n\to\infty} \mathbf{u}_\infty$, where $\mathbf{u}_\infty$ solves the equilibrium problem, $A\mathbf{u}_\infty + \Lambda\mathbf{u}_\infty = \mathbf{F}_\infty$.*

6.0 A SECOND-ORDER, UNCONDITIONALLY STABLE, PARTITIONED METHOD FOR THE EVOLUTIONARY STOKES-DARCY PROBLEM

In this chapter we present a partitioned numerical method for the evolutionary Stokes-Darcy problem (3.1)-(3.12) that is strongly stable and uniformly convergent with respect to the model parameters. The method involves a stabilization of the classical Crank-Nicolson Leapfrog (CNLF) time stepping scheme for the time discretization. We prove the method's unconditional stability and second-order, uniform convergence in space and time. Further, we prove that the method controls the unstable mode of Leapfrog, by showing asymptotic stability. Numerical tests that verify the method's stability and convergence properties, as well as tests illustrating its efficiency versus fully coupled methods, are presented in Chapter 8, in Section 8.2.

6.1 INTRODUCTION AND THE CNLF-STAB METHOD

In this section, in Algorithm 2, we present the stabilized CNLF (CNLF-stab) method for the evolutionary Stokes-Darcy system. We begin with the semi-discretization of the problem in space and then present the usual CNLF method for the discretization in time. We also discuss CNLF's stability and convergence properties, which motivated the development of the CNLf-stab method. Then, in Section 6.2, we prove unconditional, asymptotic stability of CNLF-stab, and in Section 6.3 second-order convergence in space and time.

We recall from Section 3.4 the variational formulation of the evolutionary Stokes-Darcy problem (where $0 < T \leq \infty$):

Find $(\mathbf{u}, \tilde{p}, \phi) : (0, T] \to \mathbf{X}_f \times Q_f \times X_p$ *such that for all* $(\mathbf{v}, q, \psi) \in \mathbf{X}_f \times Q_f \times X_p$,

$$n(\mathbf{u}_t, \mathbf{v})_f + nb_f(\mathbf{v}, \tilde{p}) + a_f(\mathbf{u}, \mathbf{v}) + c_I(\mathbf{v}, \phi) = n(\tilde{\mathbf{f}}_f, \mathbf{v})_f, \tag{6.1}$$

$$b_f(\mathbf{u}, q) = 0, \tag{6.2}$$

$$g(S_0 \phi_t, \psi)_p + a_p(\phi, \psi) - c_I(\mathbf{u}, \psi) = g(f_p, \psi)_p, \tag{6.3}$$

given the initial data $\mathbf{u}(\mathbf{x}, 0) = \mathbf{u}_0(\mathbf{x})$ *and* $\phi(\mathbf{x}, 0) = \phi_0(\mathbf{x})$, *where* $\tilde{p} = p/\rho$, $\tilde{\mathbf{f}}_f = \mathbf{f}_f/\rho$.

To discretize the system of equations (6.1)-(6.3) in space we use the Finite Element (FE) method. We let $\mathcal{T}_h$ be a quasiuniform triangulation of $\Omega_f \cup \Omega_p$, and $h > 0$ be the maximum triangle diameter. We choose our FE spaces based on a conforming FE triangulation,

$$\text{discrete Stokes velocity space:} \quad \mathbf{X}_f^h \subset \mathbf{X}_f,$$
$$\text{discrete Stokes pressure space:} \quad Q_f^h \subset Q_f,$$
$$\text{discrete hydraulic head space:} \quad X_p^h \subset X_p,$$

and assume that $\mathbf{X}_f^h$ and Q_f^h satisfy the discrete inf-sup condition (LBB^h), see [51, 56, 80]:

$$\exists\, \beta_h^* > 0 \quad \text{such that} \quad \inf_{\substack{q_h \in Q_f^h \\ q_h \neq 0}} \sup_{\substack{\mathbf{v}_h \in \mathbf{X}_f^h \\ \mathbf{v}_h \neq \mathbf{0}}} \frac{b_f(\mathbf{v}_h, q_h)}{\|\nabla \mathbf{v}_h\|_f \|q_h\|_f} \geq \beta_h^* > 0. \tag{6.4}$$

The LBB^h condition guarantees the stability of the discrete Stokes pressure, p_h. Notice that the FE spaces $\mathbf{X}_f^h$ and X_p^h are separate and continuity is not assumed across the interface I between the two domains. We denote by $\mathbf{V}_f^h$ the discretely divergence-free space:

$$\mathbf{V}_f^h := \{\mathbf{v}_h \in \mathbf{X}_f^h : (q_h, \nabla \cdot \mathbf{v}_h)_f = 0 \ \ \forall q_h \in Q_f^h\},$$

and point out that $\mathbf{V}_f^h$ is not necessarily a subspace of the divergence-free space $\mathbf{V}_f$. The semi-discretized formulation reads:

Find $(\mathbf{u}_h, \tilde{p}_h, \phi_h) : (0, T] \to \mathbf{X}_f^h \times Q_f^h \times X_p^h$ *such that for all* $(\mathbf{v}_h, q_h, \psi_h) \in \mathbf{X}_f^h \times Q_f^h \times X_p^h$,

$$n(\mathbf{u}_{h,t}, \mathbf{v}_h)_f + a_f(\mathbf{u}_h, \mathbf{v}_h) - n(\tilde{p}_h, \nabla \cdot \mathbf{v}_h)_f + c_I(\mathbf{v}_h, \phi_h) = n(\tilde{\mathbf{f}}_f, \mathbf{v}_h)_f, \tag{6.5}$$

$$(q_h, \nabla \cdot \mathbf{u}_h)_f = 0, \tag{6.6}$$

$$gS_0(\phi_{h,t}, \psi_h)_p + a_p(\phi_h, \psi_h) - c_I(\mathbf{u}_h, \psi_h) = g(f_p, \psi_h)_p, \tag{6.7}$$

given the initial data $\mathbf{u}_h(x, 0) = \mathbf{u}_0(x)$ *and* $\phi_h(x, 0) = \phi_0(x)$.

We further discretize the problem (6.5)-(6.7) in time with the CNLF-stab time-stepping scheme (Algorithm 2 below). Before introducing the stabilized method, we present the usual CNLF method (Algorithm 1) for discretizing the problem in time, along with its stability and accuracy properties. (For a detailed analysis of the CNLF method for the Stokes-Darcy system see [75].) Let $t^k := k\Delta t$, $k = 0, 1, \ldots, N$, with $N\Delta t = T$, $0 < T \leq \infty$ (if $T = \infty$ then $N = \infty$), and $\mathbf{v}^k := \mathbf{v}(\mathbf{x}, t^k)$ for any function $\mathbf{v}(\mathbf{x}, t)$. In the proof of Proposition 6 we will use the following inverse inequality, see [14]:

$$h\|\nabla \mathbf{w}_h\|_{f/p} \leq C_{\text{inv},f/p}\|\mathbf{w}_h\|_{f/p}, \ \forall \mathbf{w} \in \mathbf{X}^h_{f/p}, \quad C_{\text{inv},f/p} > 0. \tag{6.8}$$

Algorithm 1 (The CNLF method). *The CNLF method for the evolutionary Stokes-Darcy problem is:*

$$Given \ \left(\mathbf{u}^k_h, \tilde{p}^k_h, \phi^k_h\right), \ \left(\mathbf{u}^{k-1}_h, \tilde{p}^{k-1}_h, \phi^{k-1}_h\right) \in \mathbf{X}^h_f \times Q^h_f \times X^h_p,$$

$$find \ \left(\mathbf{u}^{k+1}_h, \tilde{p}^{k+1}_h, \phi^{k+1}_h\right) \in \mathbf{X}^h_f \times Q^h_f \times X^h_p, \quad k = 1, \ldots, N - 1,$$

$$satisfying \ \forall \left(\mathbf{v}_h, q_h, \psi_h\right) \in \mathbf{X}^h_f \times Q^h_f \times X^h_p :$$

$$n\left(\frac{\mathbf{u}^{k+1}_h - \mathbf{u}^{k-1}_h}{2\Delta t}, \mathbf{v}_h\right)_f + a_f\left(\frac{\mathbf{u}^{k+1}_h + \mathbf{u}^{k-1}_h}{2}, \mathbf{v}_h\right) - n\left(\frac{\tilde{p}^{k+1}_h + \tilde{p}^{k-1}_h}{2}, \nabla \cdot \mathbf{v}_h\right)_f$$

$$+c_I(\mathbf{v}_h, \phi^k_h) = n(\tilde{\mathbf{f}}^k_f, \mathbf{v}_h)_f, \tag{6.9}$$

$$\left(q_h, \nabla \cdot \mathbf{u}^{k+1}_h\right)_f = 0, \tag{6.10}$$

$$gS_0\left(\frac{\phi^{n+1}_h - \phi^{k-1}_h}{2\Delta t}, \psi_h\right)_p + a_p\left(\frac{\phi^{k+1}_h + \phi^{k-1}_h}{2}, \psi_h\right) - c_I(\mathbf{u}^k_h, \psi_h) = g(f^k_p, \psi_h)_p \tag{6.11}$$

where $(\mathbf{u}^0_h, \phi^0_h) = (\mathbf{u}_0, \phi_0)$.

CNLF involves three levels in time and therefore, to obtain the first approximation, $(\mathbf{u}^1_h, p^1_h, \phi^1_h)$, we need to apply a one-step method. The CNLF method (6.9)-(6.11) is very efficient, in that it decouples the Stokes-Darcy system into the two sub-physics flows by using the explicit Leapfrog method for the coupling term, $c_I(\cdot, \cdot)$. This enables us to solve the sub-physics flows at each time step in parallel by highly optimized algorithms for each sub-problem. One further advantage of CNLF is that it is second-order convergent in time with optimal convergence rates in space. However, it requires a computationally restrictive (under certain parameter regimes) time step condition for stability, given in (6.12) below.

Proposition 6 (Conditional stability of CNLF). *Consider the CNLF method* (6.9)-(6.11). *Suppose*

$$\Delta t < C_{\Omega_{f/p}}^{-1} \max\left\{\min\left\{h^2 g^{-1}, S_0 n^{-1}\right\}, \min\left\{hg^{-1}, hS_0 n^{-1}\right\}\right\}, \tag{6.12}$$

where $C_{\Omega_{f/p}} := C_{T,f} C_{T,p} C_{inv,f}^{1/2} C_{inv,p}^{1/2}$, *and* $C_{T,f/p}, C_{inv,f/p} > 0$ *are the constants from the trace* (2.9) *and inverse* (6.8) *inequalities respectively. Then for any* $N > 1$ *we have*

$$n\alpha^f\left(\|\mathbf{u}_h^N\|_f^2 + \|\mathbf{u}_h^{N-1}\|_f^2\right) + g\alpha^p\left(\|\phi_h^N\|_p^2 + \|\phi_h^{N-1}\|_p^2\right)$$

$$+ \Delta t \sum_{k=1}^{N-1}\left\{\frac{n\nu}{C_K}\|\nabla\left(\mathbf{u}_h^{k+1} + \mathbf{u}_h^{k-1}\right)\|_f^2 + \frac{gk_{min}}{2}\|\nabla\left(\phi_h^{k+1} + \phi_h^{k-1}\right)\|_p^2\right\}$$

$$\leq n(\|\mathbf{u}_h^1\|_f^2 + \|\mathbf{u}_h^0\|_f^2) + gS_0\left(\|\phi_h^1\|_p^2 + \|\phi_h^0\|_p^2\right) + 2\Delta t\left(c_I(\phi_h^0, \mathbf{u}_h^1) - c_I(\phi_h^1, \mathbf{u}_h^0)\right)$$

$$+ \Delta t \sum_{k=1}^{N-1}\left\{\frac{nC_K}{\nu}\|\tilde{\mathbf{f}}_f^k\|_{-1,f}^2 + \frac{2g}{k_{min}}\|f_p^k\|_{-1,p}^2\right\}, \tag{6.13}$$

where

$$\alpha^f := \min\{1 - \Delta t\ h^{-1} g C_{\Omega_{f/p}}, 1 - \Delta t\ h^{-2} g C_{\Omega_{f/p}}\},$$

$$\alpha^p := \min\{S_0 - \Delta t\ h^{-1} n C_{\Omega_{f/p}}, S_0 - \Delta t\ n C_{\Omega_{f/p}}\},$$

are positive constants due to (6.12).

Proof. See Appendix A.4. □

The time step condition (6.12) involves the specific storage parameter, S_0, which we recall from Table 2 can be very small in value. To illustrate how restrictive the CNLF method can be, let's assume that $S_0 = \mathcal{O}(10^{-6})$, $n = \mathcal{O}(10^{-1})$, $g = \mathcal{O}(10^1)$, and $C_{\Omega_{f/p}} = \mathcal{O}(10^1)$. Then, taking $h = 0.1$ in CNLF forces the time step to be at most $\mathcal{O}(10^{-4})$ for stability. As a result, CNLF becomes impractical for computations, especially in cases of large aquifers with low conductivity which require accurate calculations over long time intervals. Furthermore, the method cannot be applied to the quasistatic Stokes-Darcy problem, where $S_0 = 0$. The stability condition (6.12) of CNLF does not explicitly depend on the hydraulic conductivity parameter, $\mathbf{K}$. However, in computations and in the presence of round-off error, CNLF becomes unstable for small values of the minimum eigenvalue of $\mathbf{K}$, k_{min}, (see Section 5.1 for

more information about the unstable and stable modes of Leapfrog). In light of the small values of k_{min} from Table 1, this can be a serious issue when using CNLF.

The CNLF-stab method (Algorithm 2) is obtained from CNLF by adding stabilization terms to both the Stokes as well as the groundwater flow equation. The resulting method is a partitioned numerical scheme that is unconditionally, asymptotically stable and second-order convergent, uniformly with respect to the model parameters. Thus, CNLF-stab retains CNLF's second-order accuracy, while eliminating the time step restriction for stability, and while also controlling the unstable mode due to Leapfrog.

Algorithm 2 (The CNLF-stab method). *Let*

$$0 < \epsilon^* < 1, \ and \ \beta^* \geq 1/(2\epsilon^*), \ so \ that \ \beta^* > 1/2. \tag{6.14}$$

The CNLF-stab algorithm for the evolutionary Stokes-Darcy problem is:

$$Given \ \left(\mathbf{u}_h^k, \tilde{p}_h^k, \phi_h^k\right), \left(\mathbf{u}_h^{k-1}, \tilde{p}_h^{k-1}, \phi_h^{k-1}\right) \in \mathbf{X}_f^h \times Q_f^h \times X_p^h,$$

$$find \ \left(\mathbf{u}_h^{k+1}, \tilde{p}_h^{k+1}, \phi_h^{k+1}\right) \in \mathbf{X}_f^h \times Q_f^h \times X_p^h, \quad k = 1, \dots, N-1,$$

$$satisfying \ \forall \, (\mathbf{v}_h, q_h, \psi_h) \in \mathbf{X}_f^h \times Q_f^h \times X_p^h:$$

$$n\left(\frac{\mathbf{u}_h^{k+1} - \mathbf{u}_h^{k-1}}{2\Delta t}, \mathbf{v}_h\right)_f + n\left(\nabla \cdot \left(\frac{\mathbf{u}_h^{k+1} - \mathbf{u}_h^{k-1}}{2\Delta t}\right), \nabla \cdot \mathbf{v}_h\right)_f + a_f\left(\frac{\mathbf{u}_h^{k+1} + \mathbf{u}_h^{k-1}}{2}, \mathbf{v}_h\right)$$

$$-n\left(\frac{\tilde{p}_h^{k+1} + \tilde{p}_h^{k-1}}{2}, \nabla \cdot \mathbf{v}_h\right)_f + c_I(\mathbf{v}_h, \phi_h^k) = n(\tilde{\mathbf{f}}_f^k, \mathbf{v}_h)_f, \tag{6.15}$$

$$\left(q_h, \nabla \cdot \mathbf{u}_h^{k+1}\right)_f = 0, \tag{6.16}$$

$$gS_0\left(\frac{\phi_h^{n+1} - \phi_h^{k-1}}{2\Delta t}, \psi_h\right)_p + a_p\left(\frac{\phi_h^{k+1} + \phi_h^{k-1}}{2}, \psi_h\right) - c_I(\mathbf{u}_h^k, \psi_h)$$

$$+\beta^* \Delta t n g^2 C_\dagger^2 [(\nabla(\phi_h^{k+1} - \phi_h^{k-1}), \nabla \psi_h)_p + (\phi_h^{k+1} - \phi_h^{k-1}, \psi_h)_p] = g(f_p^k, \psi_h)_p, \tag{6.17}$$

where $C_\dagger$ is the constant from inequality (3.46), *and* $(\mathbf{u}_h^0, \phi_h^0) = (\mathbf{u}_0, \phi_0)$.

The stabilization terms in (6.17) are of the type studied in [4], and the added term in (6.15) is grad-div stabilization of $\mathbf{u}_t$, see [94]. CNLF-stab, like CNLF, is a two-step method, and hence we must obtain the approximation $(\mathbf{u}_h^1, p_h^1, \phi_h^1)$ by using a one-step method, for example Backward Euler Leapfrog (BELF), [83]. The error in the approximation in this first step will affect the overall convergence rate of the method. Also like CNLF, CNLF-stab

decouples the two sub-physics processes, allowing for the two symmetric positive definite sub-problems to be solved in parallel at each time step. Further, the added stabilization terms,

$$n\left(\nabla \cdot \left(\frac{\mathbf{u}_h^{k+1} - \mathbf{u}_h^{k-1}}{2\Delta t}\right), \nabla \cdot \mathbf{v}_h\right)_f \quad \text{in (6.15) and}$$

$$\beta^* \Delta t n g^2 C_\dagger^2 \left[\left(\nabla(\phi_h^{k+1} - \phi_h^{k-1}), \nabla \psi_h\right)_p + \left(\phi_h^{k+1} - \phi_h^{k-1}, \psi_h\right)_p\right] \quad \text{in (6.17),}$$

add a consistency error of order Δt^2 to the CNLF method. Thus, the CNLF-stab method retains the desired accuracy and efficiency properties of CNLF, while being unconditionally, asymptotically stable and eliminating condition (6.12). The proof of unconditional, asymptotic stability of the CNLF-stab method (6.15)-(6.17) is given in Section 6.2, and the proof of second-order convergence, uniform in the model parameters, in Section 6.3.

Remark 11. *The stabilization in* (6.15)-(6.17) *is not a direct application of the stabilization* $\boldsymbol{\beta}\boldsymbol{\Delta}\mathbf{t}\boldsymbol{\Lambda}^*\boldsymbol{\Lambda}\left(\mathbf{u}^{n+1} - \mathbf{u}^{n-1}\right)$ *in* (CNLF-stab) *from Chapter 5. If we were to implement this stabilization in the Stokes-Darcy problem, we would need to define a linear operator* $\Lambda = (\Lambda_f, \Lambda_p) : \mathbf{X}_f^h \times X_p^h \to \mathbf{X}_f^h \times X_p^h$ *via the Riesz representation theorem by*

$$(\Lambda_f(\mathbf{u}, \phi), \mathbf{v})_f + (\Lambda_p(\mathbf{u}, \phi), \psi)_p = \int_I \psi \mathbf{u} \cdot \hat{\mathbf{n}}_f \, d\boldsymbol{\sigma} - \int_I \phi \mathbf{v} \cdot \hat{\mathbf{n}}_f \, d\boldsymbol{\sigma}.$$

The stabilization motivated by $\boldsymbol{\beta}\boldsymbol{\Delta}\mathbf{t}\boldsymbol{\Lambda}^*\boldsymbol{\Lambda}\left(\mathbf{u}^{n+1} - \mathbf{u}^{n-1}\right)$, *that seems most natural in appearance, is to add only a boundary integral term in each equation:*

$$\beta \Delta t n g^2 \int_I (\phi_h^{n+1} - \phi_h^{n-1}) \psi_h \, d\boldsymbol{\sigma} \quad and \quad \beta \Delta t n \int_I \left(\left(\mathbf{u}_h^{n+1} - \mathbf{u}_h^{n-1}\right) \cdot \hat{\mathbf{n}}_f\right) (\mathbf{v}_h \cdot \hat{\mathbf{n}}_f) \, d\boldsymbol{\sigma}.$$

The analysis as to whether this stabilization is sufficient for unconditional stability of the method is an open problem. However, in light of inequality (3.42), *the stabilizations in* (6.15)-(6.17) *are closely connected.*

6.2 STABILITY ANALYSIS OF CNLF-STAB

In this section, in Theorem 9, we prove unconditional stability of CNLF-stab. We recall the definitions of the norms on the dual spaces of $\mathbf{X}_f$ and X_p:

$$\|\mathbf{f}\|_{-1,f} = \sup_{\mathbf{0} \neq \mathbf{v} \in \mathbf{X}_f} \frac{(\mathbf{f}, \mathbf{v})_f}{\|\nabla \mathbf{v}\|_f},$$

$$\|f\|_{-1,p} = \sup_{0 \neq \psi \in X_p} \frac{(f, \psi)_p}{\|\nabla \psi\|_p}.$$

Theorem 9 (Unconditional stability of CNLF-stab)**.** *The CNLF-stab method* (6.15)-(6.17) *is unconditionally stable: for any $N > 1$, there holds*

$$n\alpha_1^* \left(\|\mathbf{u}_h^N\|_{div,f}^2 + \|\mathbf{u}_h^{N-1}\|_{div,f}^2 \right) + gS_0 \left(\|\phi_h^N\|_p^2 + \|\phi_h^{N-1}\|_p^2 \right)$$
$$+ \alpha_2^* \Delta t^2 n g^2 C_\dagger^2 \left(\|\phi_h^N\|_{1,p}^2 + \|\phi_h^{N-1}\|_{1,p}^2 \right)$$
$$+ \Delta t \sum_{k=1}^{N-1} \left\{ \frac{n\nu}{C_K} \|\nabla \left(\mathbf{u}_h^{k+1} + \mathbf{u}_h^{k-1} \right)\|_f^2 + \frac{gk_{min}}{2} \|\nabla \left(\phi_h^{k+1} + \phi_h^{k-1} \right)\|_p^2 \right\} \tag{6.18}$$
$$\leq 2n \left(\|\mathbf{u}_h^1\|_{div,f}^2 + \|\mathbf{u}_h^0\|_{div,f}^2 \right) + gS_0 \left(\|\phi_h^1\|_p^2 + \|\phi_h^0\|_p^2 \right)$$
$$+ 3\Delta t^2 n g^2 C_\dagger^2 \left(\|\phi_h^1\|_{1,p}^2 + \|\phi_h^0\|_{1,p}^2 \right) + \Delta t \sum_{k=1}^{N-1} \left\{ \frac{nC_K}{\rho^2 \nu} \|\mathbf{f}_f^k\|_{-1,f}^2 + \frac{2g}{k_{min}} \|f_p^k\|_{-1,p}^2 \right\},$$

where $\alpha_1^* := 1 - \epsilon^*$, and $\alpha_2^* := (2\beta^* - 1/\epsilon^*)$ are positive constants by (6.14)*.*

Proof. We set $\mathbf{v}_h = \mathbf{u}_h^{k+1} + \mathbf{u}_h^{k-1}$, $\psi_h = \phi_h^{k+1} + \phi_h^{k-1}$ in (6.15), (6.17). Then the pressure term in (6.15) cancels by (6.16). By adding the equations together and multiplying by $2\Delta t$ we get

$$n \left(\|\mathbf{u}_h^{k+1}\|_{div,f}^2 - \|\mathbf{u}_h^{k-1}\|_{div,f}^2 \right) + gS_0 \left(\|\phi_h^{k+1}\|_p^2 - \|\phi_h^{k-1}\|_p^2 \right)$$
$$+ 2\beta^* \Delta t^2 n g^2 C_\dagger^2 \left(\|\phi_h^{k+1}\|_{1,p}^2 - \|\phi_h^{k-1}\|_{1,p}^2 \right)$$
$$+ \Delta t \left\{ a_f \left(\mathbf{u}_h^{k+1} + \mathbf{u}_h^{k-1}, \mathbf{u}_h^{k+1} + \mathbf{u}_h^{k-1} \right) + a_p \left(\phi_h^{k+1} + \phi_h^{k-1}, \phi_h^{k+1} + \phi_h^{k-1} \right) \right\} \tag{6.19}$$
$$+ 2\Delta t \left(c_I(\mathbf{u}_h^{k+1} + \mathbf{u}_h^{k-1}, \phi_h^k) - c_I(\mathbf{u}_h^k, \phi_h^{k+1} + \phi_h^{k-1}) \right)$$
$$= 2\Delta t \left\{ n(\tilde{\mathbf{f}}_f^k, \mathbf{u}_h^{k+1} + \mathbf{u}_h^{k-1})_f + g \left(f_p^k, \phi_h^{k+1} + \phi_h^{k-1} \right)_p \right\}.$$

If we let

$$C^{k+1/2} = c_I(\phi_h^k, \mathbf{u}_h^{k+1}) - c_I(\phi_h^{k+1}, \mathbf{u}_h^k),$$

then we can express the interface terms in the equation above as

$$c_I(\mathbf{u}_h^{k+1} + \mathbf{u}_h^{k-1}, \phi_h^k) - c_I(\mathbf{u}_h^k, \phi_h^{k+1} + \phi_h^{k-1}) = C^{k+\frac{1}{2}} - C^{k-\frac{1}{2}}.$$

By applying the coercivity estimates (3.34), (3.36) on the left-hand side, and also using the dual norms of $\mathbf{X}_f, X_p$, and Young's inequalities on the right-hand side of (6.19), we obtain

$$
\begin{aligned}
n &\left(\|\mathbf{u}_h^{k+1}\|_{\mathrm{div},f}^2 - \|\mathbf{u}_h^{k-1}\|_{\mathrm{div},f}^2 \right) + gS_0 \left(\|\phi_h^{k+1}\|_p^2 - \|\phi_h^{k-1}\|_p^2 \right) \\
&+ 2\beta^* \Delta t^2 n g^2 C_\dagger^2 \left(\|\phi_h^{k+1}\|_{1,p}^2 - \|\phi_h^{k-1}\|_{1,p}^2 \right) + 2\Delta t \left\{ C^{k+\frac{1}{2}} - C^{k-\frac{1}{2}} \right\} \\
&+ \Delta t \left\{ \frac{2n\nu}{C_K} \|\nabla \left(\mathbf{u}_h^{k+1} + \mathbf{u}_h^{k-1} \right) \|_f^2 + gk_{min} \|\nabla \left(\phi_h^{k+1} + \phi_h^{k-1} \right) \|_p^2 \right\} \\
&\le \Delta t \frac{n\nu}{C_K} \|\nabla \left(\mathbf{u}_h^{k+1} + \mathbf{u}_h^{k-1} \right) \|_f^2 + \Delta t \frac{nC_K}{\nu} \|\tilde{\mathbf{f}}_f^k\|_{-1,f}^2 \\
&+ \Delta t \frac{gk_{min}}{2} \|\nabla \left(\phi_h^{k+1} + \phi_h^{k-1} \right) \|_p^2 + \Delta t \frac{2g}{k_{min}} \|f_p^k\|_{-1,p}^2 .
\end{aligned}
$$

Rearranging gives

$$
\begin{aligned}
n &\left(\|\mathbf{u}_h^{k+1}\|_{\mathrm{div},f}^2 - \|\mathbf{u}_h^{k-1}\|_{\mathrm{div},f}^2 \right) + gS_0 \left(\|\phi_h^{k+1}\|_p^2 - \|\phi_h^{k-1}\|_p^2 \right) \\
&+ 2\beta^* \Delta t^2 n g^2 C_\dagger^2 \left(\|\phi_h^{k+1}\|_{1,p}^2 - \|\phi_h^{k-1}\|_{1,p}^2 \right) + 2\Delta t \left\{ C^{k+\frac{1}{2}} - C^{k-\frac{1}{2}} \right\} \\
&+ \Delta t \left\{ \frac{n\nu}{C_K} \|\nabla \left(\mathbf{u}_h^{k+1} + \mathbf{u}_h^{k-1} \right) \|_f^2 + \frac{gk_{min}}{2} \|\nabla \left(\phi_h^{k+1} + \phi_h^{k-1} \right) \|_p^2 \right\} \\
&\le \Delta t \frac{nC_K}{\nu} \|\tilde{\mathbf{f}}_f^k\|_{-1,f}^2 + \Delta t \frac{2g}{k_{min}} \|f_p^k\|_{-1,p}^2 .
\end{aligned}
\tag{6.20}
$$

We denote the energy terms by

$$
\begin{aligned}
E^{k+1/2} = \; & n \left(\|\mathbf{u}_h^{k+1}\|_{\mathrm{div},f}^2 + \|\mathbf{u}_h^k\|_{\mathrm{div},f}^2 \right) + gS_0 \left(\|\phi_h^{k+1}\|_p^2 + \|\phi_h^k\|_p^2 \right) \\
& + 2\beta^* \Delta t^2 n g^2 C_\dagger^2 \left(\|\phi_h^{k+1}\|_{1,p}^2 + \|\phi_h^k\|_{1,p}^2 \right).
\end{aligned}
$$

Then (6.20) becomes

$$
\begin{aligned}
E^{k+1/2} - E^{k-1/2} + \Delta t &\left\{ \frac{n\nu}{C_K} \|\nabla \left(\mathbf{u}_h^{k+1} + \mathbf{u}_h^{k-1} \right) \|_f^2 + \frac{gk_{min}}{2} \|\nabla \left(\phi_h^{k+1} + \phi_h^{k-1} \right) \|_p^2 \right\} \\
& + 2\Delta t \left\{ C^{k+1/2} - C^{k-1/2} \right\} \le \Delta t \frac{nC_K}{\nu} \|\tilde{\mathbf{f}}_f^k\|_{-1,f}^2 + \Delta t \frac{2g}{k_{min}} \|f_p^k\|_{-1,p}^2 .
\end{aligned}
$$

Next, we sum up the inequality from $k = 1$ to $N - 1$ to find

$$E^{N-1/2} + \Delta t \sum_{k=1}^{N-1} \left\{ \frac{n\nu}{C_K} \|\nabla \left(\mathbf{u}_h^{k+1} + \mathbf{u}_h^{k-1} \right) \|_f^2 + \frac{gk_{min}}{2} \|\nabla \left(\phi_h^{k+1} + \phi_h^{k-1} \right) \|_p^2 \right\}$$

$$+ 2\Delta t C^{N-1/2} \leq E^{1/2} + 2\Delta t C^{1/2} + \Delta t \sum_{k=1}^{N-1} \left\{ \frac{nC_K}{\nu} \|\tilde{\mathbf{f}}_f^k\|_{-1,f}^2 + \frac{2g}{k_{min}} \|f_p^k\|_{-1,p}^2 \right\}. \tag{6.21}$$

We then apply inequality (3.46) to the interface terms involved in $C^{N-1/2}$ to obtain

$$|c_I(\mathbf{u}_h^N, \phi_h^{N-1})| \leq ngC_\dagger \|\mathbf{u}_h^N\|_{\mathrm{div},f} \|\phi_h^{N-1}\|_{1,p}, \quad \text{and}$$

$$|c_I(\mathbf{u}_h^{N-1}, \phi_h^N)| \leq ngC_\dagger \|\mathbf{u}_h^{N-1}\|_{\mathrm{div},f} \|\phi_h^N\|_{1,p}.$$

Thus, by the Cauchy-Schwarz and Young's inequalities we have

$$|2\Delta t C^{N-1/2}| \leq n\epsilon^* \left(\|\mathbf{u}_h^N\|_{\mathrm{div},f}^2 + \|\mathbf{u}_h^{N-1}\|_{\mathrm{div},f}^2 \right) + \frac{\Delta t^2 n g^2 C_\dagger^2}{\epsilon^*} \left(\|\phi_h^{N-1}\|_{1,p}^2 + \|\phi_h^N\|_{1,p}^2 \right).$$

Consequently,

$$E^{N-1/2} + 2\Delta t C^{N-1/2} \geq n(1 - \epsilon^*) \left(\|\mathbf{u}_h^N\|_{\mathrm{div},f}^2 + \|\mathbf{u}_h^{N-1}\|_{\mathrm{div},f}^2 \right) + gS_0 \left(\|\phi_h^N\|_p^2 + \|\phi_h^{N-1}\|_p^2 \right)$$

$$+ \left(2\beta^* - \frac{1}{\epsilon^*} \right) \Delta t^2 n g^2 C_\dagger^2 \left(\|\phi_h^N\|_{1,p}^2 + \|\phi_h^{N-1}\|_{1,p}^2 \right). \tag{6.22}$$

After combining (6.21) and (6.22) we have

$$n\alpha_1^* \left(\|\mathbf{u}_h^N\|_{\mathrm{div},f}^2 + \|\mathbf{u}_h^{N-1}\|_{\mathrm{div},f}^2 \right) + gS_0 \left(\|\phi_h^N\|_p^2 + \|\phi_h^{N-1}\|_p^2 \right)$$

$$+ \alpha_2^* \Delta t^2 n g^2 C_\dagger^2 \left(\|\phi_h^N\|_{1,p}^2 + \|\phi_h^{N-1}\|_{1,p}^2 \right)$$

$$+ \Delta t \sum_{k=1}^{N-1} \left\{ \frac{n\nu}{C_K} \|\nabla \left(\mathbf{u}_h^{k+1} + \mathbf{u}_h^{k-1} \right) \|_f^2 + \frac{gk_{min}}{2} \|\nabla \left(\phi_h^{k+1} + \phi_h^{k-1} \right) \|_p^2 \right\}$$

$$\leq n \left(\|\mathbf{u}_h^1\|_{\mathrm{div},f}^2 + \|\mathbf{u}_h^0\|_{\mathrm{div},f}^2 \right) + gS_0 \left(\|\phi_h^1\|_p^2 + \|\phi_h^0\|_p^2 \right) \tag{6.23}$$

$$+ 2\Delta t^2 n g^2 C_\dagger^2 \left(\|\phi_h^1\|_{1,p}^2 + \|\phi_h^0\|_{1,p}^2 \right) + 2\Delta t \left\{ c_I(\phi_h^0, \mathbf{u}_h^1) - c_I(\phi_h^1, \mathbf{u}_h^0) \right\}$$

$$+ \Delta t \sum_{k=1}^{N-1} \left\{ \frac{nC_K}{\rho^2\nu} \|\mathbf{f}_f^k\|_{-1,f}^2 + \frac{2g}{k_{min}} \|f_p^k\|_{-1,p}^2 \right\},$$

where $\alpha_1^* = 1 - \epsilon^* > 0, \alpha_2^* = 2\beta^* - 1/\epsilon^* > 0$. Finally, to achieve the unconditional stability bound (6.18), we bound the coupling terms on the right-hand side using (3.46) (with $C = C_\dagger$) and Young:

$$
\begin{aligned}
2\Delta t \left\{ c_I(\phi_h^0, \mathbf{u}_h^1) - c_I(\phi_h^1, \mathbf{u}_h^0) \right\} &\leq 2\Delta t n g C_\dagger \left(\|\mathbf{u}_h^1\|_{\mathrm{div},f} \|\phi_h^0\|_{1,p} + \|\mathbf{u}_h^0\|_{\mathrm{div},f} \|\phi_h^1\|_{1,p} \right) \\
&\leq n \left(\|\mathbf{u}_h^1\|_{\mathrm{div},f}^2 + \|\mathbf{u}_h^0\|_{\mathrm{div},f}^2 \right) + \Delta t^2 n g^2 C_\dagger^2 \left(\|\phi_h^1\|_{1,p}^2 + \|\phi_h^0\|_{1,p}^2 \right),
\end{aligned}
$$

concluding the proof. $\qquad\square$

Corollary 1. *If* $\tilde{\mathbf{f}}_f \equiv \mathbf{0}, f_p \equiv 0$ *in* (6.15)-(6.17), *then*

$$
\left(\mathbf{u}_h^{n+1} + \mathbf{u}_h^{n-1} \right) \xrightarrow{n \to \infty} \mathbf{0}, \quad \left(\phi_h^{n+1} + \phi_h^{n-1} \right) \xrightarrow{n \to \infty} 0.
$$

Proof. The bound (6.18) implies that the series

$$
\sum_{n=1}^{\infty} \|\nabla(\mathbf{u}_h^{n+1} + \mathbf{u}_h^{n-1})\|_f^2, \quad \sum_{n=1}^{\infty} \|\nabla(\phi_h^{n+1} + \phi_h^{n-1})\|_p^2
$$

converge. Thus, $\|\nabla(\mathbf{u}_h^{n+1} + \mathbf{u}_h^{n-1})\|_f, \|\nabla(\phi_h^{n+1} + \phi_h^{n-1})\|_p \to 0$, as $n \to \infty$, and by the Poincaré-Friedrichs inequality, $\|\mathbf{u}_h^{n+1} + \mathbf{u}_h^{n-1}\|_f, \|\phi_h^{n+1} + \phi_h^{n-1}\|_p \to 0$ as well. $\qquad\square$

This shows that the CNLF-stab method controls the stable mode of Leapfrog, $(\mathbf{u}^{n+1} + \mathbf{u}^{n-1})$. In the next subsection, we also show that CNLF-stab controls the unstable mode of Leapfrog, $(\mathbf{u}^{n+1} - \mathbf{u}^{n-1})$, as well, proving therefore that CNLF-stab is unconditionally, asymptotically stable.

6.2.1 Unconditional, asymptotic stability of CNLF-stab

In this section, in Theorem 10, we prove that the CNLF-stab method (6.15)-(6.17) is unconditionally, asymptotically stable. We express $\mathbf{u}_h^n$ and ϕ_h^n, for any $n \geq 2$, in terms of the stable and unstable modes as follows:

$$\mathbf{u}_h^n = \frac{\mathbf{u}_h^n + \mathbf{u}_h^{n-2}}{2} + \frac{\mathbf{u}_h^n - \mathbf{u}_h^{n-2}}{2},$$
$$\phi_h^n = \frac{\phi_h^n + \phi_h^{n-2}}{2} + \frac{\phi_h^n - \phi_h^{n-2}}{2}.$$

By Corollary 1, we have for the stable modes:

$$\left(\mathbf{u}_h^n + \mathbf{u}_h^{n-2}\right) \xrightarrow{n \to \infty} \mathbf{0}, \qquad \text{and} \qquad \left(\phi_h^n + \phi_h^{n-2}\right) \xrightarrow{n \to \infty} 0. \tag{6.24}$$

Thus, for asymptotic stability of the CNLF-stab method it is enough to show that if $\tilde{\mathbf{f}}_f \equiv \mathbf{0}$, $f_p \equiv 0$, then the same is true for the unstable modes:

$$\left(\mathbf{u}_h^n - \mathbf{u}_h^{n-2}\right) \xrightarrow{n \to \infty} \mathbf{0}, \qquad \text{and} \qquad \left(\phi_h^n - \phi_h^{n-2}\right) \xrightarrow{n \to \infty} 0.$$

For the proof we will use the stability bound (6.18) from Theorem 9 and also derive a second stability bound for the unstable modes in Proposition 7, proven next.

Proposition 7. *Consider the CNLF-stab method* (6.15)-(6.17) *with* $\tilde{\mathbf{f}}_f \equiv \mathbf{0}$, $f_p \equiv 0$. *Then for any* $N > 1$ *there holds*

$$\delta^* n \lambda_1 \sum_{k=1}^{N-1} \|\mathbf{u}_h^{k+1} - \mathbf{u}_h^{k-1}\|_{div,f}^2 + \delta^* g S_0 \sum_{k=1}^{N-1} \|\phi_h^{k+1} - \phi_h^{k-1}\|_p^2$$
$$+ n \lambda_2 \sum_{k=1}^{N-1} \|\nabla \left(\mathbf{u}_h^{k+1} + \mathbf{u}_h^{k-1}\right)\|_f^2 + \frac{\Delta t g}{2} \lambda_3 \sum_{k=1}^{N-1} \|\nabla \left(\phi_h^{k+1} + \phi_h^{k-1}\right)\|_p^2 \tag{6.25}$$
$$+ \delta^* \Delta t^2 n g^2 C_\dagger \lambda_4 \sum_{k=1}^{N-1} \|\phi_h^{k+1} - \phi_h^{k-1}\|_{1,p}^2 + \delta^* \Delta t \left\{ \frac{2n\nu}{C_K} \left(\|\nabla \mathbf{u}_h^N\|_f^2 + \|\nabla \mathbf{u}_h^{N-1}\|_f^2\right) \right.$$
$$\left. + g k_{min} \left(\|\nabla \phi_h^N\|_p^2 + \|\nabla \phi_h^{N-1}\|_p^2\right) \right\} \leq \widehat{C}^{**},$$

where $\widehat{C}^{**}$ *is a positive constant that depends on* $\mathbf{u}_h^1, \mathbf{u}_h^0, \phi_h^1,$ *and* ϕ_h^0, λ_i, $i = 1, \ldots, 4$ *are positive constants given in* (6.44) *below, and* $\delta^* > 0$ *is given in* (6.43).

Proof. From (6.18), if $\tilde{\mathbf{f}}_f \equiv \mathbf{0}$, $f_p \equiv 0$, we have

$$\Delta t \sum_{k=1}^{N-1} \left\{ \frac{n\nu}{C_K} \| \nabla \left(\mathbf{u}_h^{k+1} + \mathbf{u}_h^{k-1} \right) \|_f^2 + \frac{g k_{min}}{2} \| \nabla \left(\phi_h^{k+1} + \phi_h^{k-1} \right) \|_p^2 \right\} \leq C^{**}, \qquad (6.26)$$

$$n\alpha_1^* \left(\| \mathbf{u}_h^N \|_{\text{div},f}^2 + \| \mathbf{u}_h^{N-1} \|_{\text{div},f}^2 \right) + \alpha_2^* \Delta t^2 n g^2 C_\dagger^2 \left(\| \phi_h^N \|_{1,p}^2 + \| \phi_h^{N-1} \|_{1,p}^2 \right) \leq C^{**}, \qquad (6.27)$$

for all $N > 1$, where C^{**} is a positive constant that depends on $\mathbf{u}_h^0, \mathbf{u}_h^1, \phi_h^0, \phi_h^1$ and the model parameters. In (6.15)-(6.17) with $\tilde{\mathbf{f}}_f \equiv \mathbf{0}$, $f_p \equiv 0$, we choose $\mathbf{v}_h = \mathbf{u}_h^{k+1} - \mathbf{u}_h^{k-1}$, and $\psi_h = \phi_h^{k+1} - \phi_h^{k-1}$. Then, by (6.16), the pressure term in (6.15) cancels out. After multiplying each equation by $2\Delta t$, and adding together we obtain

$$n\| \mathbf{u}_h^{k+1} - \mathbf{u}_h^{k-1} \|_{\text{div},f}^2 + g S_0 \| \phi_h^{k+1} - \phi_h^{k-1} \|_p^2 + 2\beta^* \Delta t^2 n g^2 C_\dagger \| \phi_h^{k+1} - \phi_h^{k-1} \|_{1,p}^2$$
$$+ \Delta t \left\{ a_f(\mathbf{u}_h^{k+1} + \mathbf{u}_h^{k-1}, \mathbf{u}_h^{k+1} - \mathbf{u}_h^{k-1}) + a_p(\phi_h^{k+1} + \phi_h^{k-1}, \phi_h^{k+1} - \phi_h^{k-1}) \right\} \qquad (6.28)$$
$$+ 2\Delta t \left\{ c_I(\mathbf{u}_h^{k+1} - \mathbf{u}_h^{k-1}, \phi_h^k) - c_I(\mathbf{u}_h^k, \phi_h^{k+1} - \phi_h^{k-1}) \right\} = 0.$$

By symmetry of the bilinear forms $a_{f/p}(\cdot, \cdot)$, (6.28) becomes

$$n\| \mathbf{u}_h^{k+1} - \mathbf{u}_h^{k-1} \|_{\text{div},f}^2 + g S_0 \| \phi_h^{k+1} - \phi_h^{k-1} \|_p^2 + 2\beta^* \Delta t^2 n g^2 C_\dagger \| \phi_h^{k+1} - \phi_h^{k-1} \|_{1,p}^2$$
$$+ \Delta t \left\{ a_f(\mathbf{u}_h^{k+1}, \mathbf{u}_h^{k+1}) - a_f(\mathbf{u}_h^{k-1}, \mathbf{u}_h^{k-1}) + a_p(\phi_h^{k+1}, \phi_h^{k+1}) - a_p(\phi_h^{k-1}, \phi_h^{k-1}) \right\} \qquad (6.29)$$
$$+ 2\Delta t \left\{ c_I(\mathbf{u}_h^{k+1} - \mathbf{u}_h^{k-1}, \phi_h^k) - c_I(\mathbf{u}_h^k, \phi_h^{k+1} - \phi_h^{k-1}) \right\} = 0.$$

Letting

$$A_f^{k+1/2} := a_f(\mathbf{u}_h^{k+1}, \mathbf{u}_h^{k+1}) + a_f(\mathbf{u}_h^k, \mathbf{u}_h^k),$$
$$A_p^{k+1/2} := a_p(\phi_h^{k+1}, \phi_h^{k+1}) + a_p(\phi_h^k, \phi_h^k),$$

(6.29) is equivalent to

$$n\| \mathbf{u}_h^{k+1} - \mathbf{u}_h^{k-1} \|_{\text{div},f}^2 + g S_0 \| \phi_h^{k+1} - \phi_h^{k-1} \|_p^2 + 2\beta^* \Delta t^2 n g^2 C_\dagger \| \phi_h^{k+1} - \phi_h^{k-1} \|_{1,p}^2$$
$$+ \Delta t \left\{ (A_f^{k+1/2} + A_p^{k+1/2}) - (A_f^{k-1/2} + A_p^{k-1/2}) \right\} \qquad (6.30)$$
$$+ 2\Delta t \left\{ c_I(\mathbf{u}_h^{k+1} - \mathbf{u}_h^{k-1}, \phi_h^k) - c_I(\mathbf{u}_h^k, \phi_h^{k+1} - \phi_h^{k-1}) \right\} = 0.$$

We multiply (6.30) by an arbitrary $\delta^* > 0$ (to be determined later) and sum from $k = 1$ to $N - 1$ to get

$$\delta^* n \sum_{k=1}^{N-1} \|\mathbf{u}_h^{k+1} - \mathbf{u}_h^{k-1}\|_{\text{div},f}^2 + \delta^* g S_0 \sum_{k=1}^{N-1} \|\phi_h^{k+1} - \phi_h^{k-1}\|_p^2$$

$$+ 2\delta^* \beta^* \Delta t^2 n g^2 C_\dagger \sum_{k=1}^{N-1} \|\phi_h^{k+1} - \phi_h^{k-1}\|_{1,p}^2 + \delta^* \Delta t \left\{ A_f^{N-1/2} + A_p^{N-1/2} \right\}$$

$$+ 2\delta^* \Delta t \sum_{k=1}^{N-1} \left\{ c_I(\mathbf{u}_h^{k+1} - \mathbf{u}_h^{k-1}, \phi_h^k) - c_I(\mathbf{u}_h^k, \phi_h^{k+1} - \phi_h^{k-1}) \right\}$$

$$= \delta^* \Delta t \left\{ A_f^{1/2} + A_p^{1/2} \right\}.$$

By applying the continuity and coercivity bounds (3.33)-(3.36) to the terms $A_f^{N-1/2}, A_p^{N-1/2}$ and $A_f^{1/2}, A_p^{1/2}$, we obtain

$$\delta^* n \sum_{k=1}^{N-1} \|\mathbf{u}_h^{k+1} - \mathbf{u}_h^{k-1}\|_{\text{div},f}^2 + \delta^* g S_0 \sum_{k=1}^{N-1} \|\phi_h^{k+1} - \phi_h^{k-1}\|_p^2$$

$$+ 2\delta^* \beta^* \Delta t^2 n g^2 C_\dagger \sum_{k=1}^{N-1} \|\phi_h^{k+1} - \phi_h^{k-1}\|_{1,p}^2 + \delta^* \Delta t \left\{ \frac{2n\nu}{C_K} \left(\|\nabla \mathbf{u}_h^N\|_f^2 + \|\nabla \mathbf{u}_h^{N-1}\|_f^2 \right) \right.$$

$$\left. + g k_{min} \left(\|\nabla \phi_h^N\|_p^2 + \|\nabla \phi_h^{N-1}\|_p^2 \right) \right\} \tag{6.31}$$

$$+ 2\delta^* \Delta t \sum_{k=1}^{N-1} \left\{ c_I(\mathbf{u}_h^{k+1} - \mathbf{u}_h^{k-1}, \phi_h^k) - c_I(\mathbf{u}_h^k, \phi_h^{k+1} - \phi_h^{k-1}) \right\}$$

$$\leq \delta^* \Delta t \left\{ M \left(\|\nabla \mathbf{u}_h^1\|_f^2 + \|\nabla \mathbf{u}_h^0\|_f^2 \right) + g k_{max} \left(\|\nabla \phi_h^1\|_p^2 + \|\nabla \phi_h^0\|_p^2 \right) \right\},$$

where $M := n\nu \left(2 + \frac{\alpha C_{T,f}^2 C_{PF,f}}{2\sqrt{k_{min}}}\right)$. Adding together (6.31) and (6.26) yields

$$
\begin{aligned}
\delta^* n \sum_{k=1}^{N-1} \|\mathbf{u}_h^{k+1} - \mathbf{u}_h^{k-1}\|_{\mathrm{div},f}^2 &+ \delta^* g S_0 \sum_{k=1}^{N-1} \|\phi_h^{k+1} - \phi_h^{k-1}\|_p^2 \\
&+ \Delta t \sum_{k=1}^{N-1} \left\{ \frac{n\nu}{C_K} \|\nabla(\mathbf{u}_h^{k+1} + \mathbf{u}_h^{k-1})\|_f^2 + \frac{g k_{min}}{2} \|\nabla(\phi_h^{k+1} + \phi_h^{k-1})\|_p^2 \right\} \\
&+ 2\delta^* \beta^* \Delta t^2 n g^2 C_\dagger \sum_{k=1}^{N-1} \|\phi_h^{k+1} - \phi_h^{k-1}\|_{1,p}^2 + \delta^* \Delta t \left\{ \frac{2n\nu}{C_K} \left(\|\nabla \mathbf{u}_h^N\|_f^2 + \|\nabla \mathbf{u}_h^{N-1}\|_f^2\right) \right. \\
&\left. \qquad\qquad + g k_{min} \left(\|\nabla \phi_h^N\|_p^2 + \|\nabla \phi_h^{N-1}\|_p^2\right) \right\} \\
&+ 2\delta^* \Delta t \sum_{k=1}^{N-1} \left\{ c_I(\mathbf{u}_h^{k+1} - \mathbf{u}_h^{k-1}, \phi_h^k) - c_I(\mathbf{u}_h^k, \phi_h^{k+1} - \phi_h^{k-1}) \right\} \\
&\leq \delta^* \Delta t \left\{ M \left(\|\nabla \mathbf{u}_h^1\|_f^2 + \|\nabla \mathbf{u}_h^0\|_f^2\right) + g k_{max} \left(\|\nabla \phi_h^1\|_p^2 + \|\nabla \phi_h^0\|_p^2\right) \right\} + C^{**}.
\end{aligned}
\tag{6.32}
$$

The next step involves bounding the coupling terms on the left-hand side of (6.32) and then absorbing them into the positive terms. By Cauchy-Schwarz, (3.46) (with $C = C_\dagger$), and Young, we have, for some $\xi^*, \zeta^* > 0$,

$$
\begin{aligned}
\left| 2\delta^* \Delta t \sum_{k=1}^{N-1} \left\{ c_I(\mathbf{u}_h^{k+1} - \mathbf{u}_h^{k-1}, \phi_h^k) - c_I(\mathbf{u}_h^k, \phi_h^{k+1} - \phi_h^{k-1}) \right\} \right| & \\
\leq 2\delta^* \Delta t n g C_\dagger \sum_{k=1}^{N-1} \left\{ \|\mathbf{u}_h^{k+1} - \mathbf{u}_h^{k-1}\|_{\mathrm{div},f} \|\phi_h^k\|_{1,p} + \|\mathbf{u}_h^k\|_{\mathrm{div},f} \|\phi_h^{k+1} - \phi_h^{k-1}\|_{1,p} \right\} & \\
\leq \xi^* \delta^* n \sum_{k=1}^{N-1} \|\mathbf{u}_h^{k+1} - \mathbf{u}_h^{k-1}\|_{\mathrm{div},f}^2 + \frac{\delta^* n}{\xi^*} \Delta t^2 g^2 C_\dagger^2 \sum_{k=1}^{N-1} \|\phi_h^k\|_{1,p}^2 & \\
+ \zeta^* \delta^* \Delta t^2 n g^2 C_\dagger^2 \sum_{k=1}^{N-1} \|\phi_h^{k+1} - \phi_h^{k-1}\|_{1,p}^2 + \frac{\delta^* n}{\zeta^*} \sum_{k=1}^{N-1} \|\mathbf{u}_h^k\|_{\mathrm{div},f}^2. &
\end{aligned}
\tag{6.33}
$$

We now use the identity

$$
\|a\|^2 = \frac{1}{4}\|a + b\|^2 + \frac{1}{4}\|a - b\|^2 + \frac{1}{2}\left(\|a\|^2 - \|b\|^2\right),
$$

to express $\|\mathbf{u}_h^k\|_{\mathrm{div},f}^2$ and $\|\phi_h^k\|_{1,p}^2$ as follows, for all $k \geq 2$:

$$
\|\mathbf{u}_h^k\|_{\mathrm{div},f}^2 = \frac{1}{4}\|\mathbf{u}_h^k + \mathbf{u}_h^{k-2}\|_{\mathrm{div},f}^2 + \frac{1}{4}\|\mathbf{u}_h^k - \mathbf{u}_h^{k-2}\|_{\mathrm{div},f}^2 + \frac{1}{2}\left(\|\mathbf{u}_h^k\|_{\mathrm{div},f}^2 - \|\mathbf{u}_h^{k-2}\|_{\mathrm{div},f}^2\right),
$$

$$
\|\phi_h^k\|_{1,p}^2 = \frac{1}{4}\|\phi_h^k + \phi_h^{k-2}\|_{1,p}^2 + \frac{1}{4}\|\phi_h^k - \phi_h^{k-2}\|_{1,p}^2 + \frac{1}{2}\left(\|\phi_h^k\|_{1,p}^2 - \|\phi_h^{k-2}\|_{1,p}^2\right).
$$

Then

$$\sum_{k=1}^{N-1} \|\mathbf{u}_h^k\|_{\text{div},f}^2 = \|\mathbf{u}_h^1\|_{\text{div},f}^2 + \sum_{k=2}^{N-1} \|\mathbf{u}_h^k\|_{\text{div},f}^2$$

$$= \|\mathbf{u}_h^1\|_{\text{div},f}^2 + \frac{1}{4} \sum_{k=2}^{N-1} \|\mathbf{u}_h^k + \mathbf{u}_h^{k-2}\|_{\text{div},f}^2 + \frac{1}{4} \sum_{k=2}^{N-1} \|\mathbf{u}_h^k - \mathbf{u}_h^{k-2}\|_{\text{div},f}^2$$

$$+ \frac{1}{2} \sum_{k=2}^{N-1} \left(\|\mathbf{u}_h^k\|_{\text{div},f}^2 - \|\mathbf{u}_h^{k-2}\|_{\text{div},f}^2 \right)$$

$$= \|\mathbf{u}_h^1\|_{\text{div},f}^2 + \frac{1}{4} \sum_{k=1}^{N-2} \|\mathbf{u}_h^{k+1} + \mathbf{u}_h^{k-1}\|_{\text{div},f}^2 + \frac{1}{4} \sum_{k=1}^{N-2} \|\mathbf{u}_h^{k+1} - \mathbf{u}_h^{k-1}\|_{\text{div},f}^2$$

$$+ \frac{1}{2} \left(\|\mathbf{u}_h^{N-1}\|_{\text{div},f}^2 + \|\mathbf{u}_h^{N-2}\|_{\text{div},f}^2 - \|\mathbf{u}_h^1\|_{\text{div},f}^2 - \|\mathbf{u}_h^0\|_{\text{div},f}^2 \right)$$

$$\leq \frac{1}{4} \sum_{k=1}^{N-1} \|\mathbf{u}_h^{k+1} + \mathbf{u}_h^{k-1}\|_{\text{div},f}^2 + \frac{1}{4} \sum_{k=1}^{N-1} \|\mathbf{u}_h^{k+1} - \mathbf{u}_h^{k-1}\|_{\text{div},f}^2$$

$$+ \frac{1}{2} \left(\|\mathbf{u}_h^{N-1}\|_{\text{div},f}^2 + \|\mathbf{u}_h^{N-2}\|_{\text{div},f}^2 \right) + \frac{1}{2} \left(\|\mathbf{u}_h^1\|_{\text{div},f}^2 + \|\mathbf{u}_h^0\|_{\text{div},f}^2 \right).$$

Furthermore, applying (2.6) and (2.8) to the first term, we obtain

$$\sum_{k=1}^{N-1} \|\mathbf{u}_h^k\|_{\text{div},f}^2 \leq \frac{1}{4}(C_{PF,f}^2 + d) \sum_{k=1}^{N-1} \left\|\nabla \left(\mathbf{u}_h^{k+1} + \mathbf{u}_h^{k-1}\right)\right\|_f^2 + \frac{1}{4} \sum_{k=1}^{N-1} \|\mathbf{u}_h^{k+1} - \mathbf{u}_h^{k-1}\|_{\text{div},f}^2$$

$$+ \frac{1}{2} \left(\|\mathbf{u}_h^{N-1}\|_{\text{div},f}^2 + \|\mathbf{u}_h^{N-2}\|_{\text{div},f}^2 \right) + \frac{1}{2} \left(\|\mathbf{u}_h^1\|_{\text{div},f}^2 + \|\mathbf{u}_h^0\|_{\text{div},f}^2 \right). \quad (6.34)$$

Similarly,

$$\sum_{k=1}^{N-1} \|\phi_h^k\|_{1,p}^2 \leq \frac{1}{4}(C_{PF,p}^2 + 1) \sum_{k=1}^{N-1} \left\|\nabla \left(\phi_h^{k+1} + \phi_h^{k-1}\right)\right\|_p^2 + \frac{1}{4} \sum_{k=1}^{N-1} \|\phi_h^{k+1} - \phi_h^{k-1}\|_{1,p}^2$$

$$+ \frac{1}{2} \left(\|\phi_h^{N-1}\|_{1,p}^2 + \|\phi_h^{N-2}\|_{1,p}^2 \right) + \frac{1}{2} \left(\|\phi_h^1\|_{1,p}^2 + \|\phi_h^0\|_{1,p}^2 \right). \quad (6.35)$$

Combining (6.33), (6.34), and (6.35), yields

$$
\left| 2\delta^*\Delta t \sum_{k=1}^{N-1} \left\{ c_I(\mathbf{u}_h^{k+1} - \mathbf{u}_h^{k-1}, \phi_h^k) - c_I(\mathbf{u}_h^k, \phi_h^{k+1} - \phi_h^{k-1}) \right\} \right|
$$

$$
\leq \delta^* n \left(\xi^* + \frac{1}{4\zeta^*} \right) \sum_{k=1}^{N-1} \|\mathbf{u}_h^{k+1} - \mathbf{u}_h^{k-1}\|_{\mathrm{div},f}^2 + \frac{\delta^* n}{4\zeta^*}(C_{PF,f}^2 + d) \sum_{k=1}^{N-1} \|\nabla \left(\mathbf{u}_h^{k+1} + \mathbf{u}_h^{k-1} \right)\|_f^2
$$

$$
+ \frac{\delta^*}{4\xi^*}\Delta t^2 n g^2 C_\dagger^2 (C_{PF,p}^2 + 1) \sum_{k=1}^{N-1} \|\nabla \left(\phi_h^{k+1} + \phi_h^{k-1} \right)\|_p^2 \tag{6.36}
$$

$$
+ \delta^* \Delta t^2 n g^2 C_\dagger^2 \left(\zeta^* + \frac{1}{4\xi^*} \right) \sum_{k=1}^{N-1} \|\phi_h^{k+1} - \phi_h^{k-1}\|_{1,p}^2
$$

$$
+ \frac{\delta^* n}{2\zeta^*} \left(\|\mathbf{u}_h^{N-1}\|_{\mathrm{div},f}^2 + \|\mathbf{u}_h^{N-2}\|_{\mathrm{div},f}^2 \right) + \frac{\delta^*}{2\xi^*}\Delta t^2 n g^2 C_\dagger^2 \left(\|\phi_h^{N-1}\|_{1,p}^2 + \|\phi_h^{N-2}\|_{1,p}^2 \right)
$$

$$
+ \frac{\delta^* n}{2\zeta^*} \left(\|\mathbf{u}_h^1\|_{\mathrm{div},f}^2 + \|\mathbf{u}_h^0\|_{\mathrm{div},f}^2 \right) + \frac{\delta^*}{2\xi^*}\Delta t^2 n g^2 C_\dagger^2 \left(\|\phi_h^1\|_{1,p}^2 + \|\phi_h^0\|_{1,p}^2 \right).
$$

Next, we apply (6.36) on (6.32). After combining terms, the resulting inequality is

$$
\delta^* n \left(1 - \xi^* - \frac{1}{4\zeta^*} \right) \sum_{k=1}^{N-1} \|\mathbf{u}_h^{k+1} - \mathbf{u}_h^{k-1}\|_{\mathrm{div},f}^2 + \delta^* g S_0 \sum_{k=1}^{N-1} \|\phi_h^{k+1} - \phi_h^{k-1}\|_p^2
$$

$$
+ n \left(\Delta t \frac{\nu}{C_K} - \frac{\delta^*}{4\zeta^*}(C_{PF,f}^2 + d) \right) \sum_{k=1}^{N-1} \|\nabla \left(\mathbf{u}_h^{k+1} + \mathbf{u}_h^{k-1} \right)\|_f^2
$$

$$
+ \frac{\Delta t g}{2} \left(k_{min} - \frac{\delta^*}{2\xi^*}\Delta t n g C_\dagger^2 (C_{PF,p}^2 + 1) \right) \sum_{k=1}^{N-1} \|\nabla \left(\phi_h^{k+1} + \phi_h^{k-1} \right)\|_p^2
$$

$$
+ \delta^* \Delta t^2 n g^2 C_\dagger \left(2\beta^* - \zeta^* - \frac{1}{4\xi^*} \right) \sum_{k=1}^{N-1} \|\phi_h^{k+1} - \phi_h^{k-1}\|_{1,p}^2 \tag{6.37}
$$

$$
+ \delta^* \Delta t \left\{ \frac{2n\nu}{C_K} \left(\|\nabla \mathbf{u}_h^N\|_f^2 + \|\nabla \mathbf{u}_h^{N-1}\|_f^2 \right) + g k_{min} \left(\|\nabla \phi_h^N\|_p^2 + \|\nabla \phi_h^{N-1}\|_p^2 \right) \right\}
$$

$$
\leq \delta^* \Delta t \left\{ M \left(\|\nabla \mathbf{u}_h^1\|_f^2 + \|\nabla \mathbf{u}_h^0\|_f^2 \right) + g k_{max} \left(\|\nabla \phi_h^1\|_p^2 + \|\nabla \phi_h^0\|_p^2 \right) \right\} + C^{**}
$$

$$
+ \frac{\delta^* n}{2\zeta^*} \left(\|\mathbf{u}_h^{N-1}\|_{\mathrm{div},f}^2 + \|\mathbf{u}_h^{N-2}\|_{\mathrm{div},f}^2 \right) + \frac{\delta^*}{2\xi^*}\Delta t^2 n g^2 C_\dagger^2 \left(\|\phi_h^{N-1}\|_{1,p}^2 + \|\phi_h^{N-2}\|_{1,p}^2 \right)
$$

$$
+ \frac{\delta^* n}{2\zeta^*} \left(\|\mathbf{u}_h^1\|_{\mathrm{div},f}^2 + \|\mathbf{u}_h^0\|_{\mathrm{div},f}^2 \right) + \frac{\delta^*}{2\xi^*}\Delta t^2 n g^2 C_\dagger^2 \left(\|\phi_h^1\|_{1,p}^2 + \|\phi_h^0\|_{1,p}^2 \right).
$$

In light of (6.27), (6.37), results in:

$$
\delta^* n \left(1 - \xi^* - \frac{1}{4\zeta^*}\right) \sum_{k=1}^{N-1} \|\mathbf{u}_h^{k+1} - \mathbf{u}_h^{k-1}\|_{\text{div},f}^2 + \delta^* g S_0 \sum_{k=1}^{N-1} \|\phi_h^{k+1} - \phi_h^{k-1}\|_p^2
$$
$$
+ n \left(\Delta t \frac{\nu}{C_K} - \frac{\delta^*}{4\zeta^*}(C_{PF,f}^2 + d)\right) \sum_{k=1}^{N-1} \|\nabla\left(\mathbf{u}_h^{k+1} + \mathbf{u}_h^{k-1}\right)\|_f^2
$$
$$
+ \frac{\Delta t g}{2} \left(k_{min} - \frac{\delta^*}{2\xi^*}\Delta t n g C_{\dagger}^2(C_{PF,p}^2 + 1)\right) \sum_{k=1}^{N-1} \|\nabla\left(\phi_h^{k+1} + \phi_h^{k-1}\right)\|_p^2 \qquad (6.38)
$$
$$
+ \delta^* \Delta t^2 n g^2 C_{\dagger} \left(2\beta^* - \zeta^* - \frac{1}{4\xi^*}\right) \sum_{k=1}^{N-1} \|\phi_h^{k+1} - \phi_h^{k-1}\|_{1,p}^2
$$
$$
+ \delta^* \Delta t \left\{ \frac{2n\nu}{C_K}\left(\|\nabla\mathbf{u}_h^N\|_f^2 + \|\nabla\mathbf{u}_h^{N-1}\|_f^2\right) + g k_{min}\left(\|\nabla\phi_h^N\|_p^2 + \|\nabla\phi_h^{N-1}\|_p^2\right)\right\} \le \widehat{C}^{**},
$$

where $\widehat{C}^{**}$ is a positive constant depending on $\mathbf{u}_h^1, \mathbf{u}_h^0, \phi_h^1, \phi_h^0$. Thus, (6.38) implies stability as long as:

$$
1 - \xi^* - \frac{1}{4\zeta^*} > 0 \qquad (6.39)
$$

$$
\Delta t \frac{\nu}{C_K} - \frac{\delta^*}{4\zeta^*}(C_{PF,f}^2 + d) > 0 \qquad (6.40)
$$

$$
k_{min} - \frac{\delta^*}{2\xi^*}\Delta t n g C_{\dagger}^2(C_{PF,p}^2 + 1) > 0 \qquad (6.41)
$$

$$
2\beta^* - \zeta^* - \frac{1}{4\xi^*} > 0. \qquad (6.42)
$$

To satisfy (6.40) and (6.41), we choose $\delta^* > 0$ so that

$$
\delta^* < \min\left\{\zeta^* \frac{4\Delta t \nu}{C_K(C_{PF,f}^2 + d)}, \xi^* \frac{2k_{min}}{\Delta t n g C_{\dagger}^2(C_{PF,p}^2 + 1)}\right\}. \qquad (6.43)
$$

Since $\xi^*, \zeta^* > 0$, by (6.39) we need to have $\xi^* < 1$ and by (6.42) that $\zeta^* < 2\beta^*$, where $\beta^* > 1/2$ is the constant in the stabilization term in (6.17). Therefore, (6.39) and (6.42) are true for

$$
0 < \xi^* < 1, \quad \text{and} \quad \frac{1}{4(1 - \xi^*)} < \zeta^* < 2\beta^* - \frac{1}{4\xi^*}.
$$

From the ζ^*-interval, we see that for $\xi^* = 1/2$ we achieve the optimal condition for stability, $\beta^* > 1/2$, derived in Theorem 9. Thus, we choose $\xi^* = 1/2$, which forces $1/2 < \zeta^* < 2\beta^* - 1/2$. Letting

$$
\begin{aligned}
\lambda_1 &:= 1 - \xi^* - \frac{1}{4\zeta^*} > 0 \\
\lambda_2 &:= \Delta t \frac{\nu}{C_K} - \frac{\delta^*}{4\zeta^*}(C_{PF,f}^2 + d) > 0 \\
\lambda_3 &:= k_{min} - \frac{\delta^*}{2\xi^*}\Delta t ng C_{\dagger}^2(C_{PF,p}^2 + 1) > 0 \\
\lambda_4 &:= 2\beta^* - \zeta^* - \frac{1}{4\xi^*} > 0,
\end{aligned}
\tag{6.44}
$$

in (6.38) we obtain the stability bound (6.25), concluding the proof. $\qquad\square$

Theorem 10 (Unconditional asymptotic stability of CNLF-stab)**.** *Consider the CNLF-stab method* (6.15)-(6.17) *with* $\tilde{\mathbf{f}}_f \equiv \mathbf{0}, f_p = 0$. *Then*

$$
\mathbf{u}_h^n \xrightarrow{n\to\infty} \mathbf{0}, \quad \phi_h^n \xrightarrow{n\to\infty} 0.
\tag{6.45}
$$

Proof. By (6.25) we have that both

$$
\sum_{n=1}^{N-1} \|\mathbf{u}_h^{n+1} - \mathbf{u}_h^{n-1}\|_f^2, \quad \sum_{n=1}^{N-1} \|\phi_h^{n+1} - \phi_h^{n-1}\|_p^2,
$$

are bounded for any $N > 1$. Consequently,

$$
\sum_{n=1}^{\infty} \|\mathbf{u}_h^{n+1} - \mathbf{u}_h^{n-1}\|_f^2, \quad \sum_{n=1}^{\infty} \|\phi_h^{n+1} - \phi_h^{n-1}\|_p^2 < \infty,
$$

which implies that both

$$
\|\mathbf{u}_h^{n+1} - \mathbf{u}_h^{n-1}\|_f, \quad \|\phi_h^{n+1} - \phi_h^{n-1}\|_p \xrightarrow{n\to\infty} 0,
$$

and hence

$$
(\mathbf{u}_h^{n+1} - \mathbf{u}_h^{n-1}) \xrightarrow{n\to\infty} \mathbf{0}, \quad (\phi_h^{n+1} - \phi_h^{n-1}) \xrightarrow{n\to\infty} 0.
\tag{6.46}
$$

The claim of the theorem now follows by (6.46) and Corollary 1. $\qquad\square$

6.3   ERROR ANALYSIS OF CNLF-STAB

In this section, in Theorem 11, we establish the method's second-order accuracy in time over long time intervals, with optimal convergence rates in space. An essential feature of the error analysis is that no form of Grönwall's inequality is used as a tool. The strategy for proving the error estimate in Theorem 11 is:

1. Decompose the error into the error in the FE space plus the error of the projection of the true solution onto the FE space.

2. Bound the error in the space by the projection error and the consistency errors.

3. Apply the triangle inequality to bound the total error by the projection and consistency errors.

We assume that the FE spaces, $\mathbf{X}_f^h$, X_p^h, and Q_f^h, satisfy approximation properties of piecewise polynomials of degree $r - 1$, r, and $r + 1$, $r \geq 1$:

$$\inf_{\mathbf{u}_h \in \mathbf{X}_f^h} \|\mathbf{u} - \mathbf{u}_h\|_f \leq Ch^{r+1} \|\mathbf{u}\|_{H^{r+1}(\Omega_f)}$$

$$\inf_{\mathbf{u}_h \in \mathbf{X}_f^h} \|\mathbf{u} - \mathbf{u}_h\|_{1,f} \leq Ch^r \|\mathbf{u}\|_{H^{r+1}(\Omega_f)}$$

$$\inf_{\phi_h \in X_p^h} \|\phi - \phi_h\|_p \leq Ch^{r+1} \|\phi\|_{H^{r+1}(\Omega_p)} \qquad (6.47)$$

$$\inf_{\phi_h \in X_p^h} \|\phi - \phi_h\|_{1,p} \leq Ch^r \|\phi\|_{H^{r+1}(\Omega_p)}$$

$$\inf_{p_h \in Q_f^h} \|p - p_h\|_f \leq Ch^{r+1} \|p\|_{H^{r+1}(\Omega_f)}.$$

Moreover, we assume that the spaces $\mathbf{X}_f^h$ and Q_f^h satisfy the (LBB^h) condition (6.4). As a consequence, there exists a $C > 0$ such that if $\mathbf{u} \in \mathbf{V}_f$, then

$$\inf_{\mathbf{v}_h \in \mathbf{V}_h} \|\mathbf{u} - \mathbf{v}_h\|_{1,f} \leq C \inf_{\mathbf{x}_h \in \mathbf{X}_f^h} \|\mathbf{u} - \mathbf{x}_h\|_{1,f}, \qquad (6.48)$$

(see, for example, [51, Chapter II, Proof of Theorem 1.1, Equation (1.12)]). We introduce the following discrete norms, recalling that $\mathbf{v}^k = \mathbf{v}(\mathbf{x}, t^k)$, for any function $\mathbf{v}(\mathbf{x}, t)$:

$$|||\mathbf{v}|||_{L^2(0,T;\mathbf{X})}^2 := \Delta t \sum_{k=1}^{N} \|\mathbf{v}^k\|_{\mathbf{X}}^2,$$

$$|||\mathbf{v}|||_{L^\infty(0,T;\mathbf{X})} := \max_{0 \le k \le N} \|\mathbf{v}^k\|_{\mathbf{X}}, \quad \text{for any space } \mathbf{X}.$$

For the proof of Theorem 11, we will use the consistency error bounds given next.

Lemma 4 (Consistency error bounds). *The consistency errors satisfy:*

$$\Delta t \sum_{k=1}^{N-1} \left\| \mathbf{u}_t^k - \frac{\mathbf{u}^{k+1} - \mathbf{u}^{k-1}}{2\Delta t} \right\|_f^2 \le \frac{(\Delta t)^4}{20} \|\mathbf{u}_{ttt}\|_{L^2(0,T;L^2(\Omega_f))}^2 \tag{6.49}$$

$$\Delta t \sum_{k=1}^{N-1} \left\| \phi_t^k - \frac{\phi^{k+1} - \phi^{k-1}}{2\Delta t} \right\|_p^2 \le \frac{(\Delta t)^4}{20} \|\phi_{ttt}\|_{L^2(0,T;L^2(\Omega_p))}^2 \tag{6.50}$$

$$\Delta t \sum_{k=1}^{N-1} \left\| \nabla \left(\mathbf{u}^k - \frac{\mathbf{u}^{k+1} + \mathbf{u}^{k-1}}{2} \right) \right\|_f^2 \le \frac{(\Delta t)^4}{3} \|\mathbf{u}_{tt}\|_{L^2(0,T;H^1(\Omega_f))}^2 \tag{6.51}$$

$$\Delta t \sum_{k=1}^{N-1} \left\| \nabla \left(\phi^k - \frac{\phi^{k+1} + \phi^{k-1}}{2} \right) \right\|_p^2 \le \frac{(\Delta t)^4}{3} \|\phi_{tt}\|_{L^2(0,T;H^1(\Omega_p))}^2 \tag{6.52}$$

$$\Delta t \sum_{k=1}^{N-1} \left\| \nabla \left(\mathbf{u}_t^k - \frac{\mathbf{u}^{k+1} - \mathbf{u}^{k-1}}{2\Delta t} \right) \right\|_f^2 \le \frac{(\Delta t)^4}{20} \|\nabla \mathbf{u}_{ttt}\|_{L^2(0,T;L^2(\Omega_f))}^2 \tag{6.53}$$

$$\Delta t \sum_{k=1}^{N-1} \|\phi^{k+1} - \phi^{k-1}\|_{1,p}^2 \le 4(\Delta t)^2 \|\phi_t\|_{L^2(0,T;H^1(\Omega_p))}^2. \tag{6.54}$$

Proof. See Appendix A.5. □

We are now ready to prove the main result. We denote the errors by

$$\mathbf{e}_f^n = \mathbf{u}^n - \mathbf{u}_h^n, \quad e_p^n = \phi^n - \phi_h^n, \quad n = 0, 1, \ldots, N.$$

Theorem 11 (Second-order convergence of CNLF-stab). *Consider the CNLF-stab method* (6.15)-(6.17), *and assume for simplicity that* $\beta^* = 1$ *in* (6.17). *For any* $0 < T \leq \infty$, *if* $\mathbf{u}$, p, *and* ϕ *satisfy the regularity conditions*

$$
\begin{aligned}
&\mathbf{u} \in \left(L^2(0, T; H^{r+2}(\Omega_f)) \cap L^\infty(0, T; H^{r+1}(\Omega_f)) \cap H^3(0, T; H^1(\Omega_f)) \right)^d, \\
&p \in L^2(0, T; H^{r+1}(\Omega_f)), \\
&\phi \in L^2(0, T; H^{r+2}(\Omega_p)) \cap L^\infty(0, T; H^{r+1}(\Omega_p)) \cap H^3(0, T; H^1(\Omega_p)),
\end{aligned}
\tag{6.55}
$$

then there exists a constant $\widehat{C} > 0$, *independent of the mesh width h, time step* Δt, *and final time T, such that*

$$
\begin{aligned}
&\frac{n}{2}(\|\mathbf{e}^N_f\|^2_{div,f} + \|\mathbf{e}^{N-1}_f\|^2_{div,f}) + gS_0(\|e^N_p\|^2_p + \|e^{N-1}_p\|^2_p) \\
&+ \Delta t \sum_{k=1}^{N-1} \left(\frac{n\nu}{C_K} \|\nabla(\mathbf{e}^{k+1}_f + \mathbf{e}^{k-1}_f)\|^2_f + \frac{gk_{min}}{2} \|\nabla(e^{k+1}_p + e^{k-1}_p)\|^2_p \right) \\
&\leq \widehat{C} \Big\{ h^{2r} \Big[\|\mathbf{u}_t\|^2_{L^2(0,T;H^{r+1}(\Omega_f))} + \|\|\mathbf{u}\|\|^2_{L^2(0,T;H^{r+1}(\Omega_f))} + \|\|\mathbf{u}\|\|^2_{L^\infty(0,T;H^{r+1}(\Omega_f))} \\
&+ \Delta t^4 \|\phi_t\|^2_{L^2(0,T;H^{r+1}(\Omega_p))} + \|\|\phi\|\|^2_{L^2(0,T;H^{r+1}(\Omega_p))} \Big] \\
&+ h^{2r+2} \Big[\|\|p\|\|^2_{L^2(0,T;H^{r+1}(\Omega_p))} + \|\phi_t\|^2_{L^2(0,T;H^{r+1}(\Omega_p))} + \|\|\phi\|\|^2_{L^\infty(0,T;H^{r+1}(\Omega_p))} \Big] \\
&+ \Delta t^4 \Big\{ \|\mathbf{u}_{ttt}\|^2_{L^2(0,T;H^1(\Omega_f))} + \|\mathbf{u}_{tt}\|^2_{L^2(0,T;H^1(\Omega_f))} + \|\phi_{ttt}\|^2_{L^2(0,T;L^2(\Omega_p))} \\
&+ \|\phi_t\|^2_{L^2(0,T;H^1(\Omega_p))} + \|\phi_{tt}\|^2_{L^2(0,T;H^1(\Omega_p))} \Big\} + \|\mathbf{e}^1_f\|^2_{div,f} + \|e^1_p\|^2_{1,p} \Big\}.
\end{aligned}
\tag{6.56}
$$

Proof. We consider the CNLF-stab method (6.15)-(6.17) over the discretely divergence-free space $\mathbf{V}^h$, instead of $\mathbf{X}^h_f$, so that the term $\left((\tilde{p}^{k+1}_h + \tilde{p}^{k-1}_h)/2, \nabla \cdot \mathbf{v}_h \right)$ cancels out. Subtracting (6.15) and (6.17) from the variational formulation (6.1)-(6.3) evaluated at time t^k we get:

$$
\begin{aligned}
&n \left(\mathbf{u}^k_t - \frac{\mathbf{u}^{k+1}_h - \mathbf{u}^{k-1}_h}{2\Delta t}, \mathbf{v}_h \right)_f - n \left(\nabla \cdot \left(\frac{\mathbf{u}^{k+1}_h - \mathbf{u}^{k-1}_h}{2\Delta t} \right), \nabla \cdot \mathbf{v}_h \right)_f \\
&+ a_f \left(\mathbf{u}^k - \frac{\mathbf{u}^{k+1}_h + \mathbf{u}^{k-1}_h}{2}, \mathbf{v}_h \right) - n \left(\tilde{p}^k, \nabla \cdot \mathbf{v}_h \right)_f + c_I \left(\mathbf{v}_h, \phi^k - \phi^k_h \right) = 0, \\
&gS_0 \left(\phi^k_t - \frac{\phi^{k+1}_h - \phi^{k-1}_h}{2\Delta t}, \psi_h \right)_p + a_p \left(\phi^k - \frac{\phi^{k+1}_h + \phi^{k-1}_h}{2}, \psi_h \right) \\
&- \Delta t n g^2 C^2_{\dagger} \{ (\nabla(\phi^{k+1}_h - \phi^{k-1}_h), \nabla\psi_h)_p + (\phi^{k+1}_h - \phi^{k-1}_h, \psi_h)_p \} - c_I \left(\mathbf{u}^k - \mathbf{u}^k_h, \psi_h \right) = 0.
\end{aligned}
$$

Since $\mathbf{v}_h$ is discretely divergence-free, we have that

$$\left(\tilde{p}^k, \nabla \cdot \mathbf{v}_h\right)_f = \left(\tilde{p}^k - \lambda_h^k, \nabla \cdot \mathbf{v}_h\right)_f, \text{ for any } \lambda_h \in Q_f^h.$$

Further, $\left(\nabla \cdot \mathbf{u}_t^k, \mathbf{v}_h\right) = 0$. Thus, after rearranging, we get:

$$n\left(\frac{\mathbf{e}_f^{k+1} - \mathbf{e}_f^{k-1}}{2\Delta t}, \mathbf{v}_h\right)_f + n\left(\nabla \cdot \left(\frac{\mathbf{e}_f^{k+1} - \mathbf{e}_f^{k-1}}{2\Delta t}\right), \nabla \cdot \mathbf{v}_h\right)_f + a_f\left(\frac{\mathbf{e}_f^{k+1} + \mathbf{e}_f^{k+1}}{2}, \mathbf{v}_h\right)$$

$$+ c_I\left(\mathbf{v}_h, e_p^k\right) = -n\left(\mathbf{u}_t^k - \frac{\mathbf{u}^{k+1} - \mathbf{u}^{k-1}}{2\Delta t}, \mathbf{v}_h\right)_f - n\left(\nabla \cdot \left(\mathbf{u}_t^k - \frac{\mathbf{u}^{k+1} - \mathbf{u}^{k-1}}{2\Delta t}\right), \nabla \cdot \mathbf{v}_h\right)_f$$

$$- a_f\left(\mathbf{u}^k - \frac{\mathbf{u}^{k+1} + \mathbf{u}^{k-1}}{2}, \mathbf{v}_h\right) + n\left(\tilde{p}^k - \lambda_h^k, \nabla \cdot \mathbf{v}_h\right)_f,$$

$$gS_0\left(\frac{e_p^{k+1} - e_p^{k-1}}{2\Delta t}, \psi_h\right)_p + a_p\left(\frac{e_p^{k+1} + e_p^{k-1}}{2}, \psi_h\right) + \Delta tng^2C_\dagger^2\left\{(\nabla(e_p^{k+1} - e_p^{k-1}), \nabla\psi_h)_p\right.$$

$$\left. + (e_p^{k+1} - e_p^{k-1}, \psi_h)_p\right\} - c_I\left(\mathbf{e}_f^k, \psi_h\right)$$

$$= -gS_0\left(\phi_t^k - \frac{\phi^{k+1} - \phi^{k-1}}{2\Delta t}, \psi_h\right)_p - a_p\left(\phi^k - \frac{\phi^{k+1} + \phi^{k-1}}{2}, \psi_h\right)$$

$$+ \Delta tng^2C_\dagger^2\left\{(\nabla(\phi^{k+1} - \phi^{k-1}), \nabla\psi_h)_p + (\phi^{k+1} - \phi^{k-1}, \psi_h)_p\right\}.$$

We denote the consistency errors by:

$$\varepsilon_f^k(\mathbf{v}_h) = -n\left(\mathbf{u}_t^k - \frac{\mathbf{u}^{k+1} - \mathbf{u}^{k-1}}{2\Delta t}, \mathbf{v}_h\right)_f - n\left(\nabla \cdot \left(\mathbf{u}_t^k - \frac{\mathbf{u}^{k+1} - \mathbf{u}^{k-1}}{2\Delta t}\right), \nabla \cdot \mathbf{v}_h\right)_f$$

$$- a_f\left(\mathbf{u}^k - \frac{\mathbf{u}^{k+1} + \mathbf{u}^{k-1}}{2}, \mathbf{v}_h\right),$$

$$\varepsilon_p^k(\psi_h) = -gS_0\left(\phi_t^k - \frac{\phi^{k+1} - \phi^{k-1}}{2\Delta t}, \psi_h\right)_p + \Delta tng^2C_\dagger^2\left\{(\nabla(\phi^{k+1} - \phi^{k-1}), \nabla\psi_h)_p\right.$$

$$\left. + (\phi^{k+1} - \phi^{k-1}, \psi_h)_p\right\} - a_p\left(\phi^k - \frac{\phi^{k+1} + \phi^{k-1}}{2}, \psi_h\right).$$

Next, we decompose the error terms into

$$\mathbf{e}_f^{k+1} = \mathbf{u}^{k+1} - \mathbf{u}_h^{k+1} = (\mathbf{u}^{k+1} - \tilde{\mathbf{u}}^{k+1}) + (\tilde{\mathbf{u}}^{k+1} - \mathbf{u}_h^{k+1}) =: \boldsymbol{\eta}_f^{k+1} + \boldsymbol{\xi}_f^{k+1},$$

$$e_p^{k+1} = \phi^{k+1} - \phi_h^{k+1} = (\phi^{k+1} - \tilde{\phi}^{k+1}) + (\tilde{\phi}^{k+1} - \phi_h^{k+1}) =: \eta_p^{k+1} + \xi_p^{k+1},$$

and take $\tilde{\mathbf{u}}^{k+1} \in \mathbf{V}^h$, so that $\boldsymbol{\xi}_f^{k+1} \in \mathbf{V}^h$, and $\tilde{\phi}^{k+1} \in X_p^h$. Then the error equations become:

$$n\left(\frac{\boldsymbol{\xi}_f^{k+1} - \boldsymbol{\xi}_f^{k-1}}{2\Delta t}, \mathbf{v}_h\right)_f + n\left(\nabla \cdot \left(\frac{\boldsymbol{\xi}_f^{k+1} - \boldsymbol{\xi}_f^{k-1}}{2\Delta t}\right), \mathbf{v}_h\right)_f + a_f\left(\frac{\boldsymbol{\xi}_f^{k+1} + \boldsymbol{\xi}_f^{k-1}}{2}, \mathbf{v}_h\right)$$

$$+ c_I(\mathbf{v}_h, \xi_p^k) = -n\left(\frac{\boldsymbol{\eta}_f^{k+1} - \boldsymbol{\eta}_f^{k-1}}{2\Delta t}, \mathbf{v}_h\right)_f - n\left(\nabla \cdot \left(\frac{\boldsymbol{\eta}_f^{k+1} - \boldsymbol{\eta}_f^{k-1}}{2\Delta t}\right), \nabla \cdot \mathbf{v}_h\right)_f$$

$$- a_f\left(\frac{\boldsymbol{\eta}_f^{k+1} + \boldsymbol{\eta}_f^{k-1}}{2}, \mathbf{v}_h\right) - c_I(\mathbf{v}_h, \eta_p^k) + \varepsilon_f^k(\mathbf{v}_h) + n\left(\tilde{p}^k - \lambda_h^k, \nabla \cdot \mathbf{v}_h\right)_f,$$

$$gS_0\left(\frac{\xi_p^{k+1} - \xi_p^{k-1}}{2\Delta t}, \psi_h\right)_p + a_p\left(\frac{\xi_p^{k+1} + \xi_p^{k-1}}{2}, \psi_h\right) + \Delta t n g^2 C_\dagger^2\left\{(\nabla(\xi_p^{k+1} - \xi_p^{k-1}), \nabla\psi_h)_p\right.$$

$$\left. + (\xi_p^{k+1} - \xi_p^{k-1}, \psi_h)_p\right\} - c_I(\boldsymbol{\xi}_f^k, \psi_h)$$

$$= -gS_0\left(\frac{\eta_p^{k+1} - \eta_p^{k-1}}{2\Delta t}, \psi_h\right)_p - a_p\left(\frac{\eta_p^{k+1} + \eta_p^{k-1}}{2}, \psi_h\right) + c_I(\boldsymbol{\eta}_f^k, \psi_h)$$

$$- \Delta t n g^2 C_\dagger^2\left\{(\nabla(\eta_p^{k+1} - \eta_p^{k-1}), \nabla\psi_h)_p + (\eta_p^{k+1} - \eta_p^{k-1}, \psi_h)_p\right\} + \varepsilon_p^k(\psi_h).$$

Picking $\mathbf{v}_h = \boldsymbol{\xi}_f^{k+1} + \boldsymbol{\xi}_f^{k-1} \in \mathbf{V}^h$ and $\psi_h = \xi_p^{k+1} + \xi_p^{k-1} \in X_p^h$ in the equations above and adding together, we obtain:

$$\frac{1}{2\Delta t}\left(n\|\boldsymbol{\xi}_f^{k+1}\|_{\text{div},f}^2 + gS_0\|\xi_p^{k+1}\|_p^2 + \Delta t^2 n g^2 C_\dagger^2\|\xi_p^{k+1}\|_{1,p}^2\right)$$

$$- \frac{1}{2\Delta t}\left(n\|\boldsymbol{\xi}_f^{k-1}\|_{\text{div},f}^2 + gS_0\|\xi_p^{k-1}\|_p^2 + \Delta t^2 n g^2 C_\dagger^2\|\xi_p^{k-1}\|_{1,p}^2\right)$$

$$+ \left[c_I(\boldsymbol{\xi}_f^{k+1} + \boldsymbol{\xi}_f^{k-1}, \xi_p^k) - c_I(\boldsymbol{\xi}_f^k, \xi_p^{k+1} + \xi_p^{k-1})\right]$$

$$+ \frac{1}{2}\left[a_f(\boldsymbol{\xi}_f^{k+1} + \boldsymbol{\xi}_f^{k-1}, \boldsymbol{\xi}_f^{k+1} + \boldsymbol{\xi}_f^{k-1}) + a_p(\xi_p^{k+1} + \xi_p^{k-1}, \xi_p^{k+1} + \xi_p^{k-1})\right]$$

$$= -\frac{n}{2\Delta t}\left[\left(\boldsymbol{\eta}_f^{k+1} - \boldsymbol{\eta}_f^{k-1}, \boldsymbol{\xi}_f^{k+1} + \boldsymbol{\xi}_f^{k-1}\right)_f + \left(\nabla \cdot (\boldsymbol{\eta}_f^{k+1} - \boldsymbol{\eta}_f^{k-1}), \nabla \cdot (\boldsymbol{\xi}_f^{k+1} - \boldsymbol{\xi}_f^{k+1}))\right)_f\right]$$

$$- \frac{gS_0}{2\Delta t}\left(\eta_p^{k+1} - \eta_p^{k-1}, \xi_p^{k+1} + \xi_p^{k-1}\right)_p$$

$$- \Delta t n g^2 C_\dagger^2\left\{(\nabla(\eta_p^{k+1} - \eta_p^{k-1}), \nabla(\xi_p^{k+1} + \xi_p^{k-1}))_p + (\eta_p^{k+1} - \eta_p^{k-1}, \xi_p^{k+1} + \xi_p^{k-1})_p\right\}$$

$$- \frac{1}{2}\left[a_f\left(\boldsymbol{\eta}_f^{k+1} + \boldsymbol{\eta}_f^{k-1}, \boldsymbol{\xi}_f^{k+1} + \boldsymbol{\xi}_f^{k-1}\right) + a_p\left(\eta_p^{k+1} + \eta_p^{k-1}, \xi_p^{k+1} + \xi_p^{k-1}\right)\right]$$

$$- \left[c_I(\boldsymbol{\xi}_f^{k+1} + \boldsymbol{\xi}_f^{k-1}, \eta_p^k) - c_I(\boldsymbol{\eta}_f^k, \xi_p^{k+1} + \xi_p^{k-1})\right]$$

$$+ \varepsilon_f^k(\boldsymbol{\xi}_f^{k+1} + \boldsymbol{\xi}_f^{k-1}) + n\left(\tilde{p}^k - \lambda_h^k, \nabla \cdot (\boldsymbol{\xi}_f^{k+1} + \boldsymbol{\xi}_f^{k-1})\right)_f + \varepsilon_p^k(\xi_p^{k+1} + \xi_p^{k-1}).$$

We rewrite the coupling terms on the left-hand side equivalently as follows:

$$c_I(\boldsymbol{\xi}_f^{k+1} + \boldsymbol{\xi}_f^{k-1}, \xi_p^k) - c_I(\boldsymbol{\xi}_f^k, \xi_p^{k+1} + \xi_p^{k-1})$$
$$= \left(c_I(\boldsymbol{\xi}_f^{k+1}, \xi_p^k) - c_I(\boldsymbol{\xi}_f^k, \xi_p^{k+1})\right) - \left(c_I(\boldsymbol{\xi}_f^k, \xi_p^{k-1}) - c_I(\boldsymbol{\xi}_f^{k-1}, \xi_p^k)\right)$$
$$=: C_\xi^{k+\frac{1}{2}} - C_\xi^{k-\frac{1}{2}}.$$

We denote the "ξ" energy terms by

$$E_\xi^{k+1/2} := n\|\boldsymbol{\xi}_f^{k+1}\|_{\mathrm{div},f}^2 + gS_0\|\xi_p^{k+1}\|_p^2 + \Delta t^2 ng^2 C_\dagger^2 \|\xi_p^{k+1}\|_{1,p}^2$$
$$+ n\|\boldsymbol{\xi}_f^k\|_{\mathrm{div},f}^2 + gS_0\|\xi_p^k\|_p^2 + \Delta t^2 ng^2 C_\dagger^2 \|\xi_p^k\|_{1,p}^2$$

and also apply the coercivity estimates (3.34),(3.36) for $a_{f/p}(\cdot,\cdot)$. Then, after also multiplying by $2\Delta t$, the inequality becomes

$$E_\xi^{k+1/2} + 2\Delta t C_\xi^{k+\frac{1}{2}} - E_\xi^{k-1/2} - 2\Delta t C_\xi^{k-\frac{1}{2}}$$
$$+ \Delta t \left(\frac{2n\nu}{C_K}\|\nabla(\boldsymbol{\xi}_f^{k+1} + \boldsymbol{\xi}_f^{k-1})\|_f^2 + gk_{min}\|\nabla(\xi_p^{k+1} + \xi_p^{k-1}\|_p^2\right)$$
$$\leq -n\left[\left(\boldsymbol{\eta}_f^{k+1} - \boldsymbol{\eta}_f^{k-1}, \boldsymbol{\xi}_f^{k+1} + \boldsymbol{\xi}_f^{k-1}\right)_f + \left(\nabla \cdot \left(\boldsymbol{\eta}_f^{k+1} - \boldsymbol{\eta}_f^{k-1}\right), \nabla \cdot \left(\boldsymbol{\xi}_f^{k+1} + \boldsymbol{\xi}_f^{k-1}\right)\right)_f\right]$$
$$- [gS_0\left(\eta_p^{k+1} - \eta_p^{k-1}, \xi_p^{k+1} + \xi_p^{k-1}\right)_p + 2\Delta t^2 ng^2 C_\dagger^2 \left\{(\nabla(\eta_p^{k+1} - \eta_p^{k-1}), \nabla(\xi_p^{k+1} + \xi_p^{k-1}))_p\right.$$
$$\left. + (\eta_p^{k+1} - \eta_p^{k-1}, \xi_p^{k+1} + \xi_p^{k-1})_p\right\}] \tag{6.57}$$
$$- \Delta t \left[a_f\left(\boldsymbol{\eta}_f^{k+1} + \boldsymbol{\eta}_f^{k-1}, \boldsymbol{\xi}_f^{k+1} + \boldsymbol{\xi}_f^{k-1}\right) + a_p\left(\eta_p^{k+1} + \eta_p^{k-1}, \xi_p^{k+1} + \xi_p^{k-1}\right)\right]$$
$$- 2\Delta t \left[c_I(\boldsymbol{\xi}_f^{k+1} + \boldsymbol{\xi}_f^{k-1}, \eta_p^k) - c_I(\boldsymbol{\eta}_f^k, \xi_p^{k+1} + \xi_p^{k-1})\right]$$
$$+ 2\Delta t \left[\varepsilon_f^k(\boldsymbol{\xi}_f^{k+1} + \boldsymbol{\xi}_f^{k-1}) + n(\tilde{p}^k - \lambda_h^k, \nabla \cdot (\boldsymbol{\xi}_f^{k+1} + \boldsymbol{\xi}_f^{k-1}))_f + \varepsilon_p^k(\xi_p^{k+1} + \xi_p^{k-1})\right].$$

Next, we bound each term on the right-hand side of (6.57). For the first two terms we apply the Cauchy-Schwarz and Young's inequalities along with the Poincaré-Friedrichs inequalities (4.12),(4.13) and inequality (2.8):

$$n\left(\boldsymbol{\eta}_f^{k+1} - \boldsymbol{\eta}_f^{k-1}, \boldsymbol{\xi}_f^{k+1} + \boldsymbol{\xi}_f^{k-1}\right)_f + n\left(\nabla \cdot (\boldsymbol{\eta}_f^{k+1} - \boldsymbol{\eta}_f^{k-1}), \nabla \cdot (\boldsymbol{\xi}_f^{k+1} + \boldsymbol{\xi}_f^{k-1})\right)_f$$
$$\leq \frac{3nC_K C_{PF,f}^2}{\nu\Delta t}\|\boldsymbol{\eta}_f^{k+1} - \boldsymbol{\eta}_f^{k-1}\|_f^2 + \frac{3nC_K d^2}{\nu\Delta t}\|\nabla\left(\eta_f^{k+1} - \eta_f^{k-1}\right)\|_f^2 + \Delta t\frac{n\nu}{6C_K}\|\nabla(\boldsymbol{\xi}_f^{k+1} + \boldsymbol{\xi}_f^{k-1})\|_f^2,$$

$$gS_0(\eta_p^{k+1} - \eta_p^{k-1}, \xi_p^{k+1} + \xi_p^{k-1})_p + 2\Delta t^2 ng^2 C_\dagger^2 \left\{ \left(\nabla \left(\eta_p^{k+1} - \eta_p^{k-1} \right), \nabla \left(\xi_p^{k+1} + \xi_p^{k-1} \right) \right)_p \right.$$

$$\left. + \left(\eta_p^{k+1} - \eta_p^{k-1}, \xi_p^{k+1} + \xi_p^{k-1} \right)_p \right\}$$

$$\leq \frac{15 g C_{PF,p}^2}{2 k_{min} \Delta t} \left(S_0^2 + 4\Delta t^4 n^2 g^2 C_\dagger^4 \right) \| \eta_p^{k+1} - \eta_p^{k-1} \|_p^2$$

$$+ \frac{30 \Delta t^3 n^2 g^3 C_\dagger^4}{k_{min}} \| \nabla \left(\eta_p^{k+1} - \eta_p^{k-1} \right) \|_p^2 + \Delta t \frac{g k_{min}}{10} \| \nabla (\xi_p^{k+1} + \xi_p^{k-1}) \|_p^2.$$

To bound the third term, we apply the continuity bounds (3.33),(3.35) for $a_{f/p}(\cdot, \cdot)$. Letting $M := n\nu \left(2 + \frac{\alpha C_{T,f}^2 C_{PF,f}}{2\sqrt{k_{min}}} \right)$ gives:

$$a_f(\boldsymbol{\eta}_f^{k+1} + \boldsymbol{\eta}_f^{k-1}, \boldsymbol{\xi}_f^{k+1} + \boldsymbol{\xi}_f^{k-1}) + a_p(\eta_p^{k+1} + \eta_p^{k-1}, \xi_p^{k+1} + \xi_p^{k-1})$$

$$\leq M \| \nabla(\boldsymbol{\eta}_f^{k+1} + \boldsymbol{\eta}_f^{k-1}) \|_f \| \nabla(\boldsymbol{\xi}_f^{k+1} + \boldsymbol{\xi}_f^{k-1}) \|_f + g k_{max} \| \nabla(\eta_p^{k+1} + \eta_p^{k-1}) \|_p \| \nabla(\xi_p^{k+1} + \xi_p^{k-1}) \|_p$$

$$\leq \frac{3 M^2 C_K}{2 n \nu} \| \nabla(\boldsymbol{\eta}_f^{k+1} + \boldsymbol{\eta}_f^{k-1}) \|_f^2 + \frac{5 g k_{max}^2}{2 k_{min}} \| \nabla(\eta_p^{k+1} + \eta_p^{k-1}) \|_p^2$$

$$+ \frac{n\nu}{6 C_K} \| \nabla(\boldsymbol{\xi}_f^{k+1} + \boldsymbol{\xi}_f^{k-1}) \|_f^2 + \frac{g k_{min}}{10} \| \nabla(\xi_p^{k+1} + \xi_p^{k-1}) \|_p^2.$$

We bound the coupling terms on the right-hand side using (2.9), Poincaré-Friedrichs (4.12),(4.13), and Young inequalities. Letting $C = C_{T,f}^2 C_{T,p}^2 C_{PF,f} C_{PF,p}$, this yields

$$c_I(\boldsymbol{\xi}_f^{k+1} + \boldsymbol{\xi}_f^{k-1}, \eta_p^k) - c_I(\boldsymbol{\eta}_f^k, \xi_p^{k+1} + \xi_p^{k-1})$$

$$\leq ng \left(\| (\boldsymbol{\xi}_f^{k+1} + \boldsymbol{\xi}_f^{k-1}) \cdot \hat{\mathbf{n}}_f \|_I \| \eta_p^k \|_I + \| \boldsymbol{\eta}_f^k \cdot \hat{\mathbf{n}}_f \|_I \| \xi_p^{k+1} + \xi_p^{k-1} \|_I \right)$$

$$\leq ng C_{T,f} C_{T,p} \left\{ \| \boldsymbol{\xi}_f^{k+1} + \boldsymbol{\xi}_f^{k-1} \|_f^{1/2} \| \nabla(\boldsymbol{\xi}_f^{k+1} + \boldsymbol{\xi}_f^{k-1}) \|_f^{1/2} \| \eta_p^k \|_p^{1/2} \| \nabla \eta_p^k \|_p^{1/2} \right.$$

$$\left. + \| \xi_p^{k+1} + \xi_p^{k-1} \|_p^{1/2} \| \nabla(\xi_p^{k+1} + \xi_p^{k-1}) \|_p^{1/2} \| \boldsymbol{\eta}_f^k \|_f^{1/2} \| \nabla \boldsymbol{\eta}_f^k \|_f^{1/2} \right\}$$

$$\leq ng C_{T,f} C_{T,p} C_{PF,f}^{1/2} C_{PF,p}^{1/2} \left\{ \| \nabla(\boldsymbol{\xi}_f^{k+1} + \boldsymbol{\xi}_f^{k-1}) \|_f \| \nabla \eta_p^k \|_p \right.$$

$$\left. + \| \nabla(\xi_p^{k+1} + \xi_p^{k-1}) \|_p \| \nabla \boldsymbol{\eta}_f^k \|_f \right\}$$

$$= ng\sqrt{C} \left(\| \nabla(\boldsymbol{\xi}_f^{k+1} + \boldsymbol{\xi}_f^{k-1}) \|_f \| \nabla \eta_p^k \|_p + \| \nabla \boldsymbol{\eta}_f^k \|_f \| \nabla(\xi_p^{k+1} + \xi_p^{k-1}) \|_p \right)$$

$$\leq \frac{5 n^2 g C}{k_{min}} \| \nabla \boldsymbol{\eta}_f^k \|_f^2 + \frac{3 n g^2 C C_K}{\nu} \| \nabla \eta_p^k \|_p^2$$

$$+ \frac{n\nu}{12 C_K} \| \nabla(\boldsymbol{\xi}_f^{k+1} + \boldsymbol{\xi}_f^{k-1}) \|_f^2 + \frac{g k_{min}}{20} \| \nabla(\xi_p^{k+1} + \xi_p^{k-1}) \|_p^2.$$

Finally, we bound the consistency errors, ε_f^k and ε_p^k, and the pressure term by using the Cauchy-Schwarz, Young and Poincaré-Friedrichs (4.12),(4.13) inequalities as well as (2.8):

$$
\begin{aligned}
\varepsilon_f^k(\boldsymbol{\xi}_f^{k+1} + \boldsymbol{\xi}_f^{k-1}) = & -n\left(\mathbf{u}_t^k - \frac{\mathbf{u}^{k+1} - \mathbf{u}^{k-1}}{2\Delta t}, \boldsymbol{\xi}_f^{k+1} + \boldsymbol{\xi}_f^{k-1}\right)_f \\
& -n\left(\nabla \cdot \left(\mathbf{u}_t^k - \frac{\mathbf{u}^{k+1} - \mathbf{u}^{k-1}}{2\Delta t}\right), \nabla \cdot \left(\boldsymbol{\xi}_f^{k+1} + \boldsymbol{\xi}_f^{k-1}\right)\right)_f \\
& -a_f\left(\mathbf{u}^k - \frac{\mathbf{u}^{k+1} + \mathbf{u}^{k-1}}{2}, \boldsymbol{\xi}_f^{k+1} + \boldsymbol{\xi}_f^{k-1}\right) \\
\leq & \left\{ nC_{PF,f}\left\|\mathbf{u}_t^k - \frac{\mathbf{u}^{k+1} - \mathbf{u}^{k-1}}{2\Delta t}\right\|_f + nd\left\|\nabla\left(\mathbf{u}_t^k - \frac{\mathbf{u}^{k+1} - \mathbf{u}^{k-1}}{2\Delta t}\right)\right\|_f \right.\\
& \left. +M\left\|\nabla\left(\mathbf{u}^k - \frac{\mathbf{u}^{k+1} + \mathbf{u}^{k-1}}{2}\right)\right\|_f \right\} \|\nabla(\boldsymbol{\xi}_f^{k+1} + \boldsymbol{\xi}_f^{k-1})\|_f \\
\leq & \frac{9nC_{PF,f}^2 C_K}{2\nu}\left\|\mathbf{u}_t^k - \frac{\mathbf{u}^{k+1} - \mathbf{u}^{k-1}}{2\Delta t}\right\|_f^2 + \frac{9nd^2 C_K}{2\nu}\left\|\nabla\left(\mathbf{u}_t^k - \frac{\mathbf{u}^{k+1} + \mathbf{u}^{k-1}}{2\Delta t}\right)\right\|_f^2 \\
& + \frac{9M^2 C_K}{2\nu}\left\|\nabla\left(\mathbf{u}^k - \frac{\mathbf{u}^{k+1} + \mathbf{u}^{k-1}}{2}\right)\right\|_f^2 + \frac{n\nu}{6C_K}\|\nabla(\boldsymbol{\xi}_f^{k+1} + \boldsymbol{\xi}_f^{k-1})\|_f^2,
\end{aligned}
$$

$$
\begin{aligned}
\varepsilon_p^k(\xi_p^{k+1} + \xi_p^{k-1}) = & -gS_0\left(\phi_t^k - \frac{\phi^{k+1} - \phi^{k-1}}{2\Delta t}, \xi_p^{k+1} + \xi_p^{k-1}\right)_p \\
& + \Delta tng^2 C_\dagger^2\left\{(\nabla(\phi^{k+1} - \phi^{k-1}), \nabla(\xi_p^{k+1} + \xi_p^{k-1}))_p \right.\\
& \left. +(\phi^{k+1} - \phi^{k-1}, \xi_p^{k+1} + \xi_p^{k-1})_p\right\} - a_p\left(\phi^k - \frac{\phi^{k+1} + \phi^{k-1}}{2}, \xi_p^{k+1} + \xi_p^{k-1}\right) \\
\leq & \left\{ gS_0 C_{PF,p}\left\|\phi_t^k - \frac{\phi^{k+1} - \phi^{k-1}}{2\Delta t}\right\|_p + \Delta tng^2 C_\dagger^2(1 + C_{PF,p})\|\nabla(\phi^{k+1} - \phi^{k-1})\|_p \right.\\
& \left. +gk_{max}\left\|\nabla\left(\phi^k - \frac{\phi^{k+1} + \phi^{k-1}}{2}\right)\right\|_p \right\} \|\nabla(\xi_p^{k+1} + \xi_p^{k-1})\|_p \\
\leq & \frac{10gS_0^2 C_{PF,p}^2}{k_{min}}\left\|\phi_t^k - \frac{\phi^{k+1} - \phi^{k-1}}{2\Delta t}\right\|_p^2 + \frac{10\Delta t^2 n^2 g^3 C_\dagger^4}{k_{min}}\|\nabla(\phi^{k+1} - \phi^{k-1})\|_p^2 \\
& + \frac{10\Delta t^2 n^2 g^3 C_\dagger^4 C_{PF,p}^2}{k_{min}}\|\phi^{k+1} - \phi^{k-1}\|_p^2 + \frac{10gk_{max}^2}{k_{min}}\left\|\nabla\left(\phi^k - \frac{\phi^{k+1} + \phi^{k-1}}{2}\right)\right\|_p^2 \\
& + \frac{gk_{min}}{10}\|\nabla(\xi_p^{k+1} + \xi_p^{k-1})\|_p^2,
\end{aligned}
$$

$$n\left(\tilde{p}^k - \lambda_h^k, \nabla\cdot(\boldsymbol{\xi}_f^{k+1} + \boldsymbol{\xi}_f^{k-1})\right)_f \leq n\sqrt{d}\|\tilde{p}^k - \lambda_h^k\|_f\|\nabla(\boldsymbol{\xi}_f^{k+1} + \boldsymbol{\xi}_f^{k-1})\|_f$$
$$\leq \frac{3ndC_K}{\nu}\|\tilde{p}^k - \lambda_h^k\|_f^2 + \frac{n\nu}{12C_K}\|\nabla(\boldsymbol{\xi}_f^{k+1} + \boldsymbol{\xi}_f^{k-1})\|_f^2.$$

We now absorb all the resulting "ξ" terms into the left-hand side of inequality (6.57). After also grouping together the remaining terms, the inequality becomes

$$E_\xi^{k+\frac{1}{2}} + 2\Delta t C_\xi^{k+\frac{1}{2}} - E_\xi^{k-\frac{1}{2}} - 2\Delta t C_\xi^{k-\frac{1}{2}}$$
$$+ \Delta t\left(\frac{n\nu}{C_K}\|\nabla(\boldsymbol{\xi}_f^{k+1} + \boldsymbol{\xi}_f^{k-1})\|_f^2 + \frac{gk_{min}}{2}\|\nabla(\xi_p^{k+1} + \xi_p^{k-1})\|_p^2\right)$$
$$\leq (\Delta t)^{-1}\left\{\frac{3nC_KC_{PF,f}^2}{\nu}\|\boldsymbol{\eta}_f^{k+1} - \boldsymbol{\eta}_f^{k-1}\|_f^2 + \frac{15gC_{PF,p}^2}{2k_{min}}\left(S_0^2 + 4\Delta t^4 n^2 g^2 C_\dagger^4\right)\|\eta_p^{k+1} - \eta_p^{k-1}\|_p^2\right.$$
$$\left.+ \frac{3nC_Kd^2}{\nu}\|\nabla\left(\boldsymbol{\eta}_f^{k+1} - \boldsymbol{\eta}_f^{k-1}\right)\|_f^2\right\}$$
$$+ \Delta t\left\{\frac{30\Delta t^2 n^2 g^3 C_\dagger^4}{k_{min}}\|\nabla\left(\eta_p^{k+1} - \eta_p^{k-1}\right)\|_p^2 + \frac{3M^2C_K}{2n\nu}\|\nabla(\boldsymbol{\eta}_f^{k+1} + \boldsymbol{\eta}_f^{k-1})\|_f^2\right.$$
$$+ \frac{5gk_{max}^2}{2k_{min}}\|\nabla(\eta_p^{k+1} + \eta_p^{k-1})\|_p^2 + \frac{10n^2gC}{k_{min}}\|\nabla\boldsymbol{\eta}_f^k\|_f^2 + \frac{6ng^2CC_K}{\nu}\|\nabla\eta_p^k\|_p^2$$
$$+ \frac{9nC_{PF,f}^2C_K}{\nu}\left\|\mathbf{u}_t^k - \frac{\mathbf{u}^{k+1} - \mathbf{u}^{k-1}}{2\Delta t}\right\|_f^2 + \frac{9nd^2C_K}{\nu}\left\|\nabla\left(\mathbf{u}_t^k - \frac{\mathbf{u}^{k+1} - \mathbf{u}^{k-1}}{2\Delta t}\right)\right\|_f^2$$
$$+ \frac{9M^2C_K}{\nu}\left\|\nabla\left(\mathbf{u}^k - \frac{\mathbf{u}^{k+1} + \mathbf{u}^{k-1}}{2}\right)\right\|_f^2 + \frac{6ndC_K}{\nu}\|\tilde{p}^k - \lambda_h^k\|_f^2$$
$$+ \frac{20gS_0^2C_{PF,p}^2}{k_{min}}\left\|\phi_t^k - \frac{\phi^{k+1} - \phi^{k-1}}{2\Delta t}\right\|_p^2 + \frac{20\Delta t^2 n^2 g^3 C_\dagger^4}{k_{min}}\|\nabla(\phi^{k+1} - \phi^{k-1})\|_p^2$$
$$\left.+ \frac{20\Delta t^2 n^2 g^3 C_\dagger^4 C_{PF,p}^2}{k_{min}}\|\phi^{k+1} - \phi^{k-1}\|_p^2 + \frac{20gk_{max}^2}{k_{min}}\left\|\nabla\left(\phi^k - \frac{\phi^{k+1} + \phi^{k-1}}{2}\right)\right\|_p^2\right\}.$$

Summing up the above inequality from $k = 1, ..., N-1$ yields

$$E_\xi^{N-\frac{1}{2}} + 2\Delta t C_\xi^{N-\frac{1}{2}} - E_\xi^{\frac{1}{2}} - 2\Delta t C_\xi^{\frac{1}{2}}$$

$$+ \Delta t \sum_{k=1}^{N-1} \left(\frac{n\nu}{C_K} \|\nabla(\boldsymbol{\xi}_f^{k+1} + \boldsymbol{\xi}_f^{k-1})\|_f^2 + \frac{gk_{min}}{2} \|\nabla(\xi_p^{k+1} + \xi_p^{k-1})\|_p^2 \right)$$

$$\leq (\Delta t)^{-1} \sum_{k=1}^{N-1} \left\{ \frac{3nC_K C_{PF,f}^2}{\nu} \|\boldsymbol{\eta}_f^{k+1} - \boldsymbol{\eta}_f^{k-1}\|_f^2 + \frac{15g C_{PF,p}^2}{2k_{min}} \left(S_0^2 + 4\Delta t^4 n^2 g^2 C_\dagger^4 \right) \|\eta_p^{k+1} - \eta_p^{k-1}\|_p^2 \right.$$

$$\left. + \frac{3nC_K d^2}{\nu} \|\nabla\left(\boldsymbol{\eta}_f^{k+1} - \boldsymbol{\eta}_f^{k-1}\right)\|_f^2 \right\}$$

$$+ \Delta t \sum_{k=1}^{N-1} \left\{ \frac{30\Delta t^2 n^2 g^3 C_\dagger^4}{k_{min}} \|\nabla\left(\eta_p^{k+1} - \eta_p^{k-1}\right)\|_p^2 + \frac{3M^2 C_K}{2n\nu} \|\nabla(\boldsymbol{\eta}_f^{k+1} + \boldsymbol{\eta}_f^{k-1})\|_f^2 \right.$$

$$+ \frac{5g k_{max}^2}{2k_{min}} \|\nabla(\eta_p^{k+1} + \eta_p^{k-1})\|_p^2 + \frac{10n^2 gC}{k_{min}} \|\nabla\boldsymbol{\eta}_f^k\|_f^2 + \frac{6ng^2 C C_K}{\nu} \|\nabla\eta_p^k\|_p^2 \qquad (6.58)$$

$$+ \frac{9nC_{PF,f}^2 C_K}{\nu} \left\| \mathbf{u}_t^k - \frac{\mathbf{u}^{k+1} - \mathbf{u}^{k-1}}{2\Delta t} \right\|_f^2 + \frac{9nd^2 C_K}{\nu} \left\| \nabla\left(\mathbf{u}_t^k - \frac{\mathbf{u}^{k+1} - \mathbf{u}^{k-1}}{2\Delta t} \right) \right\|_f^2$$

$$+ \frac{9M^2 C_K}{\nu} \left\| \nabla\left(\mathbf{u}^k - \frac{\mathbf{u}^{k+1} + \mathbf{u}^{k-1}}{2} \right) \right\|_f^2 + \frac{6ndC_K}{\nu} \|\tilde{p}^k - \lambda_h^k\|_f^2$$

$$+ \frac{20g S_0^2 C_{PF,p}^2}{k_{min}} \left\| \phi_t^k - \frac{\phi^{k+1} - \phi^{k-1}}{2\Delta t} \right\|_p^2 + \frac{20\Delta t^2 n^2 g^3 C_\dagger^4}{k_{min}} \|\nabla(\phi^{k+1} - \phi^{k-1})\|_p^2$$

$$+ \frac{20\Delta t^2 n^2 g^3 C_\dagger^4 C_{PF,p}^2}{k_{min}} \|\phi^{k+1} - \phi^{k-1}\|_p^2 + \frac{20g k_{max}^2}{k_{min}} \left\| \nabla\left(\phi^k - \frac{\phi^{k+1} + \phi^{k-1}}{2} \right) \right\|_p^2 \right\}.$$

Next, we bound each sum on the right-hand side using norms as follows.

$$\sum_{k=1}^{N-1} \|\boldsymbol{\eta}_f^{k+1} - \boldsymbol{\eta}_f^{k-1}\|_f^2 = \sum_{k=1}^{N-1} \left\| \int_{t^{k-1}}^{t^{k+1}} \boldsymbol{\eta}_{f,t} \, dt \right\|_f^2$$

$$\leq \sum_{k=1}^{N-1} \int_{\Omega_f} 2\Delta t \left(\int_{t^{k-1}}^{t^{k+1}} |\boldsymbol{\eta}_{f,t}|^2 \, dt \right) \, dx$$

$$\leq 4\Delta t \|\boldsymbol{\eta}_{f,t}\|_{L^2(0,T;L^2(\Omega_f))}^2, \qquad (6.59)$$

$$\sum_{k=1}^{N-1} \|\eta_p^{k+1} - \eta_p^{k-1}\|_f^2 \leq 4\Delta t \|\eta_{p,t}\|_{L^2(0,T;L^2(\Omega_p))}^2. \qquad (6.60)$$

Similarly,

$$\sum_{k=1}^{N-1} \|\nabla \left(\boldsymbol{\eta}_f^{k+1} - \boldsymbol{\eta}_f^{k-1}\right)\|_f^2 \leq 4\Delta t \|\nabla \boldsymbol{\eta}_{f,t}\|_{L^2(0,T;L^2(\Omega_f))}^2, \tag{6.61}$$

$$\sum_{k=1}^{N-1} \|\nabla \left(\eta_p^{k+1} - \eta_p^{k-1}\right)\|_p^2 \leq 4\Delta t \|\nabla \eta_{p,t}\|_{L^2(0,T;L^2(\Omega_p))}^2. \tag{6.62}$$

Inequalities (6.59) and (6.61) imply

$$\sum_{k=1}^{N-1} \left\{ \|\boldsymbol{\eta}_f^{k+1} - \boldsymbol{\eta}_f^{k-1}\|_f^2 + \|\nabla \left(\boldsymbol{\eta}_f^{k+1} - \boldsymbol{\eta}_f^{k-1}\right)\|_f^2 \right\} \leq 4\Delta t \|\boldsymbol{\eta}_{f,t}\|_{L^2(0,T;H^1(\Omega_f))}^2. \tag{6.63}$$

For the remaining "η" terms we use Cauchy-Schwarz and the discrete norms:

$$\begin{aligned}
\sum_{k=1}^{N-1} \|\nabla(\boldsymbol{\eta}_f^{k+1} + \boldsymbol{\eta}_f^{k-1})\|_f^2 &\leq 2\sum_{k=1}^{N-1} \left(\|\nabla \boldsymbol{\eta}_f^{k+1}\|_f^2 + \|\nabla \boldsymbol{\eta}_f^{k-1}\|_f^2\right) \\
&\leq 4\sum_{k=0}^{N} \|\nabla \boldsymbol{\eta}_f^k\|_f^2 \leq 4(\Delta t)^{-1} \|\nabla \boldsymbol{\eta}_f\|_{L^2(0,T;L^2(\Omega_f))}^2,
\end{aligned} \tag{6.64}$$

$$\sum_{k=1}^{N-1} \|\nabla(\eta_p^{k+1} + \eta_p^{k-1})\|_f^2 \leq 4(\Delta t)^{-1} \|\nabla \eta_p\|_{L^2(0,T;L^2(\Omega_p))}^2, \tag{6.65}$$

$$\sum_{k=1}^{N-1} \|\nabla \boldsymbol{\eta}_f^k\|_f^2 \leq (\Delta t)^{-1} \|\nabla \boldsymbol{\eta}_f\|_{L^2(0,T;L^2(\Omega_f))}^2, \tag{6.66}$$

$$\sum_{k=1}^{N-1} \|\nabla \eta_p^k\|_p^2 \leq (\Delta t)^{-1} \|\nabla \eta_p\|_{L^2(0,T;L^2(\Omega_p))}^2, \tag{6.67}$$

$$\sum_{k=1}^{N-1} \|\tilde{p}^k - \lambda_h^k\|_f^2 \leq (\Delta t)^{-1} \|\tilde{p} - \lambda_h\|_{L^2(0,T;L^2(\Omega_f))}^2. \tag{6.68}$$

We now apply the bounds (6.59)-(6.68), (6.49)-(6.54), and (6.22) from the stability proof, in (6.58). After absorbing all the constants into $\widehat{C}_1 > 0$, we obtain

$$\begin{aligned}
&\frac{n}{2}(\|\boldsymbol{\xi}_f^N\|_{\mathrm{div},f}^2 + \|\boldsymbol{\xi}_f^{N-1}\|_{\mathrm{div},f}^2) + gS_0(\|\xi_p^N\|_p^2 + \|\xi_p^{N-1}\|_p^2) \\
&\quad + \Delta t \sum_{k=1}^{N-1} \left(\frac{n\nu}{C_K}\|\nabla(\boldsymbol{\xi}_f^{k+1} + \boldsymbol{\xi}_f^{k-1})\|_f^2 + \frac{gk_{min}}{2}\|\nabla(\xi_p^{k+1} + \xi_p^{k-1})\|_p^2\right) \\
&\leq \widehat{C}_1 \left\{ \|\boldsymbol{\eta}_{f,t}\|_{L^2(0,T;H^1(\Omega_f))}^2 + \|\eta_{p,t}\|_{L^2(0,T;L^2(\Omega_p))}^2 + \Delta t^4 \|\nabla \eta_{p,t}\|_{L^2(0,T;L^2(\Omega_p))}^2 \right. \\
&\quad + \|\nabla \boldsymbol{\eta}_f\|_{L^2(0,T;L^2(\Omega_f))}^2 + \|\nabla \eta_p\|_{L^2(0,T;L^2(\Omega_p))}^2 + \Delta t^4 \left(\|\mathbf{u}_{ttt}\|_{L^2(0,T;H^1(\Omega_f))}^2\right. \\
&\quad + \|\mathbf{u}_{tt}\|_{L^2(0,T;H^1(\Omega_f))}^2 + \|\phi_{ttt}\|_{L^2(0,T;L^2(\Omega_p))}^2 + \|\phi_t\|_{L^2(0,T,H^1(\Omega_p))}^2 \\
&\quad \left.\left. + \|\phi_{tt}\|_{L^2(0,T;H^1(\Omega_p))}^2\right) + \|\tilde{p} - \lambda_h\|_{L^2(0,T;L^2(\Omega_f))}^2 \right\} + E_\xi^{1/2} + 2\Delta t C_\xi^{1/2}.
\end{aligned} \tag{6.69}$$

The final step of the proof involves applying the triangle inequality to the error terms $\mathbf{e}_f^N = \mathbf{u}^N - \mathbf{u}_h^N = \boldsymbol{\eta}_f^N + \boldsymbol{\xi}_f^N$ and $e_p^N = \phi^N - \phi_h^N = \eta_p^N + \xi_p^N$:

$$\frac{n}{4}(\|\mathbf{e}^N{}_f\|_{\text{div},f}^2 + \|\mathbf{e}_f^{N-1}\|_{\text{div},f}^2) + \frac{gS_0}{2}(\|e_p^N\|_p^2 + \|e_p^{N-1}\|_p^2)$$

$$+ \Delta t \sum_{k=1}^{N-1} \left(\frac{n\nu}{2C_K} \|\nabla(\mathbf{e}_f^{k+1} + \mathbf{e}_f^{k-1})\|_f^2 + \frac{gk_{min}}{4} \|\nabla(e_p^{k+1} + e_p^{k-1})\|_p^2 \right)$$

$$\leq \frac{n}{2}(\|\boldsymbol{\xi}_f^N\|_{\text{div},f}^2 + \|\boldsymbol{\xi}_f^{N-1}\|_{\text{div},f}^2) + gS_0(\|\xi_p^N\|_p^2 + \|\xi_p^{N-1}\|_p^2)$$

$$+ \Delta t \sum_{k=1}^{N-1} \left(\frac{n\nu}{C_K} \|\nabla(\boldsymbol{\xi}_f^{k+1} + \boldsymbol{\xi}_f^{k-1})\|_f^2 + \frac{gk_{min}}{2} \|\nabla(\xi_p^{k+1} + \xi_p^{k-1})\|_p^2 \right)$$

$$+ \frac{n}{2}(\|\boldsymbol{\eta}_f^N\|_{\text{div},f}^2 + \|\boldsymbol{\eta}_f^{N-1}\|_{\text{div},f}^2) + gS_0(\|\eta_p^N\|_p^2 + \|\eta_p^{N-1}\|_p^2)$$

$$+ \Delta t \sum_{k=1}^{N-1} \left(\frac{n\nu}{C_K} \|\nabla(\boldsymbol{\eta}_f^{k+1} + \boldsymbol{\eta}_f^{k-1})\|_f^2 + \frac{gk_{min}}{2} \|\nabla(\eta_p^{k+1} + \eta_p^{k-1})\|_p^2 \right).$$

Now, we have

$$\|\boldsymbol{\eta}_f^n\|_f^2 \leq \|\|\boldsymbol{\eta}_f\|\|_{L^\infty(0,T;L^2(\Omega_f))}^2, \quad \|\eta_p^n\|_p^2 \leq \|\|\eta_p\|\|_{L^\infty(0,T;L^2(\Omega_p))}^2, \quad \forall n,$$

and thus $\|\boldsymbol{\eta}_f^n\|_{\text{div},f}^2 \leq d\|\|\boldsymbol{\eta}_f\|\|_{L^\infty(0,T;H^1(\Omega_f))}^2, \forall n$. Applying this, along with the previous bounds on the "η" terms and (6.69), and also absorbing all constants into $\widehat{C}_2 > 0$, results in

$$\frac{n}{4}(\|\mathbf{e}^N{}_f\|_{\text{div},f}^2 + \|\mathbf{e}_f^{N-1}\|_{\text{div},f}^2) + \frac{gS_0}{2}(\|e_p^N\|_p^2 + \|e_p^{N-1}\|_p^2)$$

$$+ \Delta t \sum_{k=1}^{N-1} \left(\frac{n\nu}{2C_K} \|\nabla(\mathbf{e}_f^{k+1} + \mathbf{e}_f^{k-1})\|_f^2 + \frac{gk_{min}}{4} \|\nabla(e_p^{k+1} + e_p^{k-1})\|_p^2 \right)$$

$$\leq \widehat{C}_2 \left\{ \|\boldsymbol{\eta}_{f,t}\|_{L^2(0,T;H^1(\Omega_f))}^2 + \|\eta_{p,t}\|_{L^2(0,T;L^2(\Omega_p))}^2 + \Delta t^4 \|\nabla \eta_{p,t}\|_{L^2(0,T;L^2(\Omega_p))}^2 \right.$$

$$+ \|\|\nabla \boldsymbol{\eta}_f\|\|_{L^2(0,T;L^2(\Omega_f))}^2 + \|\|\nabla \eta_p\|\|_{L^2(0,T;L^2(\Omega_p))}^2 \tag{6.70}$$

$$+ \Delta t^4 \left(\|\mathbf{u}_{ttt}\|_{L^2(0,T;H^1(\Omega_f))}^2 + \|\mathbf{u}_{tt}\|_{L^2(0,T;H^1(\Omega_f))}^2 + \|\phi_{ttt}\|_{L^2(0,T;L^2(\Omega_p))}^2 \right.$$

$$+ \|\phi_t\|_{L^2(0,T;H^1(\Omega_p))}^2 + \|\phi_{tt}\|_{L^2(0,T;H^1(\Omega_p))}^2 \Big) + \|\|\tilde{p} - \lambda_h\|\|_{L^2(0,T;L^2(\Omega_f))}^2$$

$$+ \|\|\boldsymbol{\eta}_f\|\|_{L^\infty(0,T;H^1(\Omega_f))}^2 + \|\|\eta_p\|\|_{L^\infty(0,T;L^2(\Omega_p))}^2 \right\} + n \left(\|\boldsymbol{\xi}_f^1\|_{\text{div},f}^2 + \|\boldsymbol{\xi}_f^0\|_{\text{div},f}^2 \right)$$

$$+ gS_0(\|\xi_p^1\|_p^2 + \|\xi_p^0\|_p^2) + \Delta t^2 n g^2 C_\dagger^2 (\|\xi_p^1\|_{1,p}^2 + \|\xi_p^0\|_{1,p}^2) + 2\Delta t C_\xi^{1/2}.$$

Using (3.46) and Young, we bound the coupling term on the right-hand side as follows:

$$C_\xi^{1/2} \leq \frac{ngC_\dagger}{2} \left(\|\boldsymbol{\xi}_f^0\|_{\text{div},f}^2 + \|\boldsymbol{\xi}_f^1\|_{\text{div},f}^2 + \|\xi_p^0\|_{1,p}^2 + \|\xi_p^1\|_{1,p}^2 \right). \tag{6.71}$$

Inequality (6.70) holds for any $\tilde{\mathbf{u}} \in \mathbf{V}^h$, $\lambda_h \in Q_f^h$, and $\tilde{\phi} \in X_p^h$. By taking the infimum over $\mathbf{V}^h$, Q_f^h, and X_p^h, using (6.48) to bound the infimum over $\mathbf{V}^h$ by the infimum over $\mathbf{X}_f^h$, and using the bound (6.71), we have:

$$
\frac{n}{2}(\|\mathbf{e}^N{}_f\|^2_{\mathrm{div},f} + \|\mathbf{e}_f^{N-1}\|^2_{\mathrm{div},f}) + gS_0(\|e_p^N\|^2_p + \|e_p^{N-1}\|^2_p)
$$

$$
+ \Delta t \sum_{k=1}^{N-1} \left(\frac{n\nu}{C_K}\|\nabla(\mathbf{e}_f^{k+1} + \mathbf{e}_f^{k-1})\|^2_f + \frac{gk_{min}}{2}\|\nabla(e_p^{k+1} + e_p^{k-1})\|^2_p \right)
$$

$$
\leq \widehat{C}_3 \Bigg\{ \inf_{\tilde{\mathbf{u}}\in\mathbf{X}_f^h} \Big[\|\boldsymbol{\eta}_{f,t}\|^2_{L^2(0,T;H^1(\Omega_f))} + \||\nabla\boldsymbol{\eta}_f\||^2_{L^2(0,T;L^2(\Omega_f))}
$$

$$
+ \||\boldsymbol{\eta}_f\||^2_{L^\infty(0,T;H^1(\Omega_f))} + \|\boldsymbol{\xi}_f^1\|^2_{\mathrm{div},f} + \|\boldsymbol{\xi}_f^0\|^2_{\mathrm{div},f} \Big]
$$

$$
+ \inf_{\lambda_h\in Q_f^h} \||\tilde{p} - \lambda_h\||^2_{L^2(0,T;L^2(\Omega_f))} + \inf_{\tilde{\phi}\in X_p^h} \Big[\|\eta_{p,t}\|^2_{L^2(0,T;L^2(\Omega_p))}
$$

$$
+ \Delta t^4 \|\nabla\eta_{p,t}\|^2_{L^2(0,T;L^2(\Omega_p))} + \||\nabla\eta_p\||^2_{L^2(0,T;L^2(\Omega_p))} + \||\eta_p\||^2_{L^\infty(0,T;L^2(\Omega_p))}
$$

$$
+ \|\xi_p^1\|^2_{1,p} + \|\xi_p^0\|^2_{1,p} \Big] + \Delta t^4 \Big\{ \|\mathbf{u}_{ttt}\|^2_{L^2(0,T;H^1(\Omega_f))} + \|\mathbf{u}_{tt}\|^2_{L^2(0,T;H^1(\Omega_f))}
$$

$$
+ \|\phi_{ttt}\|^2_{L^2(0,T;L^2(\Omega_p))} + \|\phi_t\|^2_{L^2(0,T;H^1(\Omega_p))} + \|\phi_{tt}\|^2_{L^2(0,T;H^1(\Omega_p))} \Big\} \Bigg\},
$$

where all constants were absorbed into a $\widehat{C}_3 > 0$. The claim of the theorem now immediately follows by applying the approximation assumptions (6.47). $\qquad\square$

We conclude this section with a corollary about the growth rate of the errors in the CNLF-stab method.

Corollary 2. *Under the same regularity conditions as* (6.55) *of Theorem 11, the temporal growth of the error satisfies*

$$
\|\mathbf{e}_f^N\|_{div,f}, \|e_p^N\|_p = \mathcal{O}(\sqrt{T}).
$$

Proof. For any function $\mathbf{v} : [0,\infty) \to \mathbf{X}$ and any spatial norm $\|\cdot\|_{\mathbf{X}}$ we have

$$
\int_0^T \|\mathbf{v}(t)\|^2_{\mathbf{X}} \, dt \leq T\|\mathbf{v}\|^2_{L^\infty(0,\infty;\mathbf{X})},
$$

for any $0 < T \leq \infty$. Similarly, the discrete norms satisfy

$$
\Delta t \sum_{k=1}^N \|\mathbf{v}^k\|^2_{\mathbf{X}} \leq \Delta t\|\mathbf{v}\|^2_{L^\infty(0,\infty;\mathbf{X})} \sum_{k=1}^N \{1\} = T\|\mathbf{v}\|^2_{L^\infty(0,\infty;\mathbf{X})}.
$$

The claim of the corollary follows by applying the above bound to the terms on the right-hand side of (6.56). $\qquad\square$

Remark 12. *Numerical tests verifying unconditional stability and uniform, second-order convergence of the CNLF-stab method, as well as tests that illustrate the method's effectiveness over fully coupled methods, are presented in Chapter 8, in Section 8.2.*

7.0   THE QUASISTATIC NAVIER-STOKES/DARCY APPROXIMATION

In this chapter, we introduce the fully evolutionary Navier-Stokes/Darcy problem and its quasistatic approximation. We modify the previously used 'balance of normal forces' coupling condition across the interface, (3.11), to include an "inertia" term, (7.13). This addition, like others for the nonlinear problem, has deficits which are discussed in Remark 13, in Section 7.1. We obtain first-order convergence of the solution of the fully evolutionary Navier-Stokes/Darcy problem to the quasistatic solution in both two (Theorem 13) and three (Theorem 14) spatial dimensions, as the specific storage approaches zero. In three dimensions, convergence holds under a regularity assumption on the velocity. Finally, in Theorem 16, in Section 7.4, we prove convergence to the quasistatic solution in three spatial dimensions under a small-data condition, and no extra regularity assumed on the solution.

7.1   THE EVOLUTIONARY NAVIER-STOKES/DARCY PROBLEM AND ITS QUASISTATIC APPROXIMATION

We begin this chapter by introducing the continuous, fully evolutionary, Navier-Stokes/Darcy problem. All operators, variables, and problem parameters are the same as defined in Chapters 3 and 4, and we recall from Chapters 2-4 the definitions of the spaces

$$\mathbf{X}_f := \left\{ \mathbf{v} \in (H^1(\Omega_f))^d : \mathbf{v} = \mathbf{0} \text{ on } \partial\Omega_f \backslash I \right\},$$

$$X_p := \left\{ \psi \in H^1(\Omega_p) : \psi = 0 \text{ on } \partial\Omega_p \backslash I \right\},$$

$$Q_f := L_0^2(\Omega_f),$$

$$\mathbf{V}_f := \left\{ \mathbf{v} \in \mathbf{X}_f : (q, \nabla \cdot \mathbf{v}) = 0 \ \forall q \in Q_f \right\},$$

and the norms on the dual spaces of $\mathbf{X}_f$ and X_p,

$$\|\mathbf{f}\|_{-1,f} := \sup_{0 \neq \mathbf{v} \in \mathbf{X}_f} \frac{(\mathbf{f}, \mathbf{v})_f}{\|\nabla \mathbf{v}\|_f},$$

$$\|f\|_{-1,p} := \sup_{0 \neq \psi \in X_p} \frac{(f, \psi)_p}{\|\nabla \psi\|_p},$$

where $\| \cdot \|_{f/p}$ denotes the L^2 norm on $\Omega_{f/p}$, and $(\cdot, \cdot)_{f/p}$ denotes the corresponding inner product on $\Omega_{f/p}$. We further recall that

$$L^2(0, T; X) = \{v : [0, T] \to X : \int_0^T \|v(t)\|_X^2 \, dt < \infty\},$$

$$L^\infty(0, T; X) = \{v : [0, T] \to X : \sup_{t \in [0,T]} \{\|v(t)\|_X\} < \infty\},$$

for any space X, and also the Poincaré-Friedrichs inequality (2.6) for each domain $\Omega_{f/p}$,

$$\|\mathbf{v}\|_{L^2(\Omega_f)} \leq C_{PF,f}\|\nabla \mathbf{v}\|_{L^2(\Omega_f)}, \tag{7.1}$$

$$\|\phi\|_{L^2(\Omega_p)} \leq C_{PF,p}\|\nabla \phi\|_{L^2(\Omega_p)}, \tag{7.2}$$

where $C_{PF,f/p} > 0$.

We assume that the velocity, $\mathbf{u} = \mathbf{u}(\mathbf{x}, t)$, and the pressure, $p = p(\mathbf{x}, t)$, defined in $\Omega_f \times [0, T]$, $T > 0$, satisfy the Navier-Stokes equations

$$\rho(\mathbf{u}_t + \mathbf{u} \cdot \nabla \mathbf{u}) - \nabla \cdot \mathbf{\Pi}(\mathbf{u}, p) = \mathbf{f}_f \qquad \text{in } \Omega_f \times (0, T], \tag{7.3}$$

$$\nabla \cdot \mathbf{u} = 0 \qquad \text{in } \Omega_f \times (0, T], \tag{7.4}$$

$$\mathbf{u} = \mathbf{0} \qquad \text{in } (\partial \Omega_f \backslash I) \times (0, T], \tag{7.5}$$

$$\mathbf{u}(\mathbf{x}, 0) = \mathbf{u}_0(\mathbf{x}) \qquad \text{in } \Omega_f, \tag{7.6}$$

and the velocity, $\mathbf{u}_p = \mathbf{u}(\mathbf{x}, t)$, and the hydraulic head, $\phi = \phi(\mathbf{x}, t)$, defined in $\Omega_p \times [0, T]$, satisfy the groundwater flow equations, as before

$$S_0 \phi_t + \nabla \cdot \mathbf{q} = f_p \qquad \text{in } \Omega_p \times (0, T], \tag{7.7}$$

$$\mathbf{q} = -\mathbf{K} \nabla \phi \qquad \text{in } \Omega_p \times (0, T], \tag{7.8}$$

$$\mathbf{u}_p = \frac{\mathbf{q}}{n} \qquad \text{in } \Omega_p \times (0, T], \tag{7.9}$$

$$\phi = 0 \qquad \text{in } (\partial \Omega_p \backslash I) \times (0, T], \tag{7.10}$$

$$\phi(\mathbf{x}, 0) = \phi_0(\mathbf{x}) \qquad \text{in } \Omega_p, \tag{7.11}$$

where the boundary and initial conditions for each sub-domain above are the same as in Chapter 3. The two systems of equations are coupled through the following interface conditions, namely conservation of mass, balance of normal forces (plus an "intertia" term), and the Beavers-Joseph-Saffman condition across I:

$$\mathbf{u} \cdot \hat{\mathbf{n}}_f + \mathbf{u}_p \cdot \hat{\mathbf{n}}_p = 0 \qquad \text{on } I, \qquad (7.12)$$

$$\rho g \phi = p - 2\mu \, \hat{\mathbf{n}}_f \cdot \mathbf{D}(\mathbf{u}) \cdot \hat{\mathbf{n}}_f + \frac{\rho}{2}(\mathbf{u} \cdot \mathbf{u}) \qquad \text{on } I, \qquad (7.13)$$

$$-2 \, \hat{\boldsymbol{n}}_f \cdot \mathbf{D}(\mathbf{u}) \cdot \hat{\boldsymbol{\tau}}_i = \frac{\alpha}{\sqrt{\hat{\boldsymbol{\tau}}_i \cdot \mathbf{K} \cdot \hat{\boldsymbol{\tau}}_i}} \, \mathbf{u} \cdot \hat{\boldsymbol{\tau}}_i, \text{ for } i = 1, \ldots, \, d-1 \qquad \text{on } I. \qquad (7.14)$$

Remark 13. *The addition of the "inertia" term in* (7.13) *was considered in the analysis of the Navier-Stokes/Darcy coupling in [1, 52]. The basic issue is that without the "inertia" term, the energy of the coupled problem for large data cannot be bounded by the energy input from body-force flow interactions. The cause for this is an extra term in the energy equation. The "inertia" term (with the exact constant coefficient "$\rho/2$") is chosen to exactly cancel this inconvenience. However, it can also be criticized since the resulting model violates Galilean invariance, see [81], and since the term does not arise from any physical process or law. Thus, the mechanically correct coupling conditions are still an open problem. We base our analysis on the term's inclusion because analysis (in the large) cannot begin without an energy balance.*

The only differences between the evolutionary Stokes-Darcy problem (3.1)-(3.12) and the Navier-Stokes/Darcy problem (7.3)-(7.14) are the nonlinear term "$\mathbf{u} \cdot \nabla \mathbf{u}$" appearing in (7.3) and the "inertia" term "$\frac{\rho}{2}(\mathbf{u} \cdot \mathbf{u})$" appearing in (7.13). The variational formulation of the Navier-Stokes/Darcy problem is thus easily obtained by using the steps in deriving the corresponding weak formulation of the Stokes-Darcy problem from Chapter 3, Section 3.4, with the addition of two nonlinear terms, underlined below. It reads:

Find $(\mathbf{u}, \tilde{p}, \phi) : (0, T] \rightarrow \mathbf{X}_f \times Q_f \times X_p$ *such that for all* $(\mathbf{v}, q, \psi) \in \mathbf{X}_f \times Q_f \times X_p$,

$$n(\mathbf{u}_t, \mathbf{v})_f + \underline{b(\mathbf{u}, \mathbf{u}, \mathbf{v}) - \frac{n}{2}\langle \mathbf{u} \cdot \mathbf{u}, \mathbf{v} \cdot \hat{\mathbf{n}}_f \rangle_I}$$
$$+ nb_f(\mathbf{v}, \tilde{p}) + a_f(\mathbf{u}, \mathbf{v}) + c_I(\mathbf{v}, \phi) = n(\tilde{\mathbf{f}}_f, \mathbf{v})_f, \qquad (7.15)$$

$$b_f(\mathbf{u}, q) = 0, \qquad (7.16)$$

$$g(S_0 \phi_t, \psi)_p + a_p(\phi, \psi) - c_I(\mathbf{u}, \psi) = g(f_p, \psi)_p, \qquad (7.17)$$

given the initial data $\mathbf{u}(\mathbf{x}, 0) = \mathbf{u}_0(\mathbf{x})$ *and* $\phi(\mathbf{x}, 0) = \phi_0(\mathbf{x})$, *where* $b : \mathbf{X}_f \times \mathbf{X}_f \times \mathbf{X}_f \to \mathbb{R}$ *is the trilinear form*

$$b(\mathbf{u}, \mathbf{v}, \mathbf{w}) := n(\mathbf{u} \cdot \nabla \mathbf{v}, \mathbf{w})_f, \tag{7.18}$$

and where $\tilde{\mathbf{f}}_f = \mathbf{f}_f/\rho, \tilde{p} = p/\rho$ *as before, where* ρ *is the fluid density.* The well-posedness of the Navier-Stokes/Darcy problem given in (7.15)-(7.17) was established in [1, 52].

The trilinear form $b(\cdot, \cdot, \cdot)$ is continuous in the space $\mathbf{X}_f \times (H^1(\Omega_f))^d \times \mathbf{X}_f$:

$$|b(\mathbf{u}, \mathbf{v}, \mathbf{w})| \le n \, C_c \|\nabla \mathbf{u}\|_f \|\nabla \mathbf{v}\|_f \|\nabla \mathbf{w}\|_f, \qquad \forall (\mathbf{u}, \mathbf{v}, \mathbf{w}) \in \mathbf{X}_f \times (H^1(\Omega_f))^d \times \mathbf{X}_f, \tag{7.19}$$

where (e.g., [47])

$$C_c = \begin{cases} |\Omega|^{1/2}/2, & \text{for } d = 2 \\ 2\sqrt{2}|\Omega|^{1/6}/3, & \text{for } d = 3. \end{cases}$$

Moreover, the following estimate holds in dimensions $d = 2, 3$, see, e.g., [80]:

$$|b(\mathbf{u}, \mathbf{v}, \mathbf{w})| \le nC_b \|\mathbf{u}\|_f^{1/2} \|\nabla \mathbf{u}\|_f^{1/2} \|\nabla \mathbf{v}\|_f \|\nabla \mathbf{w}\|_f, \tag{7.20}$$

for all $\mathbf{u}, \mathbf{v}, \mathbf{w} \in \mathbf{X}_f$, where C_b is a positive constant. Also, by the identity

$$\nabla \cdot (\mathbf{u}(\mathbf{v} \cdot \mathbf{w})) = (\mathbf{v} \cdot \mathbf{w})(\nabla \cdot \mathbf{u}) + \mathbf{u} \cdot \nabla \mathbf{v} \cdot \mathbf{w} + \mathbf{u} \cdot \nabla \mathbf{w} \cdot \mathbf{v},$$

if we assume that $\mathbf{u} \in \mathbf{X}_f$ is such that $\nabla \cdot \mathbf{u} = 0$, then we have by the divergence theorem:

$$(\mathbf{u} \cdot \nabla \mathbf{v}, \mathbf{w})_f = \int_{\Omega_f} \nabla \cdot (\mathbf{u}(\mathbf{v} \cdot \mathbf{w})) \, d\mathbf{x} - (\mathbf{u} \cdot \nabla \mathbf{w}, \mathbf{v})_f$$

$$= \langle \mathbf{u} \cdot \hat{\mathbf{n}}_f, \mathbf{v} \cdot \mathbf{w} \rangle_I - (\mathbf{u} \cdot \nabla \mathbf{w}, \mathbf{v})_f.$$

Therefore,

$$b(\mathbf{u}, \mathbf{v}, \mathbf{w}) = n\langle \mathbf{u} \cdot \hat{\mathbf{n}}_f, \mathbf{v} \cdot \mathbf{w} \rangle_I - b(\mathbf{u}, \mathbf{w}, \mathbf{v}), \tag{7.21}$$

and, as a consequence,

$$b(\mathbf{u}, \mathbf{v}, \mathbf{v}) = \tfrac{n}{2}\langle \mathbf{u} \cdot \hat{\mathbf{n}}_f, |\mathbf{v}|^2 \rangle_I, \tag{7.22}$$

96

for all $\mathbf{u}, \mathbf{v} \in \mathbf{X}_f$ with $\nabla \cdot \mathbf{u} = 0$. In the upcoming sections, we will consider the weak formulation over the divergence-free space, $\mathbf{V}_f$,

$$\mathbf{V}_f := \left\{ \mathbf{v} \in \mathbf{X}_f : (q, \nabla \cdot \mathbf{v}) = 0 \ \forall q \in Q_f \right\},$$

where the pressure term in the fluid region is eliminated:

Find $\mathbf{u} : (0, T] \to \mathbf{V}_f$, $\phi : (0, T] \to X_p$ such that for all $(\mathbf{v}, \psi) \in \mathbf{V}_f \times X_p$,

$$n(\mathbf{u}_t, \mathbf{v})_f + b(\mathbf{u}, \mathbf{u}, \mathbf{v}) - \frac{n}{2}\langle \mathbf{u} \cdot \mathbf{u}, \mathbf{v} \cdot \hat{\mathbf{n}}_f \rangle_I + a_f(\mathbf{u}, \mathbf{v}) + c_I(\mathbf{v}, \phi) = n(\tilde{\mathbf{f}}_f, \mathbf{v})_f, \qquad (7.23)$$

$$g(S_0 \phi_t, \psi)_p + a_p(\phi, \psi) - c_I(\mathbf{u}, \psi) = g(f_p, \psi)_p, \qquad (7.24)$$

given the initial data $\mathbf{u}(\mathbf{x}, 0) = \mathbf{u}_0(\mathbf{x})$ and $\phi(\mathbf{x}, 0) = \phi_0(\mathbf{x})$.

The continuous quasistatic Navier-Stokes/Darcy model is obtained by setting $S_0 = 0$ in (7.3)-(7.14). We denote its solution by $(\mathbf{u}^{QS}, p^{QS}, \phi^{QS})$. Therefore, the weak formulation of the quasistatic Navier-Stokes/Darcy problem over the divergence-free space $\mathbf{V}_f$ is given by:

Find $\mathbf{u}^{QS} : (0, T] \to \mathbf{V}_f$, $\phi^{QS} : (0, T] \to X_p$ such that for all $(\mathbf{v}, \psi) \in \mathbf{V}_f \times X_p$,

$$n(\mathbf{u}_t^{QS}, \mathbf{v})_f + b(\mathbf{u}^{QS}, \mathbf{u}^{QS}, \mathbf{v}) - \frac{n}{2}\langle \mathbf{u}^{QS} \cdot \mathbf{u}^{QS}, \mathbf{v} \cdot \hat{\mathbf{n}}_f \rangle_I$$
$$+ a_f(\mathbf{u}^{QS}, \mathbf{v}) + c_I(\mathbf{v}, \phi^{QS}) = n(\tilde{\mathbf{f}}_f, \mathbf{v})_f, \qquad (7.25)$$

$$a_p(\phi^{QS}, \psi) - c_I(\mathbf{u}^{QS}, \psi) = g(f_p, \psi)_p, \qquad (7.26)$$

given the initial data $\mathbf{u}^{QS}(\mathbf{x}, 0) = \mathbf{u}_0(\mathbf{x})$. $\phi^{QS}(\mathbf{x}, 0)$ is determined through (7.26) by solving

$$a_p(\phi^{QS}(\mathbf{x}, 0), \psi(\mathbf{x})) = c_I(\mathbf{u}_0(\mathbf{x}), \psi(\mathbf{x})) + g(f_p(\mathbf{x}, 0), \psi(\mathbf{x}))_p, \ \forall \psi \in X_p,$$

for the unknown $\phi^{QS}(\mathbf{x}, 0)$.

Convergence to the quasistatic solution in the nonlinear Navier-Stokes/Darcy problem will rely on á-priori bounds on the time derivative of the hydraulic head, ϕ_t. In addition, because of the nonlinearity, convergence will depend upon appropriate bounds on the nonlinear term. As we will see in Theorem 14, in three spatial dimensions, we will need to assume extra regularity on the velocity in order to prove convergence. The à-priori estimates and a result of first-order convergence to the quasistatic solution are given in the next two sections, respectively.

7.2   À-PRIORI ESTIMATES

In this section we derive à-priori estimates for both the solution $(\mathbf{u}, \phi)$ of the evolutionary Navier-Stokes/Darcy problem and the solution $(\mathbf{u}^{QS}, \phi^{QS})$ of the quasistatic Navier-Stokes/Darcy problem. We define

$$\mathbf{u}_t(0) := \mathbf{u}_t(\mathbf{x}, 0) := \lim_{t \to 0^+} \mathbf{u}_t(\mathbf{x}, t) = \lim_{t \to 0^+} \left(-\mathbf{u} \cdot \nabla \mathbf{u} + \tfrac{1}{\rho} \left[\nabla \cdot \mathbf{\Pi}(\mathbf{u}, p) + \mathbf{f}_f \right] \right),$$

$$\mathbf{u}_t^{QS}(0) := \mathbf{u}_t^{QS}(\mathbf{x}, 0) := \lim_{t \to 0^+} \mathbf{u}_t^{QS}(\mathbf{x}, t) = \lim_{t \to 0^+} \left(-\mathbf{u}^{QS} \cdot \nabla \mathbf{u}^{QS} + \tfrac{1}{\rho} \left[\nabla \cdot \mathbf{\Pi}(\mathbf{u}^{QS}, p^{QS}) + \mathbf{f}_f \right] \right),$$

$$\phi_t(0) := \phi_t(\mathbf{x}, 0) := \lim_{t \to 0^+} \phi_t(\mathbf{x}, t) = \tfrac{1}{S_0} \lim_{t \to 0^+} \left(-\nabla \cdot \mathbf{q} + f_p \right).$$

We begin by stating the main result of this section.

Theorem 12. *1. In the variational formulations* (7.23)-(7.24) *and* (7.25)-(7.26) *assume that the initial data and body forces satisfy*

$$\mathbf{u}_0 \in (L^2(\Omega_f))^d, \ \mathbf{f}_f \in (L^2(0, T; H^{-1}(\Omega_f)))^d, \ f_p \in L^2(0, T; H^{-1}(\Omega_p)).$$

a. Then for $\mathbf{u}^{QS}, \phi^{QS}$ given by (7.25)-(7.26) *we have*

$$\mathbf{u}^{QS} \in (L^\infty(0, T; L^2(\Omega_f)))^d, \ \nabla \mathbf{u}^{QS} \in (L^2(0, T; L^2(\Omega_f)))^{d \times d},$$

$$\mathbf{u}^{QS} \cdot \hat{\boldsymbol{\tau}}_i \in L^2(0, T; L^2(I)), \ i = 1, \ldots, d-1, \ \nabla \phi^{QS} \in (L^2(0, T; L^2(\Omega_p)))^d. \tag{7.27}$$

b. If, in addition, $\phi_0 \in L^2(\Omega_p)$ then for $\mathbf{u}, \phi$ given by (7.23)-(7.24) *it holds*

$$\mathbf{u} \in (L^\infty(0, T; L^2(\Omega_f)))^d, \ \sqrt{S_0}\phi \in L^\infty(0, T; L^2(\Omega_p)),$$

$$\nabla \mathbf{u} \in (L^2(0, T; L^2(\Omega_f)))^{d \times d}, \ \mathbf{u} \cdot \hat{\boldsymbol{\tau}}_i \in L^2(0, T; L^2(I)), \ i = 1, \ldots, d-1, \tag{7.28}$$

$$\nabla \phi \in (L^2(0, T; L^2(\Omega_p)))^d.$$

2. Assume that the body forces satisfy

$$\mathbf{f}_{f,t} \in (L^2(0, T; H^{-1}(\Omega_f)))^d, \ f_{p,t} \in L^2(0, T; H^{-1}(\Omega_p)),$$

where $\mathbf{f}_{f,t}, f_{p,t}$ denote the derivatives of $\mathbf{f}_f, f_p$ with respect to time.

a. If $\mathbf{u}_t(0) \in (L^2(\Omega_f))^d$, $\phi_t(0) \in L^2(\Omega_p)$, then for $\mathbf{u}, \phi$ given by (7.23)-(7.24), we have

$$\mathbf{u}_t \in (L^\infty(0,T;L^2(\Omega_f)))^d, \ \sqrt{S_0}\phi_t \in L^\infty(0,T;L^2(\Omega_p)),$$

$$\nabla\mathbf{u}_t \in (L^2(0,T;L^2(\Omega_f)))^{d\times d}, \ \mathbf{u}_t \cdot \hat{\boldsymbol{\tau}}_i \in L^2(0,T;L^2(I)), \ i=1,\ldots,\ d-1, \quad (7.29)$$

$$\nabla\phi_t \in (L^2(0,T;L^2(\Omega_p)))^d.$$

b. If $\mathbf{u}_t^{QS}(0) \in (L^2(\Omega_f))^d$, then $\mathbf{u}^{QS}, \phi^{QS}$ given by (7.25)-(7.26) satisfy

$$\mathbf{u}_t^{QS} \in (L^\infty(0,T;L^2(\Omega_f)))^d, \ \nabla\mathbf{u}_t^{QS} \in (L^2(0,T;L^2(\Omega_f)))^{d\times d},$$

$$\mathbf{u}_t^{QS} \cdot \hat{\boldsymbol{\tau}}_i \in L^2(0,T;L^2(I)), \ i=1,\ldots,\ d-1, \ \nabla\phi_t^{QS} \in (L^2(0,T;L^2(\Omega_p)))^d. \quad (7.30)$$

Proof. The conclusions of the theorem, parts 1b, 1a, 2a, and 2b, are direct consequences of Propositions 8, 9, 10, and 11, respectively, given next. □

We denote by $C_i^* = C_i^*(\mathbf{u}_0, \phi_0, \mathbf{f}_f, f_p)$, $i=1,\ldots,5$, positive constants that depend on the initial data and body forces. In Proposition 8 we derive a first energy estimate for the weak formulation (7.23)-(7.24).

Proposition 8. *Consider the weak formulation of the fully evolutionary Navier-Stokes/Darcy problem over the divergence-free space* $\mathbf{V}_f$, *given in* (7.23)-(7.24). *Assume that the initial data and body forces satisfy*

$$\mathbf{u}_0 \in (L^2(\Omega_f))^d, \phi_0 \in L^2(\Omega_p), \mathbf{f}_f \in (L^2(0,T;H^{-1}(\Omega_f)))^d, f_p \in L^2(0,T;H^{-1}(\Omega_p)). \quad (7.31)$$

Then we have

$$\sup_{t\in[0,T]} \left\{ n\|\mathbf{u}(t)\|_f^2 + gS_0\|\phi(t)\|_p^2 \right\} + \int_0^T \left\{ \frac{2n\nu}{C_K}\|\nabla\mathbf{u}(t)\|_f^2 + \frac{2n\nu\alpha}{\sqrt{k_{max}}}\sum_{i=1}^{d-1}\|\mathbf{u}(t)\cdot\hat{\boldsymbol{\tau}}_i\|_I^2 \right.$$

$$\left. + gk_{min}\|\nabla\phi(t)\|_p^2 \right\} \ dt \quad (7.32)$$

$$\leq n\|\mathbf{u}_0\|_f^2 + gS_0\|\phi_0\|_p^2 + \int_0^T \left\{ \frac{nC_K}{2\rho^2\nu}\|\mathbf{f}_f(t)\|_{-1,f}^2 + \frac{g}{k_{min}}\|f_p(t)\|_{-1,p}^2 \right\} \ dt \leq C_1^*.$$

99

Proof. In the equations (7.23)-(7.24), we fix $t > 0$ and set $\mathbf{v} = \mathbf{u}(t)$ and $\psi = \phi(t)$. By adding the two equations together, the two coupling terms exactly cancel, and we have:

$$\frac{1}{2}\frac{d}{dt}\left\{n\|\mathbf{u}(t)\|_f^2 + gS_0\|\phi(t)\|_p^2\right\} + \left[b(\mathbf{u},\mathbf{u},\mathbf{u}) - \frac{n}{2}\langle\mathbf{u}\cdot\mathbf{u},\mathbf{u}\cdot\hat{\mathbf{n}}_f\rangle_I\right] + a_f(\mathbf{u},\mathbf{u}) + a_p(\phi,\phi)$$
$$= n(\tilde{\mathbf{f}}_f,\mathbf{u})_f + g(f_p,\phi)_p.$$

Now, applying (7.22), we obtain for the term in brackets:

$$b(\mathbf{u},\mathbf{u},\mathbf{u}) - \frac{n}{2}\langle\mathbf{u}\cdot\mathbf{u},\mathbf{u}\cdot\hat{\mathbf{n}}_f\rangle_I = \frac{n}{2}\langle\mathbf{u}\cdot\mathbf{u},\mathbf{u}\cdot\hat{\mathbf{n}}_f\rangle_I - \frac{n}{2}\langle\mathbf{u}\cdot\mathbf{u},\mathbf{u}\cdot\hat{\mathbf{n}}_f\rangle_I = 0. \qquad (7.33)$$

Using this along with the coercivity estimates (3.34) and (3.36) on the left hand side and Young's inequality (2.5) on the right hand side, we obtain

$$\frac{1}{2}\frac{d}{dt}\left\{n\|\mathbf{u}(t)\|_f^2 + gS_0\|\phi(t)\|_p^2\right\} + \frac{2n\nu}{C_K}\|\nabla\mathbf{u}(t)\|_f^2 + \frac{n\nu\alpha}{\sqrt{k_{max}}}\sum_{i=1}^{d-1}\|\mathbf{u}(t)\cdot\hat{\boldsymbol{\tau}}_i\|_I^2 + gk_{min}\|\nabla\phi(t)\|_p^2$$
$$\leq \frac{n}{\rho}\|\mathbf{f}_f(t)\|_{-1,f}\|\nabla\mathbf{u}(t)\|_f + g\|f_p(t)\|_{-1,p}(t)\|\nabla\phi(t)\|_p$$
$$\leq \frac{n\nu}{C_K}\|\nabla\mathbf{u}(t)\|_f^2 + \frac{nC_K}{4\rho^2\nu}\|\mathbf{f}_f(t)\|_{-1,f}^2 + \frac{gk_{min}}{2}\|\nabla\phi(t)\|_p^2 + \frac{g}{2k_{min}}\|f_p(t)\|_{-1,p}^2.$$

Rearranging and integrating over $[0,t]$ for any t in $(0,T]$ and $T < \infty$, yields

$$n\|\mathbf{u}(t)\|_f^2 + gS_0\|\phi(t)\|_p^2 + \int_0^t\left\{\frac{2n\nu}{C_K}\|\nabla\mathbf{u}(s)\|_f^2 + \frac{2n\nu\alpha}{\sqrt{k_{max}}}\sum_{i=1}^{d-1}\|\mathbf{u}(s)\cdot\hat{\boldsymbol{\tau}}_i\|_I^2\right.$$
$$\left. + gk_{min}\|\nabla\phi(s)\|_p^2\right\}\,ds$$
$$\leq n\|\mathbf{u}_0\|_f^2 + gS_0\|\phi_0\|_p^2 + \int_0^t\left\{\frac{nC_K}{2\rho^2\nu}\|\mathbf{f}_f(s)\|_{-1,f}^2 + \frac{g}{k_{min}}\|f_p(s)\|_{-1,p}^2\right\}\,ds.$$

Finally, the result in (7.32) follows by taking the supremum over $[0,T]$ and applying the assumptions (7.31) on the right hand side above. $\qquad\square$

In Proposition 9 we derive the corresponding energy estimate for the quasistatic weak formulation (7.25)-(7.26).

Proposition 9. *Consider the quasistatic Navier-Stokes/Darcy weak formulation* (7.25)-(7.26) *and assume that the initial data and body forces satisfy*

$$\mathbf{u}_0 \in (L^2(\Omega_f))^d, \mathbf{f}_f \in (L^2(0,T;H^{-1}(\Omega_f)))^d, f_p \in L^2(0,T;H^{-1}(\Omega_p)). \qquad (7.34)$$

Then we have

$$n \sup_{t\in[0,T]} \|\mathbf{u}^{QS}(t)\|_f^2 + \int_0^T \left\{ \frac{2n\nu}{C_K} \|\nabla\mathbf{u}^{QS}(t)\|_f^2 + \frac{2n\nu\alpha}{\sqrt{k_{max}}} \sum_{i=1}^{d-1} \|\mathbf{u}^{QS}(t)\cdot\hat{\boldsymbol{\tau}}_i\|_I^2 \right.$$
$$\left. + gk_{min}\|\nabla\phi^{QS}(t)\|_p^2 \right\} dt$$
$$\leq n\|\mathbf{u}_0\|_f^2 + \int_0^T \left\{ \frac{nC_K}{2\rho^2\nu} \|\mathbf{f}_f(t)\|_{-1,f}^2 + \frac{g}{k_{min}} \|f_p(t)\|_{-1,p}^2 \right\} dt \leq C_2^*.$$

Proof. We fix $t > 0$ and pick $\mathbf{v} = \mathbf{u}^{QS}(t), \psi = \phi^{QS}(t)$ in (7.25)-(7.26) so that the nonlinear terms cancel out according to (7.33). After adding the equations together, the coupling terms cancel out as well. Thus, the claim of the proposition follows by manipulations similar to the ones in the proof of Proposition 8 and the assumptions (7.34). □

In the next two propositions, 10 and 11, we obtain additional estimates for the weak formulations (7.23)-(7.24) and (7.25)-(7.26) that result in à-priori estimates for the time derivatives of $\mathbf{u}, \mathbf{u}^{QS}, \phi$, and ϕ^{QS}.

Proposition 10. *Consider the fully evolutionary Navier-Stokes/Darcy weak formulation* (7.23)-(7.24). *If the initial data and body forces satisfy*

$$\mathbf{u}_t(0) \in (L^2(\Omega_f))^d, \ \phi_t(0) \in L^2(\Omega_p),$$

$$\mathbf{f}_{f,t} \in (L^2(0,T;H^{-1}(\Omega_f)))^d, \ f_{p,t} \in L^2(0,T;H^{-1}(\Omega_p)),$$

then

$$\sup_{t\in[0,T]} \left\{ n\|\mathbf{u}_t(t)\|_f^2 + gS_0\|\phi_t(t)\|_p^2 \right\} + \int_0^T \left\{ \frac{2n\nu}{C_K} \|\nabla\mathbf{u}_t(t)\|_f^2 + \frac{2n\nu\alpha}{\sqrt{k_{max}}} \sum_{i=1}^{d-1} \|\mathbf{u}_t(t)\cdot\hat{\boldsymbol{\tau}}_i\|_I^2 \right.$$
$$\left. + gk_{min}\|\nabla\phi_t(t)\|_p^2 \right\} dt$$
$$\leq n\|\mathbf{u}_t(0)\|_f^2 + gS_0\|\phi_t(0)\|_p^2 + \int_0^T \left\{ \frac{nC_K}{2\rho^2\nu} \|\mathbf{f}_{f,t}(t)\|_{-1,f}^2 + \frac{g}{k_{min}} \|f_{p,t}(t)\|_{-1,p}^2 \right\} dt \leq C_3^*.$$

Proof. Starting with the weak formulation (7.23)-(7.24), we take the derivative with respect to time to get

$$n(\mathbf{u}_{tt}, \mathbf{v})_f + \frac{d}{dt}\left[b(\mathbf{u}, \mathbf{u}, \mathbf{v}) - \frac{n}{2}\langle \mathbf{u} \cdot \mathbf{u}, \mathbf{v} \cdot \hat{\mathbf{n}}_f\rangle\right] + a_f(\mathbf{u}_t, \mathbf{v}) + c_I(\mathbf{v}, \phi_t) = n(\tilde{\mathbf{f}}_{f,t}, \mathbf{v})_f, \quad (7.35)$$

$$g S_0(\phi_{tt}, \psi)_p + a_p(\phi_t, \psi) - c_I(\mathbf{u}_t, \psi) = g(f_{p,t}, \psi)_p. \quad (7.36)$$

We now fix $t > 0$, choose $\mathbf{v} = \mathbf{u}_t(t), \psi = \phi_t(t)$ in (7.35)-(7.36), so that the term in brackets vanishes by (7.33). Then, by adding the equations together the coupling terms cancel out, and the rest of the proof is similar to the proof of Proposition 8. $\qquad\square$

Proposition 11. *Consider the quasistatic Navier-Stokes/Darcy weak formulation* (7.25)-(7.26) *and assume that*

$$\mathbf{u}_t^{QS}(0) \in (L^2(\Omega_f))^d, \mathbf{f}_{f,t} \in (L^2(0, T; H^{-1}(\Omega_f)))^d, f_{p,t} \in L^2(0, T; H^{-1}(\Omega_p)).$$

Then,

$$n \sup_{t \in [0,T]} \|\mathbf{u}_t^{QS}(t)\|_f^2 + \int_0^T \left\{ \frac{2n\nu}{C_K}\|\nabla\mathbf{u}_t^{QS}(t)\|_f^2 + \frac{2n\nu\alpha}{\sqrt{k_{max}}}\sum_{i=1}^{d-1}\|\mathbf{u}_t^{QS}(t) \cdot \hat{\boldsymbol{\tau}}_i\|_I^2 \right.$$
$$\left. + g k_{min}\|\nabla\phi_t^{QS}(t)\|_p^2 \right\} dt$$
$$\leq n\|\mathbf{u}_t^{QS}(0)\|_f^2 + \int_0^T \left\{ \frac{nC_K}{2\rho^2\nu}\|\mathbf{f}_{f,t}(t)\|_{-1,f}^2 + \frac{g}{k_{min}}\|f_{p,t}(s)\|_{-1,p}^2 \right\} dt \leq C_4^*.$$

Proof. We take the derivative with respect to time in (7.25)-(7.26) to get:

$$(\mathbf{u}_{tt}^{QS}, \mathbf{v})_f + \frac{d}{dt}\left[b(\mathbf{u}^{QS}, \mathbf{u}^{QS}, \mathbf{v}) - \frac{n}{2}\langle \mathbf{u}^{QS} \cdot \mathbf{u}^{QS}, \mathbf{v} \cdot \hat{\mathbf{n}}_f\rangle\right] + a_f(\mathbf{u}_t^{QS}, \mathbf{v}) + c_I(\mathbf{v}, \phi_t^{QS})$$
$$= n(\tilde{\mathbf{f}}_{f,t}, \mathbf{v})_f, \quad (7.37)$$

$$a_p(\phi_t^{QS}, \psi) - c_I(\mathbf{u}_t^{QS}, \psi) = g(f_{p,t}, \psi)_p. \quad (7.38)$$

By fixing $t > 0$ and choosing $\mathbf{v} = \mathbf{u}_t^{QS}(t), \psi = \phi_t^{QS}(t)$ in (7.37)-(7.38), the nonlinear term in brackets vanishes according to (7.33). By adding the equations together the coupling terms cancel out, and we obtain the claim by following the steps from the proof of Proposition 8. $\qquad\square$

7.3 CONVERGENCE TO THE QUASISTATIC SOLUTION

In this section, in Theorem 13 for the 2d case and Theorem 16 for the 3d case, we derive estimates for the error between the solution $(\mathbf{u}, \phi)$ of the fully evolutionary Navier-Stokes/Darcy problem, (7.23)-(7.24), and the solution $(\mathbf{u}^{QS}, \phi^{QS})$ of the corresponding quasistatic problem, (7.25)-(7.26), and prove convergence to the quasistatic solution as S_0 converges to zero. For both cases, the order of convergence is one, and in the case of three spatial dimensions, the convergence result holds under a regularity assumption on the velocity.

Let the errors in $\mathbf{u}$ and ϕ be denoted respectively by

$$\mathbf{e_u}(\mathbf{x}, t) := \mathbf{u}(\mathbf{x}, t) - \mathbf{u}^{QS}(\mathbf{x}, t),$$

$$e_\phi(\mathbf{x}, t) := \phi(\mathbf{x}, t) - \phi^{QS}(\mathbf{x}, t).$$

Then $\mathbf{e_u}(\mathbf{x}, 0) = \mathbf{0}$ and $e_\phi(\mathbf{x}, 0) = \phi_0(\mathbf{x}) - \phi^{QS}(\mathbf{x}, 0)$.

7.3.1 Convergence to the quasistatic solution in 2d

Before stating the main result of this subsection, we recall an improved bound on the trilinear form "$(\mathbf{u} \cdot \nabla \mathbf{v}, \mathbf{w})_f$", which holds in two spatial dimensions.

Proposition 12. *For $\mathbf{u}, \mathbf{v}, \mathbf{w} \in \mathbf{X}_f$, we have*

$$|(\mathbf{u} \cdot \nabla \mathbf{v}, \mathbf{w})_f| \leq \sqrt{2} \|\mathbf{u}\|_f^{1/2} \|\nabla \mathbf{u}\|_f^{1/2} \|\nabla \mathbf{v}\|_f \|\mathbf{w}\|_f^{1/2} \|\nabla \mathbf{w}\|_f^{1/2}, \qquad for \ \ d = 2. \qquad (7.39)$$

Proof. First, we apply Hölder's inequality, (2.3), on $(\mathbf{u} \cdot \nabla \mathbf{v}, \mathbf{w})_f$ with $q = 2, p = r = 4$ to get

$$|(\mathbf{u} \cdot \nabla \mathbf{v}, \mathbf{w})_f| \leq \|\mathbf{u}\|_{L^4(\Omega_f)} \|\nabla \mathbf{v}\|_f \|\mathbf{w}\|_{L^4(\Omega_f)}. \qquad (7.40)$$

Then the inequality follows by combining (7.40) with the Ladyzhenskaya inequality, [79]:

$$\|\mathbf{u}\|_{L^4(\Omega_f)} \leq 2^{1/4} \|\mathbf{u}\|_f^{1/2} \|\nabla \mathbf{u}\|_f^{1/2}, \qquad for \ \ d = 2. \qquad (7.41)$$

$\square$

Theorem 13. *Assume that the initial data and body forces satisfy*

$$\mathbf{u}_0 \in (L^2(\Omega_f))^d, \ \mathbf{u}_t^{QS}(0) \in (L^2(\Omega_f))^d, \ \|\phi_t(0)\|_{-1,p} < \infty,$$

$$\mathbf{f}_f \in (L^2(0,T;H^{-1}(\Omega_f)))^d, \ f_p \in L^2(0,T;H^{-1}(\Omega_p)),$$

$$\mathbf{f}_{f,t} \in (L^2(0,T;H^{-1}(\Omega_f)))^d, \ f_{p,t} \in L^2(0,T;H^{-1}(\Omega_p)).$$

Then

$$\sup_{t\in[0,T]} \left\{ n\|\mathbf{e_u}(t)\|_f^2 + gS_0\|e_\phi(t)\|_p^2 \right\} + \int_0^T \left\{ \frac{2n\nu}{C_K}\|\nabla\mathbf{e_u}(t)\|_f^2 + \frac{2n\nu\alpha}{\sqrt{k_{max}}}\sum_{i=1}^{d-1}\|\mathbf{e_u}(t)\cdot\hat{\tau}_i\|_I^2 \right.$$

$$\left. + gk_{min}\|\nabla e_\phi(t)\|_p^2 \right\} \ dt$$

$$\leq \left(\frac{gS_0^3 C_{PF,p}^2}{(k_{min})^2}\|\phi_t(0)\|_{-1,p}^2 + \frac{S_0^2 C_{PF,p}^3}{(k_{min})^2}C_4^* \right) \exp\left(\frac{27}{4}\left[\frac{C_K^2 C_2^*}{\nu^2 n} \right]^2 \right) \leq C_B S_0^2,$$

where C_B is a positive constant with $C_B \sim \frac{\exp(\nu^{-4}n^{-2})}{(k_{min})^2}$.

Proof. We first subtract the quasistatic weak formulation (7.25)-(7.26) from the Navier-Stokes/Darcy weak formulation (7.23)-(7.24) and obtain

$$n(\mathbf{e_{u,t}},\mathbf{v})_f + \left[b(\mathbf{u},\mathbf{u},\mathbf{v}) - b(\mathbf{u}^{QS},\mathbf{u}^{QS},\mathbf{v}) \right] - \frac{n}{2}\left\{ \langle\mathbf{u}\cdot\mathbf{u},\mathbf{v}\cdot\hat{\mathbf{n}}_f\rangle_I - \langle\mathbf{u}^{QS}\cdot\mathbf{u}^{QS},\mathbf{v}\cdot\hat{\mathbf{n}}_f\rangle_I \right\}$$

$$+a_f(\mathbf{e_u},\mathbf{v}) + c_I(\mathbf{v},e_\phi) = 0, \tag{7.42}$$

$$gS_0(e_{\phi,t},\psi)_p + a_p(e_\phi,\psi) - c_I(\mathbf{e_u},\psi) = -gS_0(\phi_t^{QS},\psi)_p. \tag{7.43}$$

Next, we fix $t > 0$, choose $v = \mathbf{e_u}(t)$ and $\psi = e_\phi(t)$ in (7.42)-(7.43), and add the equations together. The coupling terms cancel out and we get

$$\frac{1}{2}\frac{d}{dt}\left\{ n\|\mathbf{e_u}(t)\|_f^2 + gS_0\|e_\phi(t)\|_p^2 \right\} + a_f(\mathbf{e_u},\mathbf{e_u}) + a_p(e_\phi,e_\phi)$$

$$+ \left[b(\mathbf{u},\mathbf{u},\mathbf{e_u}) - b(\mathbf{u}^{QS},\mathbf{u}^{QS},\mathbf{e_u}) \right] - \frac{n}{2}\left\{ \langle\mathbf{u}\cdot\mathbf{u},\mathbf{e_u}\cdot\hat{\mathbf{n}}_f\rangle_I - \langle\mathbf{u}^{QS}\cdot\mathbf{u}^{QS},\mathbf{e_u}\cdot\hat{\mathbf{n}}_f\rangle_I \right\} \tag{7.44}$$

$$= -gS_0(\phi_t^{QS},e_\phi)_p.$$

Now, we express the nonlinear terms appearing in the left-hand side of (7.44) as follows:

$$\left[b(\mathbf{u},\mathbf{u},\mathbf{e_u}) - b(\mathbf{u}^{QS},\mathbf{u}^{QS},\mathbf{e_u}) \right] - \frac{n}{2}\left\{ \langle\mathbf{u}\cdot\mathbf{u},\mathbf{e_u}\cdot\hat{\mathbf{n}}_f\rangle_I - \langle\mathbf{u}^{QS}\cdot\mathbf{u}^{QS},\mathbf{e_u}\cdot\hat{\mathbf{n}}_f\rangle_I \right\}$$

$$= b(\mathbf{e_u},\mathbf{u},\mathbf{e_u}) + b(\mathbf{u}^{QS},\mathbf{e_u},\mathbf{e_u}) - \frac{n}{2}\langle\mathbf{e_u}\cdot\mathbf{u},\mathbf{e_u}\cdot\hat{\mathbf{n}}_f\rangle_I - \frac{n}{2}\langle\mathbf{u}^{QS}\cdot\mathbf{e_u},\mathbf{e_u}\cdot\hat{\mathbf{n}}_f\rangle_I. \tag{7.45}$$

Then, we use (7.21) for the term "$b(\mathbf{e_u}, \mathbf{u}, \mathbf{e_u})$", and (7.45) becomes, after also simplifying:

$$\left[b(\mathbf{u},\mathbf{u},\mathbf{e_u}) - b(\mathbf{u}^{QS},\mathbf{u}^{QS},\mathbf{e_u})\right] - \frac{n}{2}\left\{\langle \mathbf{u}\cdot\mathbf{u}, \mathbf{e_u}\cdot\hat{\mathbf{n}}_f\rangle_I - \langle \mathbf{u}^{QS}\cdot\mathbf{u}^{QS}, \mathbf{e_u}\cdot\hat{\mathbf{n}}_f\rangle_I\right\}$$

$$= n\langle \mathbf{e_u}\cdot\mathbf{u}, \mathbf{e_u}\cdot\hat{\mathbf{n}}_f\rangle_I - b(\mathbf{e_u},\mathbf{e_u},\mathbf{u}) + b(\mathbf{u}^{QS},\mathbf{e_u},\mathbf{e_u})$$

$$\qquad - \frac{n}{2}\langle \mathbf{e_u}\cdot\mathbf{u}, \mathbf{e_u}\cdot\hat{\mathbf{n}}_f\rangle_I - \frac{n}{2}\langle \mathbf{u}^{QS}\cdot\mathbf{e_u}, \mathbf{e_u}\cdot\hat{\mathbf{n}}_f\rangle_I$$

$$= \frac{n}{2}\langle \mathbf{e_u}\cdot\mathbf{u}, \mathbf{e_u}\cdot\hat{\mathbf{n}}_f\rangle_I - b(\mathbf{e_u},\mathbf{e_u},\mathbf{u}) + b(\mathbf{u}^{QS},\mathbf{e_u},\mathbf{e_u}) - \frac{n}{2}\langle \mathbf{u}^{QS}\cdot\mathbf{e_u}, \mathbf{e_u}\cdot\hat{\mathbf{n}}_f\rangle_I$$

$$= \frac{n}{2}\langle \mathbf{e_u}\cdot\mathbf{e_u}, \mathbf{e_u}\cdot\hat{\mathbf{n}}_f\rangle_I - b(\mathbf{e_u},\mathbf{e_u},\mathbf{u}) + b(\mathbf{u}^{QS},\mathbf{e_u},\mathbf{e_u})$$

$$= \frac{n}{2}\langle \mathbf{e_u}\cdot\mathbf{e_u}, \mathbf{e_u}\cdot\hat{\mathbf{n}}_f\rangle_I - b(\mathbf{e_u},\mathbf{e_u},\mathbf{e_u}) - b(\mathbf{e_u},\mathbf{e_u},\mathbf{u}^{QS}) + b(\mathbf{u}^{QS},\mathbf{e_u},\mathbf{e_u})$$

$$\overset{(7.22)}{=} -b(\mathbf{e_u},\mathbf{e_u},\mathbf{u}^{QS}) + b(\mathbf{u}^{QS},\mathbf{e_u},\mathbf{e_u}). \tag{7.46}$$

Using (7.46) as well as the coercivity estimates (3.34)-(3.36) on the left-hand side of (7.44), we obtain after rearranging:

$$\frac{1}{2}\frac{d}{dt}\left\{n\|\mathbf{e_u}(t)\|_f^2 + gS_0\|e_\phi(t)\|_p^2\right\} + \frac{2n\nu}{C_K}\|\nabla\mathbf{e_u}\|_f^2 + \frac{n\nu\alpha}{\sqrt{k_{max}}}\sum_{i=1}^{d-1}\|\mathbf{e_u}\cdot\hat{\tau}_i\|_I^2 + gk_{min}\|\nabla e_\phi\|_p^2$$

$$\leq b(\mathbf{e_u},\mathbf{e_u},\mathbf{u}^{QS}) - b(\mathbf{u}^{QS},\mathbf{e_u},\mathbf{e_u}) - gS_0(\phi_t^{QS}, e_\phi)_p. \tag{7.47}$$

We then bound the last term on the right-hand side as follows, using Young's inequality:

$$|gS_0(\phi_t^{QS}, e_\phi)_p| \leq gS_0\|\phi_t^{QS}\|_{-1,p}\|e_\phi\|_p \leq \frac{gk_{min}}{2}\|e_\phi\|_p^2 + \frac{gS_0^2}{2k_{min}}\|\phi_t^{QS}\|_{-1,p}^2.$$

Thus, (7.47) becomes

$$\frac{1}{2}\frac{d}{dt}\left\{n\|\mathbf{e_u}(t)\|_f^2 + gS_0\|e_\phi(t)\|_p^2\right\} + \frac{2n\nu}{C_K}\|\nabla\mathbf{e_u}\|_f^2 + \frac{n\nu\alpha}{\sqrt{k_{max}}}\sum_{i=1}^{d-1}\|\mathbf{e_u}\cdot\hat{\tau}_i\|_I^2 + \frac{gk_{min}}{2}\|\nabla e_\phi\|_p^2$$

$$\leq b(\mathbf{e_u},\mathbf{e_u},\mathbf{u}^{QS}) - b(\mathbf{u}^{QS},\mathbf{e_u},\mathbf{e_u}) + \frac{gS_0^2}{2k_{min}}\|\phi_t^{QS}\|_{-1,p}^2. \tag{7.48}$$

To bound the trilinear terms on the right-hand side of (7.48), we apply (7.39) along with Young's inequality (2.4), with $p = \frac{4}{3}$, $q = 4$, and $\epsilon = \frac{4n\nu}{3C_K}$:

$$
\begin{aligned}
b(\mathbf{e_u}, \mathbf{e_u}, \mathbf{u}^{QS}) - b(\mathbf{u}^{QS}, \mathbf{e_u}, \mathbf{e_u}) &= n\left\{(\mathbf{e_u} \cdot \nabla \mathbf{e_u}, \mathbf{u}^{QS}) - (\mathbf{u}^{QS} \cdot \nabla \mathbf{e_u}, \mathbf{e_u})\right\} \\
&\leq 2\sqrt{2}\, n\|\mathbf{e_u}\|_f^{1/2}\|\nabla \mathbf{e_u}\|_f^{1/2}\|\nabla \mathbf{e_u}\|_f\|\mathbf{u}^{QS}\|_f^{1/2}\|\nabla \mathbf{u}^{QS}\|_f^{1/2} \\
&= \left(\|\nabla \mathbf{e_u}\|_f^{3/2}\right)\left(2\sqrt{2}\, n\|\mathbf{e_u}\|_f^{1/2}\|\mathbf{u}^{QS}\|_f^{1/2}\|\nabla \mathbf{u}^{QS}\|_f^{1/2}\right) \\
&\leq \frac{n\nu}{C_K}\|\nabla \mathbf{e_u}\|_f^2 + \frac{27}{4}n\left(\frac{C_K}{\nu}\right)^3 \|\mathbf{e_u}\|_f^2\|\mathbf{u}^{QS}\|_f^2\|\nabla \mathbf{u}^{QS}\|_f^2. \quad (7.49)
\end{aligned}
$$

Therefore, (7.48) becomes

$$
\begin{aligned}
\frac{1}{2}\frac{d}{dt}&\left\{n\|\mathbf{e_u}(t)\|_f^2 + gS_0\|e_\phi(t)\|_p^2\right\} + \frac{n\nu}{C_K}\|\nabla \mathbf{e_u}\|_f^2 + \frac{n\nu\alpha}{\sqrt{k_{max}}}\sum_{i=1}^{d-1}\|\mathbf{e_u} \cdot \hat{\tau}_i\|_I^2 + \frac{gk_{min}}{2}\|\nabla e_\phi\|_p^2 \\
&\leq \frac{27}{4}n\left(\frac{C_K}{\nu}\right)^3\|\mathbf{e_u}\|_f^2\|\mathbf{u}^{QS}\|_f^2\|\nabla \mathbf{u}^{QS}\|_f^2 + \frac{gS_0^2}{2k_{min}}\|\phi_t^{QS}\|_{-1,p}^2. \quad (7.50)
\end{aligned}
$$

We now multiply by 2 and integrate with respect to time over $[0, t]$, $t > 0$:

$$
\begin{aligned}
n\|\mathbf{e_u}(t)\|_f^2 &+ gS_0\|e_\phi(t)\|_p^2 + \int_0^t \left\{\frac{2n\nu}{C_K}\|\nabla \mathbf{e_u}(s)\|_f^2 + \frac{2n\nu\alpha}{\sqrt{k_{max}}}\sum_{i=1}^{d-1}\|\mathbf{e_u}(s) \cdot \hat{\tau}_i\|_I^2 \right. \\
&\left. + gk_{min}\|\nabla e_\phi(s)\|_p^2\right\}\, ds \\
&\leq gS_0\|e_\phi(0)\|_p^2 + \frac{27}{2}n\left(\frac{C_K}{\nu}\right)^3\int_0^t \|\mathbf{e_u}(s)\|_f^2\|\mathbf{u}^{QS}(s)\|_f^2\|\nabla \mathbf{u}^{QS}(s)\|_f^2\, ds \\
&\quad + \frac{gS_0^2}{k_{min}}\int_0^t \|\phi_s^{QS}(s)\|_{-1,p}^2\, ds,
\end{aligned}
\quad (7.51)
$$

where we used that $\mathbf{e_u}(0) = \mathbf{0}$. Next, we use Grönwall's lemma (2.10) with

$$
\begin{aligned}
u(t) &= n\|\mathbf{e_u}(t)\|_f^2, \\
\beta(s) &= \frac{27}{2}\left(\frac{C_K}{\nu}\right)^3\|\mathbf{u}^{QS}(s)\|_f^2\|\nabla \mathbf{u}^{QS}(s)\|_f^2, \quad \text{and} \\
\alpha(t) &= gS_0\|e_\phi(0)\|_p^2 + \frac{gS_0^2}{k_{min}}\int_0^t \|\phi_s^{QS}(s)\|_{-1,p}^2\, ds.
\end{aligned}
$$

106

This yields:

$$
n\|\mathbf{e_u}(t)\|_f^2 + gS_0\|e_\phi(t)\|_p^2 + \int_0^t \left\{ \frac{2n\nu}{C_K}\|\nabla\mathbf{e_u}(s)\|_f^2 + \frac{2n\nu\alpha}{\sqrt{k_{max}}}\sum_{i=1}^{d-1}\|\mathbf{e_u}(s)\cdot\hat{\tau}_i\|_I^2 \right.
$$
$$
\left. + gk_{min}\|\nabla e_\phi(s)\|_p^2 \right\} ds
$$
$$
\leq \left(gS_0\|e_\phi(0)\|_p^2 + \frac{gS_0^2}{k_{min}}\int_0^t \|\phi_s^{QS}(s)\|_{-1,p}^2 \, ds \right) \cdot
$$
$$
\cdot \exp\left(\frac{27}{2}\left(\frac{C_K}{\nu}\right)^3 \int_0^t \|\mathbf{u}^{QS}(s)\|_f^2\|\nabla\mathbf{u}^{QS}(s)\|_f^2 \, ds \right). \tag{7.52}
$$

After taking the supremum over $[0,T]$, we obtain

$$
\sup_{t\in[0,T]} \{n\|\mathbf{e_u}(t)\|_f^2 + gS_0\|e_\phi(t)\|_p^2\} + \int_0^T \left\{ \frac{2n\nu}{C_K}\|\nabla\mathbf{e_u}(t)\|_f^2 + \frac{2n\nu\alpha}{\sqrt{k_{max}}}\sum_{i=1}^{d-1}\|\mathbf{e_u}(t)\cdot\hat{\tau}_i\|_I^2 \right.
$$
$$
\left. + gk_{min}\|\nabla e_\phi(t)\|_p^2 \right\} dt
$$
$$
\leq \left(gS_0\|e_\phi(0)\|_p^2 + \frac{gS_0^2}{k_{min}}\int_0^T \|\phi_t^{QS}(t)\|_{-1,p}^2 \, dt \right) \cdot
$$
$$
\cdot \exp\left(\frac{27}{2}\left(\frac{C_K}{\nu}\right)^3 \int_0^T \|\mathbf{u}^{QS}(t)\|_f^2\|\nabla\mathbf{u}^{QS}(t)\|_f^2 \, dt \right). \tag{7.53}
$$

From Proposition 9 we have that

$$
\|\mathbf{u}^{QS}\|_{L^\infty(0,T;L^2(\Omega_f))}^2 \leq \frac{C_2^*}{n}, \quad \text{and} \quad \|\nabla\mathbf{u}^{QS}\|_{L^2(0,T;L^2(\Omega_f))}^2 \leq \frac{C_K C_2^*}{2n\nu}. \tag{7.54}
$$

Moreover, since

$$
\int_0^T \|\phi_t^{QS}(t)\|_{-1,p}^2 \, dt \leq C_{PF,p}\int_0^T \|\phi_t^{QS}(t)\|_p^2 \, dt \leq C_{PF,p}^3 \int_0^T \|\nabla\phi_t^{QS}(t)\|_p^2 \, dt,
$$

by Proposition 11 we also have that

$$
\int_0^T \|\phi_t^{QS}(t)\|_{-1,p}^2 \, dt \leq \frac{C_{PF,p}^3}{gk_{min}}C_4^*. \tag{7.55}
$$

Furthermore, by setting $t = 0$ in (7.24) and (7.26) and then subtracting (7.26) from (7.24) we get

$$
gS_0(\phi_t(0),\psi)_p + a_p(e_\phi(0),\psi) = 0,
$$

107

and thus, picking $\psi = e_\phi(0)$ above results in

$$a_p(e_\phi(0), e_\phi(0)) = -gS_0(\phi_t(0), e_\phi(0))_p.$$

By using the coercivity estimate (3.36), along with the definition of the $\|\cdot\|_{-1,p}$ norm and the Poincaré-Friedrichs inequality, we obtain

$$
\begin{aligned}
&k_{min}\|\nabla e_\phi(0)\|_p^2 \leq S_0\|\phi_t(0)\|_{-1,p}\|\nabla e_\phi(0)\|_p, \\
&\Rightarrow \|\nabla e_\phi(0)\|_p \leq \frac{S_0}{k_{min}}\|\phi_t(0)\|_{-1,p}, \\
&\Rightarrow \|e_\phi(0)\|_p \leq \frac{S_0 C_{PF,p}}{k_{min}}\|\phi_t(0)\|_{-1,p}.
\end{aligned}
\tag{7.56}
$$

Finally, by applying (7.54), (7.55), and (7.56) on the right-hand side of (7.53), we get

$$
\begin{aligned}
\sup_{t\in[0,T]} &\left\{ n\|\mathbf{e_u}(t)\|_f^2 + gS_0\|e_\phi(t)\|_p^2 \right\} + \int_0^T \left\{ \frac{2n\nu}{C_K}\|\nabla \mathbf{e_u}(t)\|_f^2 + \frac{2n\nu\alpha}{\sqrt{k_{max}}} \sum_{i=1}^{d-1} \|\mathbf{e_u}(t)\cdot\hat{\tau}_i\|_I^2 \right. \\
&\left. + gk_{min}\|\nabla e_\phi(t)\|_p^2 \right\} dt \\
\leq &\left(\frac{gS_0^3 C_{PF,p}^2}{(k_{min})^2}\|\phi_t(0)\|_{-1,p}^2 + \frac{S_0^2 C_{PF,p}^3}{(k_{min})^2}C_4^* \right) \exp\left(\frac{27}{4}\left[\frac{C_K^2 C_2^*}{\nu^2 n} \right]^2 \right) \leq C_B S_0^2,
\end{aligned}
$$

since also $\|\phi_t(0)\|_{-1,p} < \infty$, where $C_B \sim \frac{\exp(\nu^{-4}n^{-2})}{(k_{min})^2}$, concluding the proof. $\qquad\square$

In summary, under the assumptions of Theorem 13,

$$
\begin{aligned}
\|\mathbf{u} - \mathbf{u}^{QS}\|_{L^\infty(0,T;L^2(\Omega_f))} &= \mathcal{O}(S_0), \quad C \sim \frac{(\exp(\nu^{-4}n^{-2}))^{1/2}}{\sqrt{n}k_{min}}, \\
\|\nabla(\mathbf{u} - \mathbf{u}^{QS})\|_{L^2(0,T;L^2(\Omega_f))} &= \mathcal{O}(S_0), \quad C \sim \frac{(\exp(\nu^{-4}n^{-2}))^{1/2}}{\sqrt{n}\nu k_{min}}, \\
\|\phi - \phi^{QS}\|_{L^\infty(0,T;L^2(\Omega_p))} &= \mathcal{O}(\sqrt{S_0}), \quad C \sim \frac{(\exp(\nu^{-4}n^{-2}))^{1/2}}{k_{min}}, \\
\|\nabla(\phi - \phi^{QS})\|_{L^2(0,T;L^2(\Omega_p))} &= \mathcal{O}(S_0), \quad C \sim \frac{(\exp(\nu^{-4}n^{-2}))^{1/2}}{(k_{min})^{3/2}}.
\end{aligned}
$$

where C denotes the constant in the error estimate, and "$\sim$" means "proportional to". We conclude that the quasistatic approximation in the Navier-Stokes/Darcy problem in two spatial dimensions is justified provided $0 < S_0 << k_{min} << 1$.

7.3.2 Convergence to the quasistatic solution in 3d

In the case of three spatial dimensions, we assume more regularity on the solution in order to prove convergence to the quasistatic solution.

Theorem 14. *Assume that the initial data and body forces satisfy*

$$\mathbf{u}_t^{QS}(0) \in (L^2(\Omega_f))^d, \ \|\phi_t(0)\|_{-1,p} < \infty,$$

$$\mathbf{f}_{f,t} \in (L^2(0,T;H^{-1}(\Omega_f)))^d, \ f_{p,t} \in L^2(0,T;H^{-1}(\Omega_p)).$$

Further, assume that

$$\|\nabla \mathbf{u}^{QS}\|_{L^4(0,T;L^2(\Omega_f))} \leq C_{\mathbf{u}}, \quad 0 < C_{\mathbf{u}} < \infty. \tag{7.57}$$

Then

$$\sup_{t \in [0,T]} \left\{ n\|\mathbf{e_u}(t)\|_f^2 + gS_0\|e_\phi(t)\|_p^2 \right\} + \int_0^T \left\{ \frac{2n\nu}{C_K}\|\nabla\mathbf{e_u}(t)\|_f^2 + \frac{2n\nu\alpha}{\sqrt{k_{max}}} \sum_{i=1}^{d-1} \|\mathbf{e_u}(t) \cdot \hat{\tau}_i\|_I^2 \right.$$

$$\left. + \ gk_{min}\|\nabla e_\phi(t)\|_p^2 \right\} \ dt$$

$$\leq \left(\frac{gS_0^3 C_{PF,p}^2}{(k_{min})^2} \|\phi_t(0)\|_{-1,p}^2 + \frac{S_0^2 C_{PF,p}^3}{(k_{min})^2}C_4^* \right) \exp\left(\frac{27}{8}C_b^4 \left[\frac{C_K}{\nu}\right]^3 C_{\mathbf{u}} \right) \leq C_E S_0^2,$$

where C_E is a positive constant with $C_E \sim \frac{\exp(\nu^{-3})}{(k_{min})^2}$.

Proof. Following the same steps as in the proof of Theorem 13, we arrive at

$$\frac{1}{2}\frac{d}{dt}\left\{ n\|\mathbf{e_u}(t)\|_f^2 + gS_0\|e_\phi(t)\|_p^2 \right\} + \frac{2n\nu}{C_K}\|\nabla\mathbf{e_u}\|_f^2 + \frac{n\nu\alpha}{\sqrt{k_{max}}}\sum_{i=1}^{d-1}\|\mathbf{e_u} \cdot \hat{\tau}_i\|_I^2 + \frac{gk_{min}}{2}\|\nabla e_\phi\|_p^2$$

$$\leq b(\mathbf{e_u}, \mathbf{e_u}, \mathbf{u}^{QS}) - b(\mathbf{u}^{QS}, \mathbf{e_u}, \mathbf{e_u}) + \frac{gS_0^2}{2k_{min}}\|\phi_t^{QS}\|_{-1,p}^2. \tag{7.58}$$

To bound the trilinear forms above, we use (7.20) along with Young's inequality (2.4) with $p = \frac{4}{3}$, $q = 4$, and $\epsilon = \frac{4n\nu}{3C_K}$:

$$
\begin{aligned}
b(\mathbf{e_u}, \mathbf{e_u}, \mathbf{u}^{QS}) - b(\mathbf{u}^{QS}, \mathbf{e_u}, \mathbf{e_u}) &= n\left\{(\mathbf{e_u} \cdot \nabla\mathbf{e_u}, \mathbf{u}^{QS}) - (\mathbf{u}^{QS} \cdot \nabla\mathbf{e_u}, \mathbf{e_u})\right\} \\
&\leq 2nC_b\|\mathbf{e_u}\|_f^{1/2}\|\nabla\mathbf{e_u}\|_f^{1/2}\|\nabla\mathbf{e_u}\|_f\|\nabla\mathbf{u}^{QS}\|_f \\
&= \left(\|\nabla\mathbf{e_u}\|_f^{3/2}\right)\left(2nC_b\|\mathbf{e_u}\|_f^{1/2}\|\nabla\mathbf{u}^{QS}\|_f\right) \\
&\leq \frac{n\nu}{C_K}\|\nabla\mathbf{e_u}\|_f^2 + \frac{27}{16}nC_b^4\left(\frac{C_K}{\nu}\right)^3\|\mathbf{e_u}\|_f^2\|\nabla\mathbf{u}^{QS}\|_f^4.
\end{aligned}
\tag{7.59}
$$

(7.59) and (7.58) then give

$$
\begin{aligned}
&\frac{1}{2}\frac{d}{dt}\left\{n\|\mathbf{e_u}(t)\|_f^2 + gS_0\|e_\phi(t)\|_p^2\right\} + \frac{n\nu}{C_K}\|\nabla\mathbf{e_u}\|_f^2 + \frac{n\nu\alpha}{\sqrt{k_{max}}}\sum_{i=1}^{d-1}\|\mathbf{e_u}\cdot\hat{\tau}_i\|_I^2 + \frac{gk_{min}}{2}\|\nabla e_\phi\|_p^2 \\
&\leq \frac{27}{16}nC_b^4\left(\frac{C_K}{\nu}\right)^3\|\mathbf{e_u}\|_f^2\|\nabla\mathbf{u}^{QS}\|_f^4 + \frac{gS_0^2}{2k_{min}}\|\phi_t^{QS}\|_{-1,p}^2.
\end{aligned}
\tag{7.60}
$$

Next we integrate with respect to time over $[0, t]$, $t > 0$, and get

$$
\begin{aligned}
&n\|\mathbf{e_u}(t)\|_f^2 + gS_0\|e_\phi(t)\|_p^2 + \int_0^t\left\{\frac{2n\nu}{C_K}\|\nabla\mathbf{e_u}(s)\|_f^2 + \frac{2n\nu\alpha}{\sqrt{k_{max}}}\sum_{i=1}^{d-1}\|\mathbf{e_u}(s)\cdot\hat{\tau}_i\|_I^2\right. \\
&\left.\quad + gk_{min}\|\nabla e_\phi(s)\|_p^2\right\}\,ds \\
&\leq gS_0\|e_\phi(0)\|_p^2 + \frac{27}{8}nC_b^4\left(\frac{C_K}{\nu}\right)^3\int_0^t\|\mathbf{e_u}(s)\|_f^2\|\nabla\mathbf{u}^{QS}(s)\|_f^4\,ds \\
&\quad + \frac{gS_0^2}{k_{min}}\int_0^t\|\phi_s^{QS}(s)\|_{-1,p}^2\,ds.
\end{aligned}
\tag{7.61}
$$

By applying Grönwall's lemma (2.10) to (7.61) with

$$
\begin{aligned}
u(t) &= n\|\mathbf{e_u}(t)\|_f^2, \\
\beta(s) &= \frac{27}{8}C_b^4\left(\frac{C_K}{\nu}\right)^3\|\nabla\mathbf{u}^{QS}(s)\|_f^4, \quad \text{and} \\
\alpha(t) &= gS_0\|e_\phi(0)\|_p^2 + \frac{gS_0^2}{k_{min}}\int_0^t\|\phi_s^{QS}(s)\|_{-1,p}^2\,ds,
\end{aligned}
$$

we obtain

$$
\begin{aligned}
n\|\mathbf{e_u}(t)\|_f^2 + gS_0\|e_\phi(t)\|_p^2 &+ \int_0^t \left\{ \frac{2n\nu}{C_K}\|\nabla\mathbf{e_u}(s)\|_f^2 + \frac{2n\nu\alpha}{\sqrt{k_{max}}} \sum_{i=1}^{d-1} \|\mathbf{e_u}(s)\cdot\hat{\tau}_i\|_I^2 \right. \\
&\left. + gk_{min}\|\nabla e_\phi(s)\|_p^2 \right\} ds \\
&\leq \left(gS_0\|e_\phi(0)\|_p^2 + \frac{gS_0^2}{k_{min}} \int_0^t \|\phi_s^{QS}(s)\|_{-1,p}^2 \, ds \right) \cdot \\
&\quad \cdot \exp\left(\frac{27}{8}C_b^4 \left(\frac{C_K}{\nu}\right)^3 \int_0^t \|\nabla\mathbf{u}^{QS}(s)\|_f^4 \, ds \right).
\end{aligned}
\tag{7.62}
$$

Taking the supremum over $[0,T]$ results in

$$
\begin{aligned}
\sup_{t\in[0,T]} \left\{ n\|\mathbf{e_u}(t)\|_f^2 + gS_0\|e_\phi(t)\|_p^2 \right\} &+ \int_0^T \left\{ \frac{2n\nu}{C_K}\|\nabla\mathbf{e_u}(t)\|_f^2 + \frac{2n\nu\alpha}{\sqrt{k_{max}}} \sum_{i=1}^{d-1} \|\mathbf{e_u}(t)\cdot\hat{\tau}_i\|_I^2 \right. \\
&\left. + gk_{min}\|\nabla e_\phi(t)\|_p^2 \right\} dt \\
&\leq \left(gS_0\|e_\phi(0)\|_p^2 + \frac{gS_0^2}{k_{min}} \int_0^T \|\phi_t^{QS}(t)\|_{-1,p}^2 \, dt \right) \cdot \\
&\quad \cdot \exp\left(\frac{27}{8}C_b^4 \left(\frac{C_K}{\nu}\right)^3 \int_0^T \|\nabla\mathbf{u}^{QS}(t)\|_f^4 \, dt \right).
\end{aligned}
\tag{7.63}
$$

Finally, using (7.55) and (7.56) from the proof of Theorem 13, and also the regularity assumption (7.57), we conclude that

$$
\begin{aligned}
\sup_{t\in[0,T]} \left\{ n\|\mathbf{e_u}(t)\|_f^2 + gS_0\|e_\phi(t)\|_p^2 \right\} &+ \int_0^T \left\{ \frac{2n\nu}{C_K}\|\nabla\mathbf{e_u}(t)\|_f^2 + \frac{2n\nu\alpha}{\sqrt{k_{max}}} \sum_{i=1}^{d-1} \|\mathbf{e_u}(t)\cdot\hat{\tau}_i\|_I^2 \right. \\
&\left. + gk_{min}\|\nabla e_\phi(t)\|_p^2 \right\} dt \\
&\leq \left(\frac{gS_0^3 C_{PF,p}^2}{(k_{min})^2}\|\phi_t(0)\|_{-1,p}^2 + \frac{S_0^2 C_{PF,p}^3}{(k_{min})^2}C_4^* \right) \exp\left(\frac{27}{8}C_b^4 \left[\frac{C_K}{\nu}\right]^3 C_\mathbf{u} \right) \leq C_E S_0^2,
\end{aligned}
$$

where $C_E > 0$ is such that $C_E \sim \frac{\exp(\nu^{-3})}{(k_{min})^2}$. $\qquad\square$

To summarize, under the assumptions of Theorem 14, and the extra regularity condition (7.57), we have

$$\|\mathbf{u} - \mathbf{u}^{QS}\|_{L^\infty(0,T;L^2(\Omega_f))} = \mathcal{O}(S_0), \quad C \sim \frac{(\exp{(\nu^{-3})})^{1/2}}{\sqrt{n}k_{min}},$$

$$\|\nabla(\mathbf{u} - \mathbf{u}^{QS})\|_{L^2(0,T;L^2(\Omega_f))} = \mathcal{O}(S_0), \quad C \sim \frac{(\exp{(\nu^{-3})})^{1/2}}{\sqrt{n\nu}k_{min}},$$

$$\|\phi - \phi^{QS}\|_{L^\infty(0,T;L^2(\Omega_p))} = \mathcal{O}(\sqrt{S_0}), \quad C \sim \frac{(\exp{(\nu^{-3})})^{1/2}}{k_{min}},$$

$$\|\nabla(\phi - \phi^{QS})\|_{L^2(0,T;L^2(\Omega_p))} = \mathcal{O}(S_0), \quad C \sim \frac{(\exp{(\nu^{-3})})^{1/2}}{(k_{min})^{3/2}}.$$

where C denotes the constant in the error estimate, and "$\sim$" means "proportional to", as before. Thus, we conclude that the quasistatic approximation in the Navier-Stokes/Darcy problem in three spatial dimensions (assuming more regularity) is justified provided $0 < S_0 << k_{min} << 1$.

7.4 CONVERGENCE TO THE QUASISTATIC SOLUTION IN 3D UNDER SMALL DATA

In this section, in Theorem 16, we obtain first-order convergence of the evolutionary Navier-Stokes/Darcy solution in three spatial dimensions to the quasistatic solution, as $S_0 \to 0$, under a small-data condition. To show convergence under small data, we first derive in Theorem 15 a set of additional à-priori estimates, which hold under a small-data condition. We utilize the interface inequality obtained in Chapter 2. To this end, we restrict the domains Ω_f and Ω_p so that either the hypotheses of Theorem 1 or those of Theorem 2 hold. That is, we assume either that there exists a C^1-diffeomorphism from Ω_f to Ω_p, so that (3.45) holds, or that I is of the form $x_d = f(x_1, \ldots, x_{d-1})$, $f \in C^1(\mathbb{R}^{d-1})$, and Ω_f, Ω_p are any bounded, regular domains, and (3.47) holds instead. In either case, we assume that

$$|\langle \phi, \mathbf{u} \cdot \hat{\mathbf{n}}_f \rangle_I| = \left| \int_I \phi \mathbf{u} \cdot \hat{\mathbf{n}}_f \ d\boldsymbol{\sigma} \right| \leq C^\dagger \|\mathbf{u}\|_f \|\nabla \phi\|_p, \qquad (7.64)$$

where $C^\dagger > 0$ is either the constant from Theorem 1 or Theorem 2.

Theorem 15. *Assume that the initial data and body forces of (7.23)-(7.24) and (7.25)-(7.26) satisfy*

$$\mathbf{u}_0, \mathbf{u}_t^{QS}(0) \in (L^2(\Omega_f))^d, \ \mathbf{D}(\mathbf{u}_0) \in (L^2(\Omega_f))^{d \times d}, \ \mathbf{u}_0 \cdot \hat{\boldsymbol{\tau}}_i \in L^2(I), \ i = 1, \ldots, \ d-1,$$

$$\nabla \phi^{QS}(0) \in (L^2(\Omega_p))^d,$$

$$\mathbf{f}_f \in (L^2(0, T; L^2(\Omega_f)))^d, \ f_p \in L^2(0, T; H^{-1}(\Omega_p)), \qquad (7.65)$$

$$\mathbf{f}_{f,t} \in (L^2(0, T; H^{-1}(\Omega_f)))^d, \ f_{p,t} \in L^2(0, T; H^{-1}(\Omega_p)),$$

and that the domains Ω_f, Ω_p are such that (7.64) holds. Further, assume that the initial data and body forces satisfy the small-data condition

$$n\|\mathbf{u}_0\|_f^2 + \int_0^T \left\{ \frac{nC_K}{2\rho^2 \nu} \|\mathbf{f}_f(t)\|_{-1,f}^2 + \frac{g}{k_{min}} \|f_p(t)\|_{-1,p}^2 \right\} \ dt \leq C_2^* < \frac{2n\nu^2}{C_K^2 C_b C_{PF,f}^{1/2}}, \qquad (7.66)$$

where C_2^* is the constant from Proposition 9. Then we have

$$n \int_0^T \|\mathbf{u}_t^{QS}(t)\|_f^2 \, dt + 2n\gamma \sup_{t \in [0,T]} \|\nabla \mathbf{u}^{QS}(t)\|_f^2$$

$$+ \sup_{t \in [0,T]} \left\{ \frac{n\nu\alpha}{\sqrt{k_{max}}} \sum_{i=1}^{d-1} \|\mathbf{u}^{QS}(t) \cdot \hat{\boldsymbol{\tau}}_i\|_I^2 + \frac{gk_{min}}{2} \|\nabla\phi^{QS}(t)\|_p^2 \right\}$$

$$\leq \frac{2n}{\rho^2} \int_0^T \|\mathbf{f}_f(t)\|_f^2 \, dt + g \int_0^T \|f_p(t)\|_{-1,p}^2 \, dt + 8n(gC^\dagger)^2 \int_0^T \|\nabla\phi^{QS}(t)\|_p^2 \, dt$$

$$+ g \int_0^T \|\nabla\phi_t^{QS}(t)\|_p^2 \, dt + 2nC_bC_{PF,f}^{1/2} \int_0^T \|\nabla\mathbf{u}_t^{QS}(t)\|_f^2 \, dt$$

$$+ \frac{2n^2 g(C^\dagger)^2}{k_{min}} \sup_{t \in [0,T]} \|\mathbf{u}^{QS}(t)\|_f^2$$

$$+ 2n\nu\|\mathbf{D}(\mathbf{u}_0)\|_f^2 + \sum_{i=1}^{d-1} \int_I \frac{n\nu\alpha}{\sqrt{\hat{\boldsymbol{\tau}}_i \cdot \mathbf{K} \cdot \hat{\boldsymbol{\tau}}_i}} (\mathbf{u}_0 \cdot \hat{\boldsymbol{\tau}}_i)^2 \, d\boldsymbol{\sigma}$$

$$+ g(\mathbf{K}\nabla\phi^{QS}(0), \nabla\phi^{QS}(0))_p - 2c_I(\mathbf{u}_0, \phi^{QS}(0))$$

$$\leq \frac{10n^2 g(C^\dagger)^2}{k_{min}} \|\mathbf{u}_0\|_f^2 + n\left(\frac{1}{k_{min}} + \frac{C_bC_{PF,f}^{1/2}C_K}{\nu}\right) \|\mathbf{u}_t^{QS}(0)\|_f^2 + \frac{2n}{\rho^2} \int_0^T \|\mathbf{f}_f(t)\|_f^2 \, dt$$

$$+ \frac{5n^2 g(C^\dagger)^2 C_K}{k_{min}\nu\rho^2} \int_0^T \|\mathbf{f}_f(t)\|_{-1,f}^2 + g\left(1 + 10ng\left(C^\dagger/k_{min}\right)^2\right) \int_0^T \|f_p(t)\|_{-1,p}^2 \, dt$$

$$+ \frac{nC_K}{2\nu\rho^2} \left(\frac{n}{k_{min}} + \frac{C_bC_{PF}^{1/2}C_K}{\nu}\right) \int_0^T \|\mathbf{f}_{f,t}(t)\|_{-1,f}^2 \, dt$$

$$+ \frac{g}{k_{min}} \left(\frac{1}{k_{min}} + \frac{C_bC_{PF,f}^{1/2}C_K}{\nu}\right) \int_0^T \|f_{p,t}(t)\|_{-1,p}^2 \, dt$$

$$+ 2n\nu\|\mathbf{D}(\mathbf{u}_0)\|_f^2 + \sum_{i=1}^{d-1} \int_I \frac{n\nu\alpha}{\sqrt{\hat{\boldsymbol{\tau}}_i \cdot \mathbf{K} \cdot \hat{\boldsymbol{\tau}}_i}} (\mathbf{u}_0 \cdot \hat{\boldsymbol{\tau}}_i)^2 \, d\boldsymbol{\sigma}$$

$$+ g(\mathbf{K}\nabla\phi^{QS}(0), \nabla\phi^{QS}(0))_p - 2c_I(\mathbf{u}_0, \phi^{QS}(0)) \leq C_5^*, \tag{7.67}$$

where $\gamma := \frac{2n\nu^2 - C_2^* C_b C_{PF,f}^{1/2} C_K^2}{2n\nu C_K} > 0$ by (7.66). Then, specifically

$$\mathbf{u}_t^{QS} \in (L^2(0, T; L^2(\Omega_f)))^d, \ \nabla\mathbf{u}^{QS} \in (L^\infty(0, T; L^2(\Omega_f)))^{d \times d},$$

$$\mathbf{u}^{QS} \cdot \hat{\boldsymbol{\tau}}_i \in L^\infty(0, T; L^2(I)), \ i = 1, \ldots, \ d-1, \ \nabla\phi^{QS} \in (L^\infty(0, T; L^2(\Omega_p)))^d.$$

Proof. We consider the quasistatic Navier-Stokes/Darcy weak formulation (7.25)-(7.26). We fix $t > 0$ and choose $\mathbf{v} = \mathbf{u}_t^{QS}(t)$ and $\psi = \phi_t^{QS}(t)$. Adding the resulting equations together yields:

$$n\|\mathbf{u}_t^{QS}\|_f^2 + b(\mathbf{u}^{QS}, \mathbf{u}^{QS}, \mathbf{u}_t^{QS}) - \frac{n}{2}\langle \mathbf{u}^{QS} \cdot \mathbf{u}^{QS}, \mathbf{u}_t^{QS} \cdot \hat{\mathbf{n}}_f \rangle_I + a_f(\mathbf{u}^{QS}, \mathbf{u}_t^{QS}) + a_p(\phi^{QS}, \phi_t^{QS})$$
$$+ c_I(\mathbf{u}_t^{QS}, \phi^{QS}) - c_I(\mathbf{u}^{QS}, \phi_t^{QS}) = n(\tilde{\mathbf{f}}_f, \mathbf{u}_t^{QS})_f + g(f_p, \phi_t^{QS})_p. \tag{7.68}$$

Using

$$c_I(\mathbf{u}_t^{QS}, \phi^{QS}) - c_I(\mathbf{u}^{QS}, \phi_t^{QS}) = -\frac{d}{dt}c_I(\mathbf{u}^{QS}, \phi^{QS}) + 2c_I(\mathbf{u}_t^{QS}, \phi^{QS}),$$

(7.68) can be rewritten as

$$n\|\mathbf{u}_t^{QS}\|_f^2 + b(\mathbf{u}^{QS}, \mathbf{u}^{QS}, \mathbf{u}_t^{QS}) - \frac{n}{2}\langle \mathbf{u}^{QS} \cdot \mathbf{u}^{QS}, \mathbf{u}_t^{QS} \cdot \hat{\mathbf{n}}_f \rangle_I + \frac{1}{2}\frac{d}{dt}\left\{a_f(\mathbf{u}^{QS}, \mathbf{u}^{QS}) + a_p(\phi^{QS}, \phi^{QS})\right.$$
$$\left. -2c_I(\mathbf{u}^{QS}, \phi^{QS})\right\} = n(\tilde{\mathbf{f}}_f, \mathbf{u}_t^{QS})_f + g(f_p, \phi_t^{QS})_p - 2c_I(\mathbf{u}_t^{QS}, \phi^{QS}). \tag{7.69}$$

Using (7.22), we rewrite

$$-\frac{n}{2}\langle \mathbf{u}^{QS} \cdot \mathbf{u}^{QS}, \mathbf{u}_t^{QS} \cdot \hat{\mathbf{n}}_f \rangle_I = -b(\mathbf{u}_t^{QS}, \mathbf{u}^{QS}, \mathbf{u}^{QS}),$$

so that (7.69) becomes

$$n\|\mathbf{u}_t^{QS}\|_f^2 + \frac{1}{2}\frac{d}{dt}\left\{a_f(\mathbf{u}^{QS}, \mathbf{u}^{QS}) + a_p(\phi^{QS}, \phi^{QS}) - 2c_I(\mathbf{u}^{QS}, \phi^{QS})\right\} = b(\mathbf{u}_t^{QS}, \mathbf{u}^{QS}, \mathbf{u}^{QS})$$
$$- b(\mathbf{u}^{QS}, \mathbf{u}^{QS}, \mathbf{u}_t^{QS}) + n(\tilde{\mathbf{f}}_f, \mathbf{u}_t^{QS})_f + g(f_p, \phi_t^{QS})_p - 2c_I(\mathbf{u}_t^{QS}, \phi^{QS}). \tag{7.70}$$

Next, we bound each term on the right-hand side of (7.70):

For the trilinear form we use inequality (7.20) and then apply the Poincaré-Friedrichs inequality (7.1) and Young's inequality to get

$$b(\mathbf{u}_t^{QS}, \mathbf{u}^{QS}, \mathbf{u}^{QS}) - b(\mathbf{u}^{QS}, \mathbf{u}^{QS}, \mathbf{u}_t^{QS}) \leq nC_b\|\mathbf{u}_t^{QS}\|_f^{1/2}\|\nabla \mathbf{u}_t^{QS}\|_f^{1/2}\|\nabla \mathbf{u}^{QS}\|_f\|\nabla \mathbf{u}^{QS}\|_f$$
$$+ nC_b\|\mathbf{u}^{QS}\|_f^{1/2}\|\nabla \mathbf{u}^{QS}\|_f^{1/2}\|\nabla \mathbf{u}^{QS}\|_f\|\nabla \mathbf{u}_t^{QS}\|_f$$
$$\leq 2nC_bC_{PF,f}^{1/2}\|\nabla \mathbf{u}_t^{QS}\|_f\|\nabla \mathbf{u}^{QS}\|_f^2$$
$$\leq nC_bC_{PF,f}^{1/2}\left\{\|\nabla \mathbf{u}_t^{QS}\|_f^2 + \|\nabla \mathbf{u}^{QS}\|_f^4\right\}. \tag{7.71}$$

For the interface term, and since $\nabla \cdot \mathbf{u}_t^{QS} = 0$, we use inequality (7.64) and Young's inequality to obtain

$$-2c_I(\mathbf{u}_t^{QS}, \phi^{QS}) \leq 2ngC^{\dagger}\|\mathbf{u}_t^{QS}\|_f \|\nabla \phi^{QS}\|_p \leq \frac{n}{4}\|\mathbf{u}_t^{QS}\|_f^2 + 4n(gC^{\dagger})^2\|\nabla \phi^{QS}\|_p^2. \qquad (7.72)$$

Last, we obtain bounds for the terms involving the body forces by applying the Cauchy-Schwarz and Young inequalities:

$$n(\tilde{\mathbf{f}}_f, \mathbf{u}_t^{QS})_f \leq n\|\tilde{\mathbf{f}}_f\|_f \|\mathbf{u}_t^{QS}\|_f \leq \frac{n}{4}\|\mathbf{u}_t^{QS}\|_f^2 + n\|\tilde{\mathbf{f}}_f\|_f^2 = \frac{n}{4}\|\mathbf{u}_t^{QS}\|_f^2 + \frac{n}{\rho^2}\|\mathbf{f}_f\|_f^2, \qquad (7.73)$$

$$g(f_p, \phi_t^{QS})_p \leq g\|f_p\|_{-1,p}\|\nabla \phi_t^{QS}\|_f \leq \frac{g}{2}\|\nabla \phi_t^{QS}\|_f^2 + \frac{g}{2}\|f_p\|_{-1,p}^2. \qquad (7.74)$$

Now we apply the bounds (7.71)-(7.74) to the right-hand side of (7.70) and we have, after absorbing terms on the left-hand side,

$$
\begin{aligned}
\frac{n}{2}\|\mathbf{u}_t^{QS}\|_f^2 &+ \frac{1}{2}\frac{d}{dt}\left\{a_f(\mathbf{u}^{QS}, \mathbf{u}^{QS}) + a_p(\phi^{QS}, \phi^{QS}) - 2c_I(\mathbf{u}^{QS}, \phi^{QS})\right\} \\
&\leq \frac{n}{\rho^2}\|\mathbf{f}_f\|_f^2 + \frac{g}{2}\|f_p\|_{-1,p}^2 + 4n(gC^{\dagger})^2\|\nabla \phi^{QS}\|_p^2 + \frac{g}{2}\|\nabla \phi_t^{QS}\|_f^2 \\
&\quad + nC_bC_{PF,f}^{1/2}\left\{\|\nabla \mathbf{u}_t^{QS}\|_f^2 + \|\nabla \mathbf{u}^{QS}\|_f^4\right\}.
\end{aligned}
\qquad (7.75)
$$

Multiplying (7.75) by 2 and integrating over $[0, t]$, $0 < t \leq T$, gives:

$$
\begin{aligned}
n\int_0^t &\|\mathbf{u}_s^{QS}(s)\|_f^2\, ds + \left\{a_f(\mathbf{u}^{QS}, \mathbf{u}^{QS}) + a_p(\phi^{QS}, \phi^{QS}) - 2c_I(\mathbf{u}^{QS}, \phi^{QS})\right\}(t) \\
&\leq \frac{2n}{\rho^2}\int_0^t \|\mathbf{f}_f(s)\|_f^2\, ds + g\int_0^t \|f_p(s)\|_{-1,p}^2\, ds + 8n(gC^{\dagger})^2\int_0^t \|\nabla \phi^{QS}(s)\|_p^2\, ds \\
&\quad + g\int_0^t \|\nabla \phi_s^{QS}(s)\|_f^2\, ds + 2nC_bC_{PF,f}^{1/2}\int_0^t \|\nabla \mathbf{u}_s^{QS}(s)\|_f^2\, ds \\
&\quad + 2nC_bC_{PF,f}^{1/2}\int_0^t \|\nabla \mathbf{u}^{QS}(s)\|_f^4\, ds \\
&\quad + \left\{a_f(\mathbf{u}^{QS}, \mathbf{u}^{QS}) + a_p(\phi^{QS}, \phi^{QS}) - 2c_I(\mathbf{u}^{QS}, \phi^{QS})\right\}(0).
\end{aligned}
\qquad (7.76)
$$

Finally, by applying the coercivity estimates (3.34)-(3.36) as well as inequality (7.64) and Young's inequality, we bound the term on the left-hand side as follows:

$$
\begin{aligned}
\left\{ a_f(\mathbf{u}^{QS}, \mathbf{u}^{QS}) + a_p(\phi^{QS}, \phi^{QS}) - 2c_I(\mathbf{u}^{QS}, \phi^{QS}) \right\}(t) \\
\geq \frac{2n\nu}{C_K}\|\nabla\mathbf{u}^{QS}(t)\|_f^2 + \frac{n\nu\alpha}{\sqrt{k_{max}}}\sum_{i=1}^{d-1}\|\mathbf{u}^{QS}(t)\cdot\hat{\boldsymbol{\tau}}_i\|_I^2 + gk_{min}\|\nabla\phi^{QS}(t)\|_p^2 \\
- \frac{gk_{min}}{2}\|\nabla\phi^{QS}(t)\|_p^2 - \frac{2n^2g(C^\dagger)^2}{k_{min}}\|\mathbf{u}^{QS}(t)\|_f^2 \\
= \frac{2n\nu}{C_K}\|\nabla\mathbf{u}^{QS}(t)\|_f^2 + \frac{n\nu\alpha}{\sqrt{k_{max}}}\sum_{i=1}^{d-1}\|\mathbf{u}^{QS}(t)\cdot\hat{\boldsymbol{\tau}}_i\|_I^2 + \frac{gk_{min}}{2}\|\nabla\phi^{QS}(t)\|_p^2 \\
- \frac{2n^2g(C^\dagger)^2}{k_{min}}\|\mathbf{u}^{QS}(t)\|_f^2.
\end{aligned}
\tag{7.77}
$$

By using (7.77) on the left-hand side of (7.76) and after rearranging we obtain:

$$
\begin{aligned}
n\int_0^t \|\mathbf{u}_s^{QS}(s)\|_f^2\,ds + \frac{2n\nu}{C_K}\|\nabla\mathbf{u}^{QS}(t)\|_f^2 + \frac{n\nu\alpha}{\sqrt{k_{max}}}\sum_{i=1}^{d-1}\|\mathbf{u}^{QS}(t)\cdot\hat{\boldsymbol{\tau}}_i\|_I^2 \\
+ \frac{gk_{min}}{2}\|\nabla\phi^{QS}(t)\|_p^2 \\
\leq \frac{2n}{\rho^2}\int_0^t\|\mathbf{f}_f(s)\|_f^2\,ds + g\int_0^t\|f_p(s)\|_{-1,p}^2\,ds \\
+ 8n(gC^\dagger)^2\int_0^t\|\nabla\phi^{QS}(s)\|_p^2\,ds \\
+ g\int_0^t\|\nabla\phi_s^{QS}(s)\|_p^2\,ds + 2nC_bC_{PF,f}^{1/2}\int_0^t\|\nabla\mathbf{u}_s^{QS}(s)\|_f^2\,ds \\
+ 2nC_bC_{PF,f}^{1/2}\int_0^t\|\nabla\mathbf{u}^{QS}(s)\|_f^4\,ds + \frac{2n^2g(C^\dagger)^2}{k_{min}}\|\mathbf{u}^{QS}(t)\|_f^2 \\
+ 2n\nu\|\mathbf{D}(\mathbf{u}_0)\|_f^2 + \sum_{i=1}^{d-1}\int_I \frac{n\nu\alpha}{\sqrt{\hat{\boldsymbol{\tau}}_i\cdot\mathbf{K}\cdot\hat{\boldsymbol{\tau}}_i}}(\mathbf{u}_0\cdot\hat{\boldsymbol{\tau}}_i)^2\,d\boldsymbol{\sigma} \\
+ g(\mathbf{K}\nabla\phi^{QS}(0), \nabla\phi^{QS}(0))_p - 2c_I(\mathbf{u}_0, \phi^{QS}(0)).
\end{aligned}
\tag{7.78}
$$

Finally, by taking the supremum over $[0, T]$ for t in (7.78), yields

$$
\begin{aligned}
n \int_0^T \|\mathbf{u}_t^{QS}(t)\|_f^2 \, dt + \sup_{t \in [0,T]} \Bigg\{ & \frac{2n\nu}{C_K} \|\nabla \mathbf{u}^{QS}(t)\|_f^2 + \frac{n\nu\alpha}{\sqrt{k_{max}}} \sum_{i=1}^{d-1} \|\mathbf{u}^{QS}(t) \cdot \hat{\boldsymbol{\tau}}_i\|_I^2 \\
& + \frac{g k_{min}}{2} \|\nabla \phi^{QS}(t)\|_p^2 \Bigg\}
\end{aligned}
$$

$$
\begin{aligned}
\leq {}& \frac{2n}{\rho^2} \int_0^T \|\mathbf{f}_f(t)\|_f^2 \, dt + g \int_0^T \|f_p(t)\|_{-1,p}^2 \, dt + 8n(gC^\dagger)^2 \int_0^T \|\nabla \phi^{QS}(t)\|_p^2 \, dt \\
& + g \int_0^T \|\nabla \phi_t^{QS}(t)\|_p^2 \, dt + 2n C_b C_{PF,f}^{1/2} \int_0^T \|\nabla \mathbf{u}_t^{QS}(t)\|_f^2 \, dt \qquad (7.79) \\
& + 2n C_b C_{PF,f}^{1/2} \int_0^T \|\nabla \mathbf{u}^{QS}(t)\|_f^4 \, dt + \frac{2n^2 g (C^\dagger)^2}{k_{min}} \sup_{t \in [0,T]} \|\mathbf{u}^{QS}(t)\|_f^2 \\
& + 2n\nu \|\mathbf{D}(\mathbf{u}_0)\|_f^2 + \sum_{i=1}^{d-1} \int_I \frac{n\nu\alpha}{\sqrt{\hat{\boldsymbol{\tau}}_i \cdot \mathbf{K} \cdot \hat{\boldsymbol{\tau}}_i}} (\mathbf{u}_0 \cdot \hat{\boldsymbol{\tau}}_i)^2 \, d\boldsymbol{\sigma} \\
& + g(\mathbf{K}\nabla \phi^{QS}(0), \nabla \phi^{QS}(0))_p - 2c_I(\mathbf{u}_0, \phi^{QS}(0)).
\end{aligned}
$$

Next, we bound the term "$\int_0^T \|\nabla \mathbf{u}^{QS}(t)\|_f^4 \, dt$" that appears in the right-hand side of (7.79) as follows:

$$
\int_0^T \|\nabla \mathbf{u}^{QS}(t)\|_f^4 \, dt \leq \sup_{t \in [0,T]} \|\nabla \mathbf{u}^{QS}(t)\|_f^2 \int_0^T \|\nabla \mathbf{u}^{QS}(t)\|_f^2 \, dt. \qquad (7.80)
$$

We then apply (7.80) to the right-hand side of (7.79) and obtain

$$
\begin{aligned}
n \int_0^T \|\mathbf{u}_t^{QS}(t)\|_f^2 \, dt + \sup_{t \in [0,T]} \Bigg\{ & \frac{2n\nu}{C_K} \|\nabla \mathbf{u}^{QS}(t)\|_f^2 + \frac{n\nu\alpha}{\sqrt{k_{max}}} \sum_{i=1}^{d-1} \|\mathbf{u}^{QS}(t) \cdot \hat{\boldsymbol{\tau}}_i\|_I^2 \\
& + \frac{g k_{min}}{2} \|\nabla \phi^{QS}(t)\|_p^2 \Bigg\}
\end{aligned}
$$

$$
\begin{aligned}
\leq {}& \frac{2n}{\rho^2} \int_0^T \|\mathbf{f}_f(t)\|_f^2 \, dt + g \int_0^T \|f_p(t)\|_{-1,p}^2 \, dt + 8n(gC^\dagger)^2 \int_0^T \|\nabla \phi^{QS}(t)\|_p^2 \, dt \\
& + g \int_0^T \|\nabla \phi_t^{QS}(t)\|_p^2 \, dt + 2n C_b C_{PF,f}^{1/2} \int_0^T \|\nabla \mathbf{u}_t^{QS}(t)\|_f^2 \, dt \qquad (7.81) \\
& + 2n C_b C_{PF,f}^{1/2} \sup_{t \in [0,T]} \|\nabla \mathbf{u}^{QS}(t)\|_f^2 \int_0^T \|\nabla \mathbf{u}^{QS}(t)\|_f^2 \, dt + \frac{2n^2 g (C^\dagger)^2}{k_{min}} \sup_{t \in [0,T]} \|\mathbf{u}^{QS}(t)\|_f^2 \\
& + 2n\nu \|\mathbf{D}(\mathbf{u}_0)\|_f^2 + \sum_{i=1}^{d-1} \int_I \frac{n\nu\alpha}{\sqrt{\hat{\boldsymbol{\tau}}_i \cdot \mathbf{K} \cdot \hat{\boldsymbol{\tau}}_i}} (\mathbf{u}_0 \cdot \hat{\boldsymbol{\tau}}_i)^2 \, d\boldsymbol{\sigma} \\
& + g(\mathbf{K}\nabla \phi^{QS}(0), \nabla \phi^{QS}(0))_p - 2c_I(\mathbf{u}_0, \phi^{QS}(0)).
\end{aligned}
$$

After subtracting this new term from both sides of (7.81), it becomes

$$
n \int_0^T \|\mathbf{u}_t^{QS}(t)\|_f^2 \, dt + 2n \left[\frac{\nu}{C_K} - C_b C_{PF,f}^{1/2} \int_0^T \|\nabla \mathbf{u}^{QS}(t)\|_f^2 \, dt \right] \sup_{t \in [0,T]} \|\nabla \mathbf{u}^{QS}(t)\|_f^2
$$

$$
+ \sup_{t \in [0,T]} \left\{ \frac{n \nu \alpha}{\sqrt{k_{max}}} \sum_{i=1}^{d-1} \|\mathbf{u}^{QS}(t) \cdot \hat{\boldsymbol{\tau}}_i\|_I^2 + \frac{g k_{min}}{2} \|\nabla \phi^{QS}(t)\|_p^2 \right\}
$$

$$
\leq \frac{2n}{\rho^2} \int_0^T \|\mathbf{f}_f(t)\|_f^2 \, dt + g \int_0^T \|f_p(t)\|_{-1,p}^2 \, dt + 8n(g C^\dagger)^2 \int_0^T \|\nabla \phi^{QS}(t)\|_p^2 \, dt
$$

$$
+ g \int_0^T \|\nabla \phi_t^{QS}(t)\|_p^2 \, dt + 2n C_b C_{PF,f}^{1/2} \int_0^T \|\nabla \mathbf{u}_t^{QS}(t)\|_f^2 \, dt
$$

$$
+ \frac{2n^2 g (C^\dagger)^2}{k_{min}} \sup_{t \in [0,T]} \|\mathbf{u}^{QS}(t)\|_f^2
$$

$$
+ 2n\nu \|\mathbf{D}(\mathbf{u}_0)\|_f^2 + \sum_{i=1}^{d-1} \int_I \frac{n \nu \alpha}{\sqrt{\hat{\boldsymbol{\tau}}_i \cdot \mathbf{K} \cdot \hat{\boldsymbol{\tau}}_i}} (\mathbf{u}_0 \cdot \hat{\boldsymbol{\tau}}_i)^2 \, d\boldsymbol{\sigma}
$$

$$
+ g (\mathbf{K} \nabla \phi^{QS}(0), \nabla \phi^{QS}(0))_p - 2 c_I(\mathbf{u}_0, \phi^{QS}(0)).
$$

By Proposition 9 we have that

$$
\frac{2n\nu}{C_K} \int_0^T \|\nabla \mathbf{u}^{QS}(t)\|_f^2 \, dt \leq n \|\mathbf{u}_0\|_f^2 + \int_0^T \left\{ \frac{n C_K}{2\rho^2 \nu} \|\mathbf{f}_f(t)\|_{-1,f}^2 + \frac{g}{k_{min}} \|f_p(t)\|_{-1,p}^2 \right\} \, dt \leq C_2^*.
\tag{7.82}
$$

By combining (7.82) with the assumption (7.66) we then get

$$
\frac{2n\nu}{C_K} \int_0^T \|\nabla \mathbf{u}^{QS}(t)\|_f^2 \, dt \leq C_2^* < \frac{2n\nu^2}{C_K^2 C_b C_{PF,f}^{1/2}}.
\tag{7.83}
$$

Consequently,

$$
\frac{\nu}{C_K} - C_b C_{PF,f}^{1/2} \int_0^T \|\nabla \mathbf{u}^{QS}(t)\|_f^2 \, dt \geq \frac{2n\nu^2 - C_2^* C_b C_{PF,f}^{1/2} C_K^2}{2n\nu C_K} = \gamma > 0.
\tag{7.84}
$$

Thus,

$$
n \int_0^T \|\mathbf{u}_t^{QS}(t)\|_f^2 \, dt + 2n\gamma \sup_{t\in[0,T]} \|\nabla \mathbf{u}^{QS}(t)\|_f^2
$$

$$
+ \sup_{t\in[0,T]} \left\{ \frac{n\nu\alpha}{\sqrt{k_{max}}} \sum_{i=1}^{d-1} \|\mathbf{u}^{QS}(t)\cdot\hat{\boldsymbol{\tau}}_i\|_I^2 + \frac{gk_{min}}{2} \|\nabla\phi^{QS}(t)\|_p^2 \right\}
$$

$$
\leq \frac{2n}{\rho^2} \int_0^T \|\mathbf{f}_f(t)\|_f^2 \, dt + g \int_0^T \|f_p(t)\|_{-1,p}^2 \, dt + 8n(gC^\dagger)^2 \int_0^T \|\nabla\phi^{QS}(t)\|_p^2 \, dt
$$

$$
+ g \int_0^T \|\nabla\phi_t^{QS}(t)\|_p^2 \, dt + 2nC_bC_{PF,f}^{1/2} \int_0^T \|\nabla\mathbf{u}_t^{QS}(t)\|_f^2 \, dt \tag{7.85}
$$

$$
+ \frac{2n^2 g(C^\dagger)^2}{k_{min}} \sup_{t\in[0,T]} \|\mathbf{u}^{QS}(t)\|_f^2
$$

$$
+ 2n\nu\|\mathbf{D}(\mathbf{u}_0)\|_f^2 + \sum_{i=1}^{d-1} \int_I \frac{n\nu\alpha}{\sqrt{\hat{\boldsymbol{\tau}}_i\cdot\mathbf{K}\cdot\hat{\boldsymbol{\tau}}_i}} (\mathbf{u}_0\cdot\hat{\boldsymbol{\tau}}_i)^2 \, d\boldsymbol{\sigma}
$$

$$
+ g(\mathbf{K}\nabla\phi^{QS}(0), \nabla\phi^{QS}(0))_p - 2c_I(\mathbf{u}_0, \phi^{QS}(0)),
$$

which proves the first part of (7.67). For the second part, observe that under the assumptions (7.65) of Theorem 15, we have from Propositions 9 and 11 (recall that $\|\mathbf{f}_f\|_{-1,f} \leq C\|\mathbf{f}_f\|_f$):

$$
8n(gC^\dagger)^2 \int_0^T \|\nabla\phi^{QS}(t)\|_p^2 \, dt \leq \frac{8n^2 g(C^\dagger)^2}{k_{min}} \|\mathbf{u}_0\|_f^2
$$

$$
+ \frac{4n^2 g(C^\dagger)^2 C_K}{k_{min}\nu\rho^2} \int_0^T \|\mathbf{f}_f(t)\|_{-1,f}^2 \, dt + 8n(gC^\dagger/k_{min})^2 \int_0^T \|f_p(t)\|_{-1,p}^2 \, dt, \tag{7.86}
$$

$$
g \int_0^T \|\nabla\phi_t^{QS}(t)\|_p^2 \, dt \leq \frac{n}{k_{min}} \|\mathbf{u}_t^{QS}(0)\|_f^2
$$

$$
+ \frac{n^2 C_K}{2k_{min}\nu\rho^2} \int_0^T \|\mathbf{f}_{f,t}(t)\|_{-1,f}^2 \, dt + \frac{g}{(k_{min})^2} \int_0^T \|f_{p,t}(t)\|_{-1,p}^2 \, dt, \tag{7.87}
$$

$$
2nC_bC_{PF,f}^{1/2} \int_0^T \|\nabla\mathbf{u}_t^{QS}(t)\|_f^2 \, dt \leq \frac{nC_bC_{PF,f}^{1/2}C_K}{\nu} \|\mathbf{u}_t^{QS}(0)\|_f^2
$$

$$
+ \frac{nC_bC_{PF,f}^{1/2}C_K^2}{2\nu^2\rho^2} \int_0^T \|\mathbf{f}_{f,t}(t)\|_{-1,f}^2 \, dt + \frac{C_bC_{PF,f}^{1/2}C_Kg}{k_{min}\nu} \int_0^T \|f_{p,t}(t)\|_{-1,p}^2 \, dt, \tag{7.88}
$$

$$
\frac{2n^2 g(C^\dagger)^2}{k_{min}} \sup_{t\in[0,T]} \|\mathbf{u}^{QS}(t)\|_f^2 \leq \frac{2n^2 g(C^\dagger)^2}{k_{min}} \|\mathbf{u}_0\|_f^2
$$

$$
+ \frac{n^2 g(C^\dagger)^2 C_K}{k_{min}\nu\rho^2} \int_0^T \|\mathbf{f}_f(t)\|_{-1,f}^2 \, dt + 2n(gC^\dagger/k_{min})^2 \int_0^T \|f_p(t)\|_{-1,p}^2 \, dt. \tag{7.89}
$$

The last part of Theorem 15 now follows by substituting the bounds (7.86)-(7.89) into (7.85), concluding the proof. $\qquad\square$

We now prove convergence to the quasistatic solution as $S_0 \to 0$ under a small-data condition.

Theorem 16. *Assume that the initial data and body forces of (7.23)-(7.24) and (7.25)-(7.26) satisfy*

$$\mathbf{u}_0, \mathbf{u}_t^{QS}(0) \in (L^2(\Omega_f))^d, \ \mathbf{D}(\mathbf{u}_0) \in (L^2(\Omega_f))^{d \times d}, \ \mathbf{u}_0 \cdot \hat{\boldsymbol{\tau}}_i \in L^2(I), \ i = 1, \ldots, \ d-1,$$

$$\nabla \phi^{QS}(0) \in (L^2(\Omega_p))^d, \ \|\phi_t(0)\|_{-1,p} < \infty,$$

$$\mathbf{f}_f \in (L^2(0, T; L^2(\Omega_f)))^d, \ f_p \in L^2(0, T; H^{-1}(\Omega_p)), \tag{7.90}$$

$$\mathbf{f}_{f,t} \in (L^2(0, T; H^{-1}(\Omega_f)))^d, \ f_{p,t} \in L^2(0, T; H^{-1}(\Omega_p)),$$

and that the domains Ω_f, Ω_p are such that (7.64) holds. Further, assume that the initial data and body forces satisfy the small-data conditions

$$C_2^* < \frac{2n\nu^2}{C_K^2 C_b C_{PF,f}^{1/2}},$$

$$C_5^* < \frac{2n\nu^2\gamma}{(C_K C_b)^2 C_{PF,f}}, \tag{7.91}$$

where C_2^* is the constant from Proposition 9, C_5^* the one from Theorem 15, and γ is defined in Theorem 15. Then we have

$$\sup_{t \in [0,T]} \left\{ n\|\mathbf{e_u}(t)\|_f^2 + gS_0\|e_\phi(t)\|_p^2 \right\} + 4n\epsilon \int_0^T \|\nabla \mathbf{e_u}(t)\|_f^2 \ dt$$

$$+ \int_0^T \left\{ \frac{2n\nu\alpha}{\sqrt{k_{max}}} \sum_{i=1}^{d-1} \|\mathbf{e_u}(t) \cdot \hat{\tau}_i\|_I^2 + \frac{gk_{min}}{2}\|\nabla e_\phi(t)\|_p^2 \right\} \ dt \tag{7.92}$$

$$\leq C_D S_0^2,$$

where $\epsilon := \frac{\nu - C_K C_c \sqrt{\frac{C_5^*}{2n\gamma}}}{C_K} > 0$, by (7.91), and $C_D > 0$ is a constant such that $C_D \sim \frac{1}{(k_{min})^2}$.

121

Proof. From the proof of Theorem 13, inequality (7.48), we have

$$\frac{1}{2}\frac{d}{dt}\left\{n\|\mathbf{e_u}(t)\|_f^2 + gS_0\|e_\phi(t)\|_p^2\right\} + \frac{2n\nu}{C_K}\|\nabla\mathbf{e_u}\|_f^2 + \frac{n\nu\alpha}{\sqrt{k_{max}}}\sum_{i=1}^{d-1}\|\mathbf{e_u}\cdot\hat{\tau}_i\|_I^2 + \frac{gk_{min}}{2}\|\nabla e_\phi\|_p^2$$

$$\leq b(\mathbf{e_u},\mathbf{e_u},\mathbf{u}^{QS}) - b(\mathbf{u}^{QS},\mathbf{e_u},\mathbf{e_u}) + \frac{gS_0^2}{2k_{min}}\|\phi_t^{QS}\|_{-1,p}^2. \tag{7.93}$$

We bound the trilinear terms using (7.19):

$$b(\mathbf{e_u},\mathbf{e_u},\mathbf{u}^{QS}) - b(\mathbf{u}^{QS},\mathbf{e_u},\mathbf{e_u}) \leq nC_c\|\nabla\mathbf{e_u}\|_f\|\nabla\mathbf{e_u}\|_f\|\nabla\mathbf{u}^{QS}\|_f$$

$$+ nC_c\|\nabla\mathbf{u}^{QS}\|_f\|\nabla\mathbf{e_u}\|_f\|\nabla\mathbf{e_u}\|_f$$

$$= 2nC_c\|\nabla\mathbf{e_u}\|_f^2\|\nabla\mathbf{u}^{QS}\|_f$$

$$\leq 2nC_c\sup_{t\in[0,T]}\left\{\|\nabla\mathbf{u}^{QS}(t)\|_f\right\}\|\nabla\mathbf{e_u}\|_f^2.$$

Thus, after rearranging terms, (7.93) becomes

$$\frac{1}{2}\frac{d}{dt}\left\{n\|\mathbf{e_u}(t)\|_f^2 + gS_0\|e_\phi(t)\|_p^2\right\} + 2n\left[\frac{\nu}{C_K} - C_c\sup_{t\in[0,T]}\left\{\|\nabla\mathbf{u}^{QS}(t)\|_f\right\}\right]\|\nabla\mathbf{e_u}\|_f^2$$

$$+ \frac{n\nu\alpha}{\sqrt{k_{max}}}\sum_{i=1}^{d-1}\|\mathbf{e_u}\cdot\hat{\tau}_i\|_I^2 + \frac{gk_{min}}{2}\|\nabla e_\phi\|_p^2 \leq \frac{gS_0^2}{2k_{min}}\|\phi_t^{QS}\|_{-1,p}^2. \tag{7.94}$$

We next multiply (7.94) by 2 and integrate over $[0,t]$, $0 < t \leq T$:

$$\left\{n\|\mathbf{e_u}(t)\|_f^2 + gS_0\|e_\phi(t)\|_p^2\right\} + 4n\left[\frac{\nu}{C_K} - C_c\sup_{t\in[0,T]}\left\{\|\nabla\mathbf{u}^{QS}(t)\|_f\right\}\right]\int_0^t\|\nabla\mathbf{e_u}(s)\|_f^2\,ds$$

$$+ \int_0^t\left\{\frac{2n\nu\alpha}{\sqrt{k_{max}}}\sum_{i=1}^{d-1}\|\mathbf{e_u}(s)\cdot\hat{\tau}_i\|_I^2 + \frac{gk_{min}}{2}\|\nabla e_\phi(s)\|_p^2\right\}\,ds$$

$$\leq gS_0\|e_\phi(0)\|_p^2 + \frac{gS_0^2}{2k_{min}}\int_0^t\|\phi_t^{QS}(s)\|_{-1,p}^2\,ds.$$

Finally, we take the supremum over $[0,T]$:

$$\sup_{t\in[0,T]}\left\{n\|\mathbf{e_u}(t)\|_f^2 + gS_0\|e_\phi(t)\|_p^2\right\}$$

$$+ 4n\left[\frac{\nu}{C_K} - C_c\sup_{t\in[0,T]}\left\{\|\nabla\mathbf{u}^{QS}(t)\|_f\right\}\right]\int_0^T\|\nabla\mathbf{e_u}(t)\|_f^2\,dt$$

$$+ \int_0^T\left\{\frac{2n\nu\alpha}{\sqrt{k_{max}}}\sum_{i=1}^{d-1}\|\mathbf{e_u}(t)\cdot\hat{\tau}_i\|_I^2 + \frac{gk_{min}}{2}\|\nabla e_\phi(t)\|_p^2\right\}\,dt$$

$$\leq gS_0\|e_\phi(0)\|_p^2 + \frac{gS_0^2}{2k_{min}}\int_0^T\|\phi_t^{QS}(t)\|_{-1,p}^2\,dt. \tag{7.95}$$

122

By Theorem 15, we have that

$$2n\gamma\|\nabla\mathbf{u}^{QS}\|^2_{L^\infty(0,T;L^2(\Omega_f))} \leq C_5^*. \tag{7.96}$$

Thus, assumption (7.91) of Theorem 16, together with (7.96) give that

$$\frac{\nu}{C_K} - C_c \sup_{t\in[0,T]} \left\{\|\nabla\mathbf{u}^{QS}(t)\|_f\right\} \geq \frac{\nu}{C_K} - C_c\sqrt{\frac{C_5^*}{2n\gamma}} = \frac{\nu - C_K C_c\sqrt{\frac{C_5^*}{2n\gamma}}}{C_K} = \epsilon > 0.$$

Therefore, (7.95) becomes

$$\sup_{t\in[0,T]} \left\{n\|\mathbf{e_u}(t)\|^2_f + gS_0\|e_\phi(t)\|^2_p\right\} + 4n\epsilon \int_0^T \|\nabla\mathbf{e_u(t)}\|^2_f \, dt$$

$$+ \int_0^T \left\{\frac{2n\nu\alpha}{\sqrt{k_{max}}}\sum_{i=1}^{d-1}\|\mathbf{e_u}(t)\cdot\hat\tau_i\|^2_I + \frac{gk_{min}}{2}\|\nabla e_\phi(t)\|^2_p\right\} dt \tag{7.97}$$

$$\leq gS_0\|e_\phi(0)\|^2_p + \frac{gS_0^2}{2k_{min}}\int_0^T \|\phi_t^{QS}(t)\|^2_{-1,p} \, dt.$$

Furthermore, from (7.56) of the proof of Theorem 13 we have

$$\|e_\phi(0)\|_p \leq \frac{S_0 C_{PF,p}}{k_{min}}\|\phi_t(0)\|_{-1,p},$$

and also from (7.55) that

$$\int_0^T \|\phi_t^{QS}(t)\|^2_{-1,p} \, dt \leq \frac{C_{PF,p}^3}{gk_{min}}C_4^*.$$

Hence, (7.97) becomes

$$\sup_{t\in[0,T]} \left\{n\|\mathbf{e_u}(t)\|^2_f + gS_0\|e_\phi(t)\|^2_p\right\} + 4n\epsilon \int_0^T \|\nabla\mathbf{e_u}(t)\|^2_f \, dt$$

$$+ \int_0^T \left\{\frac{2n\nu\alpha}{\sqrt{k_{max}}}\sum_{i=1}^{d-1}\|\mathbf{e_u}(t)\cdot\hat\tau_i\|^2_I + \frac{gk_{min}}{2}\|\nabla e_\phi(t)\|^2_p\right\} dt \tag{7.98}$$

$$\leq \frac{gS_0^3 C_{PF,p}^2}{(k_{min})^2}\|\phi_t(0)\|^2_{-1,p} + \frac{S_0^2 C_{PF,p}^3 C_4^*}{2(k_{min})^2} \leq C_D S_0^2,$$

where $C_D > 0$ is a constant such that $C_D \sim \frac{1}{(k_{min})^2}$. Thus, the claim of the theorem follows. $\qquad\square$

To summarize, under the assumptions of Theorem 16, we have that

$$\|\mathbf{u} - \mathbf{u}^{QS}\|_{L^\infty(0,T;L^2(\Omega_f))} = \mathcal{O}(S_0), \quad C \sim \frac{1}{\sqrt{n}k_{min}},$$

$$\|\nabla(\mathbf{u} - \mathbf{u}^{QS})\|_{L^2(0,T;L^2(\Omega_f))} = \mathcal{O}(S_0), \quad C \sim \frac{1}{\sqrt{n\epsilon}k_{min}}, \quad \epsilon \sim \nu,$$

$$\|\phi - \phi^{QS}\|_{L^\infty(0,T;L^2(\Omega_p))} = \mathcal{O}(\sqrt{S_0}), \quad C \sim \frac{1}{k_{min}},$$

$$\|\nabla(\phi - \phi^{QS})\|_{L^2(0,T;L^2(\Omega_p))} = \mathcal{O}(S_0), \quad C \sim \frac{1}{(k_{min})^{3/2}}.$$

where C denotes the constant in the error estimate, and "$\sim$" means "proportional to". We conclude that the quasistatic approximation in the Navier-Stokes/Darcy problem in three spatial dimensions (under small data) is justified provided $0 < S_0 << k_{min} << 1$.

8.0 NUMERICAL TESTS

In this chapter we confirm the theoretical results obtained in Chapters 4, 5, and 6 with numerical tests. In Section 8.1 we introduce the test problems that will be used in the numerical tests for verification of the results from Chapters 6 and 4, given respectively in Sections 8.2 and 8.3. In Section 8.4 we present numerical tests in support of the results obtained in Chapter 5.

8.1 TEST PROBLEMS AND ASSUMPTIONS

We verify the results obtained in Chapters 4 and 6 through two test problems for which the true solutions are known. For simplicity, we will assume that $d = 2$, so that we are in two dimensions in space, and that the stress and hydraulic conductivity tensors are given respectively by:

$$\mathbf{\Pi} = -p\mathbf{I} + \mu\nabla\mathbf{u},$$

$$\mathbf{K} = k_{min}\mathbf{I}, \quad k_{min} > 0.$$

We discretize the Stokes-Darcy problem (3.27)-(3.29) in space using the finite element method and in time using the CNLF-stab method (Algorithm 2) with $\beta^* = 1$. (See Chapter 6, Section 6.1, for a detailed presentation of the discretization in space and time). In all tests, we use Taylor-Hood elements (P2-P1) (see, e.g., [97]) for the velocity-pressure pair in the Stokes problem and piecewise quadratics (P2) for the hydraulic head in the Darcy problem.
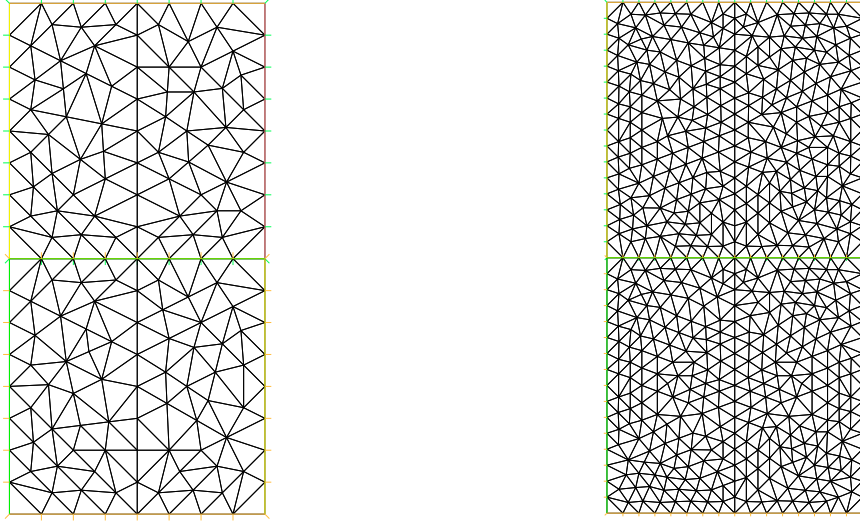
Figure 5: Mesh examples of computational domain $\Omega_f \cup \Omega_p = (0,1) \times (0,2)$ with 8 nodes (left) and 16 nodes (right) per sub-domain side.

The true solutions in each test problem below are chosen so that the interface conditions (3.10)-(3.12), as well as the incompressibility condition (3.2), are exactly satisfied. Then, the non-homogeneous Dirichlet boundary conditions at the exterior boundaries, as well as the forcing terms $\mathbf{f}_f$, f_p and the initial conditions $\mathbf{u}_0, \phi_0$ are determined by the true solutions. In both problems, the Stokes domain is given by $\Omega_f = (0,1) \times (1,2)$, the Darcy domain by $\Omega_p = (0,1) \times (0,1)$, and the interface by $I = \{(x,1) : x \in (0,1)\}$. The computational domains, and a couple of mesh examples, are depicted in Figure 5.

8.1.1   Test problem 1

In the first test problem, taken from [92], all physical parameters, except S_0, are set equal to one:

$$\rho = \mu = k_{min} = n = g = \alpha = 1.$$

The true solution is given by

$$\mathbf{u}(x, y, t) = \left([x^2(y-1)^2 + y] \cos t, \left[-\tfrac{2}{3}x(y-1)^3 + 2 - \pi \sin(\pi x) \right] \cos t \right),$$

$$p(x, y, t) = [2 - \pi \sin(\pi x)] \sin \left(\tfrac{\pi}{2}y \right) \cos t,$$

$$\phi(x, y, t) = [2 - \pi \sin(\pi x)][1 - y - \cos(\pi y)] \cos t.$$

To match the true solution, we solve the system (3.1)-(3.12) with

$$\mathbf{f}_f(x, y, t) := \left(-[x^2(y-1)^2 + y] \sin t - [\pi^2 \cos(\pi x) \sin \left(\tfrac{\pi}{2}y \right) + 2\{(y-1)^2 + x^2\}] \cos t, \right.$$

$$\left[\tfrac{2}{3}x(y-1)^3 - 2 + \pi \sin(\pi x) \right] \sin t$$

$$+ \left[\tfrac{\pi}{2}\{2 - \pi \sin(\pi x)\} \cos \left(\tfrac{\pi}{2}y \right) - \pi^3 \sin(\pi x) + 4x(y-1) \right] \cos t \right),$$

$$f_p(x, y, t) := -S_0[2 - \pi \sin(\pi x)][1 - y - \cos(\pi y)] \sin t - \pi^2 \left[\pi \sin(\pi x)(1 - y - \cos(\pi y)) \right.$$

$$+ (2 - \pi \sin(\pi x)) \cos(\pi y)] \cos t, \qquad\qquad \text{(Test problem 1)}$$

$$\mathbf{u}_0(x, y) := \mathbf{u}(x, y, 0) = \left(x^2(y-1)^2 + y, -\tfrac{2}{3}x(y-1)^3 + 2 - \pi \sin(\pi x) \right),$$

$$\phi_0(x, y) := \phi(x, y, 0) = [2 - \pi \sin(\pi x)][1 - y - \cos(\pi y)],$$

$$\mathbf{u} := \mathbf{u}(x, y, t), \quad \text{on } \partial\Omega_f \backslash I \times (0, T],$$

$$\phi := \phi(x, y, t), \quad \text{on } \partial\Omega_p \backslash I \times (0, T].$$

The true velocity field and true pressure contours at $t = 1$ for Test problem 1 are depicted in Figure 6.

8.1.2 Test problem 2

In the second test problem, taken from [92], all physical parameters can vary. The true solution is given by

$$\mathbf{u}(x, y, t) = \left((y-1)^2 \cos t, [x^2 - x] \cos t \right),$$

$$p(x, y, t) = [2\mu(x + y - 1) + \tfrac{\rho g n}{3k_{min}}] \cos t,$$

$$\phi(x, y, t) = [\tfrac{n}{k_{min}} \left\{ x(1-x)(y-1) + \tfrac{1}{3}y^3 - y^2 + y \right\} + \tfrac{2\nu}{g}x] \cos t.$$
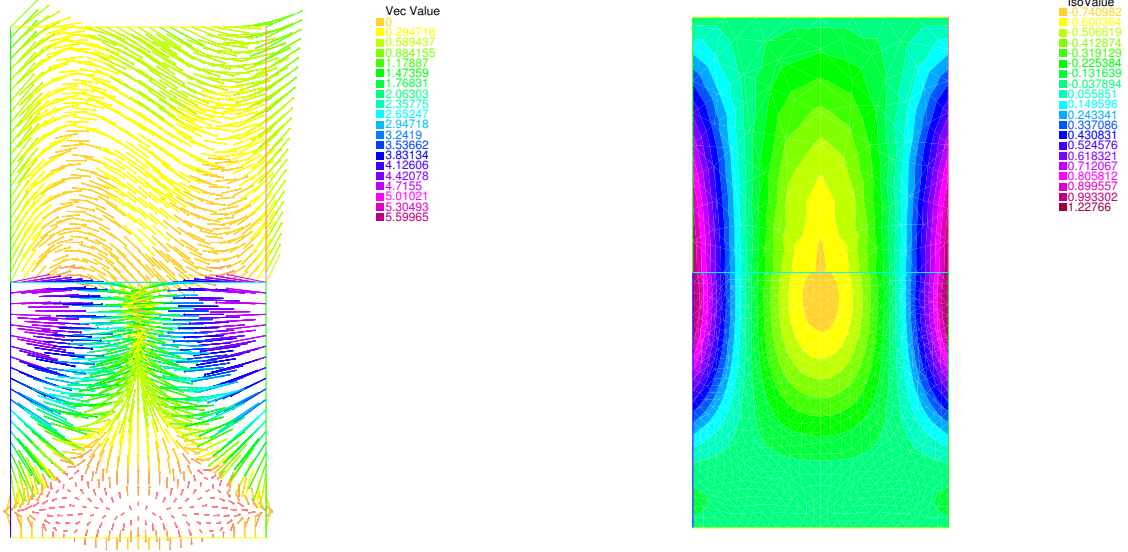
Figure 6: Test problem 1: true velocity field (left) and true pressure contours (right) at $t = 1$.

To match the true solution, we solve the system (3.1)-(3.12) with

$$
\begin{aligned}
\mathbf{f}_f(x, y, t) &:= \left(-\rho(y-1)^2 \sin t, -\rho(x^2 - x) \sin t\right), \\
f_p(x, y, t) &:= -S_0 \left[\frac{n}{k_{min}} \left\{x(1-x)(u-1) + \tfrac{1}{3}y^3 - y^2 + y\right\} + \frac{2\nu}{g}x\right] \sin t, \\
\mathbf{u}_0(x, y) &:= \mathbf{u}(x, y, 0) = \left((y-1)^2, x^2 - x\right), &&\text{(Test problem 2)} \\
\phi_0(x, y) &:= \phi(x, y, 0) = \frac{n}{k_{min}} \left\{x(1-x)(y-1) + \tfrac{1}{3}y^3 - y^2 + y\right\} + \frac{2\nu}{g}x, \\
\mathbf{u} &:= \mathbf{u}(x, y, t), \quad \text{on } \partial\Omega_f \backslash I \times (0, T], \\
\phi &:= \phi(x, y, t), \quad \text{on } \partial\Omega_p \backslash I \times (0, T].
\end{aligned}
$$

An example of the true velocity field and true pressure contours at $t = 1$ for Test problem 2 is depicted in Figure 7.
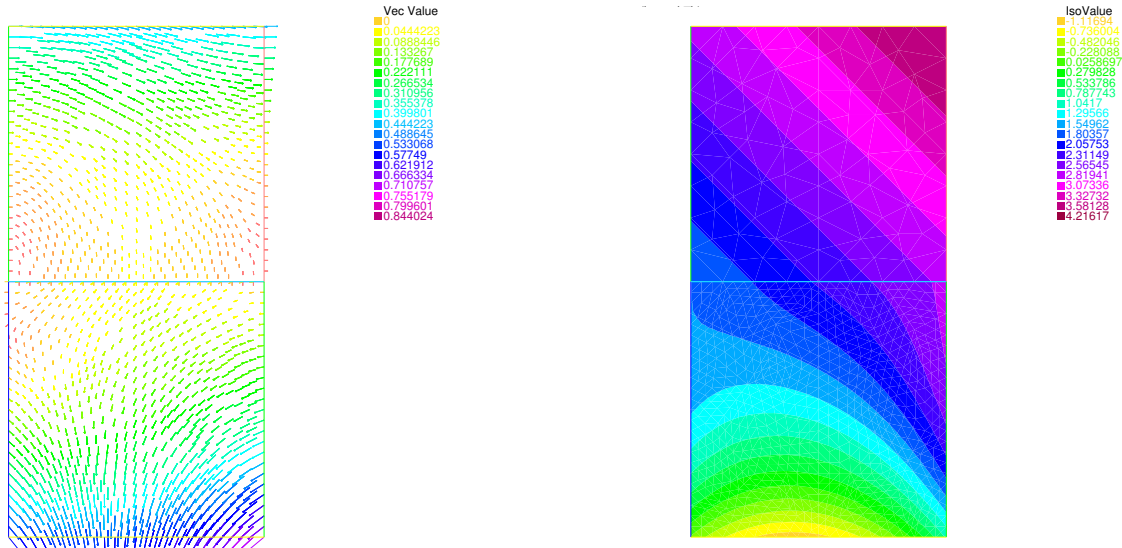
Figure 7: Test problem 2: true velocity field (left) and true pressure contours (right) at $t = 1$ with $k_{min} = 0.01$ and all other parameters equal to one.

8.2   NUMERICAL TESTS FOR THE CNLF-STAB METHOD IN THE STOKES-DARCY MODEL

In this section, we perform numerical tests to verify that the CNLF-stab method given in Algorithm 2 is: unconditionally, asymptotically stable (Theorem 10), second-order convergent in time with optimal rates in space, uniformly in the model parameters (Theorem 11), and computationally efficient when compared to fully coupled methods.

1. **Second-order convergence**

   We use the CNLF-stab method to solve Test problem 1, where all model parameters are equal to one. For simplicity, we take $\beta^* = 1$ in Algorithm 2. We solve the problem over the time interval $[0, 1]$, so that $T = 1$, with N nodes per sub-domain side and $\Delta t = 1/N$.

We check accuracy and convergence rates with the following discrete norms

$$e(\mathbf{u}) := \||\mathbf{u} - \mathbf{u}_h\|\|_{L^\infty(0,T;H^1_{\mathrm{div}}(\Omega_f))},$$

$$e(p) := \||p - p_h\|\|_{L^\infty(0,T;L^2(\Omega_f))},$$

$$e(\phi) := \||\phi - \phi_h\|\|_{L^\infty(0,T;L^2(\Omega_p))},$$

where

$$\||\mathbf{v} - \mathbf{v}_h\|\|_{L^\infty(0,T;X)} = \max_{0 \le k \le N} \|\mathbf{v}^k - \mathbf{v}_h^k\|_X, \quad \text{for } X = L^2(\Omega_{f/p}), \mathbf{v} = \mathbf{u}, p, \phi,$$

which are the analogs of the continuous norms

$$\|\mathbf{u} - \mathbf{u}^{QS}\|_{L^\infty(0,T;H^1_{\mathrm{div}}(\Omega_f))} = \sup_{t \in [0,T]} \|\mathbf{u}(t) - \mathbf{u}^{QS}(t)\|_{\mathrm{div},f},$$

$$\|p - p^{QS}\|_{L^\infty(0,T;L^2(\Omega_f))} = \sup_{t \in [0,T]} \|p(t) - p^{QS}(t)\|_f,$$

$$\|\phi - \phi^{QS}\|_{L^\infty(0,T;L^2(\Omega_p))} = \sup_{t \in [0,T]} \|\phi(t) - \phi^{QS}(t)\|_p,$$

respectively. We let $r_{\mathbf{u},p,\phi}$ denote the calculated order of convergence, given by $r = \log_2(e(N)/e(2N))$, where $e(N)$ denotes the error for each variable when using N nodes per sub-domain side. Tables 4 and 5 present the errors of CNLF (Algorithm 1) and CNLF-stab respectively, demonstrating that CNLF-stab retains CNLF's second-order accuracy, as expected.

Table 4: Test problem 1: second-order convergence of CNLF.

$\Delta t = 1/N$	$e(\mathbf{u})$	$r_{\mathbf{u}}$	$e(p)$	r_p	$e(\phi)$	r_ϕ
1/4	0.0877749	-	1.02465	-	0.0531155	-
1/8	0.0166945	2.39	0.260102	1.98	0.0112083	2.24
1/16	0.00347098	2.27	0.0622061	2.06	0.00220589	2.35
1/32	0.000949118	1.87	0.0149412	2.06	0.000546633	2.01
1/64	0.000243123	1.97	0.00357819	2.06	0.000136159	2.01

Table 5: Test problem 1: second-order convergence of CNLF-stab.

$\Delta t = 1/N$	e($\mathbf{u}$)	$r_{\mathbf{u}}$	e(p)	r_p	e(ϕ)	r_ϕ
1/4	0.0304013	-	1.10942	-	0.130579	-
1/8	0.0048835	2.64	0.272517	2.03	0.0347465	1.91
1/16	0.00105315	2.21	0.0649257	2.07	0.00878685	1.98
1/32	0.000264613	1.99	0.0163038	1.99	0.00220226	2.00
1/64	0.000064201	2.04	0.00453213	1.85	0.000550882	2.00

Next, we use CNLF-stab to solve Test problem 2, where all model parameters may vary, and take $S_0 = 10^{-4}$, $k_{min} = 10^{-1}$, and all other parameters equal to one. Like before, we solve the problem over the time interval $[0, 1]$, so that $T = 1$, with N nodes per sub-domain side and $\Delta t = 1/N$. The errors are shown in Table 6, confirming second-order accuracy of CNLF-stab once again. We observe, however, that due to the smaller values of the parameters, we need to solve the problem on finer meshes in space and time to attain second-order accuracy.

Table 6: Test problem 2 ($S_0 = 10^{-4}$, $k_{min} = 10^{-1}$): second-order convergence of CNLF-stab.

$\Delta t = 1/N$	e($\mathbf{u}$)	$r_{\mathbf{u}}$	e(p)	r_p	e(ϕ)	r_ϕ
1/8	0.00163737	-	0.214387	-	0.0819758	-
1/16	0.000464456	1.82	0.0700264	1.61	0.0264185	1.63
1/32	0.000115658	2.01	0.0187149	1.90	0.00691258	1.93
1/64	0.000029022	2.00	0.00486284	1.94	0.00174539	1.99
1/128	0.00000726908	2.00	0.00126994	1.94	0.000437368	2.00

Note 1. *The Freefem++ [59] code for the convergence tests for CNLF and CNLF-stab can be found in Section B.1.*

2. Unconditional stability

To confirm unconditional, asymptotic stability of the CNLF-stab method we solve Test problem 2 and set the body forces and source terms, $\mathbf{f}_f$ and f_p, equal to zero, and also force homogeneous Dirichlet boundary conditions at the exterior boundaries of the domains (not including the interface), so that the true solution decays rapidly to zero as $t \to \infty$. Thus, any growth in the approximate solution implies instability of the numerical method. We set $\Delta t = 1/N = 1/16$, where N is the number of nodes per sub-domain side in the FE discretization. We run tests with varying k_{min} and S_0, and all other parameters equal to one. In each test, we calculate the discrete energy of the method, given by

$$\text{Energy}(t^{n-1/2}) := \text{Energy}(t^n) + \text{Energy}(t^{n-1})$$
$$:= \|\mathbf{u}_h^n\|_f^2 + \|\mathbf{u}_h^{n-1}\|_f^2 + S_0 \left(\|\phi_h^n\|_p^2 + \|\phi_h^{n-1}\|_p^2 \right).$$

The results for CNLF-stab and CNLF are presented in Figures 8 and 9 respectively. The final time, T, is shown on each graph. Unconditional, asymptotic stability over long time intervals is confirmed for CNLF-stab for any pair of values of k_{min} and S_0, while CNLF is unstable in all cases. Notice that for these parameter values, the time-step condition of CNLF, (6.12), is violated (we estimate $C_{\Omega_{f/p}} \approx 12$ in (6.12)), so instability is expected. Further, we observe that as k_{min} becomes smaller (and S_0 is $\mathcal{O}(1)$), the growth in energy of CNLF happens sooner and is more rapid, and at the same time the energy of CNLF-stab decays to zero slower. This is because of the true solution of Test problem 2, which has large initial energy when k_{min} is small and $S_0 = 1$.

Finally, we compute the final energy of CNLF-stab,

$$\text{Final Energy} := \text{Energy}(T) + \text{Energy}(T - \Delta t), \text{ where } T = 20,$$

for Test problem 2, with zero forcing terms and homogeneous Dirichlet boundary conditions at the exterior boundaries. This time, we vary $\Delta t = 2^{-i}/100$, $i = 0, 1, 2, 3, 4$, k_{min} and S_0, and fix the number of nodes per sub-domain side, $N = 16$. In each case, the initial energy, "Energy$(0) + $Energy$(\Delta t)$", is $\mathcal{O}(10)$. The results are shown in Figure

10. Once again, CNLF-stab exhibits asymptotic, unconditional stability over long time intervals in all cases.

Note 2. *The Freefem++ [59] code for the stability tests for CNLF and CNLF-stab can be found in Section B.2.*

3. <u>Efficiency</u>

We illustrate the efficiency of CNLF-stab versus fully coupled methods, by comparing the computational time required for CNLF-stab versus that for the fully implicit Backward Euler (BE) method applied to (6.5)-(6.7).

Algorithm 3 (BE method). *The BE method for the evolutionary Stokes-Darcy problem is as follows:*

$$Given \ \left(\mathbf{u}_h^k, \tilde{p}_h^k, \phi_h^k\right) \in \mathbf{X}_f^h \times Q_f^h \times X_p^h,$$

$$find \ \left(\mathbf{u}_h^{k+1}, \tilde{p}_h^{k+1}, \phi_h^{k+1}\right) \in \mathbf{X}_f^h \times Q_f^h \times X_p^h, \quad k = 0, \ldots, N-1,$$

$$satisfying \ \forall \left(\mathbf{v}_h, q_h, \psi_h\right) \in \mathbf{X}_f^h \times Q_f^h \times X_p^h :$$

$$n \left(\frac{\mathbf{u}_h^{k+1} - \mathbf{u}_h^k}{\Delta t}, \mathbf{v}_h\right)_f + a_f \left(\mathbf{u}_h^{k+1}, \mathbf{v}_h\right) - n \left(\tilde{p}_h^{k+1}, \nabla \cdot \mathbf{v}_h\right)_f + c_I(\mathbf{v}_h, \phi_h^{k+1}) = n(\tilde{\mathbf{f}}_f^{k+1}, \mathbf{v}_h)_f,$$

$$\left(q_h, \nabla \cdot \mathbf{u}_h^{k+1}\right)_f = 0, \tag{8.1}$$

$$g S_0 \left(\frac{\phi_h^{n+1} - \phi_h^k}{\Delta t}, \psi_h\right)_p + a_p \left(\phi_h^{k+1}, \psi_h\right) - c_I(\mathbf{u}_h^{k+1}, \psi_h) = g(f_p^{k+1}, \psi_h)_p$$

where $(\mathbf{u}_h^0, \phi_h^0) = (\mathbf{u}_0, \phi_0)$.

We solve Test problem 1 with varying N (nodes per sub-domain side) and $\Delta t = 1/N$ over the interval $[0, 1]$ ($T = 1$), and compute the average computational time per time step solve for each method, and each N, and also the error in $\mathbf{u}$. The computational time comparison is given in Figure 11 and the errors in Figure 12. From the results, the efficiency of CNLF-stab when compared to BE is evident, both from the computational time perspective as well as in view of the smaller errors for fixed N and fastest (second-order) convergence. This, in combination with the method's asymptotic, unconditional stability makes CNLF-stab a very attractive choice for problems that require solutions computed over long time intervals, with small parameters, and/or on finer meshes.

Note 3. *The Freefem++ [59] code for the Backward Euler method for the evolutionary Stokes-Darcy problem is given in Section B.3.*

8.3 NUMERICAL TESTS FOR THE QUASISTATIC APPROXIMATION IN THE STOKES-DARCY MODEL

In this section we present numerical tests for the convergence of the Stokes-Darcy solution $(\mathbf{u}, p, \phi)$, that solves the system of equations (3.1)-(3.12), to the quasistatic solution $(\mathbf{u}^{QS}, p^{QS}, \phi^{QS})$ that solves the same system with $S_0 = 0$ in (3.5), as $S_0 \to 0$ (Chapter 4, Theorem 5). We verify first-order convergence as $S_0 \to 0$ with respect to the discrete analogs of the norms

$$\|\mathbf{u} - \mathbf{u}^{QS}\|_{L^\infty(0,T;L^2(\Omega_f))} = \sup_{t \in [0,T]} \|\mathbf{u}(t) - \mathbf{u}^{QS}(t)\|_f,$$

$$\|p - p^{QS}\|_{L^\infty(0,T;L^2(\Omega_f))} = \sup_{t \in [0,T]} \|p(t) - p^{QS}(t)\|_f,$$

$$\|\phi - \phi^{QS}\|_{L^\infty(0,T;L^2(\Omega_p))} = \sup_{t \in [0,T]} \|\phi(t) - \phi^{QS}(t)\|_p,$$

given by

$$\mathrm{error}(\mathbf{v}) := \||\mathbf{v} - \mathbf{v}^{QS}\||_{L^\infty(0,T;X)} = \max_{0 \le k \le N} \|\mathbf{v}^k - \mathbf{v}^{QS^k}\|_X, \quad \text{for } X = L^2(\Omega_{f/p}), \ \mathbf{v} = \mathbf{u}, p, \phi.$$

We denote the approximate order of convergence by $r_{\mathbf{u}/p/\phi}$ for $\mathbf{u}, p, \phi$, respectively, given by $r = \log_2(\mathrm{e}(S_0)/\mathrm{e}(S_0/2))$. In both test problems, the evolutionary Stokes-Darcy and quasistatic models are solved over the time interval $[0, 1]$, so that $T = 1$. In each numerical test, the mesh size, h, and the step size, Δt, are taken to be $h = \Delta t = 1/32$.

For Test problem 1, the calculated norms of the errors for $\mathbf{u}, p$, and ϕ, for each value of S_0, are shown in Table 7. The calculated order of convergence is getting closer to one as S_0 approaches zero, which is in agreement with the results of Theorem 5. To investigate how the convergence is affected by the hydraulic conductivity, we use Test problem 2 where we vary k_{min}, and set all other parameters equal to one:

$$\rho = \mu = n = g = \alpha = 1.$$

In the first run, we take $k_{min} = 1$, and we get similar errors in Table 8 as for the first test problem. Next, we let k_{min} vary, $k_{min} = 0.1, 0.01, 0.001$, and 0.0001. The corresponding results for each case can be found in Tables 9, 10, 11, and 12, respectively. The errors for the velocity from Tables 8-12 are summarized in Figure 13. We observe the expected first-order convergence, and also that as k_{min} gets small compared to S_0, the errors for fixed S_0 get bigger. This is expected in view of the main result of Theorem 5, where k_{min} appears in the denominator of the constant in the error estimate, confirming that the quasistatic approximation should be used if $0 < S_0 << k_{min} << 1$.

Note 4. *The Freefem++ [59] code for the numerical tests of this section is given in B.4.*

8.4 NUMERICAL TESTS FOR THE LINEAR STABILIZATION IN THE CNLF METHOD

In this last section, we perform numerical tests to confirm the consistency and stability properties of the (CNLF-stab) method for (5.1), analyzed in Chapter 5. We verify the consistency results obtained in Section 5.2 by comparing the errors of (CNLF-stab) with varying $\beta > 0$ and (CNLF) (which is (CNLF-stab) with $\beta = 0$), and also confirm unconditional stability of (CNLF-stab) for $\beta > 1/8$, as well as the optimal time-step conditions for $\beta = 1/12$ and $\beta = 0$, obtained in Section 5.3.

We solve (5.1) for $\mathbf{u}(t) := (u_1(t), u_2(t))^\top : [0,1] \to \mathbb{R}^2$, given $\mathbf{u}(0) = (0,1)^\top$, with

$$A := \begin{pmatrix} 1 & 0 \\ 0 & 1 \end{pmatrix}, \qquad \Lambda := \omega \begin{pmatrix} 0 & -1 \\ 1 & 0 \end{pmatrix}, \qquad \omega \in \mathbb{R}.$$

The true solution is given by

$$\mathbf{u}(t) = (\exp(-t)\sin(\omega t), \, \exp(-t)\cos(\omega t))^\top, \ t \in [0,1], \ \omega \in \mathbb{R}.$$

We denote by $\tilde{\mathbf{u}}$ the approximate solution using (CNLF-stab) with varying $\beta \geq 0$, and by

$$\varepsilon = \|\tilde{\mathbf{u}} - \mathbf{u}\|_{L^2(0,1)}$$

135

the L^2-error over $[0,1]$. We use the true solution for the approximation of $\mathbf{u}(\Delta t)$.

Figure 14 shows the error of (CNLF) ($\beta = 0$) and (CNLF-stab) (with varying $\beta > 0$). Here, we take $\omega = 40$ and Δt within $[2^{-8}/50, 1/50]$, so that the time-step condition (5.5) of (CNLF) is always satisfied. While all methods exhibit second-order accuracy, the error is smallest for (CNLF-stab) with $\beta = 1/12$, where the leading-order consistency error of (LF) vanishes. The error of (CNLF-stab) with $\beta = 1/6$ is equal to that of (CNLF), and slightly bigger than (CNLF-stab) with $\beta = 1/8$, matching the analysis in Section 5.2.

In order to confirm the unconditional (Theorem 7) and conditional (Theorems 17 and 19) stability of (CNLF) and (CNLF-stab) with varying β, we plot the computed error using fixed $\Delta t = 1/100$ and $\omega \in [40, 160]$. This implies $0.4 \leq \Delta t\, \omega \leq 1.6$. Figure 15 shows the unconditional stability of (CNLF-stab) for $\beta > 1/8$, as predicted by Theorem 7. For $A = I$, as is the case in this numerical test, Theorem 7 reveals that (CNLF-stab) is also unconditionally stable for $\beta = 1/8$ in $L^2(0,T)$, which is shown here. On the other hand, the improved time-step condition, (A.17): $\Delta t \|\Lambda\| \lesssim 1.27$, is confirmed for (CNLF-stab) with $\beta = 1/12$.

Note 5. *The Matlab code for the numerical tests of this section is given in B.5.1 and B.5.2.*
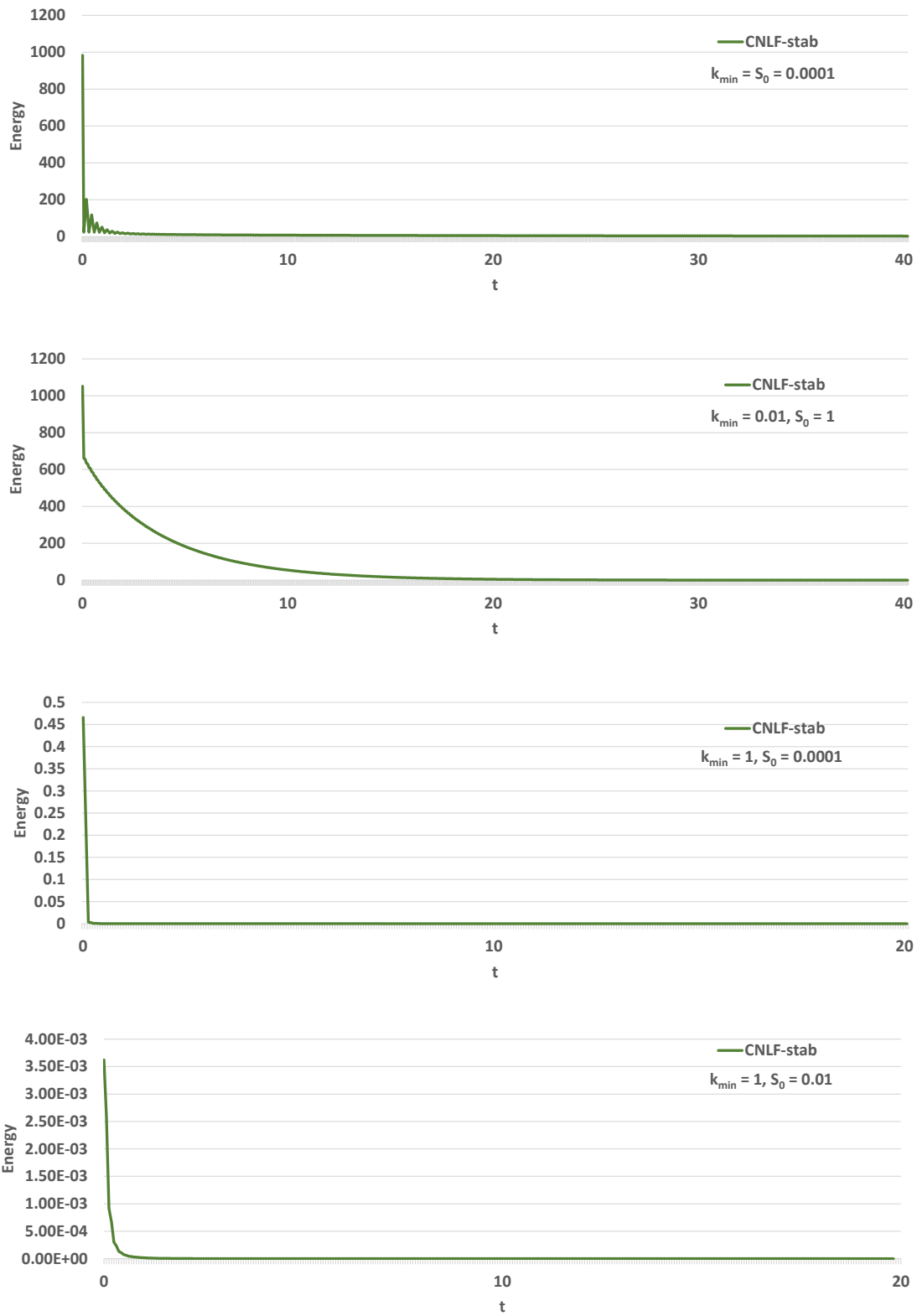
Figure 8: Unconditional stability of CNLF-stab for Test problem 2 with $N = 16 = 1/\Delta t$.
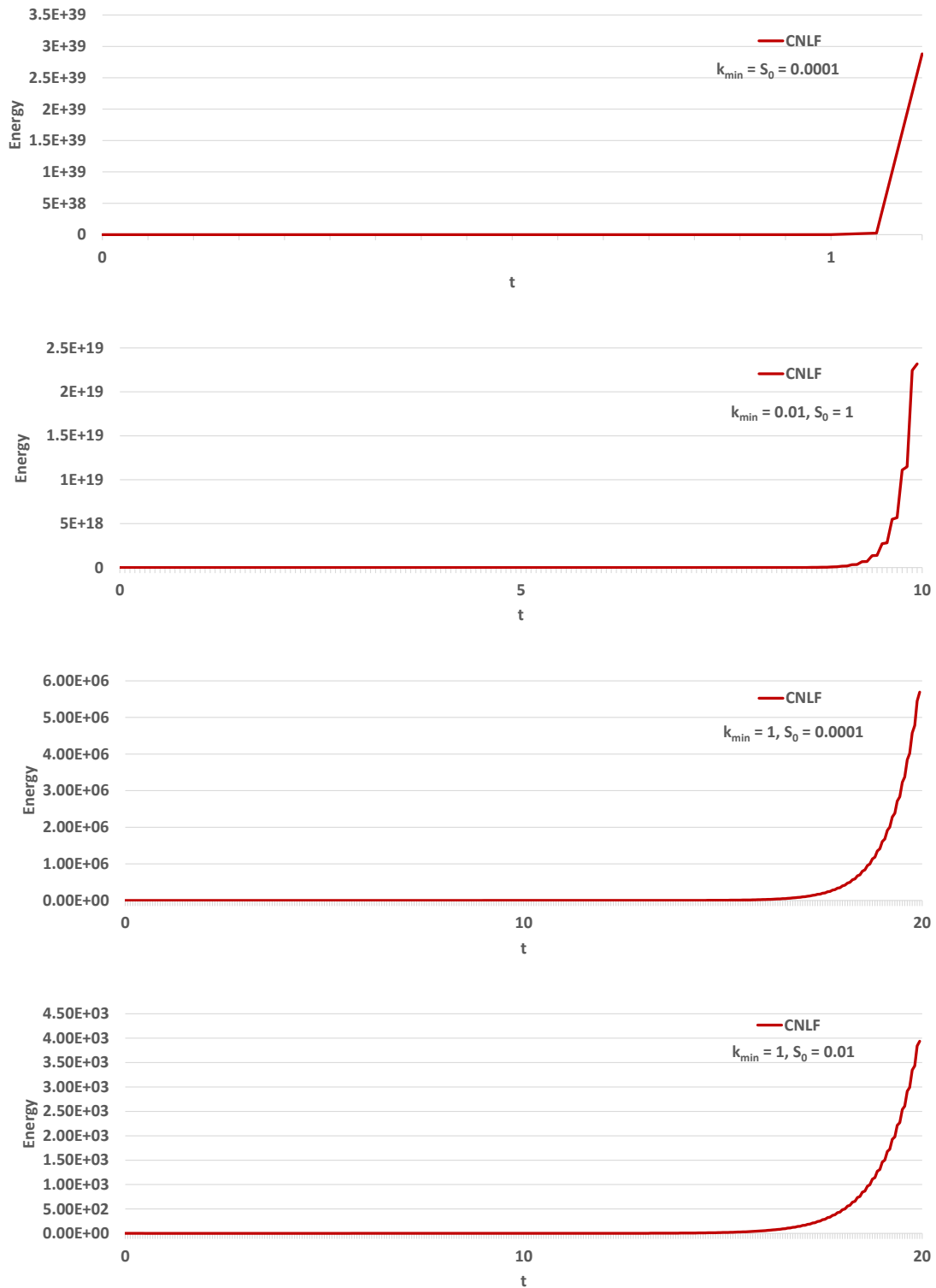
Figure 9: Instability of CNLF for Test problem 2 with $N = 16 = 1/\Delta t$.
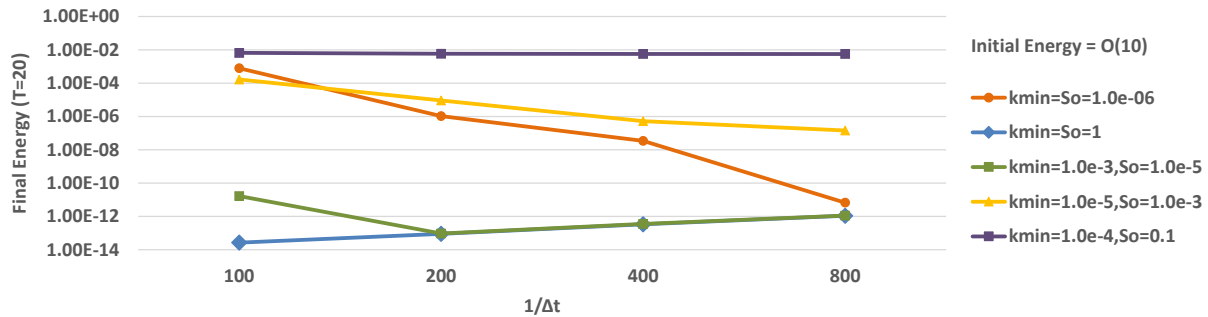
Figure 10: Final energy of CNLF-stab with varying S_0 and k_{min}.
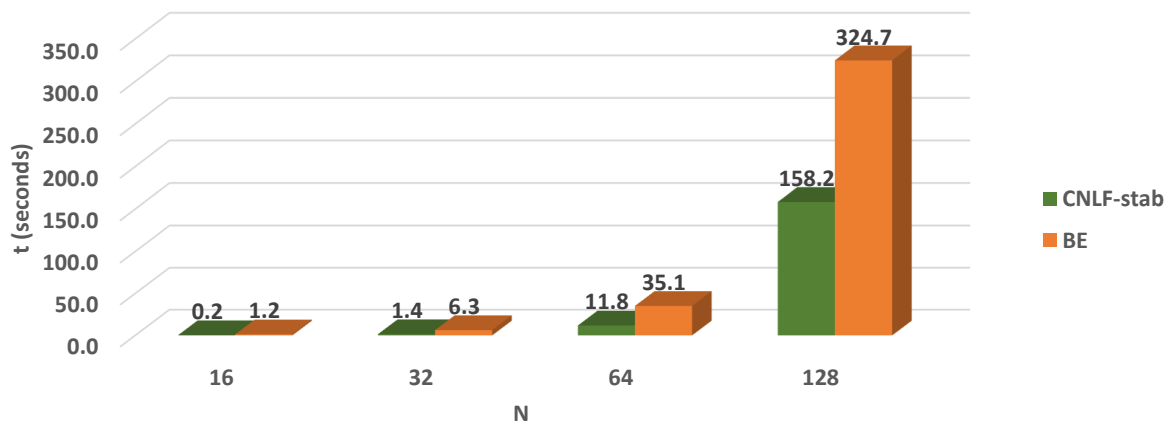
Figure 11: Average computational time per CNLF-stab/BE solve versus number of nodes per sub-domain side, N.
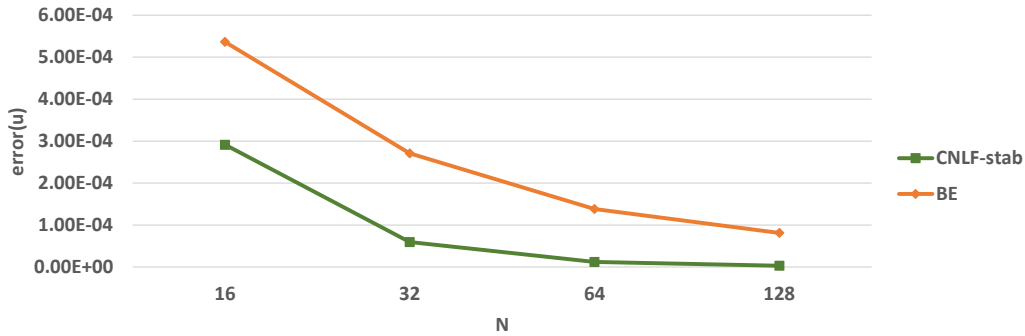
Figure 12: $\||\mathbf{u} - \mathbf{u}_h|\|_{L^\infty(0,1;L^2(\Omega_f))}$ of CNLF-stab and BE versus N.

Table 7: Test problem 1: first-order convergence to the quasistatic solution as $S_0 \to 0$, where $h = \Delta t = 1/32$, and $T = 1$.

S_0	error($\mathbf{u}$)	$r_{\mathbf{u}}$	error(p)	r_p	error(ϕ)	r_ϕ
0.01	4.11E-06	-	2.93E-03	-	8.18E-05	-
0.05	2.28E-06	0.850	1.61E-03	0.861	4.45E-05	0.878
0.025	1.20E-06	0.922	8.47E-04	0.927	2.32E-05	0.938
0.0125	6.19E-07	0.958	4.35E-04	0.962	1.19E-05	0.968
0.00625	3.15E-07	0.976	2.20E-04	0.981	6.00E-06	0.983
3.13E-03	1.59E-07	0.990	1.11E-04	0.990	3.02E-06	0.990
1.56E-04	7.96E-08	0.994	5.56E-05	0.996	1.52E-06	0.995
7.81E-05	4.00E-08	0.993	2.79E-05	0.996	7.60E-07	0.997

Table 8: Test problem 2 with $k_{min} = 1.0$: first-order convergence to the quasistatic solution as $S_0 \to 0$, where $h = \Delta t = 1/32$, and $T = 1$.

S_0	error($\mathbf{u}$)	$r_{\mathbf{u}}$	error(p)	r_p	error(ϕ)	r_ϕ
0.01	1.19E-07	-	8.44E-05	-	2.30E-06	-
0.05	6.56E-08	0.860	4.62E-05	0.869	1.25E-06	0.886
0.025	3.46E-08	0.921	2.43E-05	0.931	6.49E-07	0.941
0.0125	1.78E-08	0.957	1.24E-05	0.964	3.33E-07	0.963
0.00625	9.06E-09	0.978	6.29E-06	0.982	1.69E-07	0.981
3.13E-03	4.56E-09	0.989	3.16E-06	0.991	8.50E-08	0.990
1.56E-04	2.29E-09	0.995	1.59E-06	0.989	4.26E-08	0.995
7.81E-05	1.15E-09	0.997	7.97E-07	1.00	2.13E-08	0.997

Table 9: Test problem 2 with $k_{min} = 0.1$: first-order convergence to the quasistatic solution as $S_0 \to 0$, where $h = \Delta t = 1/32$, and $T = 1$.

S_0	error($\mathbf{u}$)	$r_{\mathbf{u}}$	error(p)	r_p	error(ϕ)	r_ϕ
0.01	2.15E-06	-	4.00E-04	-	9.90E-05	-
0.05	1.15E-06	0.910	2.25E-04	0.831	5.30E-05	0.900
0.025	5.93E-07	0.951	1.20E-04	0.902	2.75E-05	0.946
0.0125	3.02E-07	0.975	6.25E-05	0.964	1.40E-05	0.973
0.00625	1.52E-07	0.987	3.19E-05	0.972	7.07E-06	0.986
3.13E-03	7.65E-08	0.994	1.61E-05	0.985	3.55E-06	0.993
1.56E-04	3.83E-08	0.997	8.09E-06	0.992	1.78E-06	0.997
7.81E-05	1.92E-08	0.998	4.06E-06	0.996	8.91E-07	0.998

Table 10: Test problem 2 with $k_{min} = 0.01$: first-order convergence to the quasistatic solution as $S_0 \to 0$, where $h = \Delta t = 1/32$, and $T = 1$.

S_0	error($\mathbf{u}$)	$r_\mathbf{u}$	error(p)	r_p	error(ϕ)	r_ϕ
0.01	0.000302506	-	5.88E-02	-	0.0354523	-
0.05	1.55E-04	6.560	3.02E-02	7.042	1.82E-02	7.094
0.025	7.84E-05	0.984	1.54E-02	0.976	9.20E-03	0.981
0.0125	3.94E-05	0.993	7.74E-03	0.988	4.63E-03	0.991
0.00625	1.98E-05	0.994	3.89E-03	0.994	2.32E-03	0.996
3.13E-03	9.92E-06	0.997	1.95E-03	0.997	1.16E-03	0.998
1.56E-04	4.96E-06	0.998	9.75E-04	0.999	5.82E-04	0.999
7.81E-05	2.48E-06	0.999	4.88E-04	0.999	2.91E-04	0.999

Table 11: Test problem 2 with $k_{min} = 0.001$: first-order convergence to the quasistatic solution as $S_0 \to 0$, where $h = \Delta t = 1/32$, and $T = 1$.

S_0	error($\mathbf{u}$)	$r_\mathbf{u}$	error(p)	r_p	error(ϕ)	r_ϕ
0.01	1.46E-02	-	3.98E+00	-	2.48E+00	-
0.05	8.09E-03	0.851	2.21E+00	0.847	1.40E+00	0.830
0.025	4.28E-03	0.919	1.17E+00	0.916	7.44E-01	0.907
0.0125	2.20E-03	0.958	6.05E-01	0.956	3.85E-01	0.951
0.00625	1.12E-03	0.978	3.07E-01	0.977	1.96E-01	0.975
3.13E-03	5.64E-04	0.989	1.55E-01	0.989	9.87E-02	0.987
1.56E-04	2.83E-04	0.994	7.77E-02	0.994	4.96E-02	0.994
7.81E-05	1.42E-04	0.997	3.89E-02	0.997	2.49E-02	0.997

Table 12: Test problem 2 with $k_{min} = 0.0001$: first-order convergence to the quasistatic solution as $S_0 \to 0$, where $h = \Delta t = 1/32$, and $T = 1$.

S_0	error($\mathbf{u}$)	$r_{\mathbf{u}}$	error(p)	r_p	error(ϕ)	r_ϕ
0.01	1.81E-01	-	5.16E+01	-	3.19E+01	-
0.05	1.02E-01	0.825	2.91E+01	0.826	1.83E+01	0.806
0.025	5.47E-02	0.903	1.56E+01	0.903	9.84E+00	0.892
0.0125	2.83E-02	0.949	8.06E+00	0.948	5.12E+00	0.943
0.00625	1.44E-02	0.973	4.11E+00	0.973	2.61E+00	0.971
3.13E-03	7.28E-03	0.987	2.07E+00	0.987	1.32E+00	0.985
1.56E-04	3.66E-03	0.993	1.04E+00	0.993	6.64E-01	0.992
7.81E-05	1.83E-03	0.997	5.22E-01	0.997	3.33E-01	0.996
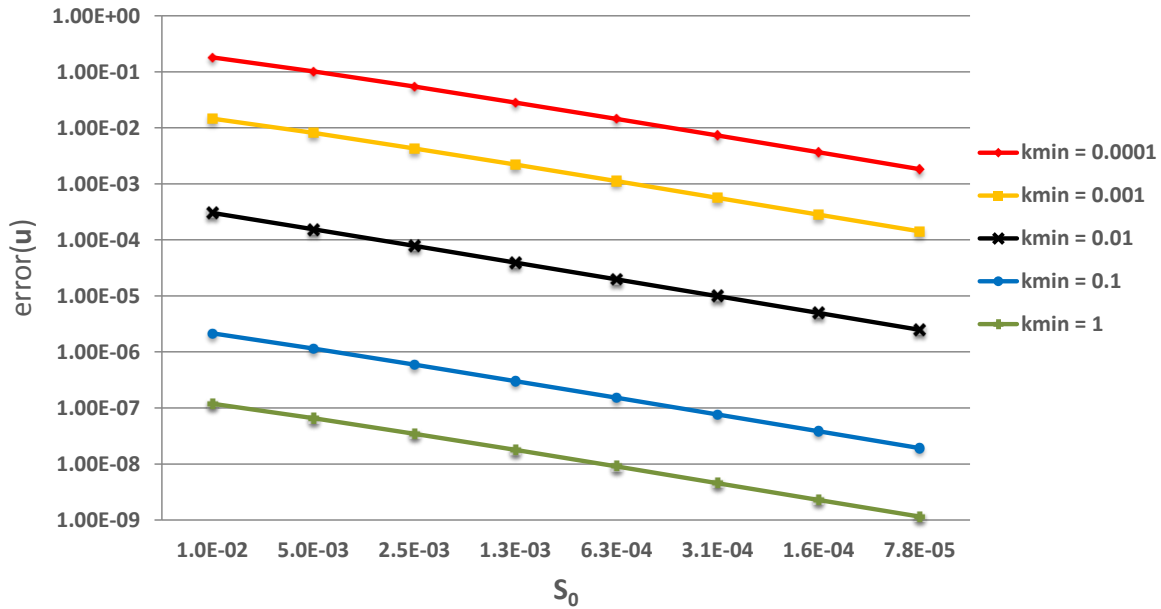
Figure 13: Test problem 2: first-order convergence to quasistatic solution with varying k_{min}.
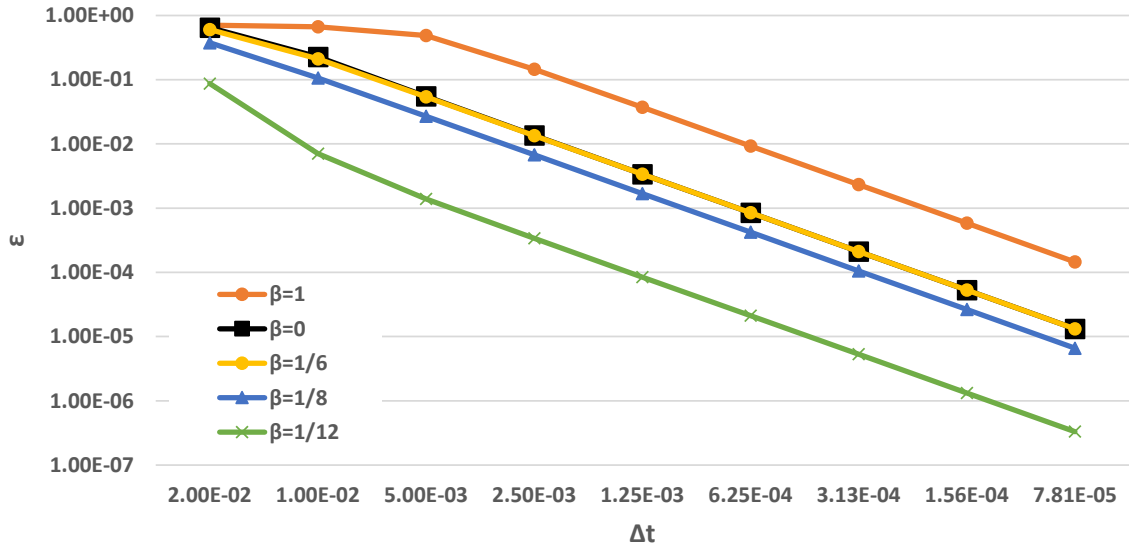
Figure 14: Second-order accuracy of (CNLF-stab) with varying $\beta \geq 0$.
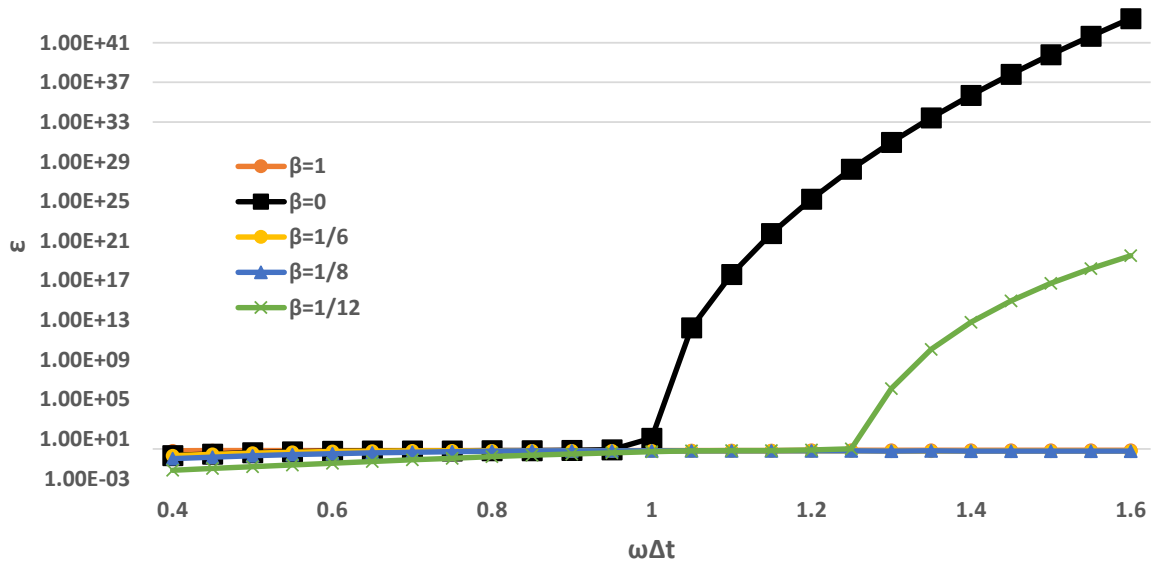
Figure 15: Unconditional stability of (CNLF-stab) for $\beta > 1/8$ and conditional for $\beta = 1/12$ and $\beta = 0$.

144

9.0 CONCLUSIONS

In this thesis, we studied the fully evolutionary Navier-Stokes/Darcy and Stokes-Darcy models for the interaction between surface and groundwater flows. We investigated the problems versus their corresponding quasistatic approximations, in which it is assumed that the hydraulic head in the groundwater flow equation adjusts instantaneously to equilibrium.

We conclude that the solution of the fully evolutionary Stokes-Darcy problem converges with order one to the quasistatic solution, as the specific storage, S_0, approaches zero, under mild assumptions on the initial data and body forces. The proof of convergence revealed that the quasistatic model is accurate in predicting the solution provided that S_0 is small and also smaller in orders of magnitude than the minimum eigenvalue of the hydraulic conductivity tensor, k_{min}. Under these assumptions, the term "$S_0\phi_t$" can be dropped from the evolutionary Stokes-Darcy equations. Numerical tests confirmed first-order convergence of the solution to the quasistatic solution, and also that the error between the two systems grows when S_0 is not small compared to k_{min}.

In the case of the nonlinear Navier-Stokes/Darcy coupling, we analyzed the problem under a modified balance of forces coupling condition, and added an "inertia" term in order to get an energy estimate. Under mild assumptions on the body forces and initial conditions, we proved that the solution of the fully evolutionary, two-dimensional, Navier-Stokes/Darcy model converges to the solution of the quasistatic model as $S_0 \to 0$. In three dimensions in space, the proof of convergence required either a small-data condition or higher regularity assumed on the fluid velocity field. The analysis showed that convergence is sensitive to k_{min}, and thus, the quasistatic model should be assumed if S_0 is small and smaller in orders of magnitude than k_{min}.

We then developed and analyzed a non-modular stabilization of the implicit-explicit

Crank-Nicolson Leapfrog (CNLF) time-stepping scheme for the solution of a general evolution equation. The CNLF method without added stabilization or modular time filters is known to have two issues: a very restrictive time step condition and slight instability exhibited in the unstable mode of Leapfrog. In contrast, we proved that the proposed stabilized CNLF method requires no time step condition for stability, is asymptotically stable, and at the same time more accurate. The claims about the stability and accuracy properties of the method were verified through numerical tests.

The stabilized CNLF method was then extended to an efficient partitioned method for the evolutionary Stokes-Darcy coupling. We proved that the added stabilization terms corrected both shortcomings of the original CNLF method for the Stokes-Darcy problem, namely the conditional stability and the instability in the unstable mode of Leapfrog, while retaining second-order accuracy, uniformly in the model parameters. In particular, we showed that the proposed partitioned method is unconditionally, asymptotically stable and uniformly, second-order convergent. To support the theoretical findings, several numerical tests were performed, confirming the method's stability and convergence properties under any parameter regime. As a result, the method can also be applied to the quasistatic Stokes-Darcy model just by setting $S_0 = 0$. Additional numerical tests were performed to show the method's effectiveness when compared to fully coupled methods.

9.1   FUTURE RESEARCH

The error estimates of Theorems 5, 6, 13, 14, and 16 have an implicit dependence on the final time, T, in the constant on the right-hand side. Since we often need to solve the evolutionary Navier-Stokes/Darcy or Stokes-Darcy problems over long-time intervals due to the large size of the computational domain and the low permeability, a first objective is to extend the analysis to long-time intervals. A second objective is evaluation of relaxation times, and also non-dimensionalization of the equations to evaluate the relative sizes of the Navier-Stokes and Darcy relaxation times.

A different modeling approach for the coupled surface and groundwater flows is the

time-dependent, one-domain Brinkman equation, which interpolates between the Stokes and Darcy flows [17, 49, 11, 3, 66, 104], when modeling faster flows. The case when the term "$S_0\phi_t$" is not dropped in the limit when obtaining Darcy's law from the Brinkman equation and the flow in the porous media is slightly compressible, is an open problem.

The stabilization of the Crank-Nicolson Leapfrog (CNLF) method developed in Chapter 5 for a general evolution equation (5.1) is restricted to semi-positive definite, symmetric operators A and autonomous, skew-symmetric operators Λ. It is an open problem to develop a stabilization of CNLF for the most general form of A and also for the non-autonomous case, $\Lambda = \Lambda(t)$.

A further goal is to adapt the stabilized CNLF method developed in Algorithm 2 to the fully evolutionary Navier-Stokes/Darcy coupling with different rates for the time step in the fluid and porous media regions to account for the difference in flow rates (fast/slow).

Finally, the next step in the analysis is the coupling of fully evolutionary Stokes-Darcy or Navier/Stokes-Darcy systems with the transport equation and the development of numerical schemes for the transport equation to track the concentration of contaminants. For the transport scheme, variants of the space-time discontinuous Galerkin method would be used that are compatible with the flow discretization schemes and that incorporate penalized jumps in both the diffusive flux and the concentration of the contaminant across the interface.

APPENDIX A

COMPLEMENTARY PROOFS

A.1 CONDITIONAL STABILITY OF CNLF FOR A GENERAL EVOLUTION EQUATION

Theorem 17 (Conditional stability of CNLF). *Consider the* (CNLF) *method under* (5.2) *and* (5.4), *and let* $\|\mathbf{u}\|_A := \sqrt{\langle A\mathbf{u}, \mathbf{u}\rangle}$ *be the norm induced by A. Assume*

$$\Delta t \|\Lambda\| < 1.$$

Then, for all $N > 1$,

$$\lambda^* \left\{ \|\mathbf{u}^N\|^2 + \|\mathbf{u}^{N-1}\|^2 \right\} + \Delta t \sum_{n=1}^{N-1} \|\mathbf{u}^{n+1} + \mathbf{u}^{n-1}\|_A^2$$
$$\leq (1 + \Delta t \|\Lambda\|) \left\{ \|\mathbf{u}^1\|^2 + \|\mathbf{u}^0\|^2 \right\}, \tag{A.1}$$

where $\lambda^* := 1 - \Delta t \|\Lambda\| > 0$.

Proof. We first take the inner product of (CNLF) with $(\mathbf{u}^{n+1} + \mathbf{u}^{n-1})$. After multiplying the equation by $2\Delta t$ we have:

$$\|\mathbf{u}^{n+1}\|^2 - \|\mathbf{u}^{n-1}\|^2 + \Delta t \langle A(\mathbf{u}^{n+1} + \mathbf{u}^{n-1}), \mathbf{u}^{n+1} + \mathbf{u}^{n-1}\rangle + 2\Delta t \langle \Lambda \mathbf{u}^n, \mathbf{u}^{n+1} + \mathbf{u}^{n-1}\rangle = 0. \tag{A.2}$$

We denote

$$E^{n+1/2} := \|\mathbf{u}^{n+1}\|^2 + \|\mathbf{u}^n\|^2,$$

148

and

$$C^{n+1/2} := \langle \Lambda \mathbf{u}^n, \mathbf{u}^{n+1} \rangle.$$

Then, using skew symmetry of Λ we write

$$
\begin{aligned}
2\Delta t \langle \Lambda \mathbf{u}^n, \mathbf{u}^{n+1} + \mathbf{u}^{n-1} \rangle &= 2\Delta t \left\{ \langle \Lambda \mathbf{u}^n, \mathbf{u}^{n+1} \rangle + \langle \Lambda \mathbf{u}^n, \mathbf{u}^{n-1} \rangle \right\} \\
&= 2\Delta t \left\{ \langle \Lambda \mathbf{u}^n, \mathbf{u}^{n+1} \rangle - \langle \Lambda \mathbf{u}^{n-1}, \mathbf{u}^n \rangle \right\} \\
&= C^{n+1/2} - C^{n-1/2}.
\end{aligned}
$$

Hence, after also applying the positivity condition (5.6) for the operator A, (A.2) becomes

$$E^{n+1/2} - E^{n-1/2} + \Delta t \|\mathbf{u}^{n+1} + \mathbf{u}^{n-1}\|_A^2 + 2\Delta t \left\{ C^{n+1/2} - C^{n-1/2} \right\} \le 0.$$

By summing up this last inequality from $n = 1$ to $N - 1$, we obtain

$$E^{N-1/2} + 2\Delta t C^{N-1/2} + \Delta t \sum_{n=1}^{N-1} \|\mathbf{u}^{n+1} + \mathbf{u}^{n-1}\|_A^2 \le E^{1/2} + 2\Delta t C^{1/2}. \qquad (\text{A.3})$$

Next, we bound the indefinite term $C^{N-1/2}$ using Cauchy-Schwarz and Young's inequalities:

$$
\begin{aligned}
2\Delta t |C^{N-1/2}| &= 2\Delta t |\langle \Lambda \mathbf{u}^N, \mathbf{u}^{N-1} \rangle| \\
&\le 2\Delta t \|\Lambda\| \|\mathbf{u}^N\| \|\mathbf{u}^{N-1}\| \\
&\le \Delta t \|\Lambda\| \left(\|\mathbf{u}^N\|^2 + \|\mathbf{u}^{N-1}\|^2 \right) \\
&= \Delta t \|\Lambda\| E^{N-1/2}. \qquad (\text{A.4})
\end{aligned}
$$

After applying (A.4) to (A.3), we arrive at

$$(1 - \Delta t \|\Lambda\|) E^{N-1/2} + \Delta t \sum_{n=1}^{N-1} \|\mathbf{u}^{n+1} + \mathbf{u}^{n-1}\|_A^2 \le (1 + \Delta t \|\Lambda\|) E^{1/2},$$

or equivalently,

$$
\begin{aligned}
(1 - \Delta t \|\Lambda\|) \left\{ \|\mathbf{u}^N\|^2 + \|\mathbf{u}^{N-1}\|^2 \right\} &+ \Delta t \sum_{n=1}^{N-1} \|\mathbf{u}^{n+1} + \mathbf{u}^{n-1}\|_A^2 \\
&\le (1 + \Delta t \|\Lambda\|) \left\{ \|\mathbf{u}^1\|^2 + \|\mathbf{u}^0\|^2 \right\}, \qquad \forall N > 1.
\end{aligned}
\qquad (\text{A.5})
$$

In light of (A.5), we conclude that the CNLF method applied to (5.1) is stable provided

$$(1 - \Delta t \|\Lambda\|) > 0 \Leftrightarrow \Delta t \|\Lambda\| < 1.$$

$\square$

A.2 THE UNSTABLE MODE OF CNLF IS STABLE UNDER CNLF'S TIME-STEP CONDITION

Theorem 18. *Consider the* (CNLF) *method under* (5.2) *and* (5.4), *and assume that the time step condition* (5.5) *holds. Then, both the stable and unstable modes of CNLF are asymptotically stable,*

$$(\mathbf{u}^{n+1} + \mathbf{u}^{n-1}) \xrightarrow{n \to \infty} \mathbf{0}, \quad (\mathbf{u}^{n+1} - \mathbf{u}^{n-1}) \xrightarrow{n \to \infty} \mathbf{0},$$

and thus,

$$\mathbf{u}^n \xrightarrow{n \to \infty} \mathbf{0}.$$

Proof. Let $\|\mathbf{u}\|_A := \sqrt{\langle A\mathbf{u}, \mathbf{u} \rangle}$ be the norm induced by A. By Theorem 17 we have that

$$\Delta t \sum_{n=1}^{N-1} \|\mathbf{u}^{n+1} + \mathbf{u}^{n-1}\|_A^2 \leq C(\mathbf{u}^1, \mathbf{u}^0), \quad \forall N > 1, \tag{A.6}$$

where $C(\mathbf{u}^1, \mathbf{u}^0)$ is a positive constant that depends on $\mathbf{u}^1, \mathbf{u}^0$. Thus, $\sum_{n=1}^{N-1} \|\mathbf{u}^{n+1} + \mathbf{u}^{n-1}\|_A^2$ is bounded for all $N > 1$, and hence it converges. It follows that $\|\mathbf{u}^{n+1} + \mathbf{u}^{n-1}\|_A \xrightarrow{n \to \infty} 0$ and therefore the stable mode is asymptotically stable, $(\mathbf{u}^{n+1} + \mathbf{u}^{n-1}) \xrightarrow{n \to \infty} \mathbf{0}$, which proves the first claim of the theorem.

To prove the second claim, we derive a second energy estimate for the CNLF method. We take the inner product of (CNLF) with $(\mathbf{u}^{n+1} - \mathbf{u}^{n-1})$ and multiply by $2\Delta t \tilde{\delta}$ where $\tilde{\delta} > 0$ (to be determined later, see (A.16)). This gives

$$\tilde{\delta} \|\mathbf{u}^{n+1} - \mathbf{u}^{n-1}\|^2 + \Delta t \tilde{\delta} \langle A(\mathbf{u}^{n+1} + \mathbf{u}^{n-1}), \mathbf{u}^{n+1} - \mathbf{u}^{n-1} \rangle$$
$$+ 2\tilde{\delta}\Delta t \langle \Lambda \mathbf{u}^n, \mathbf{u}^{n+1} - \mathbf{u}^{n-1} \rangle = 0. \tag{A.7}$$

We decompose the operator A into its symmetric and skew-symmetric parts, $A := A_s + A_{ss}$. Then, since $\|\mathbf{v}\|_A^2 = \langle A_s \mathbf{v}, \mathbf{v} \rangle$, we have

$$\langle A(\mathbf{u}^{n+1} + \mathbf{u}^{n-1}), \mathbf{u}^{n+1} - \mathbf{u}^{n-1} \rangle$$
$$= \langle A_s(\mathbf{u}^{n+1} + \mathbf{u}^{n-1}), \mathbf{u}^{n+1} - \mathbf{u}^{n-1} \rangle + \langle A_{ss}(\mathbf{u}^{n+1} + \mathbf{u}^{n-1}), \mathbf{u}^{n+1} - \mathbf{u}^{n-1} \rangle$$
$$= \langle A_s \mathbf{u}^{n+1}, \mathbf{u}^{n+1} \rangle - \langle A_s \mathbf{u}^{n-1}, \mathbf{u}^{n-1} \rangle + \langle A_{ss}(\mathbf{u}^{n+1} + \mathbf{u}^{n-1}), \mathbf{u}^{n+1} - \mathbf{u}^{n-1} \rangle$$
$$= \|\mathbf{u}^{n+1}\|_A^2 - \|\mathbf{u}^{n-1}\|_A^2 + \langle A_{ss}(\mathbf{u}^{n+1} + \mathbf{u}^{n-1}), \mathbf{u}^{n+1} - \mathbf{u}^{n-1} \rangle.$$

Letting

$$\mathcal{A}^{n+1/2} := \|\mathbf{u}^{n+1}\|_A^2 + \|\mathbf{u}^n\|_A^2,$$

([A.7](#)) becomes

$$\tilde{\delta}\|\mathbf{u}^{n+1} - \mathbf{u}^{n-1}\|^2 + \tilde{\delta}\Delta t \mathcal{A}^{n+1/2} - \tilde{\delta}\Delta t \mathcal{A}^{n-1/2}$$
$$+ \tilde{\delta}\Delta t \langle A_{ss}(\mathbf{u}^{n+1} + \mathbf{u}^{n-1}), \mathbf{u}^{n+1} - \mathbf{u}^{n-1}\rangle + 2\tilde{\delta}\Delta t \langle \Lambda \mathbf{u}^n, \mathbf{u}^{n+1} - \mathbf{u}^{n-1}\rangle = 0.$$

Summing this from $n = 1$ to $N - 1$ gives

$$\tilde{\delta}\sum_{n=1}^{N-1}\|\mathbf{u}^{n+1} - \mathbf{u}^{n-1}\|^2 + \tilde{\delta}\Delta t \mathcal{A}^{N-1/2} + \tilde{\delta}\Delta t \sum_{n=1}^{N-1}\langle A_{ss}(\mathbf{u}^{n+1} + \mathbf{u}^{n-1}), \mathbf{u}^{n+1} - \mathbf{u}^{n-1}\rangle$$
$$+ 2\tilde{\delta}\Delta t \sum_{n=1}^{N-1}\langle \Lambda \mathbf{u}^n, \mathbf{u}^{n+1} - \mathbf{u}^{n-1}\rangle = \tilde{\delta}\Delta t \mathcal{A}^{1/2}. \tag{A.8}$$

The next step is adding together ([A.6](#)) and ([A.8](#)):

$$\tilde{\delta}\sum_{n=1}^{N-1}\|\mathbf{u}^{n+1} - \mathbf{u}^{n-1}\|^2 + \Delta t \sum_{n=1}^{N-1}\|\mathbf{u}^{n+1} + \mathbf{u}^{n-1}\|_A^2 + \tilde{\delta}\Delta t \mathcal{A}^{N-1/2}$$
$$+ \tilde{\delta}\Delta t \sum_{n=1}^{N-1}\langle A_{ss}(\mathbf{u}^{n+1} + \mathbf{u}^{n-1}), \mathbf{u}^{n+1} - \mathbf{u}^{n-1}\rangle \tag{A.9}$$
$$+ 2\tilde{\delta}\Delta t \sum_{n=1}^{N-1}\langle \Lambda \mathbf{u}^n, \mathbf{u}^{n+1} - \mathbf{u}^{n-1}\rangle \leq C(\mathbf{u}^1, \mathbf{u}^0) + \tilde{\delta}\Delta t \mathcal{A}^{1/2}.$$

We now bound the last two terms on the left-hand side of ([A.9](#)). For the first term we apply Cauchy-Schwarz and Young's inequality with $\tilde{\epsilon} > 0$:

$$\left|\langle A_{ss}(\mathbf{u}^{n+1} + \mathbf{u}^{n-1}), \mathbf{u}^{n+1} - \mathbf{u}^{n-1}\rangle\right| \leq \|A_{ss}\|\|\mathbf{u}^{n+1} + \mathbf{u}^{n-1}\|\|\mathbf{u}^{n+1} - \mathbf{u}^{n-1}\|$$
$$\leq \frac{1}{2\tilde{\epsilon}}\|A_{ss}\|\|\mathbf{u}^{n+1} + \mathbf{u}^{n-1}\|^2 + \frac{\tilde{\epsilon}}{2}\|A_{ss}\|\|\mathbf{u}^{n+1} - \mathbf{u}^{n-1}\|^2,$$

and thus

$$\left|\tilde{\delta}\Delta t \sum_{n=1}^{N-1}\langle A_{ss}(\mathbf{u}^{n+1} + \mathbf{u}^{n-1}), \mathbf{u}^{n+1} - \mathbf{u}^{n-1}\rangle\right|$$
$$\leq \frac{\tilde{\delta}\Delta t}{2\tilde{\epsilon}}\|A_{ss}\|\sum_{n=1}^{N-1}\|\mathbf{u}^{n+1} + \mathbf{u}^{n-1}\|^2 + \frac{\tilde{\delta}\Delta t\tilde{\epsilon}}{2}\|A_{ss}\|\sum_{n=1}^{N}\|\mathbf{u}^{n+1} - \mathbf{u}^{n-1}\|^2. \tag{A.10}$$

For the second term, we first decompose $\mathbf{u}^n$ into the stable and unstable modes, and apply Cauchy-Schwarz and Young's inequality (with $\tilde{\epsilon} > 0$). Then, for all $n \geq 2$:

$$
\begin{aligned}
\left|\langle \Lambda \mathbf{u}^n, \mathbf{u}^{n+1} - \mathbf{u}^{n-1}\rangle\right| &= \left|\frac{1}{2}\langle \Lambda(\mathbf{u}^n - \mathbf{u}^{n-2}), \mathbf{u}^{n+1} - \mathbf{u}^{n-1}\rangle + \frac{1}{2}\langle \Lambda(\mathbf{u}^n + \mathbf{u}^{n-2}), \mathbf{u}^{n+1} - \mathbf{u}^{n-1}\rangle\right| \\
&\leq \frac{1}{2}\|\Lambda\|\|\mathbf{u}^n - \mathbf{u}^{n-2}\|\|\mathbf{u}^{n+1} - \mathbf{u}^{n-1}\| + \frac{1}{2}\|\Lambda\|\|\mathbf{u}^n + \mathbf{u}^{n-2}\|\|\mathbf{u}^{n+1} - \mathbf{u}^{n-1}\| \\
&\leq \frac{1}{2}\|\Lambda\| \left(\frac{1}{2}\|\mathbf{u}^n - \mathbf{u}^{n-2}\|^2 + \frac{1}{2}\|\mathbf{u}^{n+1} - \mathbf{u}^{n-1}\|^2\right) \\
&\quad + \frac{1}{2}\|\Lambda\| \left(\frac{1}{2\tilde{\epsilon}}\|\mathbf{u}^n + \mathbf{u}^{n-2}\|^2 + \frac{\tilde{\epsilon}}{2}\|\mathbf{u}^{n+1} - \mathbf{u}^{n-1}\|^2\right).
\end{aligned}
$$

Then,

$$
\begin{aligned}
\left|2\tilde{\delta}\Delta t \sum_{n=1}^{N-1} \langle \Lambda \mathbf{u}^n, \mathbf{u}^{n+1} - \mathbf{u}^{n-1}\rangle\right| &\leq 2\tilde{\delta}\Delta t \left|\langle \Lambda \mathbf{u}^1, \mathbf{u}^2 - \mathbf{u}^0\rangle\right| + 2\tilde{\delta}\Delta t \sum_{n=2}^{N-1} \left|\langle \Lambda \mathbf{u}^n, \mathbf{u}^{n+1} - \mathbf{u}^{n-1}\rangle\right| \\
&\leq 2\tilde{\delta}\Delta t\|\Lambda\|\|\mathbf{u}^1\|^2 + \frac{\tilde{\delta}}{2}\Delta t\|\Lambda\|\|\mathbf{u}^2 - \mathbf{u}^0\|^2 + 2\tilde{\delta}\Delta t \sum_{n=2}^{N-1} \frac{1}{2}\|\Lambda\| \left(\frac{1}{2}\|\mathbf{u}^n - \mathbf{u}^{n-2}\|^2\right. \\
&\quad \left. + \frac{1}{2}\|\mathbf{u}^{n+1} - \mathbf{u}^{n-1}\|^2\right) + 2\tilde{\delta}\Delta t \sum_{n=2}^{N-1} \frac{1}{2}\|\Lambda\| \left(\frac{1}{2\tilde{\epsilon}}\|\mathbf{u}^n + \mathbf{u}^{n-2}\|^2 + \frac{\tilde{\epsilon}}{2}\|\mathbf{u}^{n+1} - \mathbf{u}^{n-1}\|^2\right) \\
&= 2\tilde{\delta}\Delta t\|\Lambda\|\|\mathbf{u}^1\|^2 + \tilde{\delta}\Delta t\|\Lambda\|\|\mathbf{u}^2 - \mathbf{u}^0\|^2 + \tilde{\delta}\Delta t\|\Lambda\| \sum_{n=2}^{N-2} \|\mathbf{u}^{n+1} - \mathbf{u}^{n-1}\|^2 \\
&\quad + \frac{\tilde{\delta}}{2}\Delta t\|\Lambda\|\|\mathbf{u}^N - \mathbf{u}^{N-2}\|^2 + \frac{\tilde{\delta}\Delta t\|\Lambda\|}{2\tilde{\epsilon}} \sum_{n=1}^{N-2} \|\mathbf{u}^{n+1} + \mathbf{u}^{n-1}\|^2 + \frac{\tilde{\epsilon}\tilde{\delta}\Delta t\|\Lambda\|}{2} \sum_{n=2}^{N-1} \|\mathbf{u}^{n+1} - \mathbf{u}^{n-1}\|^2 \\
&\leq 2\tilde{\delta}\Delta t\|\Lambda\|\|\mathbf{u}^1\|^2 + \tilde{\delta}\Delta t\|\Lambda\| \sum_{n=1}^{N-1} \|\mathbf{u}^{n+1} - \mathbf{u}^{n-1}\|^2 + \frac{\tilde{\delta}\Delta t\|\Lambda\|}{2\tilde{\epsilon}} \sum_{n=1}^{N-1} \|\mathbf{u}^{n+1} + \mathbf{u}^{n-1}\|^2 \\
&\quad + \frac{\tilde{\epsilon}\tilde{\delta}\Delta t\|\Lambda\|}{2} \sum_{n=1}^{N-1} \|\mathbf{u}^{n+1} - \mathbf{u}^{n-1}\|^2 \\
&= 2\tilde{\delta}\Delta t\|\Lambda\|\|\mathbf{u}^1\|^2 + \tilde{\delta}\Delta t\|\Lambda\| \left(1 + \frac{\tilde{\epsilon}}{2}\right) \sum_{n=1}^{N-1} \|\mathbf{u}^{n+1} - \mathbf{u}^{n-1}\|^2 + \frac{\tilde{\delta}\Delta t\|\Lambda\|}{2\tilde{\epsilon}} \sum_{n=1}^{N-1} \|\mathbf{u}^{n+1} + \mathbf{u}^{n-1}\|^2.
\end{aligned}
$$

$$(A.11)$$

We now apply (A.10) and (A.11) to the left-hand side of (A.9). After collecting terms, we have

$$
\tilde{\delta}\left(1 - \frac{\Delta t \tilde{\epsilon}}{2}\|A_{ss}\| - \Delta t\|\Lambda\|\left(1 + \frac{\tilde{\epsilon}}{2}\right)\right)\sum_{n=1}^{N-1}\|\mathbf{u}^{n+1} - \mathbf{u}^{n-1}\|^2 + \tilde{\delta}\Delta t \mathcal{A}^{N-1/2}
$$
$$
+ \Delta t \sum_{n=1}^{N-1}\left\{\|\mathbf{u}^{n+1} + \mathbf{u}^{n-1}\|_A^2 - \frac{\tilde{\delta}}{2\tilde{\epsilon}}\left(\|A_{ss}\| + \|\Lambda\|\right)\|\mathbf{u}^{n+1} + \mathbf{u}^{n-1}\|^2\right\} \tag{A.12}
$$
$$
\leq C(\mathbf{u}^1, \mathbf{u}^0) + \tilde{\delta}\Delta t \mathcal{A}^{1/2} + 2\tilde{\delta}\Delta t\|\Lambda\|\|\mathbf{u}^1\|^2 \leq \widehat{C}(\mathbf{u}^1, \mathbf{u}^0),
$$

where $\widehat{C}(\mathbf{u}^1, \mathbf{u}^0)$ is a new positive constant that depends on $\mathbf{u}^1, \mathbf{u}^0$ and is independent of N. Thus, (A.12) implies asymptotic stability of the unstable mode provided

$$
\left(1 - \frac{\Delta t \tilde{\epsilon}}{2}\|A_{ss}\| - \Delta t\|\Lambda\|\left(1 + \frac{\tilde{\epsilon}}{2}\right)\right) > 0 \tag{A.13}
$$
$$
\left\{\|\mathbf{u}^{n+1} + \mathbf{u}^{n-1}\|_A^2 - \frac{\tilde{\delta}}{2\tilde{\epsilon}}\left(\|A_{ss}\| + \|\Lambda\|\right)\|\mathbf{u}^{n+1} + \mathbf{u}^{n-1}\|^2\right\} \geq 0. \quad \text{for} \quad \mathbf{u}^n, \mathbf{u}^{n-1} \neq \mathbf{0}. \tag{A.14}
$$

(A.13) is equivalent to

$$
\tilde{\epsilon} < \frac{2\left(1 - \Delta t\|\Lambda\|\right)}{\Delta t\left(\|\Lambda\| + \|A_{ss}\|\right)}. \tag{A.15}
$$

Since $\tilde{\epsilon} > 0$ is arbitrary, and $\Delta t\|\Lambda\| < 1$ holds, we can choose $\tilde{\epsilon}$ so that (A.15) is satisfied. For (A.14) to be true, it suffices that

$$
\tilde{\delta} \leq \frac{2\tilde{\epsilon}\lambda_{\min}(A_s)}{\|A_{ss}\| + \|\Lambda\|}, \tag{A.16}
$$

where $\lambda_{\min}(A_s) > 0$ is the minimum eigenvalue of A_s. Since $\tilde{\delta} > 0$ is arbitrary, we can choose it so that (A.16) is satisfied. Therefore, we conclude from (A.12) that

$$
\sum_{n=1}^{N-1}\|\mathbf{u}^{n+1} - \mathbf{u}^{n-1}\|^2
$$

is bounded for all $N > 1$, and thus convergent. It follows that $(\mathbf{u}^{n+1} - \mathbf{u}^{n-1}) \xrightarrow{n\to\infty} \mathbf{0}$, concluding the proof. $\qquad\square$

A.3 CONDITIONAL STABILITY OF CNLF-STAB WITH $\beta = 1/12$ FOR A GENERAL EVOLUTION EQUATION

Theorem 19 (Conditional stability of the CNLF-stab method with $\beta = 1/12$). (CNLF-stab) *with $\beta = 1/12$ is stable under the time step condition:*

$$\Delta t \|\Lambda\| < 1.268. \tag{A.17}$$

Proof. We rewrite the stabilization parameter as $\beta = \gamma - (\gamma - \beta)$ where $\gamma > 1/8$ and $\gamma - \beta > 0$. Following the steps of the proof of Theorem 7, the system energy is

$$\begin{aligned}
\text{Energy}^{n+1/2} =& \|\mathbf{u}^{n+1}\|^2 + \|\mathbf{u}^n\|^2 + 2\gamma\Delta t^2(\|\Lambda\mathbf{u}^{n+1}\|^2 + \|\Lambda\mathbf{u}^n\|^2) \\
& + 2\Delta t \langle \Lambda\mathbf{u}^n, \mathbf{u}^{n+1} \rangle - 2(\gamma - \beta)\Delta t^2(\|\Lambda\mathbf{u}^{n+1}\|^2 + \|\Lambda\mathbf{u}^n\|^2).
\end{aligned}$$

Since $\gamma > 1/8$, Theorem 7 gives

$$\begin{aligned}
\|\mathbf{u}^{n+1}\|^2 + \|\mathbf{u}^n\|^2 + 2\gamma\Delta t^2(\|\Lambda\mathbf{u}^{n+1}\|^2 + \|\Lambda\mathbf{u}^n\|^2) + 2\Delta t\langle\Lambda\mathbf{u}^n, \mathbf{u}^{n+1}\rangle \\
\geq (1 - \tfrac{1}{8\gamma})\left(\|\mathbf{u}^{n+1}\|^2 + \|\mathbf{u}^n\|^2\right).
\end{aligned}$$

Hence,

$$\begin{aligned}
\text{Energy}^{n+1/2} \geq& (1 - \tfrac{1}{8\gamma})\|\mathbf{u}^{n+1}\|^2 - 2(\gamma - \beta)\Delta t^2\|\Lambda\mathbf{u}^{n+1}\|^2 \\
& + (1 - \tfrac{1}{8\gamma})\|\mathbf{u}^n\|^2 - 2(\gamma - \beta)\Delta t^2\|\Lambda\mathbf{u}^n\|^2.
\end{aligned}$$

The bound above implies stability provided

$$1 - \tfrac{1}{8\gamma} - 2(\gamma - \beta)\Delta t^2\|\Lambda\|^2 > 0 \iff \Delta t\|\Lambda\| < \left(\tfrac{8\gamma - 1}{16\gamma(\gamma - \beta)}\right)^{1/2}.$$

For $\beta = 1/12$, the maximum value of this quantity (for $\gamma > 1/12$) is attained at $\gamma \cong 0.19717$, and thus

$$\Delta t\|\Lambda\| < \sqrt{1.6077} \cong 1.268.$$

$\square$

A.4 CONDITIONAL STABILITY OF CNLF IN THE STOKES-DARCY MODEL

Proof of Proposition 6:

Proof. In (6.9)-(6.11), we choose $\mathbf{v}_h = \mathbf{u}_h^{k+1} + \mathbf{u}_h^{k-1}$, $\psi_h = \phi_h^{k+1} + \phi_h^{k-1}$. Then the pressure term in (6.9) cancels by (6.10). By adding together the equations and multiplying by $2\Delta t$ we get

$$n \left(\|\mathbf{u}_h^{k+1}\|_f^2 - \|\mathbf{u}_h^{k-1}\|_f^2 \right) + gS_0 \left(\|\phi_h^{k+1}\|_p^2 - \|\phi_h^{k-1}\|_p^2 \right)$$
$$+ \Delta t \left\{ a_f \left(\mathbf{u}_h^{k+1} + \mathbf{u}_h^{k-1}, \mathbf{u}_h^{k+1} + \mathbf{u}_h^{k-1} \right) + a_p \left(\phi_h^{k+1} + \phi_h^{k-1}, \phi_h^{k+1} + \phi_h^{k-1} \right) \right\}$$
$$+ 2\Delta t \left(c_I(\mathbf{u}_h^{k+1} + \mathbf{u}_h^{k-1}, \phi_h^k) - c_I(\mathbf{u}_h^k, \phi_h^{k+1} + \phi_h^{k-1}) \right)$$
$$= 2\Delta t \left\{ n(\tilde{\mathbf{f}}_f^k, \mathbf{u}_h^{k+1} + \mathbf{u}_h^{k-1})_f + g \left(f_p^k, \phi_h^{k+1} + \phi_h^{k-1} \right)_p \right\}.$$

We let

$$C^{k+1/2} = c_I(\phi_h^k, \mathbf{u}_h^{k+1}) - c_I(\phi_h^{k+1}, \mathbf{u}_h^k),$$

and express the interface terms above as

$$c_I(\mathbf{u}_h^{k+1} + \mathbf{u}_h^{k-1}, \phi_h^k) - c_I(\mathbf{u}_h^k, \phi_h^{k+1} + \phi_h^{k-1}) = C^{k+\frac{1}{2}} - C^{k-\frac{1}{2}}.$$

By the coercivity estimates (3.34), (3.36), the dual norms of $\mathbf{X}_f$, X_p, and Young's inequality, we obtain

$$n \left(\|\mathbf{u}_h^{k+1}\|_f^2 - \|\mathbf{u}_h^{k-1}\|_f^2 \right) + gS_0 \left(\|\phi_h^{k+1}\|_p^2 - \|\phi_h^{k-1}\|_p^2 \right) + 2\Delta t \left\{ C^{k+\frac{1}{2}} - C^{k-\frac{1}{2}} \right\}$$
$$+ \Delta t \left\{ \frac{2n\nu}{C_K} \|\nabla \left(\mathbf{u}_h^{k+1} + \mathbf{u}_h^{k-1} \right)\|_f^2 + gk_{min} \|\nabla \left(\phi_h^{k+1} + \phi_h^{k-1} \right)\|_p^2 \right\}$$
$$\leq \Delta t \frac{n\nu}{C_K} \|\nabla \left(\mathbf{u}_h^{k+1} + \mathbf{u}_h^{k-1} \right)\|_f^2 + \Delta t \frac{nC_K}{\nu} \|\tilde{\mathbf{f}}_f^k\|_{-1,f}^2$$
$$+ \Delta t \frac{gk_{min}}{2} \|\nabla \left(\phi_h^{k+1} + \phi_h^{k-1} \right)\|_p^2 + \Delta t \frac{2g}{k_{min}} \|f_p^k\|_{-1,p}^2.$$

Rearranging gives

$$n \left(\|\mathbf{u}_h^{k+1}\|_f^2 - \|\mathbf{u}_h^{k-1}\|_f^2 \right) + gS_0 \left(\|\phi_h^{k+1}\|_p^2 - \|\phi_h^{k-1}\|_p^2 \right) + 2\Delta t \left\{ C^{k+\frac{1}{2}} - C^{k-\frac{1}{2}} \right\}$$

$$+ \Delta t \left\{ \frac{n\nu}{C_K} \|\nabla \left(\mathbf{u}_h^{k+1} + \mathbf{u}_h^{k-1} \right)\|_f^2 + \frac{gk_{min}}{2} \|\nabla \left(\phi_h^{k+1} + \phi_h^{k-1} \right)\|_p^2 \right\} \qquad \text{(A.18)}$$

$$\leq \Delta t \frac{nC_K}{\nu} \|\tilde{\mathbf{f}}_f^k\|_{-1,f}^2 + \Delta t \frac{2g}{k_{min}} \|f_p^k\|_{-1,p}^2.$$

We denote the energy terms by

$$E^{k+1/2} = n \left(\|\mathbf{u}_h^{k+1}\|_f^2 + \|\mathbf{u}_h^k\|_f^2 \right) + gS_0 \left(\|\phi_h^{k+1}\|_p^2 + \|\phi_h^k\|_p^2 \right).$$

Then (A.18) becomes

$$E^{k+1/2} - E^{k-1/2} + \Delta t \left\{ \frac{n\nu}{C_K} \|\nabla \left(\mathbf{u}_h^{k+1} + \mathbf{u}_h^{k-1} \right)\|_f^2 + \frac{gk_{min}}{2} \|\nabla \left(\phi_h^{k+1} + \phi_h^{k-1} \right)\|_p^2 \right\}$$

$$+ 2\Delta t \left\{ C^{k+1/2} - C^{k-1/2} \right\} \leq \Delta t \frac{nC_K}{\nu} \|\tilde{\mathbf{f}}_f^k\|_{-1,f}^2 + \Delta t \frac{2g}{k_{min}} \|f_p^k\|_{-1,p}^2.$$

Next, we sum up this inequality from $k = 1$ to $N - 1$ to find

$$E^{N-1/2} + \Delta t \sum_{k=1}^{N-1} \left\{ \frac{n\nu}{C_K} \|\nabla \left(\mathbf{u}_h^{k+1} + \mathbf{u}_h^{k-1} \right)\|_f^2 + \frac{gk_{min}}{2} \|\nabla \left(\phi_h^{k+1} + \phi_h^{k-1} \right)\|_p^2 \right\}$$

$$+ 2\Delta t C^{N-1/2} \leq E^{1/2} + 2\Delta t C^{1/2} + \Delta t \sum_{k=1}^{N-1} \left\{ \frac{nC_K}{\nu} \|\tilde{\mathbf{f}}_f^k\|_{-1,f}^2 + \frac{2g}{k_{min}} \|f_p^k\|_{-1,p}^2 \right\}. \qquad \text{(A.19)}$$

We then apply the trace (2.9), and inverse (6.8) inequalities to bound the interface terms in $C^{N-1/2}$ as follows:

$$|c_I(\mathbf{u}_h^N, \phi_h^{N-1})| = ng \left| \int_I \phi_h^{N-1} \mathbf{u}_h^N \cdot \hat{\mathbf{n}}_f \, d\sigma \right|$$

$$\leq ng \|\mathbf{u}_h^N\|_I \|\phi_h^{N-1}\|_I = ng \|\mathbf{u}_h^N\|_{L^2(\partial\Omega_f)} \|\phi_h^{N-1}\|_{L^2(\partial\Omega_p)}$$

$$\leq ng C_{T,f} C_{T,p} \|\mathbf{u}_h^N\|_f^{1/2} \|\nabla \mathbf{u}_h^N\|_f^{1/2} \|\phi_h^{N-1}\|_p^{1/2} \|\nabla \phi_h^{N-1}\|_p^{1/2}$$

$$\leq ng C_{T,f} C_{T,p} h^{-1} C_{inv,f}^{1/2} C_{inv,p}^{1/2} \|\mathbf{u}_h^N\|_f \|\phi_h^{N-1}\|_p.$$

Letting $C_{\Omega_{f/p}} := C_{T,f} C_{T,p} C_{inv,f}^{1/2} C_{inv,p}^{1/2} > 0$, and applying Young's inequality we have

$$|c_I(\mathbf{u}_h^N, \phi_h^{N-1})| \leq \frac{h^{-1} ng C_{\Omega_{f/p}}}{2} \left(\|\mathbf{u}_h^N\|_f^2 + \|\phi_h^{N-1}\|_p^2 \right),$$

$$\text{or} \quad |c_I(\mathbf{u}_h^N, \phi_h^{N-1})| \leq \frac{h^{-2} ng C_{\Omega_{f/p}}}{2} \|\mathbf{u}_h^N\|_f^2 + \frac{ng C_{\Omega_{f/p}}}{2} \|\phi_h^{N-1}\|_p^2,$$

156

and, similarly,

$$|c_I(\mathbf{u}_h^{N-1}, \phi_h^N)| \leq \frac{h^{-1}ngC_{\Omega_{f/p}}}{2}\left(\|\mathbf{u}_h^{N-1}\|_f^2 + \|\phi_h^N\|_p^2\right),$$

$$\text{or} \quad |c_I(\mathbf{u}_h^{N-1}, \phi_h^N)| \leq \frac{h^{-2}ngC_{\Omega_{f/p}}}{2}\|\mathbf{u}_h^{N-1}\|_f^2 + \frac{ngC_{\Omega_{f/p}}}{2}\|\phi_h^N\|_p^2.$$

Thus,

$$|2\Delta t C^{N-1/2}| \leq \Delta t \; h^{-1}ngC_{\Omega_{f/p}}\left(\|\mathbf{u}_h^N\|_f^2 + \|\mathbf{u}_h^{N-1}\|_f^2 + \|\phi_h^N\|_p^2 + \|\phi_h^{N-1}\|_p^2\right),$$

$$\text{or} \quad |2\Delta t C^{N-1/2}| \leq \Delta t \; h^{-2}ngC_{\Omega_{f/p}}\left(\|\mathbf{u}_h^N\|_f^2 + \|\mathbf{u}_h^{N-1}\|_f^2\right) + \Delta t \; ngC_{\Omega_{f/p}}\left(\|\phi_h^N\|_p^2 + \|\phi_h^{N-1}\|_p^2\right).$$

Consequently,

$$\begin{aligned} E^{N-1/2} + 2\Delta t C^{N-1/2} &\geq n\left[1 - \Delta t \; h^{-1}gC_{\Omega_{f/p}}\right]\left(\|\mathbf{u}_h^N\|_f^2 + \|\mathbf{u}_h^{N-1}\|_f^2\right) \\ &\quad + g\left[S_0 - \Delta t \; h^{-1}nC_{\Omega_{f/p}}\right]\left(\|\phi_h^N\|_p^2 + \|\phi_h^{N-1}\|_p^2\right), \end{aligned} \tag{A.20}$$

$$\begin{aligned} \text{or} \quad E^{N-1/2} + 2\Delta t C^{N-1/2} &\geq n\left[1 - \Delta t \; h^{-2}gC_{\Omega_{f/p}}\right]\left(\|\mathbf{u}_h^N\|_f^2 + \|\mathbf{u}_h^{N-1}\|_f^2\right) \\ &\quad + g\left[S_0 - \Delta t \; nC_{\Omega_{f/p}}\right]\left(\|\phi_h^N\|_p^2 + \|\phi_h^{N-1}\|_p^2\right). \end{aligned} \tag{A.21}$$

After combining (A.19) with (A.20) or with (A.21), we obtain

$$\begin{aligned} &n\left[1 - \Delta t \; h^{-1}gC_{\Omega_{f/p}}\right]\left(\|\mathbf{u}_h^N\|_f^2 + \|\mathbf{u}_h^{N-1}\|_f^2\right) + g\left[S_0 - \Delta t \; h^{-1}nC_{\Omega_{f/p}}\right]\left(\|\phi_h^N\|_p^2 + \|\phi_h^{N-1}\|_p^2\right) \\ &\quad + \Delta t \sum_{k=1}^{N-1}\left\{\frac{n\nu}{C_K}\|\nabla\left(\mathbf{u}_h^{k+1} + \mathbf{u}_h^{k-1}\right)\|_f^2 + \frac{gk_{min}}{2}\|\nabla\left(\phi_h^{k+1} + \phi_h^{k-1}\right)\|_p^2\right\} \\ &\leq n(\|\mathbf{u}_h^1\|_f^2 + \|\mathbf{u}_h^0\|_f^2) + gS_0\left(\|\phi_h^1\|_p^2 + \|\phi_h^0\|_p^2\right) + 2\Delta t\left(c_I(\phi_h^0, \mathbf{u}_h^1) - c_I(\phi_h^1, \mathbf{u}_h^0)\right) \\ &\quad + \Delta t \sum_{k=1}^{N-1}\left\{\frac{nC_K}{\nu}\|\tilde{\mathbf{f}}_f^k\|_{-1,f}^2 + \frac{2g}{k_{min}}\|f_p^k\|_{-1,p}^2\right\}, \end{aligned}$$

or

$$\begin{aligned} &n\left[1 - \Delta t \; h^{-2}gC_{\Omega_{f/p}}\right]\left(\|\mathbf{u}_h^N\|_f^2 + \|\mathbf{u}_h^{N-1}\|_f^2\right) + g\left[S_0 - \Delta t \; nC_{\Omega_{f/p}}\right]\left(\|\phi_h^N\|_p^2 + \|\phi_h^{N-1}\|_p^2\right) \\ &\quad + \Delta t \sum_{k=1}^{N-1}\left\{\frac{n\nu}{C_K}\|\nabla\left(\mathbf{u}_h^{k+1} + \mathbf{u}_h^{k-1}\right)\|_f^2 + \frac{gk_{min}}{2}\|\nabla\left(\phi_h^{k+1} + \phi_h^{k-1}\right)\|_p^2\right\} \\ &\leq n(\|\mathbf{u}_h^1\|_f^2 + \|\mathbf{u}_h^0\|_f^2) + gS_0\left(\|\phi_h^1\|_p^2 + \|\phi_h^0\|_p^2\right) + 2\Delta t\left(c_I(\phi_h^0, \mathbf{u}_h^1) - c_I(\phi_h^1, \mathbf{u}_h^0)\right) \\ &\quad + \Delta t \sum_{k=1}^{N-1}\left\{\frac{nC_K}{\nu}\|\tilde{\mathbf{f}}_f^k\|_{-1,f}^2 + \frac{2g}{k_{min}}\|f_p^k\|_{-1,p}^2\right\}. \end{aligned}$$

From these, we have stability if

$$1 - \Delta t \; h^{-1} g C_{\Omega_{f/p}} > 0 \quad \text{and} \quad S_0 - \Delta t \; h^{-1} n C_{\Omega_{f/p}} > 0$$
$$\text{or} \quad 1 - \Delta t \; h^{-2} g C_{\Omega_{f/p}} > 0 \quad \text{and} \quad S_0 - \Delta t \; n C_{\Omega_{f/p}} > 0,$$

which are equivalent to (6.12). Thus, if we let

$$\alpha^f := \min \left\{ 1 - \Delta t \; h^{-1} g C_{\Omega_{f/p}}, 1 - \Delta t \; h^{-2} g C_{\Omega_{f/p}} \right\} > 0, \quad \text{and}$$
$$\alpha^p := \min \left\{ S_0 - \Delta t \; h^{-1} n C_{\Omega_{f/p}}, S_0 - \Delta t \; n C_{\Omega_{f/p}} \right\} > 0,$$

we obtain the stability bound (6.13) conditional on (6.12), concluding the proof. $\qquad \square$

A.5   CONSISTENCY ERROR BOUNDS

Proof of Lemma 4:

Proof. First we prove (6.49). By applying integration by parts twice, we have

$$
\begin{aligned}
\mathbf{u}_t^k - \frac{\mathbf{u}^{k+1} - \mathbf{u}^{k-1}}{2\Delta t} &= \frac{1}{2\Delta t} \left((t^{k+1} - t^k) \, \mathbf{u}_t^k - (\mathbf{u}^{k+1} - \mathbf{u}^k) + (t^k - t^{k-1}) \, \mathbf{u}_t^k - (\mathbf{u}^k - \mathbf{u}^{k-1}) \right) \\
&= \frac{1}{2\Delta t} \left(\int_{t^k}^{t^{k+1}} (t - t^{k+1}) \, \mathbf{u}_{tt} \; dt + \int_{t^{k-1}}^{t^k} (t - t^{k-1}) \, \mathbf{u}_{tt} \; dt \right) \\
&= \frac{1}{2\Delta t} \left(\int_{t^k}^{t^{k+1}} \frac{(t - t^{k+1})^2}{2} \, \mathbf{u}_{ttt} \; dt + \int_{t^{k-1}}^{t^k} \frac{(t - t^{k-1})^2}{2} \, \mathbf{u}_{ttt} \; dt \right).
\end{aligned}
$$

Thus, by Cauchy-Schwarz we obtain

$$
\sum_{k=1}^{N-1} \left\| \mathbf{u}_t^k - \frac{\mathbf{u}^{k+1} - \mathbf{u}^{k-1}}{2\Delta t} \right\|_f^2
$$

$$
= \frac{1}{4(\Delta t)^2} \int_{\Omega_f} \sum_{k=1}^{N-1} \left| \int_{t^k}^{t^{k+1}} \frac{(t - t^{k+1})^2}{2} \mathbf{u}_{ttt} \, dt + \int_{t^{k-1}}^{t^k} \frac{(t - t^{k-1})^2}{2} \mathbf{u}_{ttt} \, dt \right|^2 \, d\mathbf{x}
$$

$$
\leq \frac{1}{2(\Delta t)^2} \int_{\Omega_f} \sum_{k=1}^{N-1} \left\{ \left| \int_{t^k}^{t^{k+1}} \frac{(t - t^{k+1})^2}{2} \mathbf{u}_{ttt} \, dt \right|^2 + \left| \int_{t^{k-1}}^{t^k} \frac{(t - t^{k-1})^2}{2} \mathbf{u}_{ttt} \, dt \right|^2 \right\} \, d\mathbf{x}
$$

$$
\leq \frac{1}{2(\Delta t)^2} \int_{\Omega_f} \sum_{k=1}^{N-1} \left\{ \int_{t^k}^{t^{k+1}} \frac{(t - t^{k+1})^4}{4} \, dt \int_{t^k}^{t^{k+1}} |\mathbf{u}_{ttt}|^2 \, dt \right.
$$

$$
\left. + \int_{t^{k-1}}^{t^k} \frac{(t - t^{k-1})^4}{4} \, dt \int_{t^{k-1}}^{t^k} |\mathbf{u}_{ttt}|^2 \, dt \right\} \, d\mathbf{x}
$$

$$
= \frac{(\Delta t)^3}{40} \int_{\Omega_f} \sum_{k=1}^{N-1} \left\{ \int_{t^{k-1}}^{t^{k+1}} |\mathbf{u}_{ttt}|^2 \, dt \right\} \, d\mathbf{x}
$$

$$
\leq \frac{(\Delta t)^3}{20} \int_{\Omega_f} \int_0^T |\mathbf{u}_{ttt}|^2 \, dt \, d\mathbf{x} = \frac{(\Delta t)^3}{20} \|\mathbf{u}_{ttt}\|_{L^2(0,T;L^2(\Omega_f))}.
$$

The proofs of (6.50) and (6.53) are similar. Next, we prove (6.51). By applying integration by parts we have

$$
\nabla \left(\mathbf{u}^k - \frac{\mathbf{u}^{k+1} + \mathbf{u}^{k-1}}{2} \right) = \frac{1}{2} \left((\nabla \mathbf{u}^k - \nabla \mathbf{u}^{k-1}) - (\nabla \mathbf{u}^{k+1} - \nabla \mathbf{u}^k) \right)
$$

$$
= \frac{1}{2} \left(\int_{t^{k-1}}^{t^k} \nabla \mathbf{u}_t \, dt - \int_{t^k}^{t^{k+1}} \nabla \mathbf{u}_t \, dt \right)
$$

$$
= \frac{1}{2} \left(- \int_{t^{k-1}}^{t^k} (t - t^{k-1}) \nabla \mathbf{u}_{tt} \, dt + \int_{t^k}^{t^{k+1}} (t - t^{k+1}) \nabla \mathbf{u}_{tt} \, dt \right).
$$

By Cauchy-Schwarz we then have

$$\sum_{k=1}^{N-1} \left\| \nabla \left(\mathbf{u}^k - \frac{\mathbf{u}^{k+1} + \mathbf{u}^{k-1}}{2} \right) \right\|_f^2$$

$$= \frac{1}{4} \int_{\Omega_f} \sum_{k=1}^{N-1} \left| -\int_{t^{k-1}}^{t^k} (t - t^{k-1}) \nabla \mathbf{u}_{tt} \, dt + \int_{t^k}^{t^{k+1}} (t - t^{k+1}) \nabla \mathbf{u}_{tt} \, dt \right|^2 \, d\mathbf{x}$$

$$\leq \frac{1}{2} \int_{\Omega_f} \sum_{k=1}^{N-1} \left\{ \left| \int_{t^{k-1}}^{t^k} (t - t^{k-1}) \nabla \mathbf{u}_{tt} \, dt \right|^2 + \left| \int_{t^k}^{t^{k+1}} (t - t^{k+1}) \nabla \mathbf{u}_{tt} \, dt \right|^2 \right\} \, d\mathbf{x}$$

$$\leq \frac{1}{2} \int_{\Omega_f} \sum_{k=1}^{N-1} \left\{ \int_{t^{k-1}}^{t^k} (t - t^{k-1})^2 \, dt \int_{t^{k-1}}^{t^k} |\nabla \mathbf{u}_{tt}|^2 \, dt + \int_{t^k}^{t^{k+1}} (t - t^{k+1})^2 \, dt \int_{t^k}^{t^{k+1}} |\nabla \mathbf{u}_{tt}|^2 \, dt \right\} \, d\mathbf{x}$$

$$= \frac{(\Delta t)^3}{6} \int_{\Omega_f} \sum_{k=1}^{N-1} \int_{t^{k-1}}^{t^{k+1}} |\nabla \mathbf{u}_{tt}|^2 \, dt \, d\mathbf{x}$$

$$\leq \frac{(\Delta t)^3}{3} \int_{\Omega_f} \int_0^T |\nabla \mathbf{u}_{tt}|^2 \, dt \, d\mathbf{x} \leq \frac{(\Delta t)^3}{3} \|\mathbf{u}_{tt}\|_{L^2(0,T;H^1(\Omega_f))}^2.$$

The bound (6.52) is proved similarly. Finally, for (6.54), we have

$$\sum_{k=1}^{N-1} \|\phi^{k+1} - \phi^{k-1}\|_p^2 = \sum_{k=1}^{N-1} \int_{\Omega_f} \left(\int_{t^{k-1}}^{t^{k+1}} \phi_t \, dt \right)^2 \, d\mathbf{x}$$

$$\leq \int_{\Omega_f} \sum_{k=1}^{N-1} \int_{t^{k-1}}^{t^{k+1}} dt \int_{t^{k-1}}^{t^{k+1}} \phi_t^2 \, dt \, d\mathbf{x}$$

$$= \int_{\Omega_f} \sum_{k=1}^{N-1} 2\Delta t \int_{t^{k-1}}^{t^{k+1}} \phi_t^2 \, dt \, d\mathbf{x}$$

$$\leq 2\Delta t \int_{\Omega_f} 2 \sum_{k=1}^{N} \int_{t^{k-1}}^{t^k} \phi_t^2 \, dt \, d\mathbf{x}$$

$$= 4\Delta t \|\phi_t\|_{L^2(0,T;L^2(\Omega_p))}^2 \leq 4\Delta t \|\phi_t\|_{L^2(0,T;H^1(\Omega_p))}^2.$$

$\square$

APPENDIX B

CODE

B.1 FREEFEM++ CODE FOR CONVERGENCE OF CNLF-STAB (STOKES-DARCY)

```
/*
Solves the Stokes−Darcy problem
1. using the three level Crank−Nicolson LeapFrog (CNLF) method
2. using CNLF with added grad−div stabilization in the Stokes equation and 2nd
    order difference terms in the groundwater flow equation (CNLF−stab).

[To pick CNLF or CNLF−stab replace and (un)comment accordingly:

i. string ster CNLF <−−> CNLFstab
ii. pick method: right after Solve for [u1,u2], p, phi

To pick Test Problem 1 or 2 replace and un(comment) accordingly:

i. string ster TestProb1 <−−> TestProb2
ii. pick test problem: right after true solutions and body forces
]

Includes tests for convergence.

Marina Moraiti, October 2014
*/

// Initialize timer
real startTime = clock();
real initTime, compTime;
real totalTime = 0.0;


string ster = "CNLFstabBetaConvergence_TestProb1_L2erroru"; // CNLF or
    CNLFstab, TestProb1 or TestProb2
```

```
int showplots = 0; // set equal to 1 to show plots

verbosity = 0;

// Directories for saving data
string plotdir   = "plots/";
string datadir   = "data/";
string reportdir = "reports/";

// Create directories
exec("mkdir -p " + plotdir);
exec("mkdir -p " + datadir);
exec("mkdir -p " + reportdir);

real beta = 0.49; // stabilization constant in CNLF-stab
for(int l=0;l<2;l++){
if(l==1){
  beta = 0.51;
}

/*───────────────────────────The Mesh───────────────────────────────*/

for(int N=2;N<65;N=N*2){ // loop over boundary nodes per side
//int N=64;

border D1(t=0.0,1.0){x=t;y=0.0;}; // Darcy's bottom
border D2(t=0.0,1.0){x=1.0;y=t;}; // Darcy's right
border D3(t=0.0,1.0){x=1.0-t;y=1.0;}; // Darcy's top (interface traced <--)
border D4(t=0.0,1.0){x=0.0;y=1.0-t;}; // Darcy's left

border S1(t=0.0,1.0){x=t;y=1.0;}; // Stokes' bottom (interface traced -->)
border S2(t=1.0,2.0){x=1.0;y=t;}; // Stokes' right
border S3(t=0.0,1.0){x=1.0-t;y=2.0;}; // Stokes' top
border S4(t=0.0,1.0){x=0.0;y=2.0-t;}; // Stokes' left

mesh Omegaf=buildmesh(S1(N)+S2(N)+S3(N)+S4(N));
mesh Omegap=buildmesh(D1(N)+D2(N)+D3(N)+D4(N));

if(showplots == 1){
plot(Omegaf,Omegap,wait=1);
}

savemesh(Omegaf,datadir + ster + "_N_" + N + "_Omega_f.msh");
savemesh(Omegap,datadir + ster + "_N_" + N + "_Omega_p.msh");

/*───────────────────────────FEM Spaces─────────────────────────────*/

fespace Xf(Omegaf,P2); //FEM space for Stokes velocity
fespace Qf(Omegaf,P1); //FEM space for Stokes pressure
fespace Xp(Omegap,P2); //FEM space for Darcy pressure (hydraulic head)

/*───────────────Velocity, Pressure, Hydraulic Head─────────────────*/
```

162

```
Xf u1, u2, u1old, u2old, u1old2, u2old2, v1, v2, u1temp, u2temp, u1T, u2T;
Qf p, pold, pold2, q, ptemp, ptempold2, pT;
Xp phi, phiold, phiold2, psi, phitemp, up1, up2, up1temp, up2temp, up1old,
    up1old2, up2old, up2old2, phiT, up1T, up2T, pp, ppT;

/*————————————————————Problem Parameters————————————————————————*/

real pressurepenalty=1.0e−8; // pressure stabilization
real rho = 1.0; // fluid density
real nu = 1.0; // kinematic viscosity of fluid
real g = 1.0; // gravitational acceleration constant
real So = 1.0; // specific storage
real kmin = 1.0; // minimum eigenvalue of the hydraulic conductivity tensor
real alpha = 1.0; // slip coefficient in BJS interface condition
real Cfp = 1.0; // interface inequality constant
real n = 1.0; // volumetric porosity

//for(real So=0.1;So>0.000001;So=So/10.0){ // loop over So values
//for(real kmin=1.0;kmin>0.000001;kmin=kmin/10.0){ // loop over kmin values

/*————————————————————Body Forces————————————————————————*/

//Test Problem 1

func real f1(real t) {return − sin(t)*( x^2 * (y−1.)^2 + y )
                                       − 2. * cos(t) * ( x^2 + (y−1.)
                                         ^2 )
                                       − pi^2 * cos(pi*x) * sin(pi*y
                                         /(2.)) * cos(t) ;}
func real f2(real t) {return − sin(t)*( −2. * x * (y−1.)^3 / (3.) + 2. − pi *
    sin(pi*x) )
                                       − ( pi^3 * sin(pi*x) * cos(t)
                                         + 4. * x * (1.−y) * cos(t)
                                         )
                                       + (2. − pi * sin(pi*x)) * (pi
                                         /(2.)) * cos(pi*y/(2.)) *
                                         cos(t) ;}
func real fp(real t) {return − So * sin(t) * (2. − pi * sin(pi*x)) * (1. − y −
    cos(pi*y) )
                                       − pi^3 * sin(pi*x) * (1. − y −
                                         cos(pi*y)) * cos(t)
                                       − pi^2 * cos(pi*y) * (2. − pi
                                         * sin(pi*x)) * cos(t) ;}


//Test Problem 2
/*
func real f1(real t) {return − rho * ( y − 1. )^2 * sin(t) ;}
func real f2(real t) {return − rho * ( x^2 − x ) * sin(t) ;}
func real fp(real t) {return − So * sin(t) * ( ( n / kmin ) * ( x * ( 1. − x )
    * ( y − 1.              ) + y^3 / 3. − y^2 + y ) + 2. * nu * x / g ) ;}
*/

/*————————————————————True Solution————————————————————————*/
```

163

```
//Test Problem 1

func real u1true(real t) {return ( x^2 * (y-1.)^2 + y ) * cos(t) ;}
func real u2true(real t) {return ( -2. * x * (y-1.)^3 / (3.) + 2. - pi * sin(
    pi*x) ) * cos(t) ;}
func real phitrue(real t) {return ( 2. - pi * sin(pi*x) ) * (1. - y - cos(pi*y
    )) * cos(t) ;}
func real ptrue(real t) {return ( 2. - pi * sin(pi*x) ) * sin(pi*y/(2.)) * cos
    (t) ;}
func real up1true(real t) {return ( pi^2 * cos(pi*x) * (1. - y - cos(pi*y)) *
    cos(t) ) ;}
func real up2true(real t) {return ( (2. - pi * sin(pi*x)) * ( 1. - pi * sin(pi
    *y)) * cos(t) ) ;}


//Test Problem 2
/*
func real u1true(real t) {return ( y^2 - 2. * y + 1. ) * cos(t) ;}
func real u2true(real t) {return ( x^2 - x ) * cos(t) ;}
func real phitrue(real t) {return ( (n / kmin ) * ( x * ( 1. - x ) * ( y - 1.
    ) + y^3 / 3. - y^2 + y ) + 2. * nu * x / g ) * cos(t) ;}
func real ptrue(real t) {return rho * ( 2. * nu * ( x + y - 1. ) + g * n / (
    3. * kmin ) ) * cos(t) ;}
func real up1true(real t) {return - ( ( 1. - 2. * x ) * ( y - 1. ) + 2. * kmin
     * nu / ( n * g )  ) * cos(t) ;}
func real up2true(real t) {return - ( x * ( 1. - x ) + y^2 - 2. * y + 1. ) *
    cos(t) ;}
*/

/*————————————————————Macros————————————————————————*/

macro dot(u1,u2,v1,v2) (u1*v1 + u2*v2) //
macro div(v1,v2) (dx(v1)+dy(v2)) //
macro dotgrad(u1,u2,v1,v2) (dx(u1)*dx(v1) + dy(u1)*dy(v1) + dx(u2)*dx(v2) + dy
    (u2)*dy(v2)) //

/*————————————————————Time Stepping Loop————————————————————————*/

real dt = 1.0/N; // time step size for convergence tests (h=dt)
//real dt = 1.0/10;
int itmax = 1.0/dt; // T = 1 for convergence tests
real T = itmax*dt; // final time T
int itmaxtemp = itmax - 1; // number of CNLF(stab) iterations (3 level method)

real tnminus1 = 0.0; // t_0
real tn = dt; // t_1
real tnplus1 = 2.0*dt; // t_2

/*————Initialize u, p, and phi for 1st CNLF(Stab) iteration————————————*/

u1old2 = u1true(tnminus1);
u1old = u1true(tn);
```

164

```
u2old2 = u2true(tnminus1);
u2old = u2true(tn);

phiold2 = phitrue(tnminus1);
phiold = phitrue(tn);

up1old2 = up1true(tnminus1);
up1old = up1true(tn);

up2old2 = up2true(tnminus1);
up2old = up2true(tn);

pold2 = ptrue(tnminus1);
pold = ptrue(tn);

if(showplots == 1){
        plot([u1old2,u2old2],[up1old2,up2old2],cmm="True_velocity_field_at_t_=
            _:_"+tnminus1,wait=1);
        plot([u1old,u2old],[up1old,up2old],cmm="True_velocity_field_at_t_=_:_"
            +tn,wait=1);
}

/*————Initialize max error norms for u, p and phi (convergence)—————*/

real uLinftyHdiverrorcurr = 0.0;
real uLinftyHdiverror = 0.0;

real uLinftyL2errorcurr = 0.0;
real uLinftyL2error = 0.0;

real pLinftyL2errorcurr = 0.0;
real pLinftyL2error = 0.0;

real phiLinftyL2errorcurr = 0.0;
real phiLinftyL2error = 0.0;

/*———————————————Begin time stepping loop———————————————————*/

for(int i=1;i<itmax;i++){

        // body forces and BC functions for convergence tests:

        func f1 = f1(tn);
        func f2 = f2(tn);
        func fp = fp(tn);

        func U1 = u1true(tnplus1);
        func U2 = u2true(tnplus1);
        func PHI = phitrue(tnplus1);

/*————————————————Stokes CNLF–stab Problem———————————————————*/

problem StokesCNLFstab([u1,u2,p],[v1,v2,q],solver=LU) =
```

```
        int2d(Omegaf)( ( 0.5 / dt ) * ( dot(u1,u2,v1,v2) + div(u1,u2) * div(v1
            ,v2) ) ) + 0.5 * nu * dotgrad(u1,u2,v1,v2)   //level n+1
                - 0.5 * p * div(v1,v2) + q * div(u1,u2) + p * q *
                    pressurepenalty ) //level n+1
    + int1d(Omegaf,S1)( 0.5 * ( alpha / sqrt(kmin) ) * u1 * v1 )
                        //level n+1
    + int1d(Omegaf,S1)( g * phiold * (-1.0) * v2  )
                                //level n (coupling term)
    + int2d(Omegaf)( ( -0.5 / dt) * ( dot(u1old2,u2old2,v1,v2) + div(
        u1old2,u2old2) * div(v1,v2) ) )     //level n-1
    + int2d(Omegaf)( 0.5 * nu * dotgrad(u1old2,u2old2,v1,v2) - 0.5 * pold2
        * div(v1,v2) )//+ 0.5 * pold2 * q * pressurepenalty ) //level n-1
    + int1d(Omegaf,S1)( 0.5 * ( alpha / sqrt(kmin) ) * u1old2 * v1 )
            // level n-1
    - int2d(Omegaf)( dot(f1,f2,v1,v2) )
                                    //RHS Stokes (level n)
    + on(S2,S3,S4, u1 = U1, u2 = U2 );      //Dirichlet BC on exterior
        boundary of Omegaf
```

/*————————————————————————————Stokes CNLF Problem————————————————————————————*/

```
problem StokesCNLF([u1,u2,p],[v1,v2,q],solver=LU) =
        int2d(Omegaf)( ( 0.5 / dt ) * ( dot(u1,u2,v1,v2) ) ) + 0.5 * nu *
            dotgrad(u1,u2,v1,v2)   //level n+1
                - 0.5 * p * div(v1,v2) + q * div(u1,u2) + p * q *
                    pressurepenalty ) //level n+1
    + int1d(Omegaf,S1)( 0.5 * ( alpha / sqrt(kmin) ) * u1 * v1 )
                        //level n+1
    + int1d(Omegaf,S1)( g * phiold * (-1.0) * v2  )
                                //level n (coupling term)
    + int2d(Omegaf)( ( -0.5 / dt) * ( dot(u1old2,u2old2,v1,v2) ) )     //
        level n-1
    + int2d(Omegaf)( 0.5 * nu * dotgrad(u1old2,u2old2,v1,v2) - 0.5 * pold2
        * div(v1,v2) )//+ 0.5 * pold2 * q * pressurepenalty ) //level n-1
    + int1d(Omegaf,S1)( 0.5 * ( alpha / sqrt(kmin) ) * u1old2 * v1 )
            // level n-1
    - int2d(Omegaf)( dot(f1,f2,v1,v2) )
                                    //RHS Stokes (level n)
    + on(S2,S3,S4, u1 = U1, u2 = U2 );      //Dirichlet BC on exterior
        boundary of Omegaf
```

/*————————————————————————Darcy CNLF-stab Problem————————————————————————————*/

```
problem DarcyCNLFstab(phi,psi,solver=LU) =
        int2d(Omegap)( ( 0.5 / dt ) * g * So * phi * psi + 0.5 * g * kmin * (
            dx(phi) * dx(psi) + dy(phi) * dy(psi) )   //level n+1
                + beta * dt * g^2 * (Cfp)^2 * ( dx(phi) * dx(psi) + dy(phi) *
                    dy(psi) + phi * psi ) )
                    //level n+1
    - int1d(Omegap,D3)( g * psi * (-1.0) * u2old )
                //level n (coupling term)
    + int2d(Omegap)( ( - 0.5 / dt ) * g * So * phiold2 * psi + 0.5 * g *
        kmin * ( dx(phiold2) * dx(psi) + dy(phiold2) * dy(psi) )   //level
            n-1
```

```
                    − beta ∗ dt ∗ g^2 ∗ (Cfp)^2 ∗ ( dx(phiold2) ∗ dx(psi) + dy(
                        phiold2) ∗ dy(psi) + phiold2 ∗ psi ) )
                                //level n−1
        − int2d(Omegap)( g ∗ fp ∗ psi )
                                    //RHS Darcy (level n)
        + on(D1,D2,D4, phi = PHI );              //Dircichlet BC on exterior
            boundary of Omegap


/*————————————————Darcy CNLF Problem————————————————————*/

problem DarcyCNLF(phi, psi, solver=LU) =
        int2d(Omegap)( ( 0.5 / dt ) ∗ g ∗ So ∗ phi ∗ psi + 0.5 ∗ g ∗ kmin ∗ (
            dx(phi) ∗ dx(psi) + dy(phi) ∗ dy(psi) ) )
                    //level n+1
        − int1d(Omegap,D3)( g ∗ psi ∗ (−1.0) ∗ u2old )
                    //level n (coupling term)
        + int2d(Omegap)( ( − 0.5 / dt ) ∗ g ∗ So ∗ phiold2 ∗ psi + 0.5 ∗ g ∗
            kmin ∗ ( dx(phiold2) ∗ dx(psi) + dy(phiold2) ∗ dy(psi) ) )
                                //level n−1
        − int2d(Omegap)( g ∗ fp ∗ psi )
                                //RHS Darcy (level n)
        + on(D1,D2,D4, phi = PHI );              //Dircichlet BC on exterior
            boundary of Omegap

initTime = clock();

/*————————————————Solve for [u1,u2], p, phi————————————————*/

        startTime = clock();

        StokesCNLFstab;
        DarcyCNLFstab;

        //StokesCNLF;
        //DarcyCNLF;

        compTime = clock();
        totalTime = totalTime + compTime − startTime;

        cout << "␣Time␣=␣" << compTime − startTime << endl;

        u1temp = u1true(tnplus1);
        u2temp = u2true(tnplus1);
        ptemp = ptrue(tnplus1);
        ptempold2 = ptrue(tnminus1);
        phitemp = phitrue(tnplus1);

        up1 = − kmin ∗ dx(phi) / n;
        up2 = − kmin ∗ dy(phi) / n;

        pp = rho ∗ g ∗ phi;

        up1temp = − kmin ∗ dx(phitemp) / n;
        up2temp = −kmin ∗ dy(phitemp) / n;
```

167

```
        if (showplots == 1){
        plot([u1temp,u2temp],[up1temp,up2temp],cmm="True u and up at t = : "+
            tnplus1,wait=1);
        plot([u1,u2],[up1,up2],cmm="Approximate u and up at t = : "+tnplus1,
            wait=1);
        }

/*————————————Calculation  of  max  error  norms————————————————————*/

uLinftyHdiverrorcurr = ( int2d(Omegaf)( ( u1 − u1temp )^2 + ( u2 − u2temp )^2
    + ( dx(u1) − dx(u1temp) + dy(u2) − dy(u2temp) )^2 ) )^(0.5);
        if (uLinftyHdiverrorcurr > uLinftyHdiverror){
                uLinftyHdiverror = uLinftyHdiverrorcurr;
                }

uLinftyL2errorcurr = ( int2d(Omegaf)( ( u1 − u1temp )^2 + ( u2 − u2temp )^2  )
    )^(0.5);
        if (uLinftyL2errorcurr > uLinftyL2error){
                uLinftyL2error = uLinftyL2errorcurr;
                }

pLinftyL2errorcurr = ( int2d(Omegaf)( ( p − ptemp )^2 ) )^(0.5);
        if (pLinftyL2errorcurr > pLinftyL2error){
                pLinftyL2error = pLinftyL2errorcurr;
                }

phiLinftyL2errorcurr = ( int2d(Omegap)( ( phi − phitemp )^2 ) )^(0.5);
        if (phiLinftyL2errorcurr > phiLinftyL2error){
                phiLinftyL2error = phiLinftyL2errorcurr;
                }

/*————————————————Update  Time  and  Functions————————————————————*/

        u1old2 = u1old;
        u1old = u1;

        u2old2 = u2old;
        u2old = u2;

        phiold2 = phiold;
        phiold = phi;

        pold2 = pold;
        pold = p;

        tnminus1 = tn;
        tn = tnplus1;
        tnplus1 = tnplus1 + dt;

        cout << "Completed iteration " << i << " of " << itmaxtemp << endl;

} // end time stepping loop
```

```
cout << "N_=_" << N << endl;
cout << "dt_=_" << dt << endl;
cout << "iterations_=_" << itmaxtemp << endl;

cout << "LinftyHdiv-error_of_u_=_"<< uLinftyHdiverror << endl;
cout << "LinftyL2-error_of_u_=_"<< uLinftyL2error << endl;
cout << "LinftyL2-error_of_p_=_"<< pLinftyL2error << endl;
cout << "LinftyL2-error_of_phi_=_"<< phiLinftyL2error << endl;

cout << "Total_time_=_" << totalTime << endl;

string prefix = ster + "_N_" + N + "_T_" + tn + "_dt_" + dt + "_So_" + So + "
    _kmin_" + kmin + "_beta_" + beta;

exec("mkdir_-p_" + prefix);
ofstream report(prefix+"/"+prefix+"_report.txt");


report << "_____" + ster + "_____" << endl;
report << "_Boundary_nodes_per_side:_N_=_" << N << endl;
report << "_Step_size:_dt_=_" << dt << endl;
report << "_Iterations_=_" << itmaxtemp << endl;
report << "_Final_time:_T_=_" << tn << endl;
report << "_Pressure_penalty_=_" << pressurepenalty << endl;
report << "_Physical_parameters:_" << endl;
report << "_Fluid_density:_rho_=_" << rho << endl;
report << "_Fluid_kinematic_viscosity:_nu_=_" << nu << endl;
report << "_Gravitational_acceleration:_g_=_" << g << endl;
report << "_Hydraulic_conductivity:_kmin_=_" << kmin << endl;
report << "_Specific_storage:_So_=_" << So << endl;
report << "_Volumetric_porosity:_n_=_" << n << endl;
report << "_Slip_coefficent_in_BJS:_alpha_=_" << alpha << endl;
report << "_Interface_inequality_constant:_Cfp_=_" << Cfp << endl;

report << "_L_infinity_norms:_" << endl;
report << "_LinftyHdiv-error_of_u_=_" << uLinftyHdiverror << endl;
report << "_LinftyL2-error_of_u_=_" << uLinftyL2error << endl;
report << "_LinftyL2-error_of_p_=_" << pLinftyL2error << endl;
report << "_LinftyL2-error_of_phi_=_" << phiLinftyL2error << endl;

report << "_Total_time_in_seconds_=_" << totalTime << endl;

  {
    ofstream file(prefix+"/" + prefix + "_approx_u1.txt");
    file << u1[] << endl;
  }
  {
    ofstream file(prefix+"/" + prefix + "_approx_u2.txt");
    file << u2[] << endl;
  }
  {
    ofstream file(prefix+"/" + prefix + "_approx_p.txt");
    file << p[] << endl;
  }
```

```
  {
    ofstream file(prefix+"/" + prefix + "_approx_phi.txt");
    file << phi[] << endl;
  }

u1T = u1true(tn); // True Stokes x-velocity at final time T
u2T = u2true(tn); // True Stokes y-velocity at final time T
pT = ptrue(tn); // True Stokes pressure at final time T
up1T = up1true(tn); // True Darcy x-velocity at final time T
up2T = up2true(tn); // True Darcy y-velocity at final time T
phiT = phitrue(tn); // True hydraulic head at final time T
ppT = rho * g * phiT; // True Darcy pressure at final time T

plot(Omegaf,Omegap,cmm="Mesh_with_" + N + "_nodes_per_side",ps=prefix+"/"+
    prefix+"_mesh.eps");
plot([u1,u2],[up1,up2],value=1,coef=0.1,cmm="Approximate_velocity_field_at_t="
    +tn,ps=prefix+"/"+prefix+"_ApproxVelocity_T_" + tn + "_N_" + N + "_dt_" +
    dt + "_So_" + So + "_kmin_" + kmin + ".eps");
plot([u1T,u2T],[up1T,up2T],value=1,coef=0.1,cmm="True_velocity_field_at_t="+tn
    ,ps=prefix+"/"+prefix+"_TrueVelocity_T_" + tn + "_N_" + N + "_dt_" + dt +
    "_So_" + So + "_kmin_" + kmin + ".eps");
plot(p,pp,value=1,fill=1,cmm="Contour_of_approximate_pressures_(p_and_p_p)_at_
    t=" + tn,ps=prefix+"/"+prefix+"_ApproxPressures_T_" + tn + "_N_" + N + "
    _dt_" + dt + "_So_" + So + "_kmin_" + kmin + ".eps");
plot(pT,ppT,value=1,fill=1,cmm="Contour_of_true_pressures_(p_and_p_p)_at_t=" +
    tn,ps=prefix+"/"+prefix+"_TruePressures_T_" + tn + "_N_" + N + "_dt_" +
    dt + "_So_" + So + "_kmin_" + kmin + ".eps");
//} // end kmin values loop
//} // end So values loop
} // end N values loop
} // end beta values loop
```

B.2 FREEFEM++ CODE FOR STABILITY OF CNLF-STAB (STOKES-DARCY)

```
/*
Solves the Stokes-Darcy problem
1. using the three level Crank-Nicolson LeapFrog (CNLF) method
2. using CNLF with added grad-div stabilization in the Stokes equation and 2nd
    order difference terms in the groundwater flow equation (CNLF-stab).

[To pick CNLF or CNLF-stab replace and (un)comment accordingly:

i. string ster CNLF <--> CNLFstab
ii. pick method: right after Solve for [u1,u2], p, phi

To pick Test Problem 1 or 2 replace and un(comment) accordingly:

i. string ster TestProb1 <--> TestProb2
ii. pick test problem: right after true solutions and body forces
```

```
]

Includes tests for stability.

Marina Moraiti, November 2014
*/

/*————————Initialize timer—————————*/
real startTime = clock();
real initTime, compTime;
real totalTime = 0.0;

string ster = "CNLFstabStability_TestProb2_"; // CNLF or CNLFstab, TestProb1
    or TestProb2

verbosity = 0;

real beta =1.0;


/*————————————————The Mesh————————————————————*/

//for(int N=2;N<65;N=N*2){ // loop over boundary nodes per side
int N=16;

border D1(t=0.0,1.0){x=t;y=0.0;}; // Darcy's bottom
border D2(t=0.0,1.0){x=1.0;y=t;}; // Darcy's right
border D3(t=0.0,1.0){x=1.0-t;y=1.0;}; // Darcy's top (interface traced <--)
border D4(t=0.0,1.0){x=0.0;y=1.0-t;}; // Darcy's left

border S1(t=0.0,1.0){x=t;y=1.0;}; // Stokes' bottom (interface traced -->)
border S2(t=1.0,2.0){x=1.0;y=t;}; // Stokes' right
border S3(t=0.0,1.0){x=1.0-t;y=2.0;}; // Stokes' top
border S4(t=0.0,1.0){x=0.0;y=2.0-t;}; // Stokes' left

mesh Omegaf=buildmesh(S1(N)+S2(N)+S3(N)+S4(N));
mesh Omegap=buildmesh(D1(N)+D2(N)+D3(N)+D4(N));

/*————————————FEM Spaces————————————————————*/

fespace Xf(Omegaf,P2); //FEM space for Stokes velocity
fespace Qf(Omegaf,P1); //FEM space for Stokes pressure
fespace Xp(Omegap,P2); //FEM space for Darcy pressure (hydraulic head)

/*————————Velocity, Pressure, Hydraulic Head————————————————*/

Xf u1, u2, u1old, u2old, u1old2, u2old2, v1, v2, u1temp, u2temp, gradxp,
    gradyp, gradxptemp, gradyptemp, u1T, u2T;
Qf p, pold, pold2, q, ptemp, ptempold2, pT;
Xp phi, phiold, phiold2, psi, phitemp, up1, up2, up1temp, up2temp, up1old,
    up1old2, up2old, up2old2, phiT, up1T, up2T, pp, ppT;

/*————————————Problem Parameters————————————————————*/
```

```
real pressurepenalty=1.0e-8; // pressure stabilization
real rho = 1.0; // fluid density
real nu = 1.0; // kinematic viscosity of fluid
real g = 1.0; // gravitational acceleration constant
real So = 0.01; // specific storage
real kmin = 1.0; // minimum eigenvalue of the hydraulic conductivity tensor
real alpha = 1.0; // slip coefficient in BJS interface condition
real Cfp = 1.0; // interface inequality constant
real n = 1.0; // volumetric porosity

//for(real So=0.1;So>0.000001;So=So/10.0){ // loop over So values
//for(real kmin=1.0;kmin>0.000001;kmin=kmin/10.0){ // loop over kmin values

/*————————————————————Body Forces————————————————————————*/

//Test Problem 1
/*
func real f1(real t) {return - sin(t)*( x^2 * (y-1.)^2 + y )
                                      - 2. * cos(t) * ( x^2 + (y-1.)
                                        ^2 )
                                      - pi^2 * cos(pi*x) * sin(pi*y
                                        /(2.)) * cos(t) ;}
func real f2(real t) {return - sin(t)*( -2. * x * (y-1.)^3 / (3.) + 2. - pi *
    sin(pi*x) )
                                      - ( pi^3 * sin(pi*x) * cos(t)
                                        + 4. * x * (1.-y) * cos(t)
                                        )
                                      + (2. - pi * sin(pi*x)) * (pi
                                        /(2.)) * cos(pi*y/(2.)) *
                                        cos(t) ;}
func real fp(real t) {return - So * sin(t) * (2. - pi * sin(pi*x)) * (1. - y -
    cos(pi*y) )
                                      - pi^3 * sin(pi*x) * (1. - y -
                                        cos(pi*y)) * cos(t)
                                      - pi^2 * cos(pi*y) * (2. - pi
                                        * sin(pi*x)) * cos(t) ;}
*/

//Test Problem 2

func real f1(real t) {return - rho * ( y - 1. )^2 * sin(t) ;}
func real f2(real t) {return - rho * ( x^2 - x ) * sin(t) ;}
func real fp(real t) {return - So * sin(t) * ( ( n / kmin ) * ( x * ( 1. - x )
    * ( y - 1.                  ) + y^3 / 3. - y^2 + y ) + 2. * nu * x / g ) ;}


/*————————————————————True Solutions————————————————————————*/

//Test Problem 1
/*
func real u1true(real t) {return ( x^2 * (y-1.)^2 + y ) * cos(t) ;}
func real u2true(real t) {return ( -2. * x * (y-1.)^3 / (3.) + 2. - pi * sin(
    pi*x) ) * cos(t) ;}
```

172

```
func real phitrue(real t) {return ( 2. - pi * sin(pi*x) ) * (1. - y - cos(pi*y
    )) * cos(t) ;}
func real ptrue(real t) {return ( 2. - pi * sin(pi*x) ) * sin(pi*y/(2.)) * cos
    (t) ;}
func real up1true(real t) {return ( pi^2 * cos(pi*x) * (1. - y - cos(pi*y)) *
    cos(t) ) ;}
func real up2true(real t) {return ( (2. - pi * sin(pi*x)) * ( 1. - pi * sin(pi
    *y)) * cos(t) ) ;}
*/


//Test Problem 2

func real u1true(real t) {return ( y^2 - 2. * y + 1. ) * cos(t) ;}
func real u2true(real t) {return ( x^2 - x ) * cos(t) ;}
func real phitrue(real t) {return ( (n / kmin ) * ( x * ( 1. - x ) * ( y - 1.
    ) + y^3 / 3. - y^2 + y ) + 2. * nu * x / g ) * cos(t) ;}
func real ptrue(real t) {return rho * ( 2. * nu * ( x + y - 1. ) + g * n / (
    3. * kmin ) ) * cos(t) ;}
func real up1true(real t) {return - ( ( 1. - 2. * x ) * ( y - 1. ) + 2. * kmin
     * nu / ( n * g ) ) * cos(t) ;}
func real up2true(real t) {return - ( x * ( 1. - x ) + y^2 - 2. * y + 1. ) *
    cos(t) ;}


/*————————————————————————Macros————————————————————————*/

macro dot(u1,u2,v1,v2) (u1*v1 + u2*v2) //
macro div(v1,v2) (dx(v1)+dy(v2)) //
macro dotgrad(u1,u2,v1,v2) (dx(u1)*dx(v1) + dy(u1)*dy(v1) + dx(u2)*dx(v2) + dy
    (u2)*dy(v2)) //

/*————————————————————Time Stepping Loop————————————————————*/

//real dt = 1.0/N; // time step size for convergence tests (h=dt)
real dt = 1.0/16; //
int itmax = 20.0/dt; //
real T = itmax*dt; // final time T
int itmaxtemp = itmax - 1; // number of CNLF(stab) iterations (3 level method)

real tnminus1 = 0.0; // t_0
real tn = dt; // t_1
real tnplus1 = 2.0*dt; // t_2


/*————————Initialize u, p, and phi for 1st CNLF(stab) iteration————————*/

u1old2 = u1true(tnminus1);
u1old = u1true(tn);

u2old2 = u2true(tnminus1);
u2old = u2true(tn);

phiold2 = phitrue(tnminus1);
phiold = phitrue(tn);
```

```
up1old2 = up1true(tnminus1);
up1old = up1true(tn);

up2old2 = up2true(tnminus1);
up2old = up2true(tn);

pold2 = ptrue(tnminus1);
pold = ptrue(tn);


/*————————————————————Energy and Modes————————————————————*/

real Energyzeroplusone =  int2d(Omegaf)( (u1old2)^2 + (u2old2)^2 + (u1old)^2 +
    (u2old)^2) + g * So * int2d(Omegap)( (phiold2)^2 + (phiold)^2);

real [int] Energy(itmax);
real [int] uUnstable(itmax);   // unstable mode of u
real [int] uStable(itmax);   // stable mode of u
real [int] phiUnstable(itmax);   // unstable mode of phi
real [int] phiStable(itmax);   // stable mode of phi
real [int] UnstableMode(itmax);
real [int] StableMode(itmax);

Energy[0] = int2d(Omegaf)( (u1old2)^2 + (u2old2)^2 + (u1old)^2 + (u2old)^2) +
    g * So * int2d(Omegap)( (phiold2)^2 + (phiold)^2);


/*————————————————Begin time stepping loop————————————————*/

for(int i=1;i<itmax;i++){

        // body forces and BC functions for stability tests:

        func f1 = 0.0;
        func f2 = 0.0;
        func fp = 0.0;

        func U1 = 0.0;
        func U2 = 0.0;
        func PHI = 0.0;

/*————————————————Stokes CNLF–stab Problem————————————————*/

problem StokesCNLFstab([u1,u2,p],[v1,v2,q],solver=LU) =
        int2d(Omegaf)( ( 0.5 / dt ) * ( dot(u1,u2,v1,v2) + div(u1,u2) * div(v1
            ,v2) ) + 0.5 * nu * dotgrad(u1,u2,v1,v2)   //level n+1
                - 0.5 * p * div(v1,v2) + q * div(u1,u2) + p * q *
                    pressurepenalty ) //level n+1
        + int1d(Omegaf,S1)( 0.5 * ( alpha / sqrt(kmin) ) * u1 * v1 )
                        //level n+1
        + int1d(Omegaf,S1)( g * phiold * (−1.0) * v2  )
                            //level n (coupling term)
```

174

```
        + int2d(Omegaf)( ( -0.5 / dt) * ( dot(u1old2,u2old2,v1,v2) + div(
            u1old2,u2old2) * div(v1,v2) ) )      //level n-1
        + int2d(Omegaf)( 0.5 * nu * dotgrad(u1old2,u2old2,v1,v2) - 0.5 * pold2
            * div(v1,v2) )//+ 0.5 * pold2 * q * pressurepenalty ) //level n-1
        + int1d(Omegaf,S1)( 0.5 * ( alpha / sqrt(kmin) ) * u1old2 * v1 )
                    // level n-1
        - int2d(Omegaf)( dot(f1,f2,v1,v2) )
                                            //RHS Stokes (level n)
        + on(S2,S3,S4, u1 = U1, u2 = U2 );       //Dirichlet BC on exterior
            boundary of Omegaf


/*————————————————Stokes CNLF Problem————————————————*/

problem StokesCNLF([u1,u2,p],[v1,v2,q],solver=LU) =
        int2d(Omegaf)( ( 0.5 / dt ) * ( dot(u1,u2,v1,v2) ) + 0.5 * nu *
            dotgrad(u1,u2,v1,v2)   //level n+1
                - 0.5 * p * div(v1,v2) + q * div(u1,u2) + p * q *
                    pressurepenalty ) //level n+1
        + int1d(Omegaf,S1)( 0.5 * ( alpha / sqrt(kmin) ) * u1 * v1 )
                    //level n+1
        + int1d(Omegaf,S1)( g * phiold * (-1.0) * v2  )
                                    //level n (coupling term)
        + int2d(Omegaf)( ( -0.5 / dt) * ( dot(u1old2,u2old2,v1,v2) ) )     //
            level n-1
        + int2d(Omegaf)( 0.5 * nu * dotgrad(u1old2,u2old2,v1,v2) - 0.5 * pold2
            * div(v1,v2) )//+ 0.5 * pold2 * q * pressurepenalty ) //level n-1
        + int1d(Omegaf,S1)( 0.5 * ( alpha / sqrt(kmin) ) * u1old2 * v1 )
                    // level n-1
        - int2d(Omegaf)( dot(f1,f2,v1,v2) )
                                            //RHS Stokes (level n)
        + on(S2,S3,S4, u1 = U1, u2 = U2 );       //Dirichlet BC on exterior
            boundary of Omegaf


/*————————————————Darcy CNLF-stab Problem————————————————*/

problem DarcyCNLFstab(phi,psi,solver=LU) =
        int2d(Omegap)( ( 0.5 / dt ) * g * So * phi * psi + 0.5 * g * kmin * (
            dx(phi) * dx(psi) + dy(phi) * dy(psi) )    //level n+1
                + beta * dt * g^2 * (Cfp)^2 * ( dx(phi) * dx(psi) + dy(phi) *
                    dy(psi) + phi * psi ) )
                    //level n+1
        - int1d(Omegap,D3)( g * psi * (-1.0) * u2old )
                    //level n (coupling term)
        + int2d(Omegap)( ( - 0.5 / dt ) * g * So * phiold2 * psi + 0.5 * g *
            kmin * ( dx(phiold2) * dx(psi) + dy(phiold2) * dy(psi) )    //level
            n-1
                - beta * dt * g^2 * (Cfp)^2 * ( dx(phiold2) * dx(psi) + dy(
                    phiold2) * dy(psi) + phiold2 * psi ) )
                        //level n-1
        - int2d(Omegap)( g * fp * psi )
                                    //RHS Darcy (level n)
        + on(D1,D2,D4, phi = PHI );                //Dircichlet BC on exterior
            boundary of Omegap
```

```
/*————————————————Darcy CNLF Problem————————————————————————*/

problem DarcyCNLF(phi,psi,solver=LU) =
        int2d(Omegap)( ( 0.5 / dt ) * g * So * phi * psi + 0.5 * g * kmin * (
            dx(phi) * dx(psi) + dy(phi) * dy(psi) ) )
                    //level n+1
        − int1d(Omegap,D3)( g * psi * (−1.0) * u2old )
                    //level n (coupling term)
        + int2d(Omegap)( ( − 0.5 / dt ) * g * So * phiold2 * psi + 0.5 * g *
            kmin * ( dx(phiold2) * dx(psi) + dy(phiold2) * dy(psi) ) )
                            //level n−1
        − int2d(Omegap)( g * fp * psi )
                            //RHS Darcy (level n)
        + on(D1,D2,D4, phi = PHI );           //Dircichlet BC on exterior
            boundary of Omegap


initTime = clock();

/*————————————————Solve for [u1,u2], p, phi————————————————————*/

        startTime = clock();

        StokesCNLFstab;
        DarcyCNLFstab;

        //StokesCNLF;
        //DarcyCNLF;

        compTime = clock();
        totalTime = totalTime + compTime − startTime;

        cout << " Time = " << compTime − startTime << endl;

/*————————————Calculate Energy, Stable, Unstable Modes————————————————*/

        Energy[i] = int2d(Omegaf)((u1)^2 + (u2)^2)+ g * So * int2d(Omegap)((
            phi)^2) +                           int2d(Omegaf)((u1old)^2 + (u2old)^2) +
            g * So * int2d(Omegap)((phiold)^2);
        uUnstable[i] = (1./2) * int2d(Omegaf)( (u1 − u1old2)^2 + (u2 − u2old2)
            ^2 );
        uStable[i] = (1./2) * int2d(Omegaf)( (u1 + u1old2)^2 + (u2 + u2old2)^2
            );
        phiUnstable[i] = (1./2) * int2d(Omegap)( (phi − phiold2)^2 );
        phiStable[i]= (1./2) * int2d(Omegap)( (phi + phiold2)^2 );
        UnstableMode[i] = uUnstable[i] + phiUnstable[i]; // Unstable Mode
        StableMode[i] = uStable[i] + phiStable[i]; // Stable Mode

        u1temp = u1true(tnplus1);
        u2temp = u2true(tnplus1);
        ptemp = ptrue(tnplus1);
        ptempold2 = ptrue(tnminus1);
        phitemp = phitrue(tnplus1);

/*————————————————Update Time and Functions————————————————————*/
```

```
            u1old2 = u1old;
            u1old = u1;

            u2old2 = u2old;
            u2old = u2;

            phiold2 = phiold;
            phiold = phi;

            pold2 = pold;
            pold = p;

            tnminus1 = tn;
            tn = tnplus1;
            tnplus1 = tnplus1 + dt;

            cout << "Completed iteration " << i << " of " << itmaxtemp << endl;

    } //end time stepping loop

    cout << "N = " << N << endl;
    cout << "dt = " << dt << endl;
    cout << "iterations = " << itmaxtemp << endl;

    cout << "Total time = " << totalTime << endl;

    string prefix = ster + " N " + N + " T " + tn + " dt " + dt + " So " + So + "
        kmin " + kmin;
    exec("mkdir -p " + prefix);
    ofstream report(prefix+"/"+prefix+" report.txt");

    report << "——————————" + ster + "——————————————————" <<
        endl;
    report << " Boundary nodes per side: N = " << N << endl;
    report << " Step size: dt = " << dt << endl;
    report << " Iterations = " << itmaxtemp << endl;
    report << " Final time: T = " << tn << endl;
    report << " Pressure penalty = " << pressurepenalty << endl;
    report << " Physical parameters: " << endl;
    report << " Fluid density: rho = " << rho << endl;
    report << " Fluid kinematic viscosity: nu = " << nu << endl;
    report << " Gravitational acceleration: g = " << g << endl;
    report << " Hydraulic conductivity: kmin = " << kmin << endl;
    report << " Specific storage: So = " << So << endl;
    report << " Volumetric porosity: n = " << n << endl;
    report << " Slip coefficent in BJS: alpha = " << alpha << endl;
    report << " Interface inequality constant: Cfp = " << Cfp << endl;

    report << " Total time in seconds = " << totalTime << endl;
    report << "E^1 + E^0 =" << Energyzeroplusone << endl;

      {
        ofstream file(prefix+"/" + prefix + " Energy.txt");
```

```
    file << Energy << endl;
  }
  {
    ofstream file(prefix+"/" + prefix + "_uUnstableMode.txt");
    file << uUnstable << endl;
  }
  {
    ofstream file(prefix+"/" + prefix + "_uStableMode.txt");
    file << uStable << endl;
  }
  {
    ofstream file(prefix+"/" + prefix + "_phiUnstableMode.txt");
    file << phiUnstable << endl;
  }
  {
    ofstream file(prefix+"/" + prefix + "_phiStableMode.txt");
    file << phiStable << endl;
  }
  {
    ofstream file(prefix+"/" + prefix + "_UnstableMode.txt");
    file << UnstableMode << endl;
  }
  {
    ofstream file(prefix+"/" + prefix + "_StableMode.txt");
    file << StableMode << endl;
  }

//} // end kmin values loop
//} // end So values loop
//} // end N values loop
```

B.3 FREEFEM++ CODE FOR BACKWARD EULER (STOKES-DARCY)

```
/*
Solves the evolutionary Stokes−Darcy problem with the Backward Euler method.

Marina Moraiti, October 2014
*/

verbosity=0;

/*————————————————Initialize timer————————————————————*/
real startTime = clock();
real initTime, compTime;
real totalTime = 0.0;


for(int N=16;N<129;N=N*2){

/*————————————————————The Mesh————————————————————————*/

border D1(t=0.0,1.0){x=t;y=0.0;}; // Darcy's bottom
```

```
border D2( t =0.0 ,1.0){ x=1.0;y=t ;};  // Darcy's right
border D4( t =0.0 ,1.0){ x=0.0;y=1.0−t ;};  // Darcy's left

border S2( t =1.0 ,2.0){ x=1.0;y=t ;};  // Stokes' right
border S3( t =0.0 ,1.0){ x=1.0−t ;y=2.0;};  // Stokes' top
border S4( t =0.0 ,1.0){ x=0.0;y=2.0−t ;};  // Stokes' left

border I1 ( t =0.0 ,1.0){ x=t ;y=1.0;};  // Stokes' bottom (** interface **)

mesh Omega =  buildmesh ( S2 (N)+S3 (N)+S4 (N)+D4(N)+D1(N)+D2(N)+I1 (N) ) ;

/*————————————————FE Spaces————————————————*/

fespace Xh(Omega,P2);  // FEM space for Stokes velocity and Darcy pressure
fespace Qh(Omega,P1);  // FEM space for Stokes pressure

fespace Ch(Omega,P0);  // space for characteristic function

/*———————————Characteristic Function————————————————*/

Ch reg=region ;

int nupper = reg (0.5 ,1.5);  // can be replaced by any point in Stokes region

Ch chi = (region==nupper);  // chi = 1.0 when x in Stokes region and chi = 0.0
    when x in Darcy region

/*———————————Velocity , Pressure , Hydraulic Head————————————*/

Xh u1 , u2 , u1old , u2old , v1 , v2 , phi , phiold , psi , up1 , up2 , up1old , up2old ,
    u1temp , u2temp , phitemp , up1temp , up2temp ;
Qh p , pold , q , ptemp ;

/*———————————Problem Parameters————————————————*/

real pressurepenalty =1.0e −8;
real rho = 1.0;  // fluid density
real nu = 1.0;  // kinematic viscosity of fluid
real g = 1.0;  // gravitational acceleration constant
real So = 1.0;  // specific storage
real kmin = 1.0;  // minimum eigenvalue of hydraulic conductivity tensor
real alpha = 1.0;  // slip coefficient in BJS interface condition
real Cfp = 1.0;  // interface inequality constant
real n = 1.0;  // porosity

/*———————————True Solution————————————————*/

func real u1true(real t) {return ( y^2 − 2. ∗ y + 1. ) ∗ cos(t) ;}
func real u2true(real t) {return x ∗ ( x − 1. ) ∗ cos(t) ;}
func real phitrue(real t) {return ( ( n / kmin ) ∗ ( x ∗ ( 1. − x ) ∗ ( y − 1.
    ) + y^3 / (3.) − y^2 + y ) + 2. ∗ nu ∗ x / g ) ∗ cos(t) ;}
func real ptrue(real t) {return ( 2. ∗ nu  ∗ ( x + y − 1. ) + g ∗ n / ( 3. ∗
    kmin ) ) ∗ cos(t) ;}
```

179

```
func real up1true(real t) {return − ( ( 1. − 2. ∗ x ) ∗ ( y − 1. ) + 2 ∗ kmin
    ∗ nu / ( n ∗ g ) ) ∗ cos(t) ;}
func real up2true(real t) {return − ( x − x^2 + y^2 − 2. ∗ y + 1. ) ∗ cos(t)
    ;}

/*————————————————————Body Forces————————————————————*/

func real f1(real t) {return − ( y^2 − 2. ∗ y + 1. ) ∗ sin(t) ;}
func real f2(real t) {return − ( x^2 − x ) ∗ sin(t) ;}
func real fp(real t) {return So ∗ ( − 1. ) ∗ ( ( n / kmin ) ∗ ( x ∗ ( 1. − x )
    ∗ ( y − 1. ) + y^3 / (3.) − y^2 + y ) + 2. ∗ nu ∗ x / g ) ∗ sin(t) ;}

/*————————————————————Macros————————————————————*/

macro dot(u1,u2,v1,v2) (u1∗v1 + u2∗v2) //
macro div(v1,v2) (dx(v1)+dy(v2)) //
macro dotgrad(u1,u2,v1,v2) (dx(u1)∗dx(v1) + dy(u1)∗dy(v1) + dx(u2)∗dx(v2) + dy
    (u2)∗dy(v2)) //

/*————————————————————Time Stepping Loop————————————————————*/

real dt = 1.0/N; // time step size for convergence tests (h=dt)

int itmax = 1.0/dt; // Iterations (Final Time = 1)
real T = itmax∗dt; // Final Time T (T=1)

string ster = "SD_BE_TestProb2_Efficiency";

// Report for convergence tests (uncomment for convergence tests):

ofstream report(ster + "_N_" + N + "_T_" + T + "_dt_" + dt + "_So_" + So + "
    _kmin_" + kmin + ".txt");

report << "————BE_convergence_report,_Marina_Moraiti————" << endl;
report << "_Boundary_nodes_per_side:_N_=_" << N << endl;
report << "_Step_Size:_dt_=_" << dt << endl;
report << "_BE_Iterations_=_" << itmax << endl;
report << "_Final_Time:_T_=_" << T << endl;
report << "_Pressure_Penalty_=_" << pressurepenalty << endl;

real tn = 0.0; // t_0
real tnplus1 = dt; // t_1

/*————————Initialize u, p, and phi for 1st iteration————————————*/

u1old = u1true(tn);
u2old = u2true(tn);

pold = ptrue(tn);

phiold = phitrue(tn);

/*————————————Initialize max error norms for u, p and phi————————————*/
```

```
real uLinftyL2errorcurr = 0.0;
real uLinftyL2error = 0.0;

real pLinftyL2errorcurr = 0.0;
real pLinftyL2error = 0.0;

real phiLinftyL2errorcurr = 0.0;
real phiLinftyL2error = 0.0;

/*————————————————Begin time stepping loop————————————————————*/

for(int i=1;i<itmax;i++){

/*————————————————Body forces and BC————————————————————————*/

        func f1 = f1(tnplus1);
        func f2 = f2(tnplus1);
        func fp = fp(tnplus1);

        func U1 = u1true(tnplus1);
        func U2 = u2true(tnplus1);
        func PHI = phitrue(tnplus1);

/*————————————————BE Stokes−Darcy problem————————————————————*/

problem StokesDarcyBE([u1,u2,p,phi],[v1,v2,q,psi],solver=GMRES,eps=1.0e−8,
    nbiter=40000) =
        int2d(Omega)( chi * ( 1. / dt ) * ( u1 * v1 + u2 * v2 ) + chi * nu *
            dotgrad(u1,u2,v1,v2) ) // terms 1 and 3
        + int1d(Omega,I1)( ( alpha / sqrt(kmin) ) * u1 * v1 ) // term 4
        − int2d(Omega)( chi * ( 1. / rho ) * p * div(v1,v2) ) // term 5
        + int1d(Omega,I1)( g * phi * ( −1. ) * v2 ) // term 6
        + int2d(Omega)( chi * q * div(u1,u2) ) // term 8
        − int2d(Omega)( chi * ( 1. / dt ) * ( u1old * v1 + u2old * v2 ) ) //
            term 2
        − int2d(Omega)( chi * p * q * pressurepenalty ) // pressure penalty
            term
        − int2d(Omega)( chi * ( 1. / rho ) * ( f1 * v1 + f2 * v2 ) ) // term 7
        + int2d(Omega)( ( 1. − chi ) * g * So * ( 1. / dt ) * phi * psi  + (
            1. − chi ) * g * kmin * ( dx(phi) * dx(psi) + dy(phi) * dy(psi) )
            ) // terms 9 & 11
        − int1d(Omega,I1)( g * psi * ( −1. ) * u2 ) // term 12
        − int2d(Omega)( ( 1. − chi ) * g * So * ( 1. / dt ) * phiold * psi )
            // term 10
        − int2d(Omega)( ( 1. − chi) * fp * psi ) // term 13
        + on(S2,S3,S4,u1=U1,u2=U2)
        + on(D1,D2,D4,phi=PHI);

/*————————————————Solve for [u1,u2], p, phi————————————————————*/

        initTime = clock();

        startTime = clock();
```

```
        StokesDarcyBE;

        compTime = clock();
        totalTime = totalTime + compTime - startTime;

        cout << " Time = " << compTime - startTime << endl;
        report << " Time = " << compTime - startTime << endl;

        u1temp = u1true(tnplus1);
        u2temp = u2true(tnplus1);
        ptemp = ptrue(tnplus1);
        phitemp = phitrue(tnplus1);


/*————————————————Calculation of max error————————————————*/


uLinftyL2errorcurr = ( int2d(Omega)( ( chi * u1 - chi * u1temp )^2 + ( chi *
    u2 - chi * u2temp )^2  ) )^(0.5);
        if (uLinftyL2errorcurr > uLinftyL2error){
                uLinftyL2error = uLinftyL2errorcurr;
                }

pLinftyL2errorcurr = ( int2d(Omega)( ( chi * p - chi * ptemp )^2 ) )^(0.5);
        if (pLinftyL2errorcurr > pLinftyL2error){
                pLinftyL2error = pLinftyL2errorcurr;
                }

phiLinftyL2errorcurr = ( int2d(Omega)( ( ( 1. - chi ) * phi - ( 1. - chi ) *
    phitemp )^2 ) )^(0.5);
        if (phiLinftyL2errorcurr > phiLinftyL2error){
                phiLinftyL2error = phiLinftyL2errorcurr;
                }

/*————————————————Update Time and Functions————————————————*/

        u1old = u1;
        u2old = u2;
        phiold = phi;
        pold = p;

        tn = tnplus1;
        tnplus1 = tnplus1 + dt;

        cout << "Completed iteration " << i << " of " << itmax << endl;


} // end time stepping loop

cout << "N = " << N << endl;
cout << "dt = " << dt << endl;
cout << "iterations = " << itmax << endl;
cout << "LinftyL2-error of u = "<< uLinftyL2error << endl;
cout << "LinftyL2-error of p = "<< pLinftyL2error << endl;
```

```
cout << "LinftyL2−error_of_phi_=_"<< phiLinftyL2error << endl;
cout << "Total_time_=_" << totalTime << endl;

report << "_LinftyL2−error_of_u_=_" << uLinftyL2error << endl;
report << "_LinftyL2−error_of_p_=_" << pLinftyL2error << endl;
report << "_LinftyL2−error_of_phi_=_" << phiLinftyL2error << endl;
report << "_Total_time_in_seconds_=_" << totalTime << endl;

} // end loop over N
```

B.4 FREEFEM++ CODE FOR CONVERGENCE TO QUASISTATIC STOKES-DARCY SOLUTION

```
/*
Solves the evolutionary Stokes−Darcy (SD) and quasistatic Stokes−Darcy (qsSD)
    problems for varying So to check the rate of convergence of the SD
    solution to the qsSD solution as So converges to 0.

Discretization in time: stabilized Crank−Nicolson Leapfrog (CNLF−stab)

Marina Moraiti, October 2014
*/

verbosity=0;

/*―――――――――――――――――Mesh―――――――――――――――――*/

int N=32;

border D1(t=0.0,1.0){x=t;y=0.0;}; // Darcy's bottom
border D2(t=0.0,1.0){x=1.0;y=t;}; // Darcy's right
border D3(t=0.0,1.0){x=1.0−t;y=1.0;}; // Darcy's top (interface traced <−−)
border D4(t=0.0,1.0){x=0.0;y=1.0−t;}; // Darcy's left

border S1(t=0.0,1.0){x=t;y=1.0;}; // Stokes' bottom (interface traced −−>)
border S2(t=1.0,2.0){x=1.0;y=t;}; // Stokes' right
border S3(t=0.0,1.0){x=1.0−t;y=2.0;}; // Stokes' top
border S4(t=0.0,1.0){x=0.0;y=2.0−t;}; // Stokes' left

mesh Omegaf=buildmesh(S1(N)+S2(N)+S3(N)+S4(N));
mesh Omegap=buildmesh(D1(N)+D2(N)+D3(N)+D4(N));

/*―――――――――――――FE Spaces―――――――――――――*/

fespace Xf(Omegaf,P2); // FE space for Stokes velocity
fespace Qf(Omegaf,P1); // FE space for Stokes pressure
fespace Xp(Omegap,P2); // FE space for Darcy pressure

/*―――――Velocity, Pressure, Hydraulic Head―――――*/
```

```freefem
Xf u1, u2, u1old, u2old, u1old2, u2old2, v1, v2, u1QS, u2QS, u1QSold, u2QSold,
    u1QSold2, u2QSold2;
Qf p, pold, pold2, q, pQS, pQSold, pQSold2;
Xp phi, phiold, phiold2, psi, phiQS, phiQSold, phiQSold2;

/*————————————————Problem Parameters————————————————————————*/

real pressurepenalty=1.0e−8; // pressure stabilization

// all physical parameters equal to 1 (except for So, kmin)

real rho = 1.0; // density of fluid
real nu = 1.0; // kinematic viscosity of fluid
real g = 1.0; // gravitational acceleration constant
real kmin = 0.0001; // minimum eigenvalue of the hydraulic conductivity tensor
real alpha = 1.0; // slip coefficient in BJS interface condition
real Cfp = 1.0; // interface inequality constant
real n = 1.0; // volumetric porosity

for(real So=0.01;So>0.000078124;So=0.5*So){ // loop over So values

/*————————————————————Body Forces————————————————————————*/

// Test Problem 1

/*
func real f1(real t) {return − sin(t)*( x^2 * (y−1.)^2 + y ) − 2. * cos(t) * (
    x^2 + (y−1.)^2 ) − pi^2 * cos(pi*x) * sin(pi*y/(2.)) * cos(t) ;}
func real f2(real t) {return − sin(t)*( −2. * x * (y−1.)^3 / (3.) + 2. − pi *
    sin(pi*x) ) − ( pi^3 * sin(pi*x) * cos(t) + 4. * x * (1.−y) * cos(t) ) +
    (2. − pi * sin(pi*x)) * (pi/(2.)) * cos(pi*y/(2.)) * cos(t) ;}
func real fpQS(real t) {return − pi^3 * sin(pi*x) * ( 1. − y − cos(pi*y) ) *
    cos(t) − pi^2 * cos(pi*y) * ( 2. − pi * sin(pi*x) ) * cos(t) ;}
func real fp(real t) {return − So * sin(t) * ( 2. − pi * sin(pi*x) ) * ( 1. −
    y − cos(pi*y) ) − pi^3 * sin(pi*x) * ( 1. − y − cos(pi*y) ) * cos(t) − pi
    ^2 * cos(pi*y) * ( 2. − pi * sin(pi*x) ) * cos(t) ;}
*/

// Test Problem 2

func real f1(real t) {return − rho * ( y − 1. )^2 * sin(t) ;}
func real f2(real t) {return − rho * ( x^2 − x ) * sin(t) ;}
func real fpQS(real t) {return 0.0 ;}
func real fp(real t) {return − So * sin(t) * ( ( n / kmin ) * ( x * ( 1. − x )
    * ( y − 1.) + y^3 / 3. − y^2 + y ) + 2. * nu * x / g ) ;}

/*————————————————————True Solutions————————————————————————*/

// Test Problem 1

/*
func real u1true(real t) {return ( x^2 * (y−1.)^2 + y ) * cos(t) ;}
func real u2true(real t) {return ( −2. * x * (y−1.)^3 / (3.) + 2. − pi * sin(
    pi*x) ) * cos(t) ;}
```

```
func real phitrue(real t) {return ( 2. − pi * sin(pi*x) ) * (1. − y − cos(pi*y
    )) * cos(t) ;}
func real ptrue(real t) {return ( 2. − pi * sin(pi*x) ) * sin(pi*y/(2.)) * cos
    (t) ;}
func real up1true(real t) {return ( pi^2 * cos(pi*x) * (1. − y − cos(pi*y)) )
    * cos(t) ;}
func real up2true(real t) {return ( (2. − pi * sin(pi*x)) * ( 1. − pi * sin(pi
    *y)) * cos(t) ) ;}
*/

// Test Problem 2

func real u1true(real t) {return ( y^2 − 2. * y + 1. ) * cos(t) ;}
func real u2true(real t) {return ( x^2 − x ) * cos(t) ;}
func real phitrue(real t) {return ( (n / kmin ) * ( x * ( 1. − x ) * ( y − 1.
    ) + y^3 / 3. − y^2 + y ) + 2. * nu * x / g ) * cos(t) ;}
func real ptrue(real t) {return rho * ( 2. * nu * ( x + y − 1. ) + g * n / (
    3. * kmin ) ) * cos(t) ;}
func real up1true(real t) {return − ( ( 1. − 2. * x ) * ( y − 1. ) + 2. * kmin
    * nu / ( n * g ) ) * cos(t) ;}
func real up2true(real t) {return − ( x * ( 1. − x ) + y^2 − 2. * y + 1. ) *
    cos(t) ;}

/*————————————————————Macros————————————————————————*/

macro dot(u1,u2,v1,v2) (u1*v1 + u2*v2) //
macro div(v1,v2) (dx(v1)+dy(v2)) //
macro dotgrad(u1,u2,v1,v2) (dx(u1)*dx(v1) + dy(u1)*dy(v1) + dx(u2)*dx(v2) + dy
    (u2)*dy(v2)) //

/*————————————————————Time Stepping Loop————————————————————————*/

real dt = 1.0/N; // time step size for convergence tests (h=dt)

int itmax = 1.0/dt;
real T = itmax*dt;

int itmaxtemp = itmax − 1; // CNLF−stab iterations (3 level method)

string ster = "QSSD_Convergence_CNLFstab_TestProblem2";

// Report for convergence tests:

ofstream report(ster + "_N_" + N + "_T_" + T + "_dt_" + dt + "_So_" + So + "
    _kmin_" + kmin + ".txt");

report << "————qsSD_CNLFstab_convergence_report,_Marina_Moraiti————" << endl;
report << "_Boundary_nodes_per_side:_N_=_" << N << endl;
report << "_Step_Size:_dt_=_" << dt << endl;
report << "_CNLF+stab_Iterations_=_" << itmaxtemp << endl;
report << "_Final_Time:_T_=_" << T << endl;
report << "_Pressure_Penalty_=_" << pressurepenalty << endl;

real tnminus1 = 0.0; // t_0
```

```
real tn = dt; // t_1
real tnplus1 = 2.0*dt; // t_2

/*———Initialize u, p, and phi for 1st CNLF–stab iteration (SD)————*/

u1old2 = u1true(tnminus1);
u1old = u1true(tn);

u2old2 = u2true(tnminus1);
u2old = u2true(tn);

phiold2 = phitrue(tnminus1);
phiold = phitrue(tn);

pold2 = ptrue(tnminus1);
pold = ptrue(tn);

/*———Initialize u, p, and phi for 1st CNLF–stab iteration (qsSD)———*/

u1QSold2 = u1true(tnminus1);
u1QSold = u1true(tn);

u2QSold2 = u2true(tnminus1);
u2QSold = u2true(tn);

phiQSold2 = phitrue(tnminus1);
phiQSold = phitrue(tn);

pQSold2 = ptrue(tnminus1);
pQSold = ptrue(tn);

/*———Initialize max error norms for u, p and phi (SD —> QSSD)————*/

real uLinftyL2errorcurr = 0.0;
real uLinftyL2error = 0.0;

real pLinftyL2errorcurr = 0.0;
real pLinftyL2error = 0.0;

real phiLinftyL2errorcurr = 0.0;
real phiLinftyL2error = 0.0;

/*————————Begin time stepping loop——————————————————*/

for(int i=1;i<itmax;i++){

        // body forces and BC

        func f1 = f1(tn);
        func f2 = f2(tn);
        func fp = fp(tn);
        func fpQS = fpQS(tn);

        func U1 = u1true(tnplus1);
```

```
        func U2 = u2true(tnplus1);
        func PHI = phitrue(tnplus1);


/*————————Stokes CNLF–stab problem————————————————————*/

problem StokesCNLFstab([u1,u2,p],[v1,v2,q],solver=LU) =
        int2d(Omegaf)( ( 0.5 / dt ) * ( dot(u1,u2,v1,v2) + div(u1,u2) * div(v1
            ,v2) ) + 0.5 * nu * dotgrad(u1,u2,v1,v2)   // level n+1
                - 0.5 * p * div(v1,v2) + q * div(u1,u2) + p * q *
                        pressurepenalty  )      // level n+1
        + int1d(Omegaf,S1)( 0.5 * ( alpha / sqrt(kmin) ) * u1 * v1   )
                        // level n+1
        + int1d(Omegaf,S1)( g * phiold * (−1.0) * v2   )
                                        // level n (coupling term)
        + int2d(Omegaf)( ( −0.5 / dt) * ( dot(u1old2,u2old2,v1,v2) + div(
            u1old2,u2old2) * div(v1,v2) ) )      // level n−1
        + int2d(Omegaf)( 0.5 * nu * dotgrad(u1old2,u2old2,v1,v2) − 0.5 * pold2
             * div(v1,v2) ) // level n−1
        + int1d(Omegaf,S1)( 0.5 * ( alpha / sqrt(kmin) ) * u1old2 * v1 )
                    // level n−1
        − int2d(Omegaf)( dot(f1,f2,v1,v2) )
                                            // RHS Stokes (level n)
        + on(S2,S3,S4, u1 = U1, u2 = U2 );       // Dirichlet BC on exterior
            boundary of Omegaf

/*————————qs Stokes CNLF–stab problem————————————————*/

problem QSStokesCNLFstab([u1QS,u2QS,pQS],[v1,v2,q],solver=LU) =
        int2d(Omegaf)( ( 0.5 / dt ) * ( dot(u1QS,u2QS,v1,v2) + div(u1QS,u2QS)
            * div(v1,v2) ) + 0.5 * nu * dotgrad(u1QS,u2QS,v1,v2)   // level n+1
                - 0.5 * pQS * div(v1,v2) + q * div(u1QS,u2QS) + pQS * q *
                        pressurepenalty  )      // level n+1
        + int1d(Omegaf,S1)( 0.5 * ( alpha / sqrt(kmin) ) * u1QS * v1   )
                        // level n+1
        + int1d(Omegaf,S1)( g * phiQSold * (−1.0) * v2   )
                                            // level n (coupling term)
        + int2d(Omegaf)( ( −0.5 / dt) * ( dot(u1QSold2,u2QSold2,v1,v2) + div(
            u1QSold2,u2QSold2) * div(v1,v2) ) )      // level n−1
        + int2d(Omegaf)( 0.5 * nu * dotgrad(u1QSold2,u2QSold2,v1,v2) − 0.5 *
            pQSold2 * div(v1,v2) ) // level n−1
        + int1d(Omegaf,S1)( 0.5 * ( alpha / sqrt(kmin) ) * u1QSold2 * v1 )
                    // level n−1
        − int2d(Omegaf)( dot(f1,f2,v1,v2) )
                                            // RHS Stokes (level n)
        + on(S2,S3,S4, u1QS = U1, u2QS = U2 );   // Dirichlet BC on exterior
            boundary of Omegaf

/*————————Darcy CNLF–stab problem————————————————————*/

problem DarcyCNLFstab(phi, psi, solver=LU) =
        int2d(Omegap)( ( 0.5 / dt ) * g * So * phi * psi + 0.5 * g * kmin * (
            dx(phi) * dx(psi) + dy(phi) * dy(psi) )    // level n+1
                + dt * g^2 * (Cfp)^2 * ( dx(phi) * dx(psi) + dy(phi) * dy(psi)
                    + phi * psi ) )                                    // level
```

187

```
                              n+1
          − int1d(Omegap,D3)( g * psi * (−1.0) * u2old )
                                      // level n (coupling term)
          + int2d(Omegap)( ( − 0.5 / dt ) * g * So * phiold2 * psi + 0.5 * g *
              kmin * ( dx(phiold2) * dx(psi) + dy(phiold2) * dy(psi) )    //
              level n−1
                  − dt * g^2 * (Cfp)^2 * ( dx(phiold2) * dx(psi) + dy(phiold2) *
                      dy(psi) + phiold2 * psi ) )                        // level
                      n−1
          − int2d(Omegap)( g * fp * psi )
                                      // RHS Darcy (level n)
          + on(D1,D2,D4, phi = PHI );            // Dircichlet BC on exterior
              boundary of Omegap


/*——————————qs Darcy CNLF−stab problem——————————————————*/

problem QSDarcyCNLFstab(phiQS,psi,solver=LU) =
          int2d(Omegap)( ( 0.5 / dt ) * g * 0.0 * phiQS * psi + 0.5 * g * kmin *
              ( dx(phiQS) * dx(psi) + dy(phiQS) * dy(psi) )     // level n+1
                  + dt * g^2 * (Cfp)^2 * ( dx(phiQS) * dx(psi) + dy(phiQS) * dy(
                      psi) + phiQS * psi ) )
                      // level n+1
          − int1d(Omegap,D3)( g * psi * (−1.0) * u2QSold )
                                            // level n (coupling term)
          + int2d(Omegap)( ( − 0.5 / dt ) * g * 0.0 * phiQSold2 * psi + 0.5 * g
              * kmin * ( dx(phiQSold2) * dx(psi) + dy(phiQSold2) * dy(psi) )
              // level n−1
                  − dt * g^2 * (Cfp)^2 * ( dx(phiQSold2) * dx(psi) + dy(
                      phiQSold2) * dy(psi) + phiQSold2 * psi ) )
                      // level n−1
          − int2d(Omegap)( g * fpQS * psi )
                                  // RHS Darcy (level n)
          + on(D1,D2,D4, phiQS = PHI );            // Dircichlet BC on exterior
              boundary of Omegap



/*————————Solve for [u1,u2], p, phi, [u1Qs, u2QS], pQS, phiQS——————————*/

        StokesCNLFstab;
        DarcyCNLFstab;
        QSStokesCNLFstab;
        QSDarcyCNLFstab;

/*—————————Calculation of max error norms———————————————————————*/


uLinftyL2errorcurr = ( int2d(Omegaf)( ( u1 − u1QS )^2 + ( u2 − u2QS )^2   ) )
    ^(0.5);
        if (uLinftyL2errorcurr > uLinftyL2error){
                uLinftyL2error = uLinftyL2errorcurr;
                }

pLinftyL2errorcurr = ( int2d(Omegaf)( ( p − pQS )^2 ) )^(0.5);
        if (pLinftyL2errorcurr > pLinftyL2error){
```

```
                    pLinftyL2error = pLinftyL2errorcurr;
                    }

phiLinftyL2errorcurr = ( int2d(Omegap)( ( phi - phiQS )^2 ) )^(0.5);
          if (phiLinftyL2errorcurr > phiLinftyL2error){
                    phiLinftyL2error = phiLinftyL2errorcurr;
                    }

/*————————Update time and functions————————————————————————————*/

          u1old2 = u1old;
          u1old = u1;

          u2old2 = u2old;
          u2old = u2;

          phiold2 = phiold;
          phiold = phi;

          pold2 = pold;
          pold = p;

          u1QSold2 = u1QSold;
          u1QSold = u1QS;

          u2QSold2 = u2QSold;
          u2QSold = u2QS;

          phiQSold2 = phiQSold;
          phiQSold = phiQS;

          pQSold2 = pQSold;
          pQSold = pQS;

          tnminus1 = tn;
          tn = tnplus1;
          tnplus1 = tnplus1 + dt;

          cout << "Completed iteration " << i << " of " << itmaxtemp << endl;

} // end time stepping loop

cout << "N = " << N << endl;
cout << "dt = " << dt << endl;
cout << "iterations = " << itmaxtemp << endl;

cout << "LinftyL2-norm of u - uQS = "<< uLinftyL2error << endl;
cout << "LinftyL2-norm of p - QS = "<< pLinftyL2error << endl;
cout << "LinftyL2-norm of phi - phiQS = "<< phiLinftyL2error << endl;

report << " LinftyL2-norm of u - uQS = " << uLinftyL2error << endl;
report << " LinftyL2-norm of p - pQS = " << pLinftyL2error << endl;
report << " LinftyL2-norm of phi - phiQS = " << phiLinftyL2error << endl;
```

} // end loop over So values

B.5   MATLAB CODE FOR CNLF-STAB (EVOLUTION EQUATION)

B.5.1   Consistency of CNLF-stab

```
function epsilon = CNLFstabConsistency
%Solves the problem u_t+Au+Lu=0, u=(u_1,u_2), A=I, Lu=omega(-u2,u1), over
%(0,1], u(0)=(0,1), with the CNLF-stab method: (u^{n+1}-u^{n-1})/(2*dt)+
%beta*dt*L^*L(u^{n+1}-u^{n-1})+A(u^{n+1}+u^{n-1})/2 + Lu^n = 0, beta>=0.
%True solution: u(t)=exp(-t)(sin(omega*t),cos(omega*t))
%Calculates the error, epsilon, between the true and approximate solution for
    fixed omega and varying dt.
%Marina Moraiti, November 2014
omega = 40;
epsilon = zeros(9,5);
beta = [1,0,1/6,1/8,1/12];
for k=1:5
    for i=1:9
        dt = 2^(1-i)/50;
        N = 1/dt + 1;
        t = 0:dt:1;
        u = zeros(2,N);
        utrue = zeros(2,N);
        utrue(1,:) = exp(-t).*sin(omega*t);
        utrue(2,:) = exp(-t).*cos(omega*t);
        u(1,1) = 0;
        u(2,1) = 1;
        u(1,2) = utrue(1,2);
        u(2,2) = utrue(2,2);
            for j=2:N-1
                u(1,j+1) = 2*dt*omega*u(2,j)/(1+2*beta(k)*(dt)^2*(omega)^2+dt)
                    + (1+2*beta(k)*(dt)^2*(omega)^2-dt)*u(1,j-1)/(1+2*beta(k)
                    *(dt)^2*(omega)^2+dt);
                u(2,j+1) = -2*dt*omega*u(1,j)/(1+2*beta(k)*(dt)^2*(omega)^2+dt
                    ) + (1+2*beta(k)*(dt)^2*(omega)^2-dt)*u(2,j-1)/(1+2*beta(k
                    )*(dt)^2*(omega)^2+dt);
            end
        epsilon(i,k) = sqrt(dt)*norm(u(:,3:N)-utrue(:,3:N));
    end
end
```

B.5.2   Stability of CNLF-stab

```
function epsilon = CNLFstabStability
%Solves the problem u_t+Au+Lu=0, u=(u_1,u_2), A=I, Lu=omega(-u2,u1), over
%(0,1], u(0)=(0,1), with the CNLF-stab method: (u^{n+1}-u^{n-1})/(2*dt)+
%beta*dt*L^*L(u^{n+1}-u^{n-1})+A(u^{n+1}+u^{n-1})/2 + Lu^n = 0 True
%solution: u(t)=exp(-t)(sin(omega*t),cos(omega*t)).
```

```
%Calculates the error, epsilon, between the true and approximate solution for
    fixed dt and varying omega.
%Marina Moraiti, November 2014
epsilon = zeros(25,5);
beta = [1,0,1/6,1/8,1/12];
dt = 0.01;
t = 0:dt:1;
N = 1/dt + 1;
omega = 40:5:160;
u = zeros(2,N);
utrue = zeros(2,N);
u(1,1) = 0;
u(2,1) = 1;
for k=1:5
    for i=1:25
        utrue(1,:) = exp(-t).*sin(omega(i)*t);
        utrue(2,:) = exp(-t).*cos(omega(i)*t);
        u(1,2) = utrue(1,2);
        u(2,2) = utrue(2,2);
            for j=2:N-1
                u(1,j+1) = 2*dt*omega(i)*u(2,j)/(1+2*beta(k)*(dt)^2*(omega(i))
                    ^2+dt) + (1+2*beta(k)*(dt)^2*(omega(i))^2-dt)*u(1,j-1)
                    /(1+2*beta(k)*(dt)^2*(omega(i))^2+dt);
                u(2,j+1) = -2*dt*omega(i)*u(1,j)/(1+2*beta(k)*(dt)^2*(omega(i)
                    )^2+dt) + (1+2*beta(k)*(dt)^2*(omega(i))^2-dt)*u(2,j-1)
                    /(1+2*beta(k)*(dt)^2*(omega(i))^2+dt);
            end
        epsilon(i,k) = sqrt(dt)*norm(u(:,3:N)-utrue(:,3:N));
    end
end
```

BIBLIOGRAPHY

[1] A. Cesmelioglu and B. Rivière. Analysis of time-dependent Navier-Stokes flow coupled with Darcy flow. *J. Numer. Math.*, 2008.

[2] M. P. Anderson and W. W. Woessner. *Applied groundwater modeling: simulation of flow and advective transport.* Number v. 4 in Applied Groundwater Modeling: Simulation of Flow and Advective Transport. Academic Press, 1992.

[3] P. Angot. Analysis of singular perturbations on the Brinkman problem for fictitious domain models of viscous flows. *Math. Methods Appl. Sci.*, 22(16):1395–1412, 1999.

[4] M. Anitescu, W. Layton, and F. Pahlevani. Implicit for local effects, explicit for nonlocal is unconditionally stable. *Electron. Trans. Numer. Anal.*, 18:174–187, 2004.

[5] T. Arbogast and D. S. Brunson. A computational method for approximating a Darcy-Stokes system governing a vuggy porous medium. *Comput. Geosci.*, 11(3):207–218, 2007.

[6] U. Ascher, S. Ruuth, and B. Wetton. Implicit-explicit methods for time dependent partial differential equations. *SIAM J. Numer. Anal.*, 32:797–823, 1995.

[7] R. Asselin. Frequency filter for time integrations. *Mon. Weather Rev.*, 100(6):487–490, 1972.

[8] L. Badea, M. Discacciati, and A. Quarteroni. Numerical analysis of the Navier-Stokes/Darcy coupling. *Numer. Math.*, 115:195–227, 2010. 10.1007/s00211-009-0279-6.

[9] V. Batu. *Aquifer hydraulics: a comprehensive guide to hydrogeologic data analysis.* Wiley, 1998.

[10] J. Bear. *Hydraulics of groundwater.* McGraw-Hill series in water resources and environmental engineering. McGraw-Hill International Book Co., 1979.

[11] J. Bear. *Dynamics of fluids in porous media.* Dover, 1988.

[12] G. Beavers and D. Joseph. Boundary conditions at a naturally impermeable wall. *J. Fluid Mech.*, 30:197–207, 1967.

[13] M. A. Biot. General theory of three-dimensional consolidation. *J. Appl. Phys.*, 12(2):155–164, 1941.

[14] S. Brenner and R. Scott. *The Mathematical Theory of Finite Element Methods.* Springer, 3 edition, 2008.

[15] H. Brézis. *Functional Analysis, Sobolev Spaces and Partial Differential Equations.* Universitext Series. Springer, 2010.

[16] F. Brezzi. On the existence, uniqueness and approximation of saddle-point problems arising from lagrangian multipliers. *ESAIM Math. Model. Numer. Anal. - Modlisation Mathmatique et Analyse Numrique*, 8(R2):129–151, 1974.

[17] H. C. Brinkman. A calculation of the viscous force exerted by a flowing fluid on a dense swarm of particles. *Appl. Sci. Res.*, 1(1):27–34, 1949.

[18] J. Bundschuh and M. C. S. Arriaga. *Numerical Modeling of Isothermal Groundwater and Geothermal Systems: Mass, Solute and Heat Transport.* Multiphysics Modeling Series. Taylor & Francis Group, 2010.

[19] E. Burman and P. Hansbo. A unified stabilized method for Stokes and Darcy's equations. *J. Comput. Appl. Math.*, 198(1):35–51, 2007.

[20] M. Cai, M. Mu, and J. Xu. Preconditioning techniques for a mixed Stokes/Darcy model in porous media applications. *J. Comput. Appl. Math.*, 233(2):346 – 355, 2009.

[21] Y. Cao, M. Gunzburger, X. He, and X. Wang. Parallel, non-iterative, multi-physics domain decomposition methods for time-dependent Stokes-Darcy systems. *Math. Comput.*, 83(288):1617–1644, 2014.

[22] Y. Cao, M. Gunzburger, X. Hu, F. Hua, X. Wang, and W. Zhao. Finite element approximations for Stokes-Darcy flow with Beavers-Joseph interface conditions. *SIAM J. Numer. Anal.*, 47(6):4239–4256, 2010.

[23] Y. Cao, M. Gunzburger, X.-M. Hu, and X. Wang. Robin-Robin domain decomposition methods for the steady-state Stokes-Darcy system with the Beavers-Joseph interface condition. *Numer. Math.*, 117:601–629, 2010.

[24] Y. Cao, M. Gunzburger, F. Hua, and X. Wang. Coupled Stokes-Darcy model with Beavers-Joseph interface boundary condition. *Comm. Math. Sci.*, 2010.

[25] A. Cesmelioglu and B. Rivière. Analysis of weak solutions for the fully coupled Stokes-Darcy-transport problem. Technical report, University of Pittsburgh, 2009.

[26] J. M. Connors, J. S. Howell, and W. J. Layton. Partitioned time stepping for a parabolic two domain problem. *SIAM J. Numer. Anal.*, 47(5):3526–3549, 2009.

[27] J. M. Connors, J. S. Howell, and W. J. Layton. Decoupled time stepping methods for fluid-fluid interaction. *SIAM J. Numer. Anal.*, 50(3):1297–1319, 2012.

[28] J. M. Connors and A. Miloua. Partitioned time discretization for parallel solution of coupled ODE systems. *BIT Numer. Math.*, 51(2):253–273, 2011.

[29] M. Crouzeix. Une méthode multipas implicite-explicite pour l'approximation des équationes d'évolution paraboliques. *Numer. Math.*, 1980.

[30] C. D'Angelo and P. Zunino. A finite element method based on weighted interior penalties for heterogeneous incompressible flows. *SIAM J. Numer. Anal.*, 47(5):3990–4020, 2009.

[31] L. Davis and F. Pahlevani. Semi-implicit schemes for transient Navier-Stokes equations and eddy viscosity models. *Numer. Methods Partial Differential Equations*, 2009.

[32] M. Discacciati. *Domain decomposition methods for the coupling of surface and groundwater flows.* PhD thesis, École Polytechnique Fédérale de Lausanne, Switzerland, 2004.

[33] M. Discacciati, E. Miglio, and A. Quarteroni. Mathematical and numerical models for coupling surface and groundwater flows. *Appl. Numer. Math.*, 43(1-2):57–74, 2002. 19th Dundee Biennial Conference on Numerical Analysis (2001).

[34] M. Discacciati and A. Quarternoni. Navier-Stokes/Darcy coupling: modeling, analysis, and numerical approximation. *Rev. Mat. Complut.*, 22(2):315–426, 2009.

[35] M. Discacciati and A. Quarteroni. Analysis of a domain decomposition method for the coupling of Stokes and Darcy equations. In F. Brezzi, A. Buffa, S. Corsaro, and A. Murli, editors, *Numerical Analysis and Advanced Applications - Enumath 2001*, pages 3–20. Springer, 2001.

[36] M. Discacciati and A. Quarteroni. Convergence analysis of a subdomain iterative method for the finite element approximation of the coupling of Stokes and Darcy equations. *Comput. Vis. Sci.*, 6(2-3):93–103, 2004.

[37] M. Discacciati, A. Quarteroni, and A. Valli. Robin-Robin domain decomposition methods for the Stokes-Darcy coupling. *SIAM J. Numer. Anal.*, 45(3):1246–1268, 2007.

[38] P. Domenico and M. Mifflin. Water from low-permeability sediments and land subsidence. *Water Resour. Res.*, 1(4):563–576, 1965.

[39] P. A. Domenico. *Concepts and models in groundwater hydrology.* International series in the earth and planetary sciences. McGraw-Hill, 1972.

[40] J. Douglas and T. Dupont. Alternating-direction galerkin methods on rectangles. In *Numerical Solutions of Partial Differential Equations*, volume II, pages 133–214. SYNSPADE, 1970.

[41] D. Durran. *Numerical Methods for Wave Equations in Geophysical Fluid Dynamics.* Springer, 1999.

[42] V. Ervin, Jenkin E., and S. Sun. Coupling nonlinear Stokes and Darcy flow using mortar finite elements. *Appl. Numer. Math.*, 61(11):1198–1222, 2011.

[43] V. Ervin, W. Layton, and M. Neda. Numerical analysis of filter-based stabilization for evolution equations. *SIAM J. Numer. Anal.*, 50(5):2307–2335, 2012.

[44] J. Frank, W. Hundsdorfer, and J. Verwer. On the stability of implicit-explicit linear multistep methods. *Appl. Numer. Math.*, 25(2):193–205, 1997.

[45] R. A. Freeze and J. A. Cherry. *Groundwater.* Prentice-Hall, 1979.

[46] G. P. Galdi. *An Introduction to the Mathematical Theory of the Navier-Stokes Equations: Linearized steady problems.* Number v. 1 in An Introduction to the Mathematical Theory of the Navier-Stokes Equations. Springer-Verlag, 1994.

[47] G. P. Galdi. *Nonlinear Steady Problems.* An introduction to the mathematical theory of the Navier-Stokes equations. Springer, 1998.

[48] G. P. Galdi, J. G. Heywood, and R. Rannacher. *Fundamental directions in mathematical fluid mechanics.* Advances in mathematical fluid mechanics. Birkhäuser Verlag, 2000.

[49] G. P. Galdi and B. Straughan. Exchange of stabilities, symmetry, and nonlinear stability. *Archive for Rational Mechanics and Analysis*, 89(3):211–228, 1985.

[50] G. N. Gatica, R. Oyarza, and F.-J. Sayas. Convergence of a family of Galerkin discretizations for the StokesDarcy coupled problem. *Numer. Methods Partial Differential Equations*, 27(3):721–748, 2011.

[51] V. Girault and P. A. Raviart. *Finite Element Approximation of the Navier-Stokes Equations.* Lecture Notes in Mathematics. Springer-Verlag, Berlin, 1979.

[52] V. Girault and B. Rivière. DG approximation of coupled Navier-Stokes and Darcy equations by Beaver-Joseph-Saffman interface condition. *SIAM J. Numer. Anal.*, 47(3):2052–2089, 2009.

[53] J. Gobert. Sur une inégalité de coercivité. *J. Math. Anal. Appl.*, 36(3):518 – 528, 1971.

[54] S. Gottlieb, F. Tone, C. Wang, X. Wang, and D. Wirosoetisno. Long time stability of a classical efficient scheme for two-dimensional NavierStokes equations. *SIAM J. Numer. Anal.*, 50(1):126–150, 2012.

[55] P. Gresho and R. Sani. *Incompressible flow and the finite element method: Advection-diffusion and isothermal laminar flow.*, volume 1. Wiley, 1998.

[56] M. Gunzburger. *Finite Element Methods for Viscous Incompressible Flows - A Guide to Theory, Practices, and Algorithms.* Academic Press, 1989.

[57] N. S. Hanspal, A. N. Waghode, V. Nassehi, and R. J. Wakeman. Numerical analysis of coupled Stokes/Darcy flows in industrial filtrations. *Transport Porous Med.*, 64(1):73–101, 2006.

[58] M. S. Hantush. *Flow to an eccentric well in a leaky circular aquifer.* American Geophysical Union, 1960.

[59] F. Hecht and O. Pironneau. Freefem++. http://www.freefem.org.

[60] R. H. W. Hoppe, P. Porta, and Y. Vassilevski. Computational issues related to iterative coupling of subsurface and channel flows. *Calcolo*, 44(1):1–20, 2007.

[61] F. Hua. *Modeling, analysis and simulation of Stokes-Darcy system with Beavers-Joseph interface condition.* PhD thesis, Florida State University, 2009.

[62] W. Hundsdorfer and J. Verwer. *Numerical solution of time dependent advection-diffusion-reaction equations.* Springer, Berlin, edition edition, 2003.

[63] N. Hurl. Energy stability of the Crank-Nicolson Leap Frog method with time filters. Technical report, www.mathematics.pitt.edu/research/technical-reports, University of Pittsburgh, 2012.

[64] N. Hurl, W. Layton, Y. Li, and M. Moraiti. The unstable mode in the Crank-Nicolson Leap-Frog method is stable. Technical report, www.mathematics.pitt.edu/research/technical-reports, University of Pittsburgh, 2015.

[65] N. Hurl, W. Layton, Y. Li, and C. Trenchea. Stability analysis of the CrankNicolson-Leapfrog method with the RobertAsselinWilliams time filter. *BIT Numer. Math.*, pages 1–13, 2014.

[66] R. Ingram. Finite element approximation of nonsolenoidal, viscous flows around porous and solid obstacles. *SIAM J. Numer. Anal.*, 49(2):491–520, 2011.

[67] W. Jäger and A. Mikelić. On the boundary conditions at the interface between a porous medium and a free fluid. *SIAM J. Appl. Math.*, 60:1111–1127, 2000.

[68] B. Jiang. A parallel domain decomposition method for coupling of surface and groundwater flows. *Comput. Methods Appl. Mech. Eng.*, 198(912):947 – 957, 2009.

[69] N. Jiang, M. Kubacki, W. Layton, M. Moraiti, and H. Tran. A Crank-Nicolson Leapfrog stabilization: Unconditional stability and two applications. *Journal of Computational and Applied Mathematics*, 281(0):263 – 276, 2015.

[70] O. Johansson and H. Kreiss. Über das Verfahren der zentralen Differenzen zur Lösung des Cauchy problems für partielle Differentialgleichungen, Nordisk Tidskr. *Informations-Behandling*, 3(2):97–107, 1963.

[71] A. I. Johnson. *Specific yield - compilation of specific yields for various materials.* Hydrologic properties of earth materials; Geological Survey water-supply paper. U.S. Gov. Print. Off., Washington D.C., 1967.

[72] I. Jones. Low Reynolds number flow past a porous spherical shell. *Math. Proc. Cambridge*, 73(01):231–238, 1973.

[73] N. Ju. On the global stability of a temporal discretization scheme for the Navier-Stokes equations. *IMA J. Numer. Anal.*, 22(4):577–597, 2002.

[74] E. Kalnay. *Atmospheric Modeling, data assimilation and predictability.* Cambridge Univ. Press, Cambridge, 2003.

[75] M. Kubacki. Uncoupling evolutionary groundwater-surface water flows using the Crank-Nicolson Leapfrog method. *Numer. Methods Partial Differential Equations*, 29:1192–1216, 2013.

[76] M. Kubacki and M. Moraiti. Analysis of a second-order, unconditionally stable, partitioned method for the evolutionary Stokes-Darcy problem. *International Journal of Numerical Analysis and Modeling*, 12(4):704–730, 2015.

[77] A. Labovsky, W. Layton, C. Manica, M. Neda, and L. Rebholz. The stabilized, extrapolated trapezoidal finite element method for the Navier-Stokes equations. *Comput. Methods Appl. Mech. Eng.*, 198:958–974, 2009.

[78] O. A. Ladyzhenskaya. New equations for the description of motion of viscous incompressible fluids and solvability in the large of boundary value problems for them. *Tr. Mat. Inst. Steklov*, 102:85–104, 1967.

[79] O. A. Ladyzhenskaya. *The Mathematical Theory of Viscous Incompressible: Flow.* Mathematics and Its Applications. Gordon and Breach Science Publishers, 1969.

[80] W. Layton. *Introduction to the Numerical Analysis of Incompressible, Viscous Flows.* SIAM, 2008.

[81] W. Layton. Fluid-porous interface conditions with the "inertia term" $\frac{1}{2}|u_{fluid}|^2$ are not Galilean invariant. Technical report, www.mathematics.pitt.edu/research/technical-reports, University of Pittsburgh, 2009.

[82] W. Layton, F. Schieweck, and I. Yotov. Coupling fluid flow with porous media flow. *SIAM J. Numer. Anal.*, 40(6):2195–2218, 2003.

[83] W. Layton, H. Tran, and C. Trenchea. Analysis of long time stability and errors of two partitioned methods for uncoupling evolutionary groundwater–surface water flows. *SIAM J. Numer. Anal.*, 51(1):248–272, 2013.

[84] W. Layton, H. Tran, and X. Xiong. Long time stability of four methods for splitting the evolutionary Stokes-Darcy problem into stokes and darcy subproblems. *J. Comput. Appl. Math.*, 236(13):3198–3217, 2012.

[85] W. Layton and C. Trenchea. Stability of two IMEX methods, CNLF and BDF2-AB2, for uncoupling systems of evolution equations. *Appl. Numer. Math.*, 62:112–120, 2012.

[86] T. Levy and E. Sánchez-Palencia. On boundary conditions for fluid flow in porous media. *Int. J. Eng. Sci.*, 13(11):923–940, 1975.

[87] J. L. Lions. *Perturbations Singulieres dans les Problemes aux Limites et en Controle Optimal.* Springer, 1973.

[88] E. Miglio, A. Quarteroni, and F. Saleri. Coupling of free surface and groundwater flows. *Comput. Fluids*, 32(1):73–83, 2003.

[89] A. Mikelić and W. Jäger. On the interface boundary condition of Beavers, Joseph, and Saffman. *SIAM J. Appl. Math.*, 60(4):1111–1127, 2000.

[90] M. Moraiti. On the quasistatic approximation in the Stokes-Darcy model of groundwater-surface water flows. *J. Math. Anal. Appl.*, 394(2):796–808, 2012.

[91] M. Mu and J. Xu. A two-grid method of a mixed StokesDarcy model for coupling fluid flow with porous media flow. *SIAM J. Numer. Anal.*, 45(5):1801–1813, 2007.

[92] M. Mu and X. Zhu. Decoupled schemes for a non-stationary mixed Stokes-Darcy model. *Math. Comp.*, 79(270):707–731, 2010.

[93] NC Department of Health and Human Services. http://epi.publichealth.nc.gov/oii/pdf/ProtectYourselfArsenicWellWater.pdf.

[94] M. Olshanskii and A. Reusken. Grad-Div stabilization for the Stokes equations. *Math. Comp.*, 73:1699–1718, 2004.

[95] L. Payne and B. Straughan. Analysis of the boundary condition at the interface between a viscous fluid and a porous medium and related modeling questions. *J. Math. Pures Appl.*, 77:317–354, 1998.

[96] G. Pinder and M. Celia. *Subsurface Hydrology.* John Wiley and Sons, 2006.

[97] A. Quarteroni and A. Valli. *Numerical approximation of partial differential equations.* Springer, Berlin, 1994.

[98] B. Rivière. Analysis of a discontinuous finite element method for the coupled Stokes and Darcy problems. *SIAM J. Sci. Comput.*, 22:479–500, 2005.

[99] B. Rivière and I. Yotov. Locally conservative coupling of Stokes and Darcy flows. *SIAM J. Numer. Anal.*, 42(5):50–292, 2005.

[100] A. Robert. The integration of a spectral model of the atmosphere by the implicit method. In *WMO/IUGG Symposium on NWP*, volume 7, pages 19–24, Tokyo, Japan, 1969. Japan Meteorological Agency.

[101] P. Saffman. On the boundary condition at the interface of a porous medium. *Stud. Appl. Math.*, 1:93–101, 1971.

[102] L. Shan and H. Zheng. Partitioned time stepping method for fully evolutionary Stokes-Darcy flow with Beavers-Joseph interface conditions. *SIAM J. Num. Anal.*, 51(2):813–839, 2013.

[103] L. Shan, H. Zheng, and W. Layton. A decoupling method with different subdomain time steps for the nonstationary Stokes-Darcy model. *Numer. Methods Partial Differential Equations*, 29(2):549–583, 2013.

[104] B. Straughan. Nonlinear stability of convection in a porous layer with solid partitions. *J. Math. Fluid Mech.*, 16(4):727–736, 2014.

[105] S. Thomas and D. Loft. The NCAR spectral element climate dynamical core: semi-implicit Eulerian formulation. *J. Sci. Comput.*, 25:307–322, 2005.

[106] F. Tone and D. Wirosoetisno. On the long-time stability of the implicit Euler scheme for the two-dimensional Navier-Stokes equations. *SIAM J. Num. Anal.*, 44(1):29–40, 2006.

[107] A. M. P. Valli, G. F. Carey, and A. L. G. A. Coutinho. On decoupled time step/sub-cycling and iteration strategies for multiphysics problems. *Commun. Numer. Methods Eng.*, 24(12):1941–1952, 2008.

[108] J. Varah. Stability restrictions on a second order, three level finite difference schemes for parabolic equations. *SIAM J. Numer. Anal.*, 17:300–309, 1980.

[109] V. Vassilev and I. Yotov. Domain decomposition for coupled Stokes and Darcy flows. Technical report, www.mathematics.pitt.edu/research/technical-reports, University of Pittsburgh, 2011.

[110] J. Verwer. Convergence and component splitting for the Crank-Nicolson–Leap-Frog integration method. *Modelling, Analysis and Simulation*, (E0902):1–15, 2009.

[111] H. Wang. *Theory of linear poroelasticity with applications to geomechanics and hydrogeology*. Princeton series in geophysics. Princeton University Press, 2000.

[112] X. Wang. On the coupled continuum pipe flow model (CCPF) for flows in karst aquifer. *Discrete Contin. Dyn. Syst. Ser. B*, 13:489–501, 2010.

[113] I. Watson and A. Burnett. *Hydrology: An Environmental Approach.* CRC Press, Inc., 1995.

[114] P. Williams. The RAW filter: An improvement to the Robert-Asselin filter in semi-implicit integrations. *Mon. Weather Rev.*, 139(6):1996–2007, 2011.

[115] P. Zunino. *Mathematical and Numerical Modeling of Mass Transfer in the Vascular System.* PhD thesis, École Polytechnique Fédérale de Lausanne, Switzerland, 2002.